



D-STABILITY

Slope stability software for
soft soil engineering



Installation manual | Tutorial | Scientific background |
Reliability background



User Manual

D-Stability



User Manual

D-Stability

Authors

R. van der Meij

Partners

RWS-WVL, HWBP

\coverPhoto{...}

User Manual

D-Stability

Client	Users of D-Stability
Contact	Raymond.vanderMeij@Deltares.nl
Reference	D-GEO Suite Stability
Keywords	D-GEO Suite, D-Stability, Macro Stability, slope stability, Reliability

Document control

Version	2023.01.2
Date	June 2023
Project number	11209269
Document ID	2023.01.2
Pages	171
Status	General availability Check the release notes for version history

Summary

D-Stability is free to use slope stability software for soft soil engineering.

This document contains the installation manual, tutorial and scientific manual of D-Stability

Samenvatting

D-Stability is gratis software voor het berekenen van macrostabiliteit.

Dit document bevat de installatiehandleiding, tutorial en wetenschappelijke handleiding van D-Stability.

Contents

	Summary	4
	List of Tables	9
	List of Figures	10
1	Introduction	13
	Installation manual	14
2	Installation manual	15
2.1	Downloading D-Stability	15
2.2	Installing D-Stability	17
2.3	Checking the installation	18
	Tutorial	20
3	Tutorial: probabilistic analysis	21
3.1	Creating a new project: Project description	21
3.2	The surface line	22
3.3	Setting up the geometry	25
3.4	Berms and excavations	26
3.5	Zooming	26
3.6	The drawing aid	28
3.7	Assigning material	29
3.8	Defining the water pressures	30
3.9	Defining the state	31
3.10	Construction stages	35
3.11	Loads	39
3.12	Running the calculation	40
3.13	Results	41
3.14	Safety overview	41
3.15	Using stages for further analysis	43
3.16	Probabilistic analysis: design values	46
3.17	Correlation of state points	50
3.18	Probabilistic analysis: FORM analysis	51
3.19	Probabilistic analysis: Monte Carlo Importance Sampling (MCIS) analysis	52
3.20	Berms and excavations	54
3.21	Exporting the fragility curve	59
3.22	Parameter list in the application	61
	Scientific Manual	66
4	Soil profile	67
4.1	Coordinate system	67
4.2	Soil profile definition	67
4.3	Vertexes	68
4.4	Soil and water pressure	68
5	Pore pressure	70

5.1	Hydraulic pore pressure	70
5.1.1	Hydraulic heads by lines	70
5.2	Pore pressure due to degree of consolidation	71
5.3	Pore pressure from loads	72
5.4	Pore pressure due to earthquake	73
5.5	Total pore pressure and effective stress	73
6	Shear strength models	75
6.1	MohrCoulomb model (drained): classic and advanced	75
6.1.1	Introduction	75
6.1.2	Theoretical background	76
6.1.3	Numerical simulation	82
6.1.4	Advice on the use of the dilatancy angle ψ in D-Stability	83
6.1.5	References regarding Mohr Coulomb advanced model	85
6.2	SHANSEP (undrained)	85
6.2.1	Yield stress	85
6.2.2	Calculating the undrained shear stress	86
6.2.3	Yield stress field	86
6.2.4	Construction stages	87
6.3	Su table (undrained)	88
6.3.1	Introduction	88
6.3.2	Format of the table	89
6.3.3	Scaling over 'm'	90
6.3.4	Graphical representation of the scaling over 'm'	90
6.3.5	SU tables in probabilistic analysis	91
6.4	Calculation shear strength	92
7	Limit equilibrium methods	93
7.1	Safety factor	93
7.2	Method of slices	93
7.2.1	Subdivision into slices	93
7.2.2	Slice properties	94
7.2.2.1	Geometrical properties	95
7.3	Driving and resisting moments	96
7.3.1	Driving moments	96
7.3.1.1	Driving soil moment	96
7.3.1.2	Driving water moment	96
7.3.1.3	Driving load moment	98
7.3.1.4	Driving earthquake moment	99
7.3.1.5	Total driving moment	100
7.3.2	Resisting moments	100
7.3.2.1	Resisting moment from soil	100
7.3.2.2	Resisting moment from end section	101
7.3.2.3	Total resisting moment	102
7.4	Bishop	102
7.4.1	Method according to A. W. Bishop	102
7.4.2	Equilibrium	103
7.4.3	Safety factor	104
7.5	Uplift-Van	105
7.5.1	Method according to M. Van	105
7.5.2	Driving moment of the circular parts	105
7.5.2.1	Driving water moments of the circular parts	106
7.5.2.2	Determination of active and passive sides	109
7.5.3	Resisting moment of the circular parts	109

7.5.4	Horizontal forces	110
7.5.4.1	Soil resistance force along horizontal part I_s	110
7.5.4.2	Earthquake force along horizontal part $F_{\text{quake;horiz}}$	110
7.5.4.3	Resulting water force along horizontal part $F_{\text{water;horiz}}$	110
7.5.4.4	Resulting horizontal force at active side I_a	111
7.5.4.5	Resulting horizontal force at passive side I_p	111
7.5.5	Safety factor	112
7.5.5.1	Determination of the arm of the active force I_a	112
7.5.5.2	Equilibrium of horizontal forces	113
7.6	Spencer	114
7.6.1	Method according to E. Spencer	114
7.6.2	Safety factor	114
8	Optimization procedures	118
8.1	Search area	118
8.1.1	Search area for Bishop	118
8.1.2	Search area for Uplift-Van	118
8.1.3	Search area for Spencer	118
8.2	Slip plane constraints	118
8.2.1	General constraints on all slip planes	118
8.2.1.1	Minimal circle depth	118
8.2.1.2	Minimal circle length	119
8.2.1.3	Entry and exit point constraints	119
8.2.2	Constraints on Spencer slip planes	119
8.3	Single slip plane	119
8.4	Grid search (Bishop)	119
8.4.1	Move grid if optimum is on edge	119
8.5	Genetic algorithm (Spencer)	120
8.5.1	General genetic algorithm	120
8.5.1.1	Initialization	120
8.5.1.2	Parental selection	122
8.5.1.3	Mutation	123
8.5.1.4	Child selection	125
8.5.1.5	Elitism	125
8.5.1.6	Stop Criterion	125
8.5.1.7	Chaos in the algorithm	125
8.6	APSO algorithm (Uplift-Van)	125
9	External loads	127
9.1	Line loads	127
9.2	Uniform loads	129
9.3	Earthquake	130
9.4	Tree on slope	131
10	Reinforcements	133
10.1	Resisting moment from geotextiles	133
10.2	Resisting moment from nails	134
10.2.1	Tensile resistance at soil-nail interaction during pull-out	136
10.2.2	Soil/nail normal reaction: soil fails in bearing below the nail	136
10.2.3	Tensile and shear resistance of the nail	137
10.2.4	Soil/nail normal reaction: nail breaks in bending	138
11	Waternet Creator	139
11.1	Waternet lines	139
11.1.1	Conditions under which the automatic generation works	139

11.1.2	Required input	139
11.1.3	Schematisation of phreatic plane	141
11.1.3.1	Particular cases	143
11.1.3.2	Minimum values below dike crest	144
11.1.4	Schematisation of the piezometric heads	144
11.1.4.1	Schematisation of piezometric head PL2	144
11.1.4.2	Schematisation of piezometric heads PL3 and PL4	145
11.1.4.3	Checking for uplift	148
11.1.5	Schematisation of the pore pressures by means of waternet-lines	149
	Reliability analysis	151
12	Introduction	152
13	Stochastic distributions	153
13.1	Distribution properties	153
13.1.1	Mean	153
13.1.2	Standard deviation	153
13.1.2.1	Determining standard deviation	153
13.1.3	Density functions	154
13.2	Distribution types	154
13.2.1	Standard normal distribution	154
13.2.2	Normal distribution	155
13.2.3	Log-normal distribution	155
14	Semi probabilistic analysis	157
14.1	Design value	157
14.2	Characteristic value	157
14.2.1	Charateristic value (normal)	157
14.2.2	Characteristic value (lognormal)	158
14.3	Stress tables	158
15	Full probabilistic analysis	159
15.1	FORM analysis	159
15.1.1	Convergence	161
15.1.2	Correlations	162
15.2	Monte Carlo and Monte Carlo Importance Sampling analysis	162
15.2.1	Crude Monte Carlo (MC)	163
15.2.2	Adaptive Importance Sampling (MCIS)	165
15.3	Fragility curve	166
15.4	Combining Fragility Curve and water level	166
	References	168
16	References	169

List of Tables

5.2	Different degrees of consolidation in different layers	72
11.1	Parameters for generating water pressures in geometry, inner stability	140
11.2	Schematisation of the phreatic plane for the different scenario's	141
11.3	Overview and description of piezometric lines	144
11.4	Points of PL2	145
11.5	Points of head lines PL3 and PL4	146
15.3	Required number of samples with crude Monte Carlo for combinations of the acceptable relative error ε and actual probability of failure P_f . The value of k in equation (15.13) is taken equal to 1.96.	165

List of Figures

2.1	<i>Deltares website</i>	15
2.2	<i>Software</i>	15
2.3	<i>Download portal</i>	16
2.4	<i>D-Stability Download portal</i>	16
2.5	<i>MSI</i>	17
2.6	<i>Installation wizard</i>	17
2.7	<i>Repair or remove</i>	18
2.8	<i>Open tutorial</i>	18
2.9	<i>Calculate the second stage</i>	19
2.10	<i>Successful run and therefore successful installation</i>	19
3.1	<i>Opening screen</i>	21
3.2	<i>Project information</i>	22
3.3	<i>Surface line data</i>	23
3.4	<i>Imported surface line</i>	24
3.5	<i>Surface line fully valid</i>	24
3.6	<i>Only the left half of the surface line is valid</i>	25
3.7	<i>Constructed subsoil schematization using divide and draw</i>	26
3.8	<i>Scaling the geometry to fit the canvas by clicking the vertical (z direction) and the horizontal (x direction) double arrows at the right bottom of the program interface</i>	27
3.9	<i>Same scale for x and z by double-clicking on the "+" where the axes intersect, on the top left corner of the canvas</i>	27
3.10	<i>Drawing aid toggle activated while drawing</i>	28
3.11	<i>Drawing an excavation</i>	28
3.12	<i>Assignment of a material to a layer</i>	29
3.13	<i>Use of the profile inspector</i>	29
3.14	<i>Completed head line</i>	30
3.15	<i>Inspecting water pressures with profile inspector</i>	31
3.16	<i>Defining state point in layer</i>	31
3.17	<i>State pinned in layer</i>	32
3.18	<i>State point parameters</i>	33
3.19	<i>State line drawn along the boundary of a layer</i>	33
3.20	<i>State point placed on a state line</i>	34
3.21	<i>State inspector</i>	35
3.22	<i>State inspector II</i>	35
3.23	<i>Construction stages</i>	36
3.24	<i>Defining water in high water stage</i>	36
3.25	<i>High water pressure in aquifer</i>	37
3.26	<i>Assigning hydrostatic pressures to reference line</i>	37
3.27	<i>Assigning high water pressures to aquifer</i>	38
3.28	<i>Inspecting the high water pressures and resulting POP</i>	38
3.29	<i>Definition of a uniform load</i>	39
3.30	<i>Inspecting the effect of a uniform load</i>	39
3.31	<i>Selecting calculation method</i>	40
3.32	<i>Defining search area</i>	40
3.33	<i>Resulting slip plane</i>	41
3.34	<i>Safety overview for $F_s < 1,024$</i>	42
3.35	<i>Safety overview with Spencer for $F_s < 1,175$</i>	42
3.36	<i>New building stage for other Limit Equilibrium Method</i>	43
3.37	<i>Import water pressures from another stage</i>	43
3.38	<i>Choose another LEM</i>	44

3.39	<i>Define Spencer search area</i>	44
3.40	<i>Spencer result</i>	45
3.41	<i>Slip plane inspector</i>	45
3.42	<i>Design values</i>	46
3.43	<i>Making a single Bishop calculation</i>	47
3.44	<i>Import slip circle from another phase</i>	47
3.45	<i>Defining probabilistic material properties and correlation</i>	48
3.46	<i>Choosing a design calculation</i>	49
3.47	<i>Results with design values</i>	49
3.48	<i>Correlation of state points</i>	50
3.49	<i>Fully probabilistic calculation</i>	51
3.50	<i>Result of a probabilistic calculation</i>	51
3.51	<i>The MCIS analysis</i>	53
3.52	<i>The result of an MCIS analysis</i>	54
3.53	<i>Creating a berm</i>	55
3.54	<i>Filling up the ditch and drawing a new excavation</i>	55
3.55	<i>Assigning material to berm</i>	56
3.56	<i>Inspecting POP besides the berm</i>	56
3.57	<i>Inspecting POP underneath the berm</i>	57
3.58	<i>Inspecting the yield stress in the ditch</i>	57
3.59	<i>Making an Uplift-Van analysis</i>	58
3.60	<i>Defining the Uplift-Van search area</i>	58
3.61	<i>Increasing the berm length</i>	59
3.62	<i>Determining the final conditional probability of failure</i>	59
3.63	<i>Export fragility curve screen</i>	60
3.64	<i>Exporting a fragility curve</i>	60
4.1	Coordinate system	67
4.2	Soil profile	68
5.1	Calculation of the hydraulic pore pressures (from piezometric level lines)	70
6.1	Definition of a-angle of principle stress, θ , b- the angle of principal strain increment, ξ and c-the angle of principal stress increment. χ	76
6.2	Results of Direct Simple Shear tests on Leighton Buzzard sand, from Roscoe (1970). The symbol ψ in this figure stands for the angle of principal effective stress, θ 19 lb/sq in = 131 kPa and 56 lb/ sq in = 386 kPa	77
6.3	Typical test result from Roscoe (1970)	78
6.4	Stress and strain increments observed after a rotation of a retaining wall, from Roscoe (1970), the symbol ν is used for angle of dilatancy which is represented by ψ in this text	79
6.5	Development of a failure plane in clay in a triaxial compression test, from: Kwak et al. (2020)	81
6.6	Stress – strain relation for simulations 1 and 2, $K_0 = 0.5$	82
6.7	Stress – strain relationship for simulations 3 and 4, $K_0 = 2,0$	83
6.8	The difference in using triaxial compression and plain strain	84
6.9	Yield stress points	86
6.10	Average and design values of the undrained shear strength - effective stress relationship based upon statistical analysis of lab tests	89
6.11	Scaling over m along the five construction stages	91
7.1	Slip plane including method of slices	93
7.2	Global view of one slice	94
7.3	Horizontal water pressures (due to free water) acting on the side of a slice in case of vertical layer boundary	97

7.4	Relation angle α - Shear Stress for $\alpha_{\min} = 35^\circ$	101
7.5	Force equilibrium for one slice in the method of slices	103
7.6	Uplift failure mechanism	105
7.7	Van-Uplift Stability derivation	105
7.8	Schematization of the pore pressure distribution on bars	108
7.9	Interslice forces according to Spencer method	114
8.1	Procedure of the genetic algorithm	120
8.2	An entire population of uniformly defined individuals	121
8.3	An entire population of quadratically defined individuals	121
8.4	Scattered crossover between two parents	122
8.5	Double point crossover between two parents	123
8.6	Left: initial genome; Right: genome after jump mutation	124
8.7	Left: initial genome; Right: genome after creep mutation	124
8.8	Left: initial genome; Right: genome after inversion	125
9.1	Line load	127
9.2	Uniform Load	129
9.3	Representation of the effect of wind on trees	131
10.1	Resisting contribution by geotextiles	133
10.2	Resisting contribution by nails	134
10.3	Representation of the four criteria in the $F_N - F_D$ diagram to determine F_{nail}	135
10.4	Representation of the Tresca's criterion by Mohr's circle	138
11.1	Schematisation of the phreatic plane for clay dikes (scenario's 1A and 1B)	142
11.2	Schematisation of the phreatic plane for sand dike on clay/peat underground (scenario 2A), without drainage construction	142
11.3	Schematisation of the phreatic plane for sand dike on clay/peat underground (scenario 2A), with drainage construction	142
11.4	Schematisation of the phreatic plane for sand dike on sand underground (scenario 2B), without drainage construction	143
11.5	Schematisation of the phreatic plane for sand dike on sand underground (scenario 2B), with drainage construction	143
11.6	Schematisation of the hydraulic heads for dikes on clay underground (scenario's 1A and 2A)	147
11.7	Schematisation of the hydraulic heads for clay dike on sand underground (scenario 1B)	147
11.8	Lowering of piezometric head in the presence of uplift. D-Stability checks for uplift starting at the inner toe and extending to the edge of the profile and adapts the piezometric head accordingly until an unstable equilibrium is attained.	148
11.9	Schematisation of pore pressures when there is a single aquifer	149
11.10	Schematisation of pore pressures when there is an in-between aquifer	150
15.1	Schematic representation of FORM	160
15.2	Schematic view of Monte Carlo sampling for an example with two random variables. Each dot represents a sampled pair (x_1, x_2) . Red dots indicate failure ($Z < 0$), green dots indicate no failure ($Z \geq 0$).	163
15.3	Relation between k and P_k according to equation (15.13). Function ϕ is the standard normal density function	164
15.4	The algorithm of Adaptive Importance Sampling.	165

1 Introduction

D-Stability is software for soft soil slope stability.

Deltares is an independent institute for applied research in the field of water, subsurface and infrastructure. Throughout the world, we work on smart solutions, innovations and applications for people, environment and society. Knowledge is our core business. Deltares employs over 800 people and is based in Delft and Utrecht, the Netherlands.

D-Stability is made in cooperation with the HWBP and Rijkswaterstaat.

Rijkswaterstaat is the executive agency of the Ministry of Infrastructure and Water Management, dedicated to promote safety, mobility and the quality of life in the Netherlands.

This is the user manual for D-Stability. The user manual contains the following sections:

- 1 Installation manual;
- 2 Tutorial;
- 3 Scientific background information;
- 4 Reliability information.

Deltares dares to share. D-Stability is free to use.

Installation manual

2 Installation manual

2.1 Downloading D-Stability

D-Stability is free to use and available through the IPLO and the Deltares website. To download D-Stability from the Deltares website, go to the [Deltares website](https://www.deltares.nl) (www.deltares.nl) and click on Software and data.

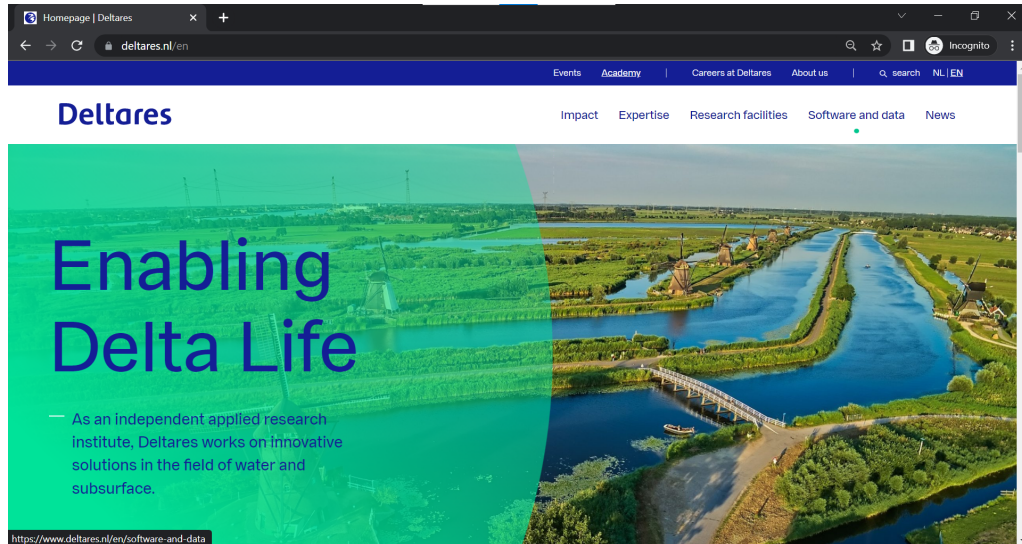


Figure 2.1 *Deltares website*

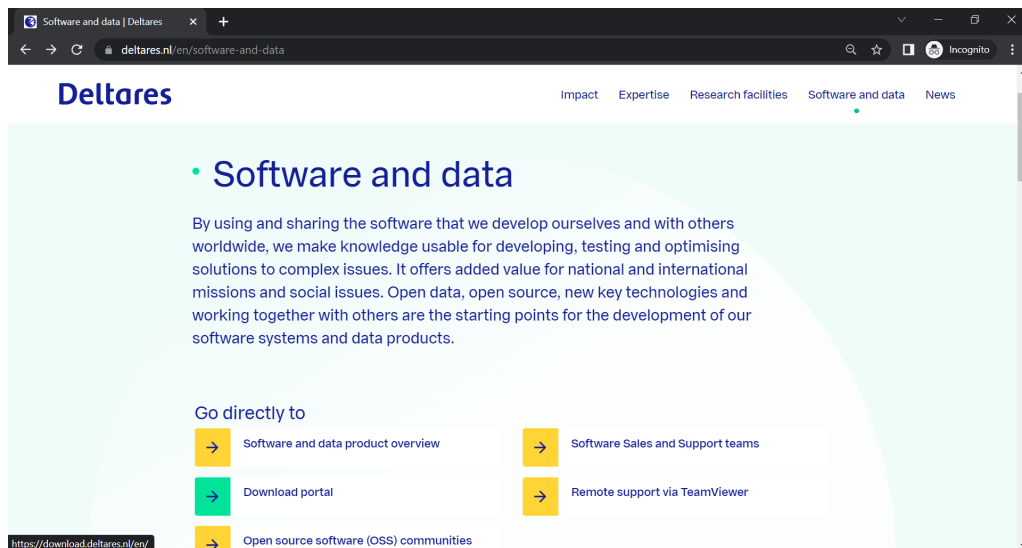


Figure 2.2 *Software*

Next, click on the Download portal, where you can find the available software downloads.

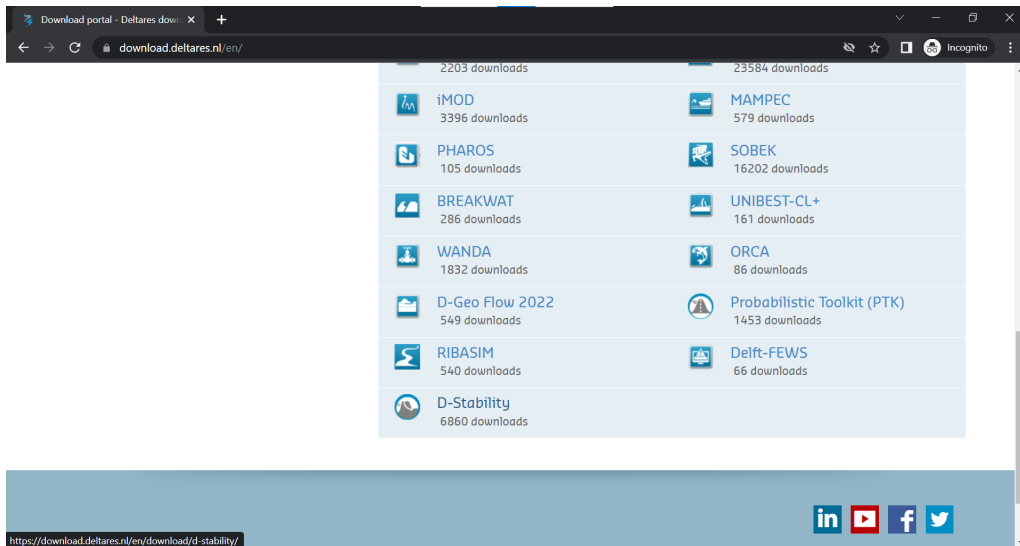


Figure 2.3 *Download portal*

On this webpage, you have access to all available software of a range of Deltares software products and solutions. Click on the D-Stability name or logo in the table to navigate to the [D-Stability download page](#).

On the download page, you can submit your name and email address. A link will be sent to your email address directly. If you don't receive the email directly, please check your spam folder. Using this link, you can download the installer of the software.

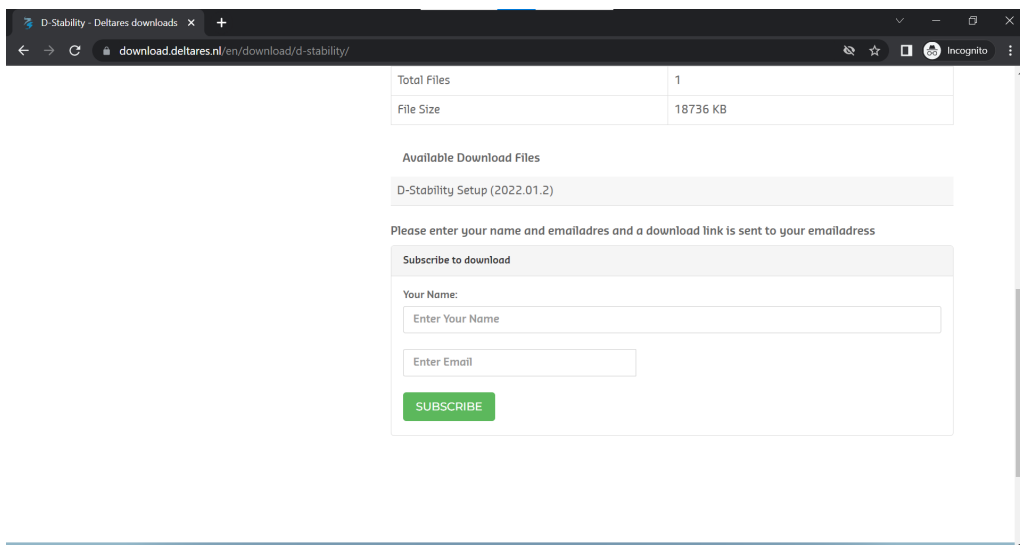


Figure 2.4 *D-Stability Download portal*

2.2 Installing D-Stability

After downloading the software, you can either choose to run the software directly from the browser or double click on the downloaded .msi file from windows explorer.

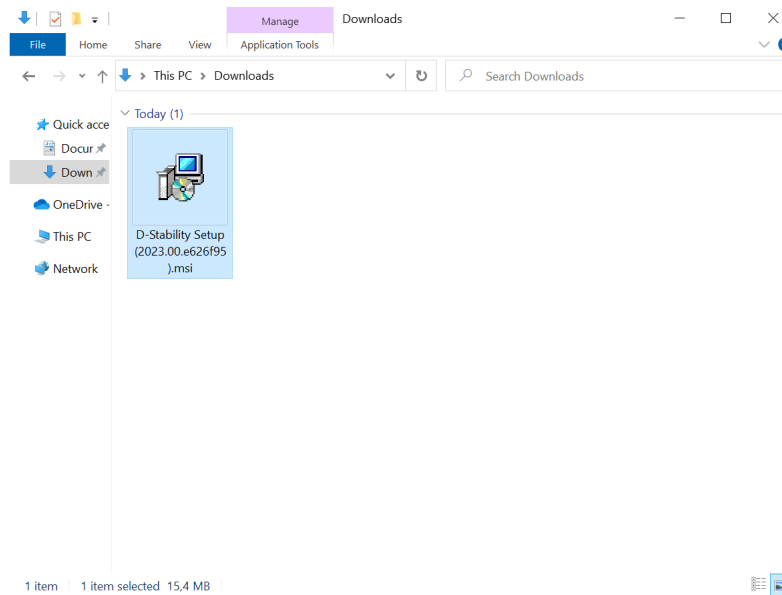


Figure 2.5 MSI

The software does not require any privileges, besides the fact that the user needs to be allowed to run a .msi file. If you don't have privileges to install software, please contact your system administrator.

Note: When you start the installation, please note that the installation is from a trusted publisher: Deltares.



The installation wizard starts and will guide you through the installation process.

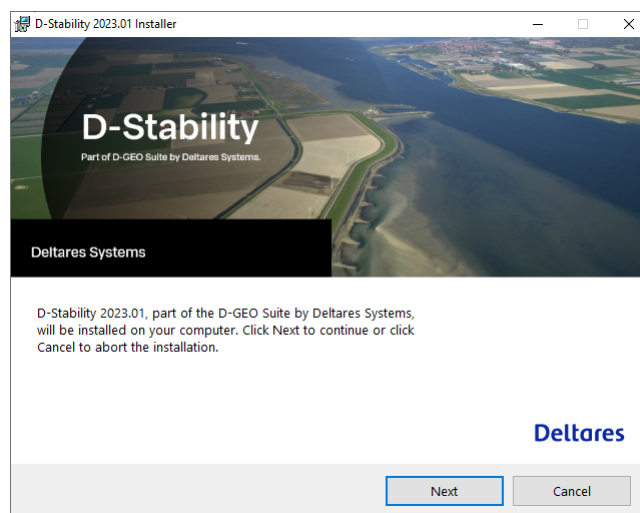


Figure 2.6 Installation wizard

If you already have installed the version of D-Stability, you can use the installer to

repair or remove the software.

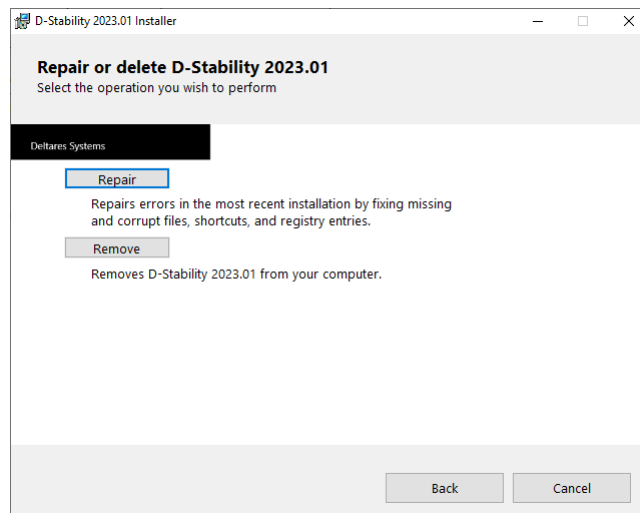


Figure 2.7 *Repair or remove*

2.3 Checking the installation

After installing D-Stability, you can start it from your start menu where it initially appears at the top, or find it using the search function in your taskbar.

To check whether the installation was successful, you can open the installed .stix file that accompanies the installation called "tutorial.stix". By doing so, the following geometry will appear.

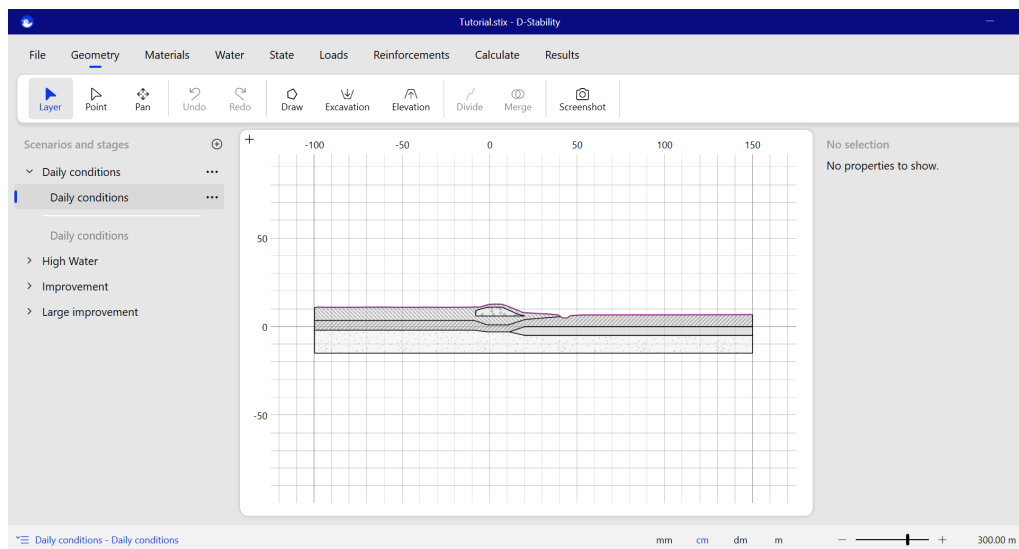


Figure 2.8 *Open tutorial*

Next, go to the second construction phase "High Water" (section tab from the left bottom) and go to "calculate" in the file menu. Then, press the "calculate" button. The software should start running, and after a while, the calculation result should appear.

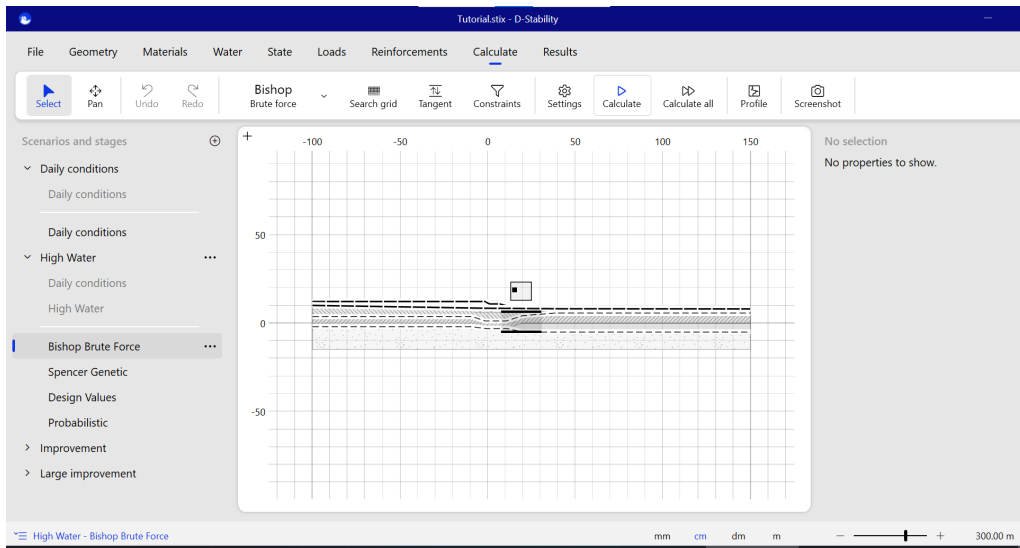


Figure 2.9 Calculate the second stage

If you see a resulting slip plane on the "results" tab, the calculation is performed successfully and you know that all software components are working.

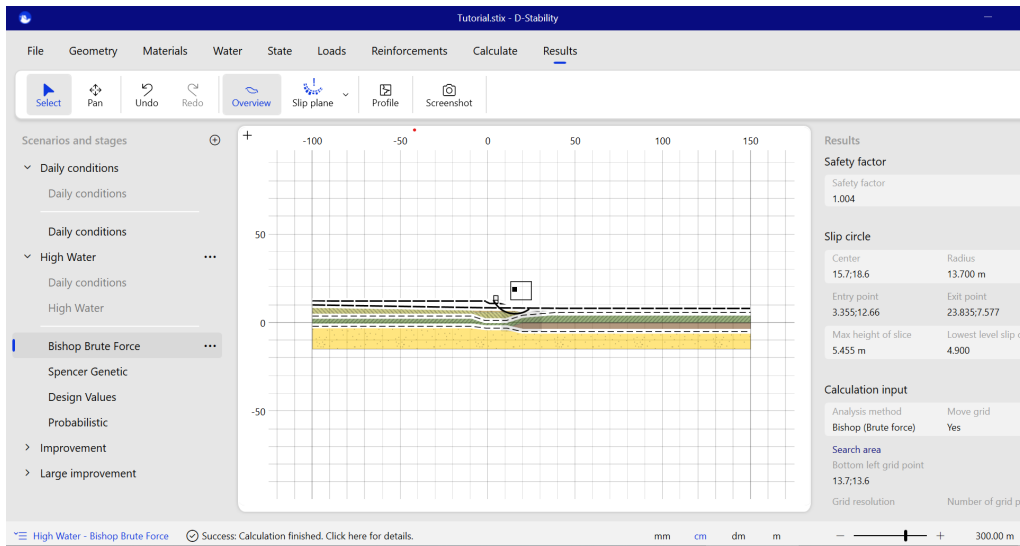


Figure 2.10 Successful run and therefore successful installation

Tutorial

3 Tutorial: probabilistic analysis

This tutorial will guide a user through most of the application by walking through the steps to determine a conditional failure probability and thereafter improving the design of the embankment. The tutorial gives an overview of D-Stability. Many detailed aspects like moving a point or defining constraints to a slip plane are not addressed. The software ought to be sufficiently intuitive to discover the use without having each field explained.

Note: This example is for instruction purposes only. It is not a guide to perform a complete calculation.



3.1 Creating a new project: Project description

A new project can be started by opening an existing file, or starting a new file. For this example, a new project is started from scratch by pressing the "new project" button.

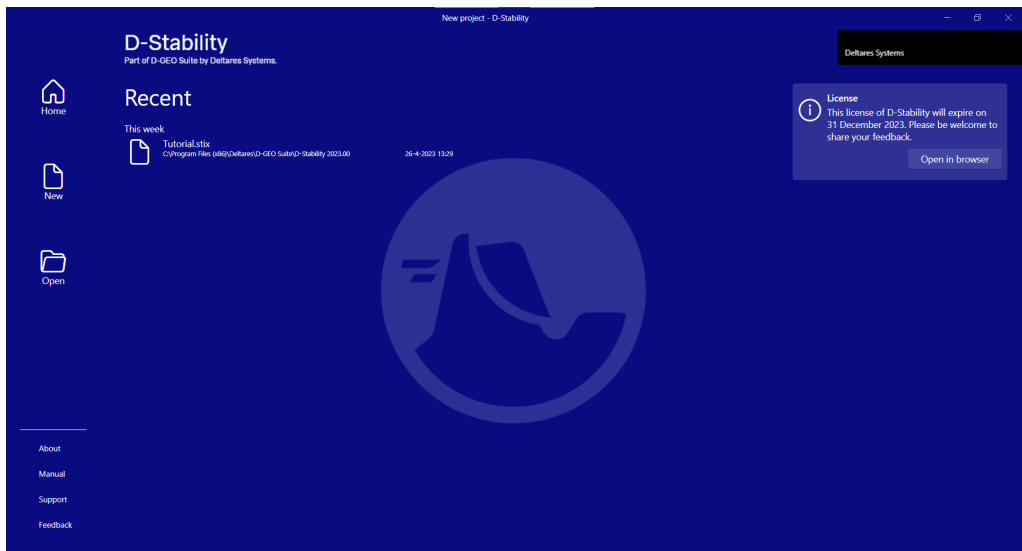


Figure 3.1 *Opening screen*

The user can enter the project information as name, owner, date to describe the current project.

Note: this information will also appear on the stamp when the canvas is later copied to the clipboard.



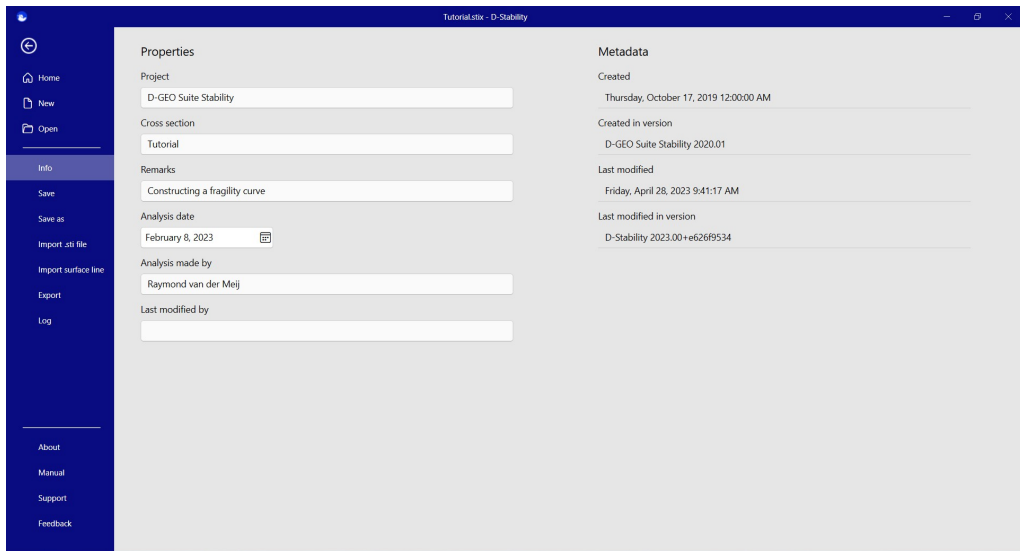


Figure 3.2 *Project information*

A logical way to build up a schematization is to work from left to right, both in the ribbon tabs and through the construction stages.

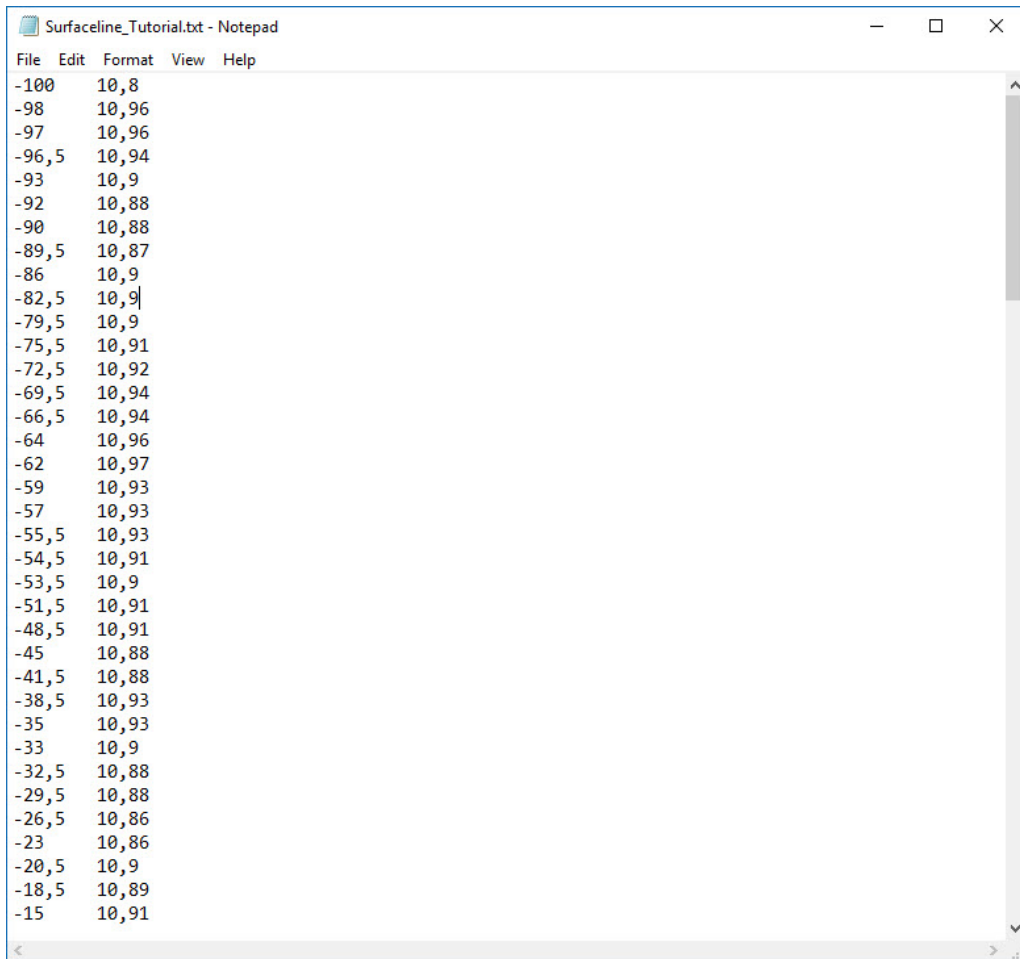
3.2 The surface line

The user can choose to import an .sti file from the old D-Geo Stability version 18.1. D-Stability formally only supports the .sti import of version 18.1. Older versions can possibly be imported as well, but it is strongly advised to save the .sti file in D-Geo Stability 18.1 before importing it into D-Stability.

For this tutorial, a surface line is imported. This line is described in a text file in ASCII format which can be edited in, for example, Notepad. The file may have any extension. It must contain two columns with horizontal and vertical coordinates according to the following specifications:

- the decimal separator must be a comma (,) or a period (.);
- the list separator must be a semicolon (;), a colon (:) or a tab character;
- the horizontal coordinates must be strictly in ascending or descending order.

The beginning of the imported surface line is shown in Notepad in the following figure.



```
Surfaceline_Tutorial.txt - Notepad
File Edit Format View Help
-100 10,8
-98 10,96
-97 10,96
-96,5 10,94
-93 10,9
-92 10,88
-90 10,88
-89,5 10,87
-86 10,9
-82,5 10,9
-79,5 10,9
-75,5 10,91
-72,5 10,92
-69,5 10,94
-66,5 10,94
-64 10,96
-62 10,97
-59 10,93
-57 10,93
-55,5 10,93
-54,5 10,91
-53,5 10,9
-51,5 10,91
-48,5 10,91
-45 10,88
-41,5 10,88
-38,5 10,93
-35 10,93
-33 10,9
-32,5 10,88
-29,5 10,88
-26,5 10,86
-23 10,86
-20,5 10,9
-18,5 10,89
-15 10,91
```

Figure 3.3 *Surface line data*

Note: Please note that a geometry with a large number of nodes may slow down the user interface as the yield administration is computationally expensive. It is therefore advised to keep the number of imported surface line nodes to a minimum. If, after importing, the software becomes sluggish, remove unnecessary nodes from the surface line.



A box is automatically drawn below the surface line after import to make a shape out of the line.

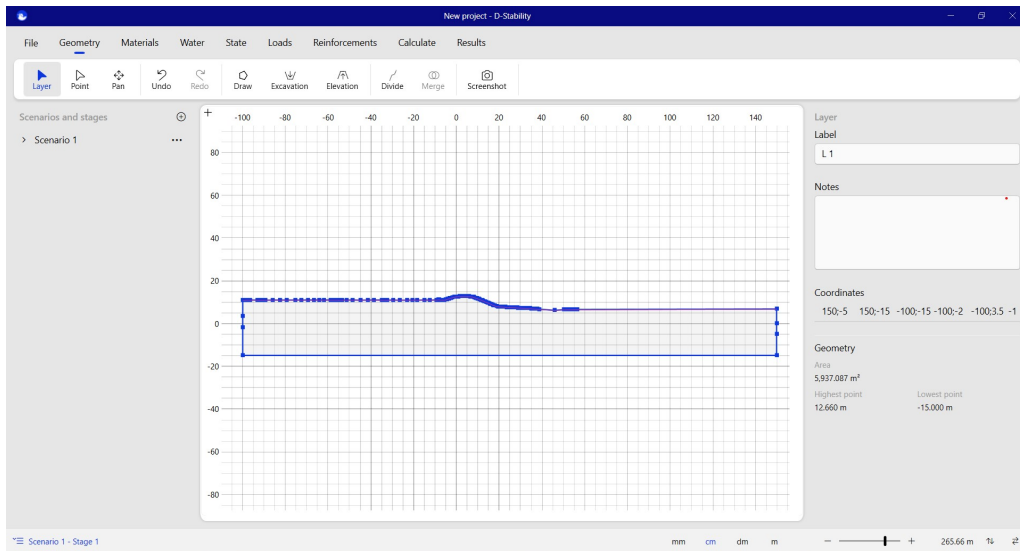


Figure 3.4 *Imported surface line*

Note: A valid surface line can always be imported on an empty canvas. In some cases, it is also possible to import a surface line on a non-empty canvas. The software will then assume it is a berm and try to place it on top of the existing geometry, instead of boxing it. If this is feasible, the imported line will appear on the canvas. If importing is not possible because, for example, the new line would intersect the current geometry or it would lay beside it, an error will appear in the log. This log is shown both at the left bottom of the GUI and under the file menu.



D-Stability has no pre-defined boundaries under which an analysis can be made. A slip circle analysis can only be made underneath the surface line. The surface line must adhere to certain specifications. D-Stability communicates to the user which part of the geometry is considered to be the surface line, by drawing it in purple. The following figure shows a valid surface line on top.

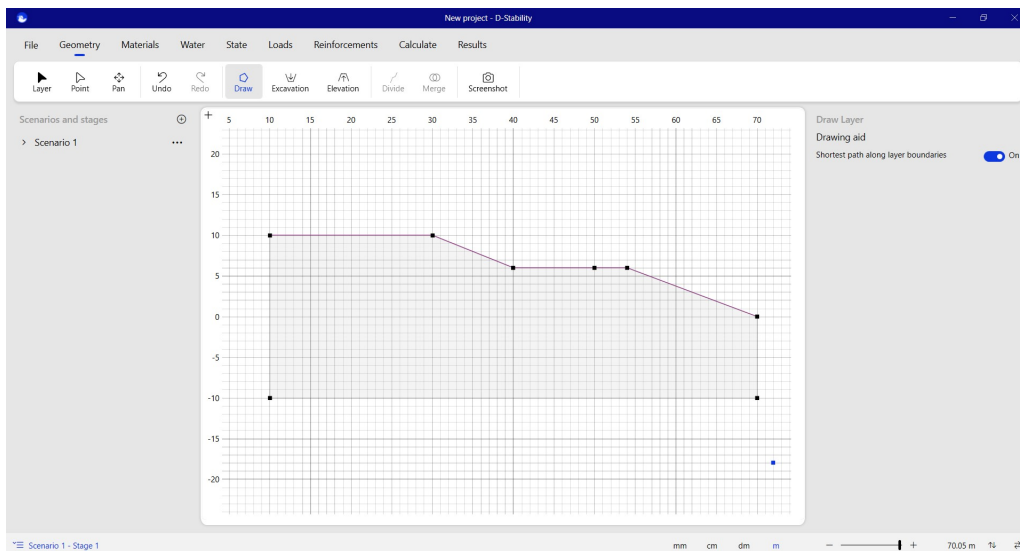


Figure 3.5 *Surface line fully valid*

If the uppermost line goes back at any point (e.g. point a in the figure below) the following situation will appear.

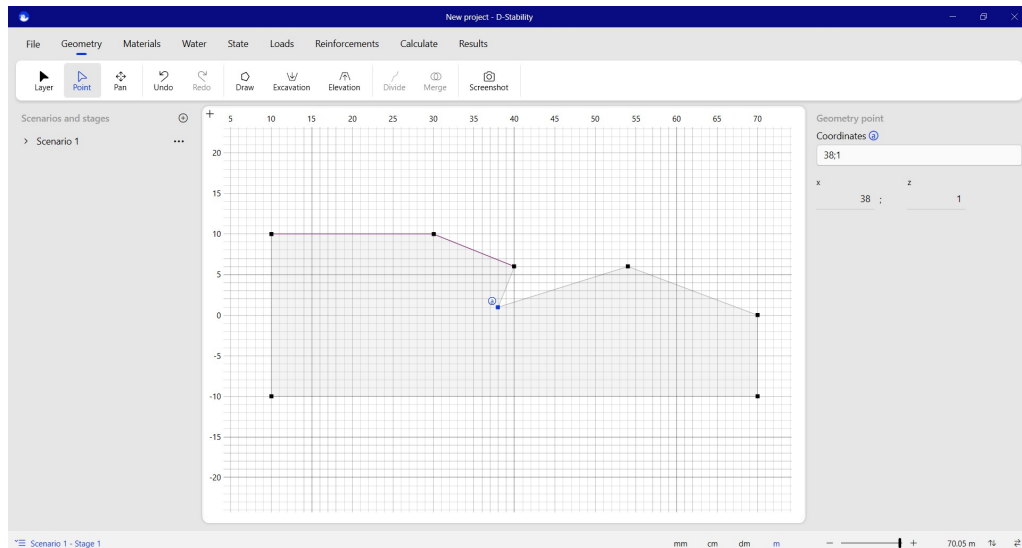


Figure 3.6 Only the left half of the surface line is valid

In this case, the surface line is only valid up to that third point of the surface line. The purple coloring stops after this point. No slip circle analysis can be made to the right of this point, unless the surface line is corrected.

3.3 Setting up the geometry

After importing the surface line, the user can make the subsoil schematization by using the "Divide" or the "Draw" options. "Divide" splits an existing layer into two separate layers, so both the start and the end point need to lay on the edge of the layer. This function is activated once a layer is selected. "Draw" creates a new independent shape which can interfere with some existing layers, but does not have to. Be aware that drawing a shape through an existing layer replaces the lines of that layer (and thus may split the layer). This functionality is always enabled, unless berms or excavations are active.

Several layers can be merged into one if they are adjacent to one another. The "Merge" button becomes active when contiguous layers are selected, which will be merged after clicking the button. Multiple selection can be accomplished either by holding down the "Ctrl" button while clicking on different layers, or by using rectangular select by dragging the mouse while pressing the primary button.

Note: a layer containing an inner layer cannot be divided by a line.



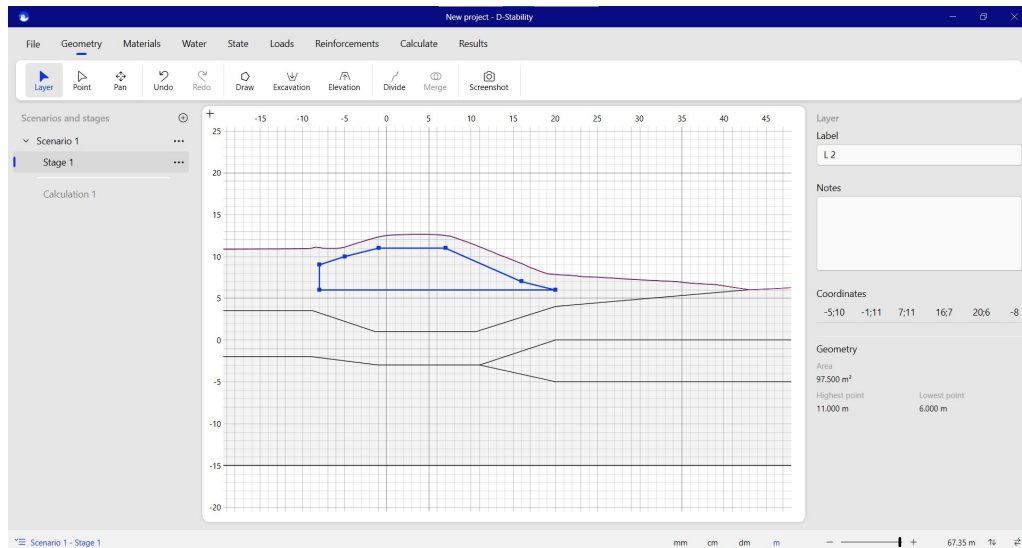


Figure 3.7 *Constructed subsoil schematization using divide and draw*

3.4 Berms and excavations

It is possible to draw berms or excavations with the "Draw" option. To further facilitate construction stages, though, berms and excavations can be drawn explicitly. The corresponding shapes must start and end on the surface line.

As drawing a free shape can affect the surface line, it is no longer possible to draw freely using "Draw" if one chooses to draw a berm or excavation. For the same reason, berms and excavations cannot be on the same location. An advantage of using an excavation is that the underlying geometry is kept. Moving the excavation will not affect existing points in the current geometry.

When a new stage is created, berms and excavations are made permanent in that stage.

3.5 Zooming

The user has different options to scale the geometry via zoom control:

- Simultaneously zooming x and z by scrolling the mouse wheel on the canvas;
- Zooming either x or z by scrolling the mouse wheel on, respectively, the x or y axis;
- Zooming x and z by clicking the "+" or "-" at the bottom right of the screen;
- Having the same scale for x and z by double clicking the "+" at the top left corner.

The value on the right of the zoom control shows the width of the canvas. The two double arrows buttons on the right of that value allow the user to zoom in the z or x direction, respectively.

The "mm", "cm", "dm" and "m" buttons near the zoom control dictate the clicking accuracy on the canvas. When choosing, for example "dm", all mouse clicks will be

rounded up to the nearest decimetre. Note that a deviation can be caused if snapping to a nearby line occurs.

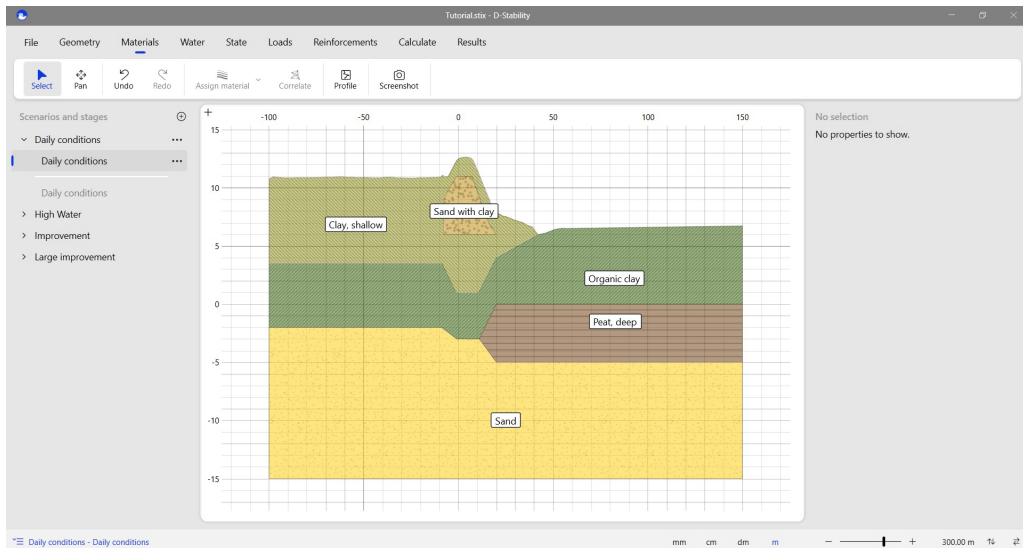


Figure 3.8 *Scaling the geometry to fit the canvas by clicking the vertical (z direction) and the horizontal (x direction) double arrows at the right bottom of the program interface*

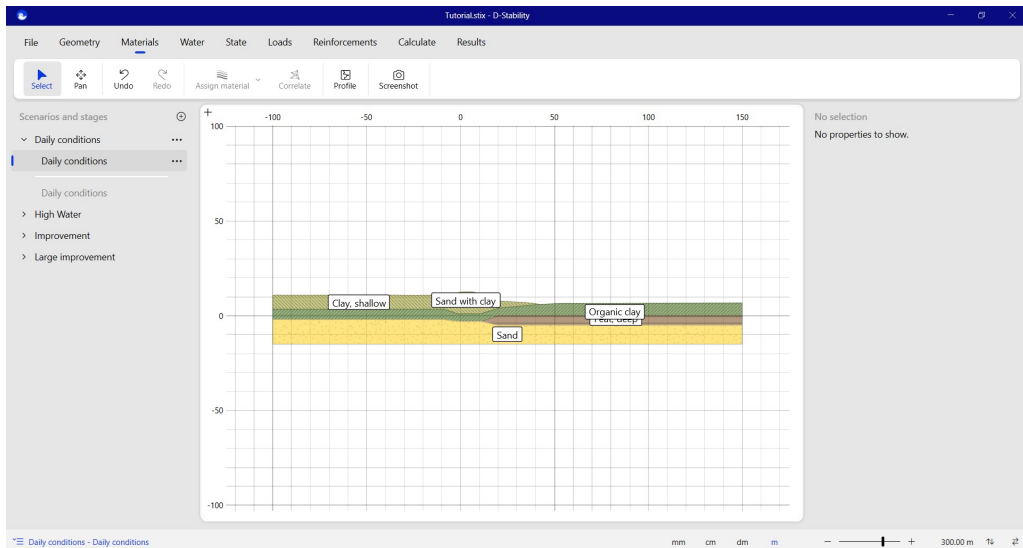


Figure 3.9 *Same scale for x and z by double-clicking on the "+" where the axes intersect, on the top left corner of the canvas*

3.6 The drawing aid

While drawing a shape along the surface line, one may have to click many points in order to draw two adjacent layers. The drawing aid is a tool that, when switched on, draws a poly line along the shortest route of existing points. Additionally, it can be used to draw an excavation as shown in the following two figures.

The drawing aid toggle is visible while drawing.

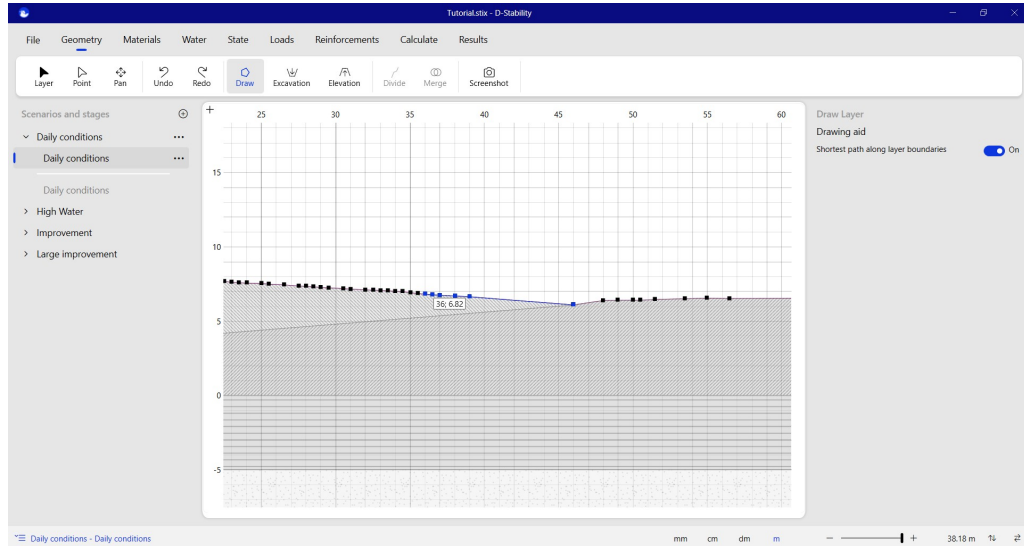


Figure 3.10 Drawing aid toggle activated while drawing

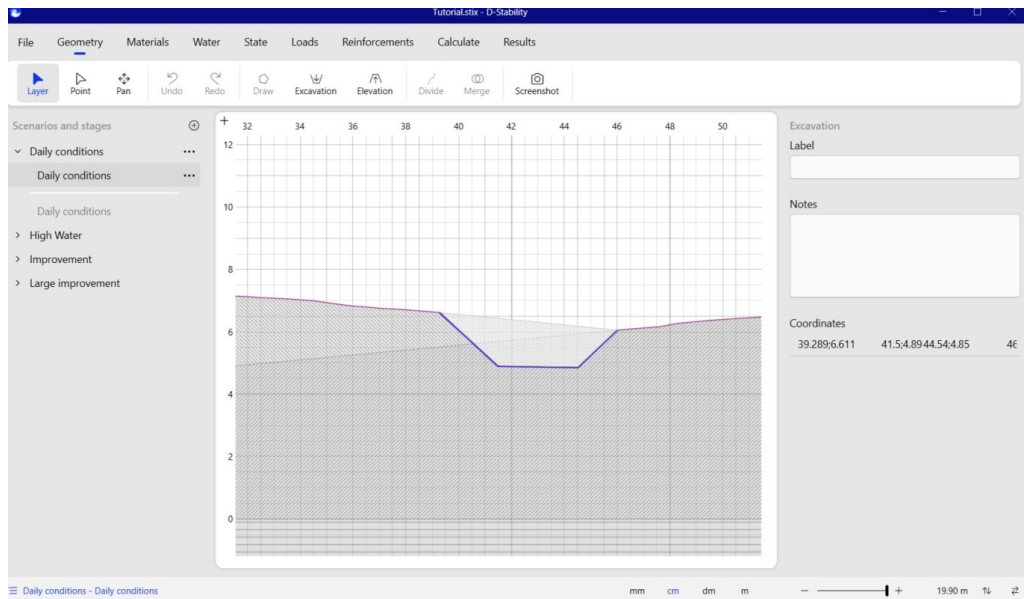


Figure 3.11 Drawing an excavation

Note: If a poly line trough existing points is not wanted, for example to take a shortcut through the material, the drawing aid must be switched off. It can be deactivated and activated at any time while drawing.



3.7 Assigning material

After the schematization is complete, the user can continue to the "Material" tab of the ribbon to assign material properties. By selecting a layer, the button "Assign material" becomes active. For each layer in the profile, a material can be selected from the drop-down list. One material can be applied to multiple layers.

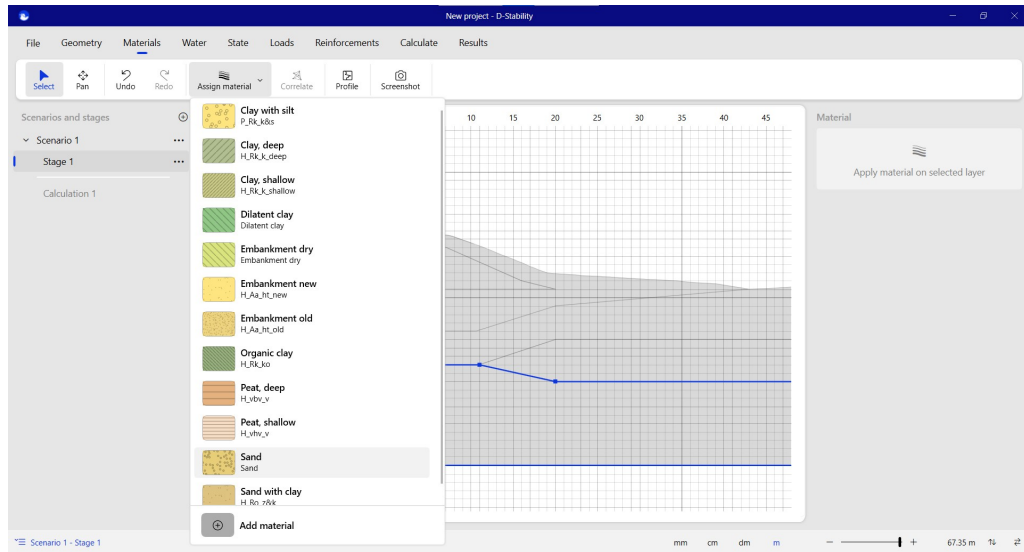


Figure 3.12 Assignment of a material to a layer

Once layers contain materials, the "Profile" option, when turned on, will plot the stresses as a function of depth.

Note: The profile inspector will only produce a chart if all layers have materials properties assigned. If the profile inspector does not work, previous stages without assigned materials could be the cause.

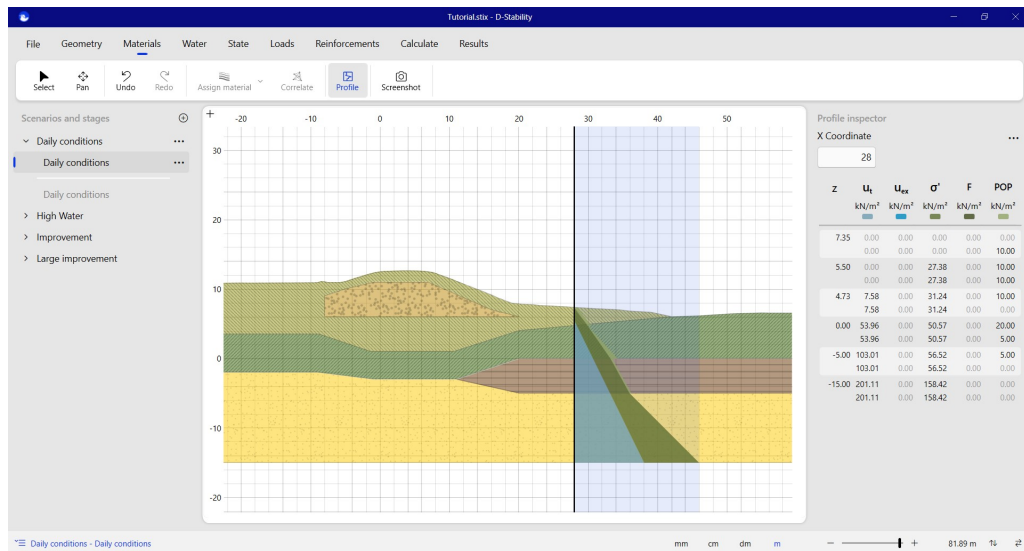


Figure 3.13 Use of the profile inspector

3.8 Defining the water pressures

Water pressures can be defined in the "Water" tab.

Water pressures are defined by head lines and reference lines. A head line represents a value or set of values of water pressure. The reference line represents the location in the geometry where this pressure is acting.

Between the reference lines, the software uses linear interpolation in z direction. Water pressures over depth can be viewed with the profile inspector. Angles in these water pressures charts can only take place at the location of a reference line.

The firstly drawn headline is considered to be phreatic. The water will act as open water and exert pressure perpendicular to the surface. Another line can be assigned to be phreatic by the user by selecting the headline and pressing the button "Mark as phreatic line" on the ribbon. In the figure below, the first headline and therefore the phreatic line is drawn.

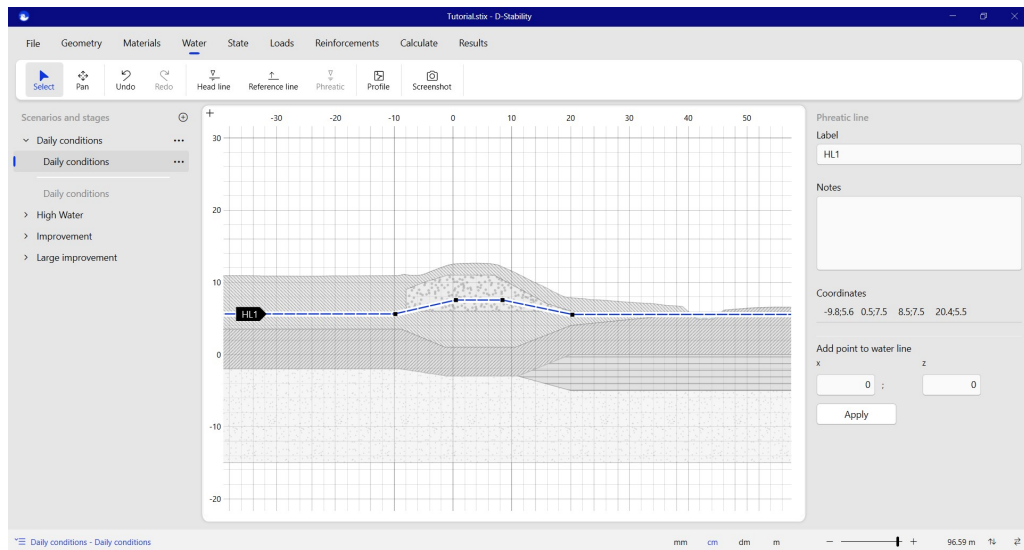



Figure 3.14 Completed head line

Note: The drawing aid is by default turned on while drawing a reference line as these lines usually lie on layer boundaries. 

Turning on the profile inspector shows the newly defined water pressures in the geometry, along with the total and effective stresses.

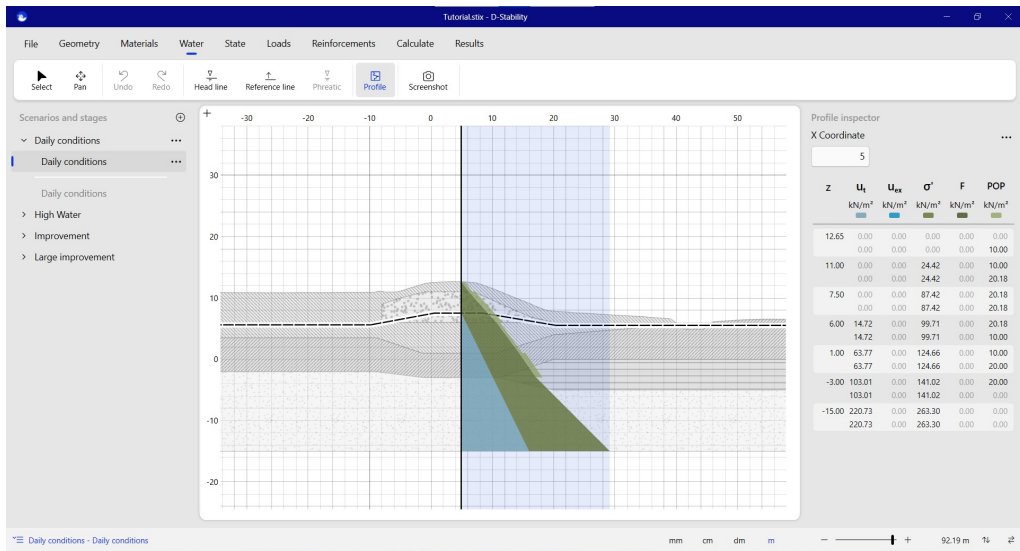


Figure 3.15 Inspecting water pressures with profile inspector

3.9 Defining the state

The state parameters like the yield stress, OCR or POP can be defined in the "State" tab.

State administration is kept for the SHANSEP method. This strength representation needs to know the yield stress at each point in the geometry. Later on in this manual, building stages are presented to further aid this administration. This section shows how to define the state in the current stage.

Two methods are available to define the state: inside a layer and along a state line. This section first explains the method inside a layer and thereafter on a state line.

When defining the state in a layer, the user first needs to select the layer.

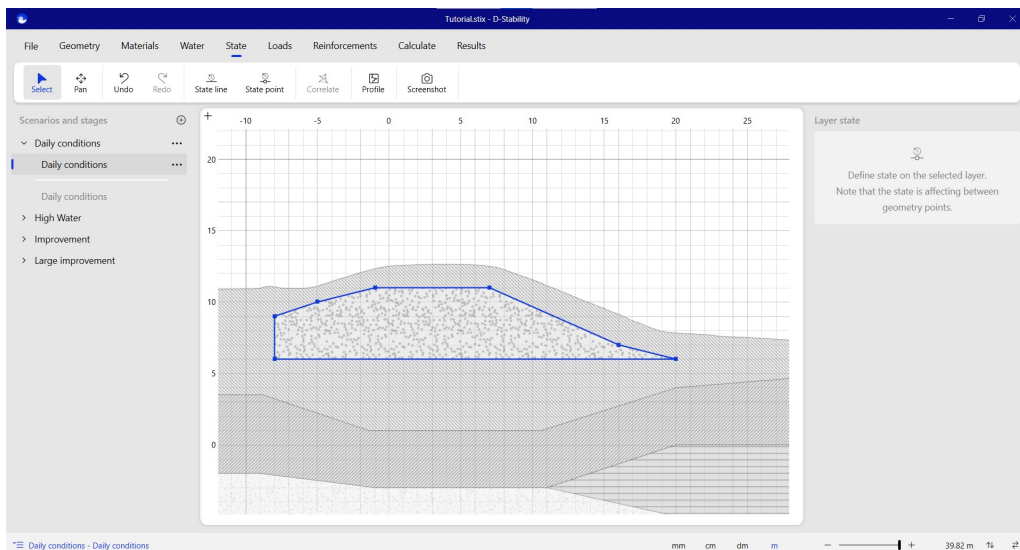


Figure 3.16 Defining state point in layer

Next, a state point can be placed anywhere within the layer.

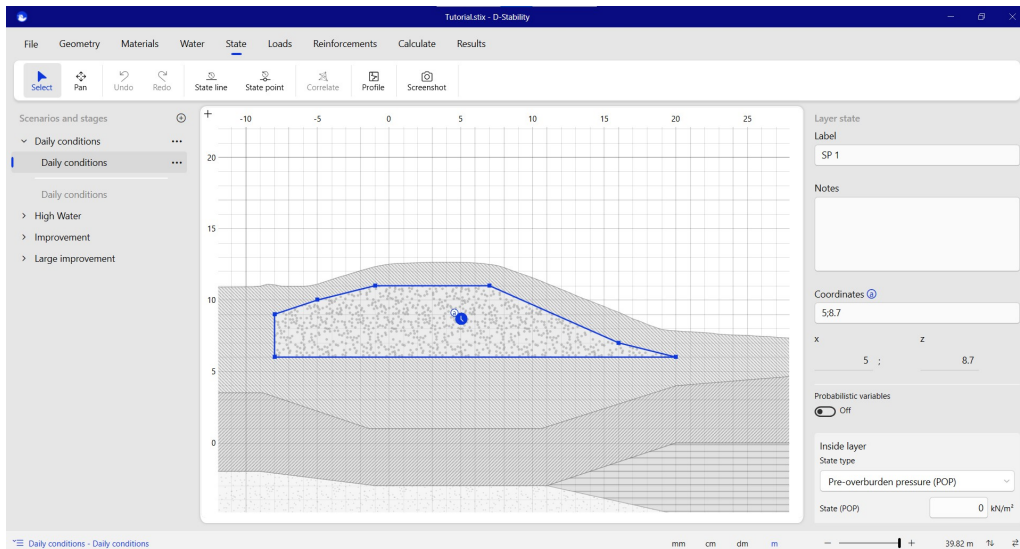


Figure 3.17 State pinned in layer

After placing the point, the user has three options:

- Enter the POP at that point. The POP will be constant in that layer.
- Entering a Yield stress at that point. That stress will be translated to a POP-value at that point. This derived POP value will be constant in that entire layer.
- Entering an OCR at that point. The OCR will be translated to a POP. This constant POP will be assigned to the whole layer.

A state point will always lead to a constant POP in a layer. This POP can later on be overridden due to higher yield stresses in previous stages. The sequential order of the stages (from left to right) is important, and will be elaborated in section 3.8.

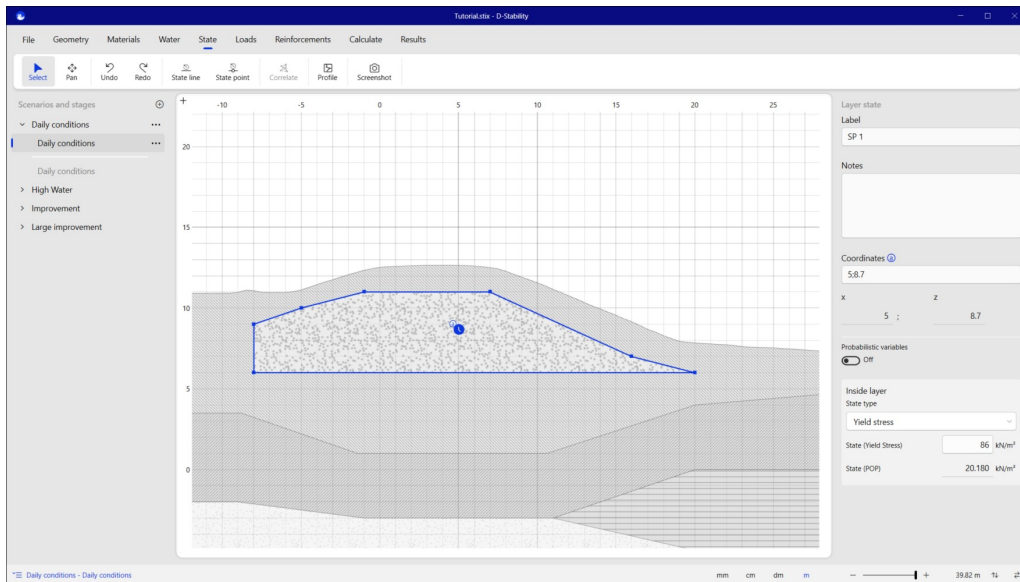


Figure 3.18 State point parameters

Alternatively, the state can be defined along a reference line, a so-called "state line". State lines can be defined along a layer boundary with the help of the drawing aid.

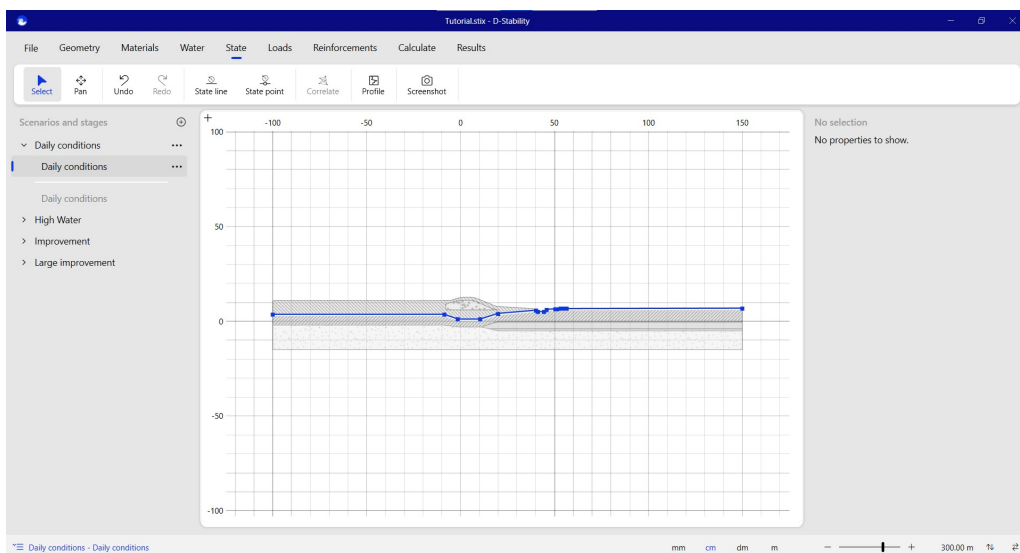


Figure 3.19 State line drawn along the boundary of a layer

After drawing a state line, it can be selected and a state point can be placed on top of the state line.

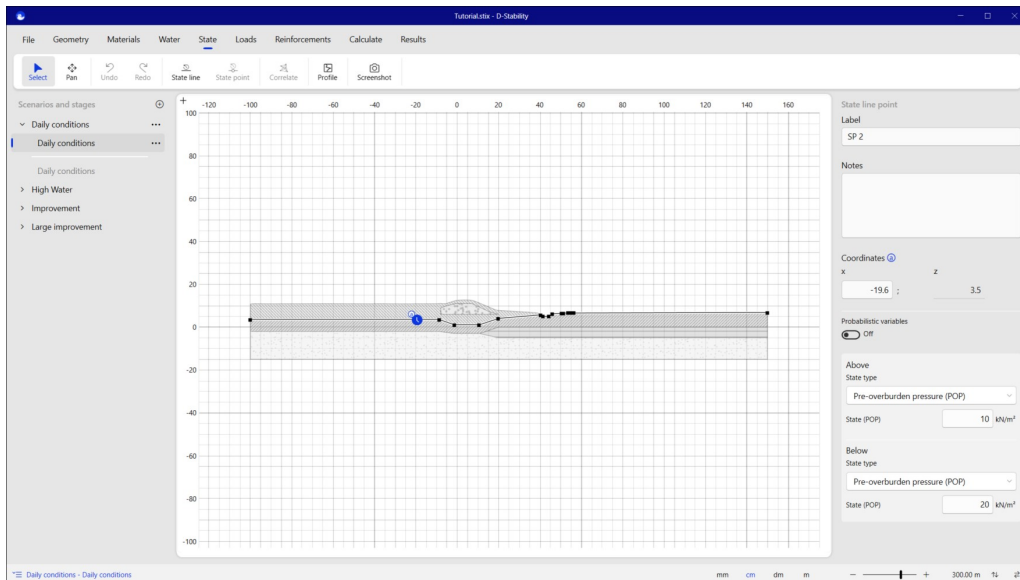


Figure 3.20 State point placed on a state line

When multiple points are placed upon a state line, the software uses linear interpolation to determine the state between them on the line. Further these points along the line, the state value is kept constant. No extrapolation will be used.

When using multiple state lines, the state is first interpolated along the line. Subsequently, linear interpolation is used in the z direction between the state lines. Again, no extrapolation is used above the top or below the bottom line; the value is kept constant.

Note: When defining the state inside a layer, the inner value is assigned while zero is assigned outside the layer so the state does not "radiate" into other layers. When combining state in layers with state on lines, the user needs to make sure the software does not accidentally interpolate to zero outside a layer. **Always use the stress inspector thoroughly while defining the state.** It is a good option to define state in layers and on lines over two different construction stages.



More information about the interpolation of the state can be found in the scientific background information in section 7.2.3.

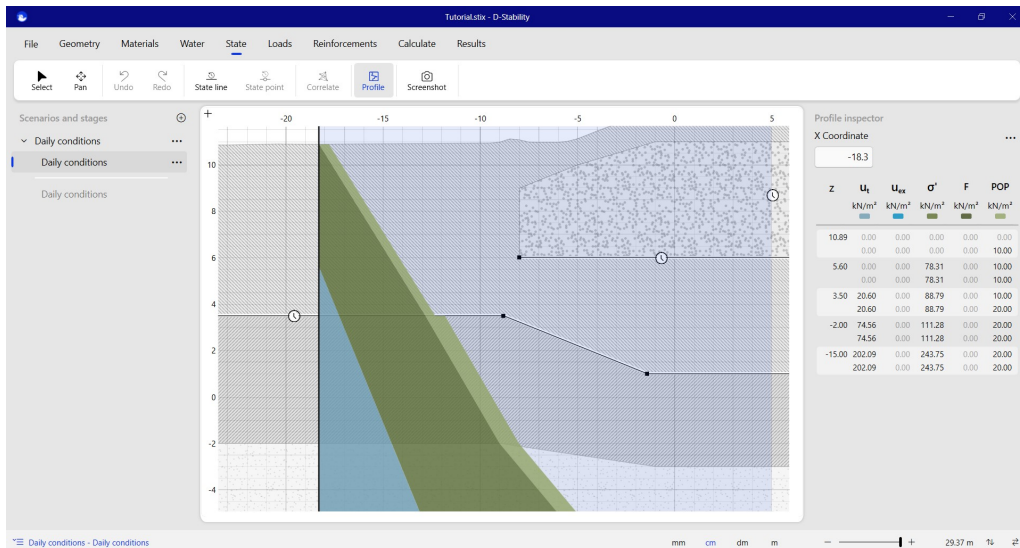


Figure 3.21 State inspector

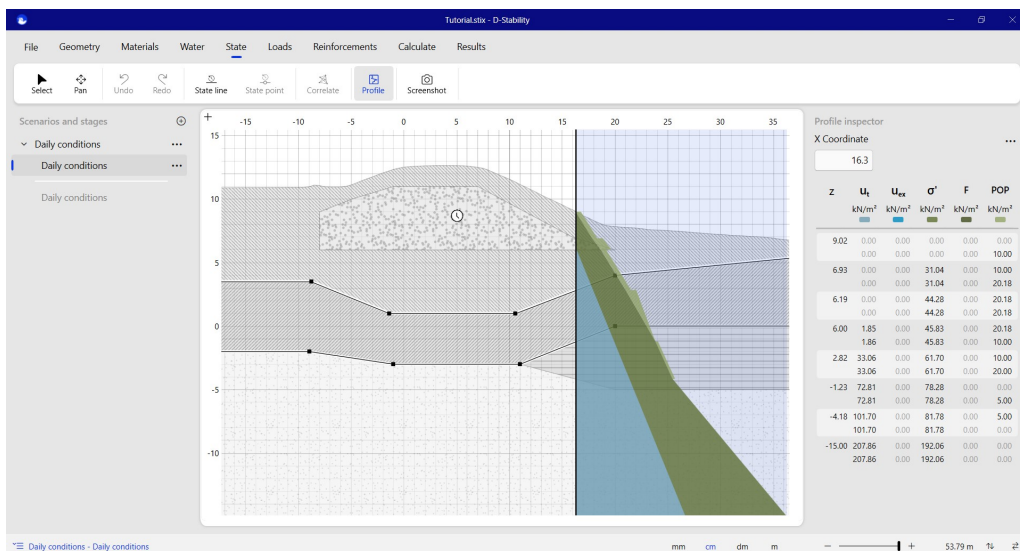


Figure 3.22 State inspector II

3.10 Construction stages

The construction stages are defined on the left of the canvas. These stages represent sequential moments in time. The first stage is the one at the top, which is followed by the one on beneath it.

The order of the stages is important for the yield stress administration. All stages above the current stage (the history) are taken into account to determine the yield stress in that stage. Stages beneath the current stage (the future) do not have any effect for the SHANSEP yield stress administration.

It is possible to calculate the safety for every construction stage.

Note: Stages can be dragged and dropped to change the order and, therefore, their mutual influence (history).



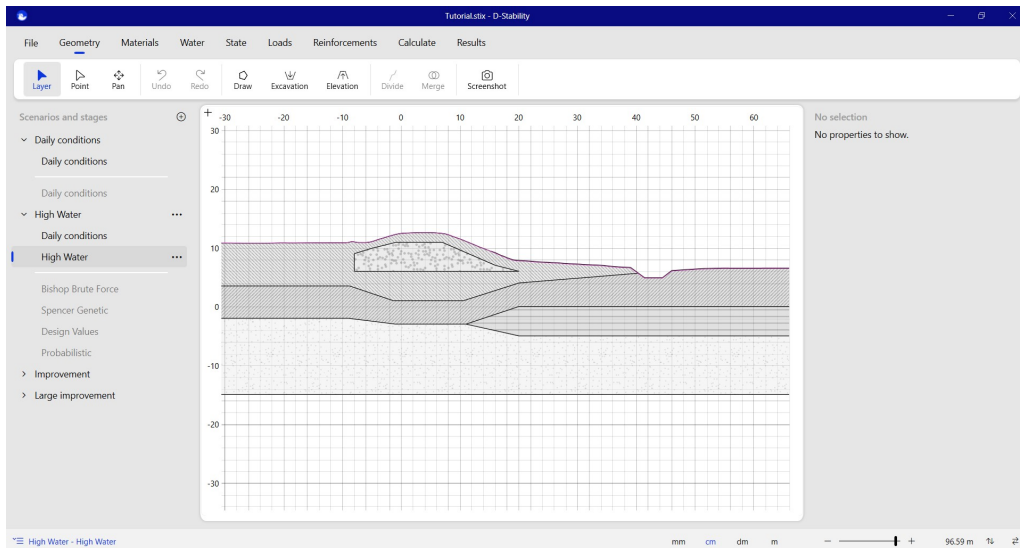


Figure 3.23 Construction stages

When defining a new stage, the geometry is copied from the currently selected one. Berms and excavations, however, are made permanent. Factors that might affect the state, like water pressures or loads, are not copied to the new stage and need to be redefined or imported.

In the next figure, high water pressures are defined in the second construction stage.

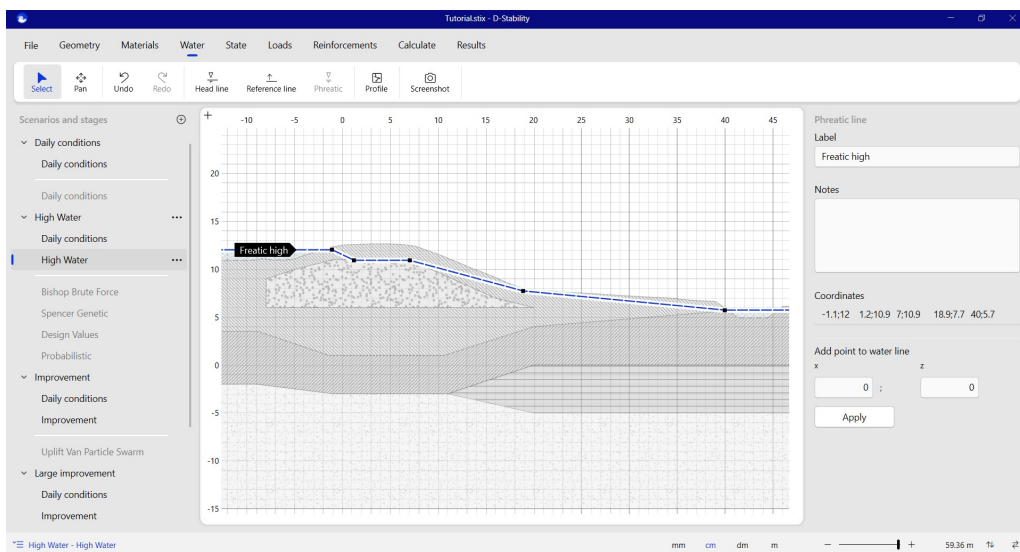


Figure 3.24 Defining water in high water stage

High water pressures are also defined in the bottom aquifer layer.

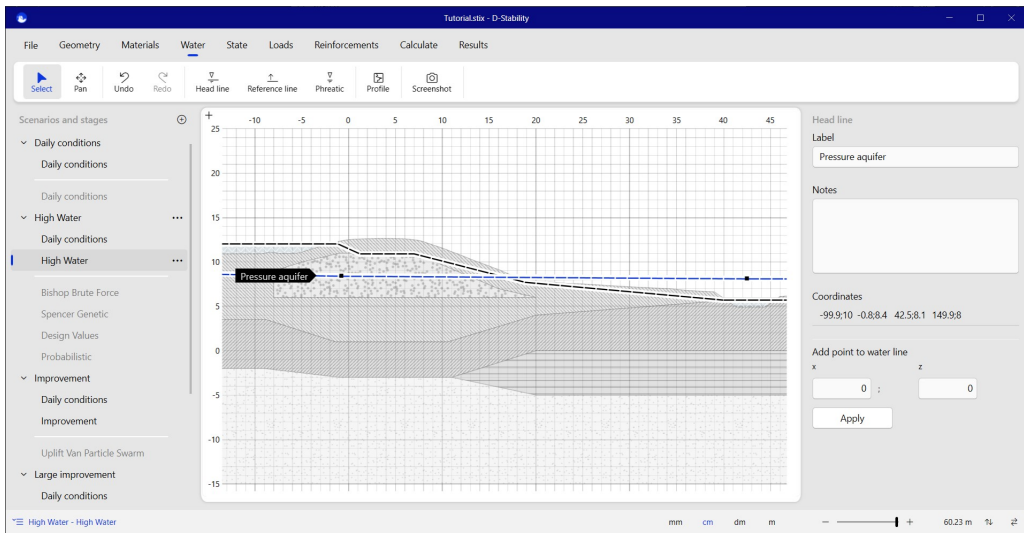


Figure 3.25 High water pressure in aquifer

The high water pressure is assigned to the top of the aquifer layer.

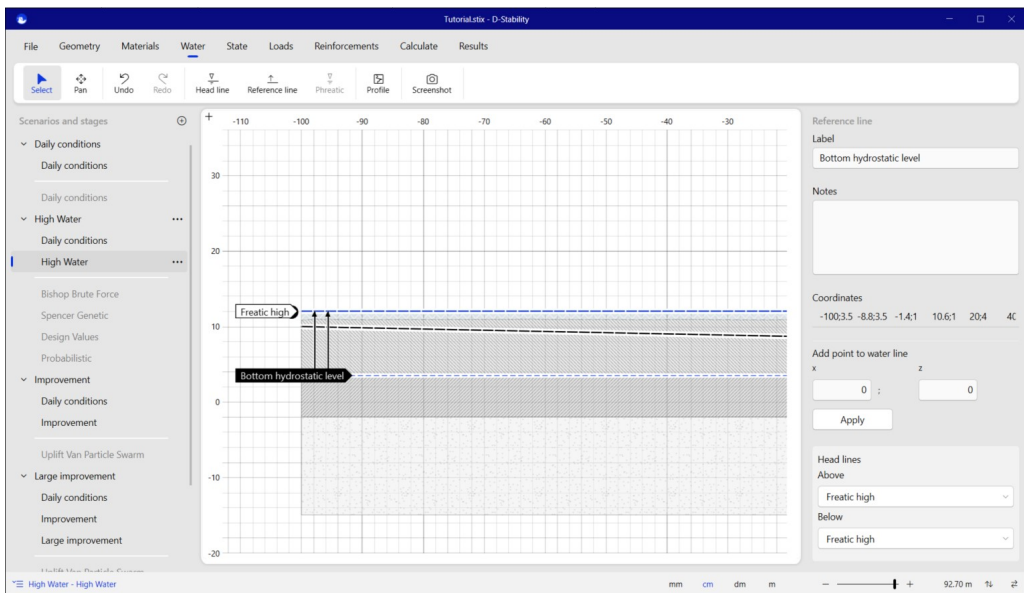


Figure 3.26 Assigning hydrostatic pressures to reference line

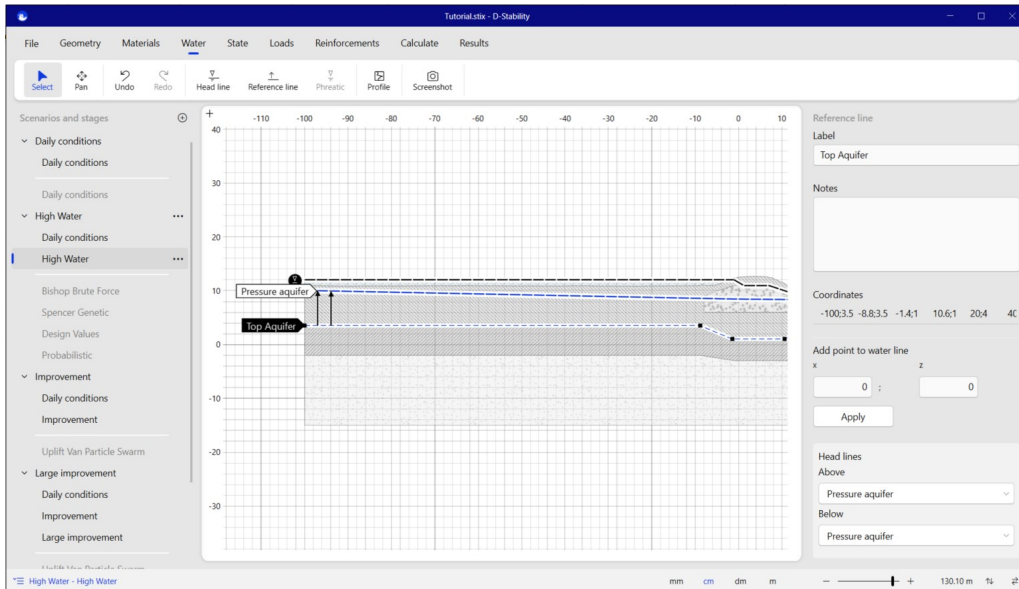


Figure 3.27 Assigning high water pressures to aquifer

The influence of assigning the water pressures on the stresses can be seen if the profile inspector is turned on. The line at which the inspector is applied can be dragged over the geometry. Alternatively, a specific location for the profile inspector can also be given at the properties of the profile inspector.

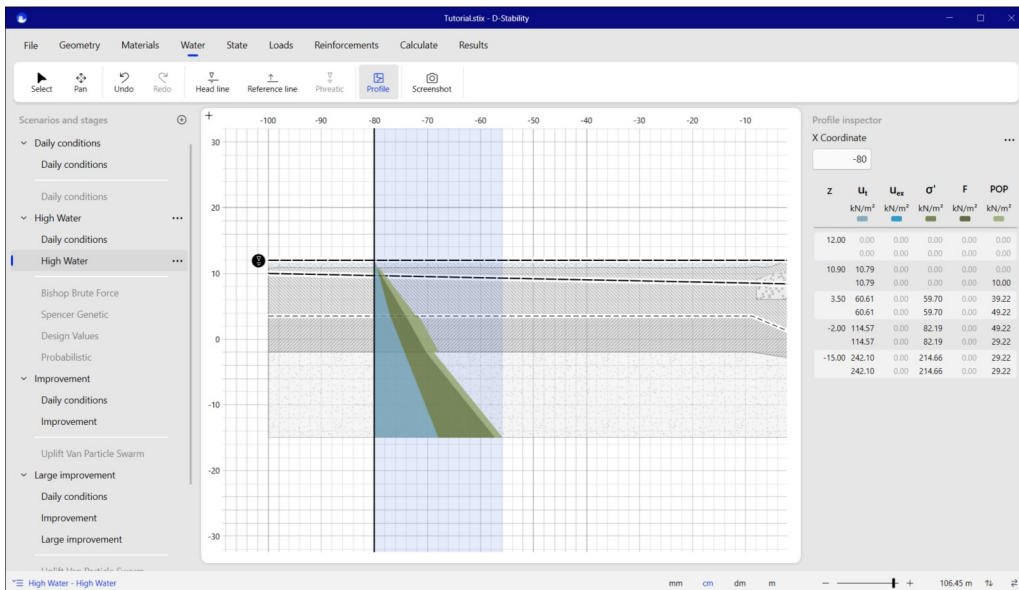


Figure 3.28 Inspecting the high water pressures and resulting POP

3.11 Loads

In the "loads" tab, the user can define a uniform, line-, tree- or earthquake-load. More information on these loads can be found in chapter 5 of the scientific background document.

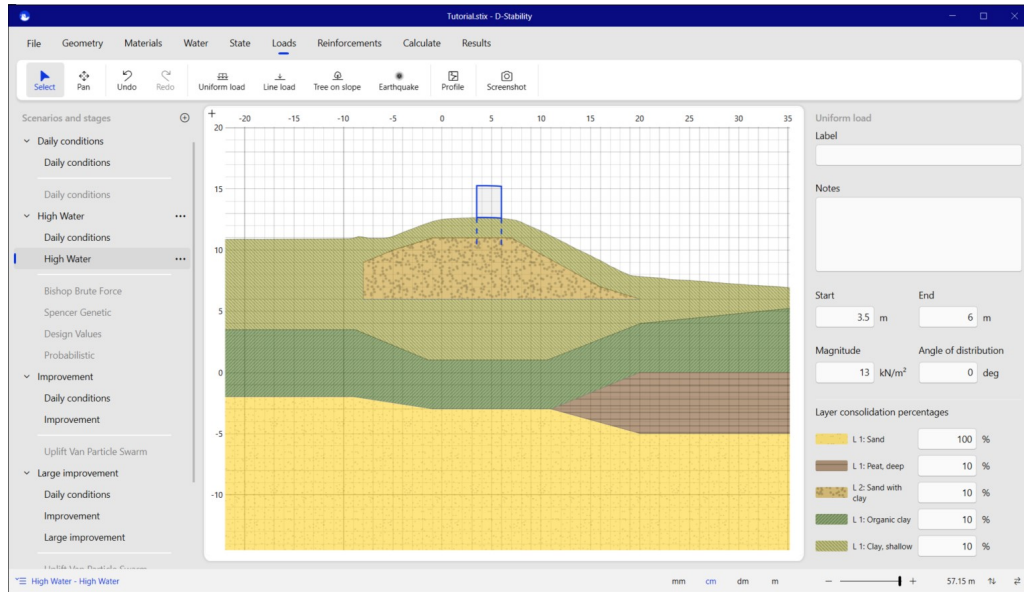


Figure 3.29 Definition of a uniform load

Consolidation percentages of the load upon the underlying layers can be entered on the right of the canvas. Load stresses and excess pore pressures due to the load can be inspected using profile inspector.

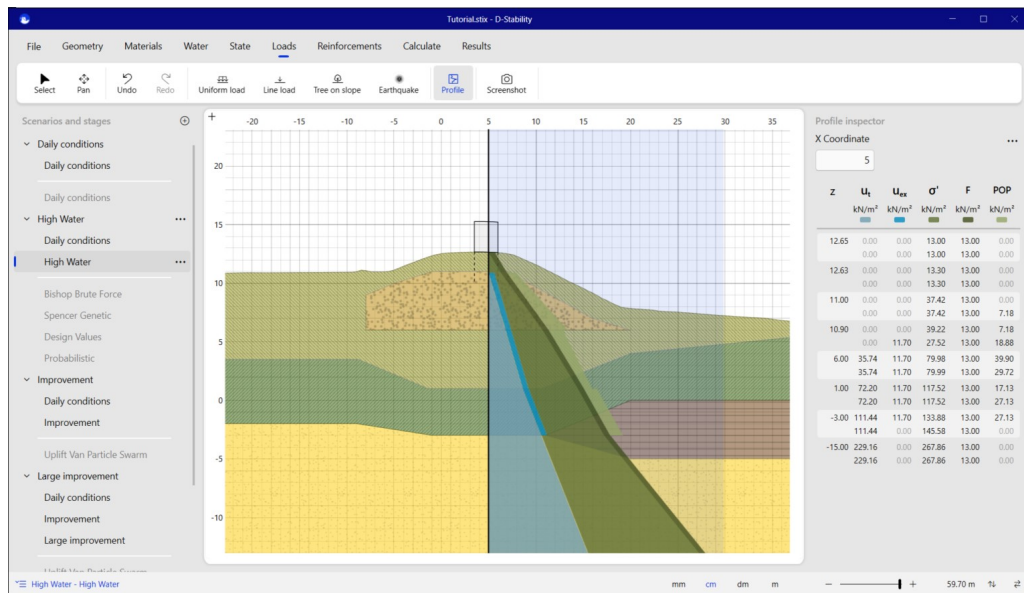


Figure 3.30 Inspecting the effect of a uniform load

3.12 Running the calculation

D-Stability has three Limit Equilibrium Methods implemented: Bishop, Uplift-Van and Spencer. Chapter 9 describes the implementation of these methods. They can be used with an optimization routine or as a single calculation. In each stage, you can switch the calculation method. For this tutorial, first, in the "calculate" tab, Bishop Brute Force is selected.

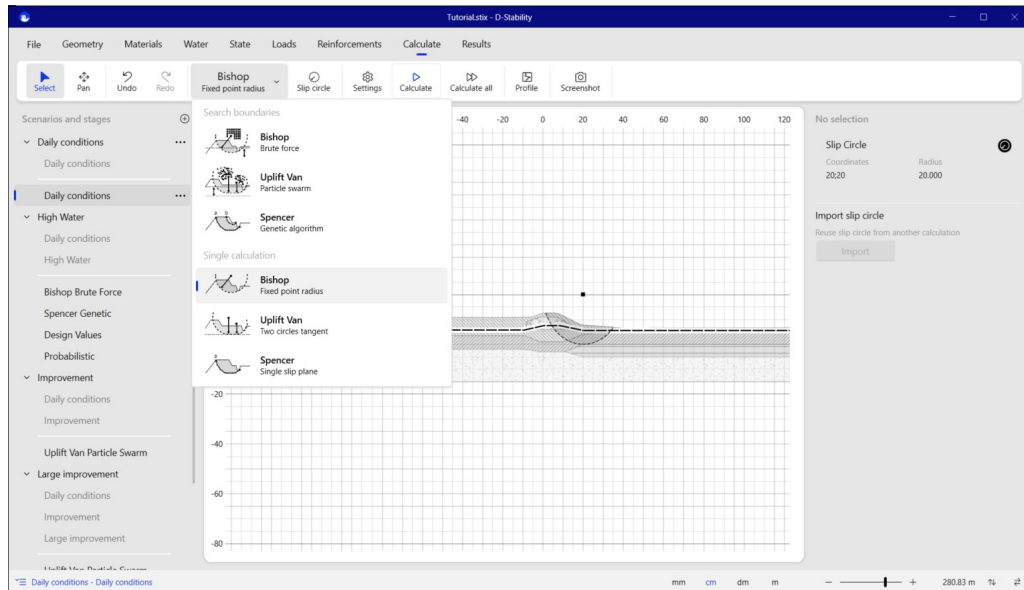


Figure 3.31 Selecting calculation method

The centre points and tangent lines of the slip circle need to be defined next. The "move grid" option is standard turned on, in case the optimum lies on the edge of the search space.

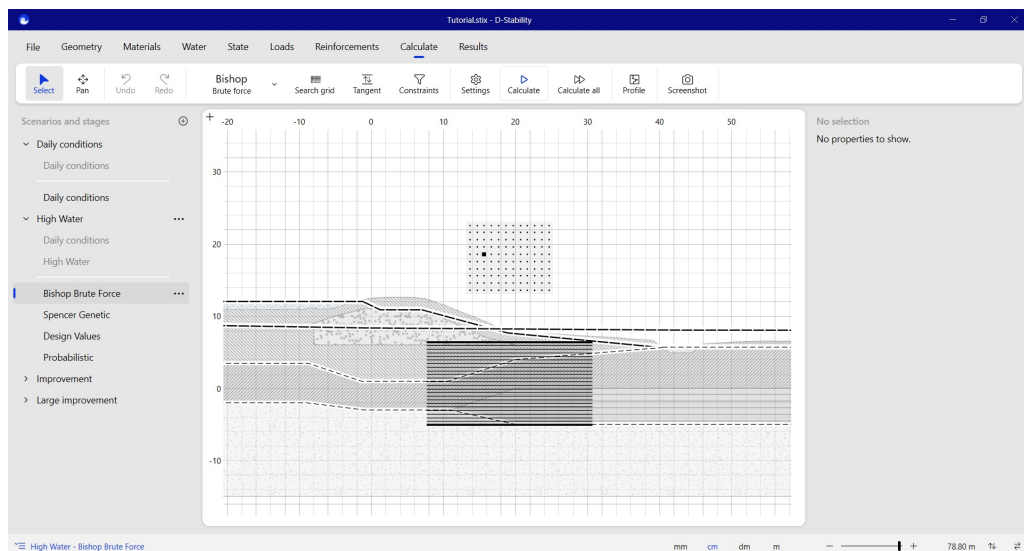


Figure 3.32 Defining search area

Note: The automated search algorithms only follow computational routines. Searching for the lowest safety factor must be the result of an intelligent interaction



between user and the software. Never rely on the first search of the software. Moving the initial location of the search grid or swarm scope may result in (very) different answers. It is the responsibility of the user to find the representative slip circle. The implemented search algorithms are only an aid.

Pressing the "Calculate" button on the ribbon causes the analysis to run. Once the calculation has finished, the program automatically jumps to the "Results" tab.

3.13 Results

The calculation overview shows the normative slip circle. Information about the safety factor and the slip plane can be found on the right side.

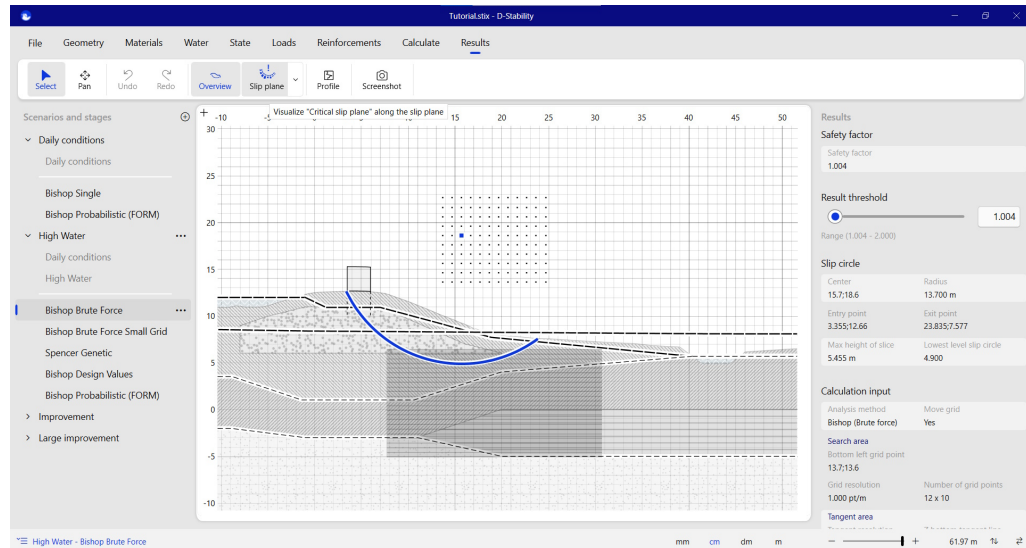


Figure 3.33 Resulting slip plane

More details about the slip plane, forces and slices can be found using the "Slip plane inspector" button. The upper half of this button is used to turn the view on and off, the lower half of the button enables selecting which parameter is plotted on the bottom of the circle.

3.14 Safety overview

D-Stability shows by default the representative slip plane. This is the slip plane with the lowest safety factor. The slider in the inspector allows to plot all slip planes from the minimal safety factor to the minimal safety factor plus one. It also plots the center points of the slip circles. This way, the user can assess the risk of bigger slip planes and see whether there are multiple minima. It can also give an indication about possible minima outside the chosen search scope.

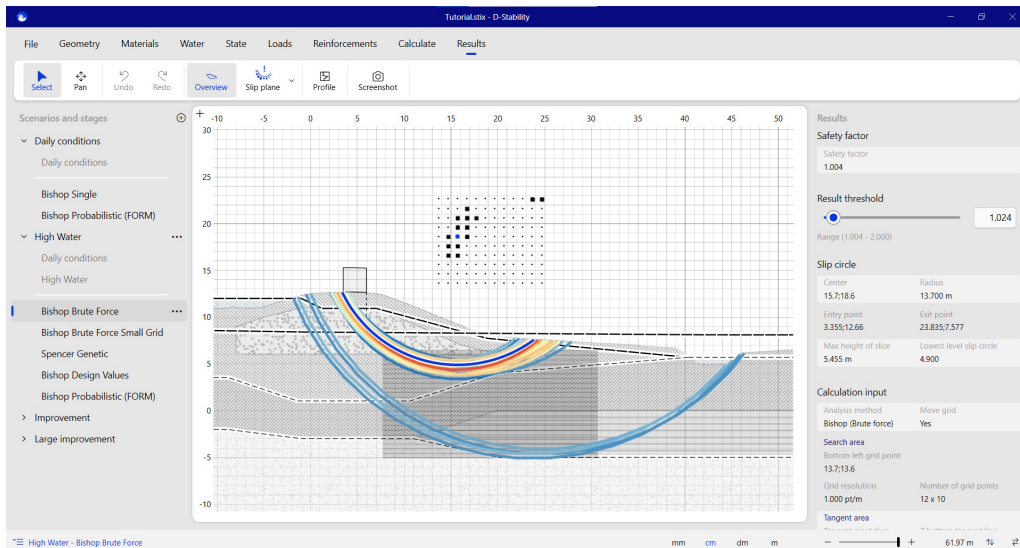


Figure 3.34 Safety overview for $F_s < 1,024$

Note that the "move grid" option is only relevant for the minimal safety factor. The safety plot shows no information regarding slip planes outside the defined search area, unless it was found on the move towards the minimal safety factor. Local minima are not found outside the grid.

The safety overview is enabled for Bishop, Uplift-Van and Spencer.

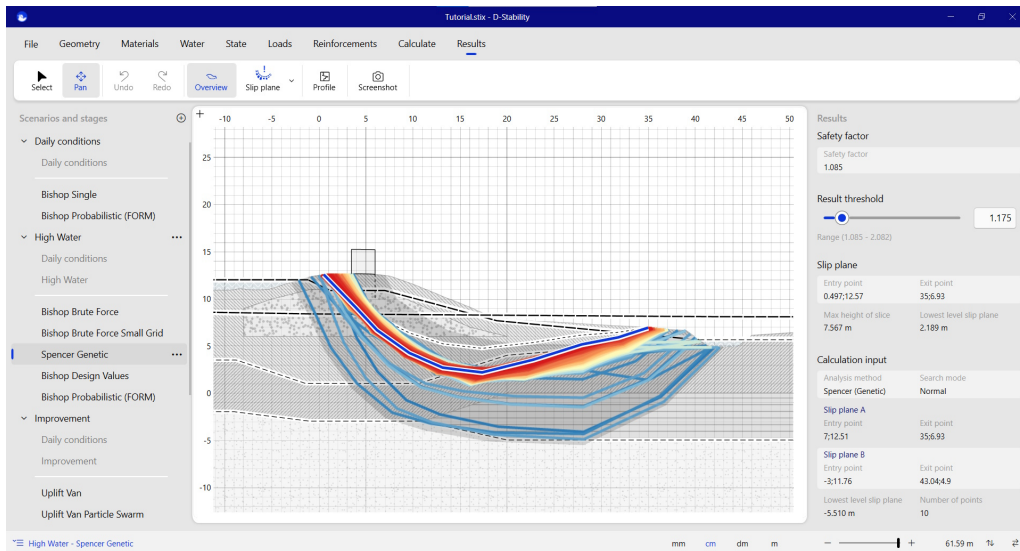


Figure 3.35 Safety overview with Spencer for $F_s < 1,175$

Regarding the Uplift Van Bee Swarm and the Spencer Genetic Algorithm, the user needs to be aware that these search algorithms optimize towards the global minimum. Fewer analyses are made around local minima. While showing slip planes farther away from the minimum, precision becomes less. The safety overview gives an indication of the influence zone of slip planes with a higher safety factor, but for these methods, the precision can be less than around the optimized minimum.

3.15 Using stages for further analysis

For the remainder of this tutorial, new building stages are defined for probabilistic analysis and reinforcement. A new building stage is defined for a Spencer analysis.

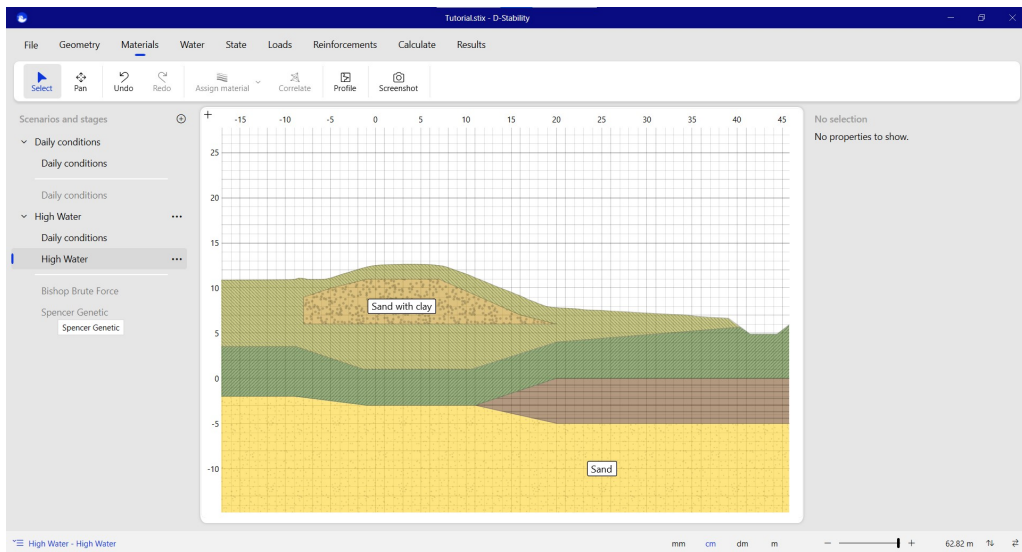


Figure 3.36 New building stage for other Limit Equilibrium Method

As stated before, no water pressures are directly copied from a previous stage as they might change in time. However, in the water tab, users can easily import water pressures from another building phase.

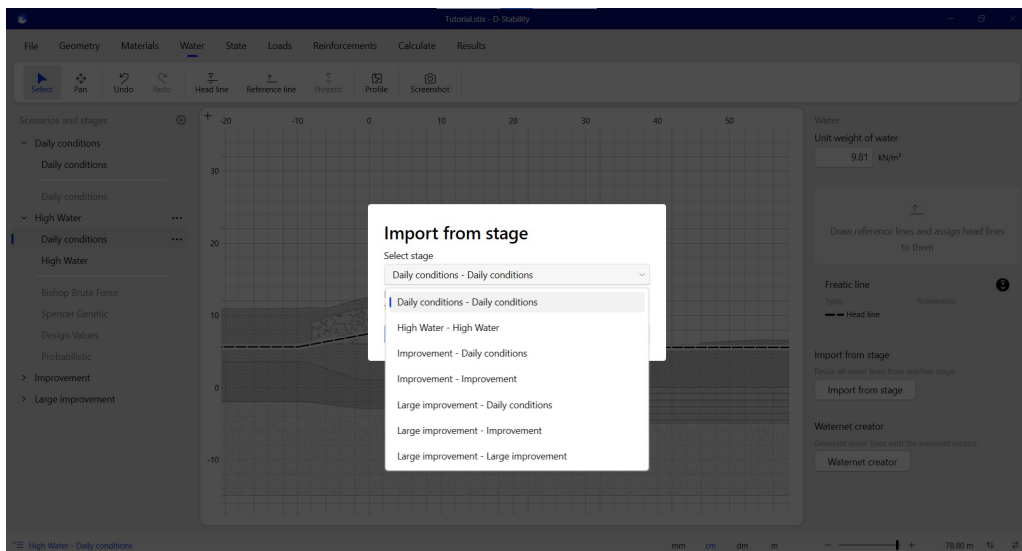


Figure 3.37 Import water pressures from another stage

There is then freedom to select any other Limit Equilibrium Method in this building stage.

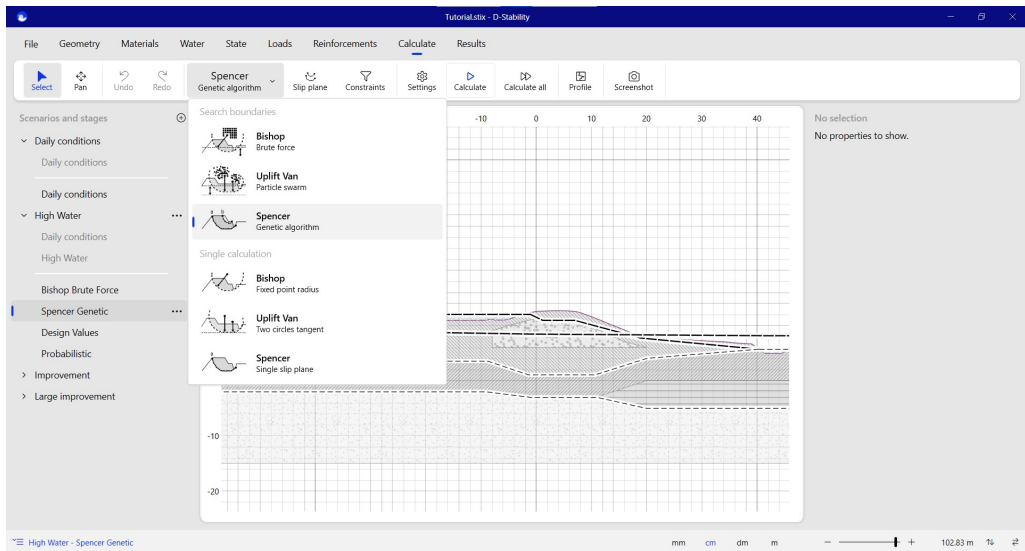


Figure 3.38 Choose another LEM

The Spencer search area can be defined as indicated in the figure below.

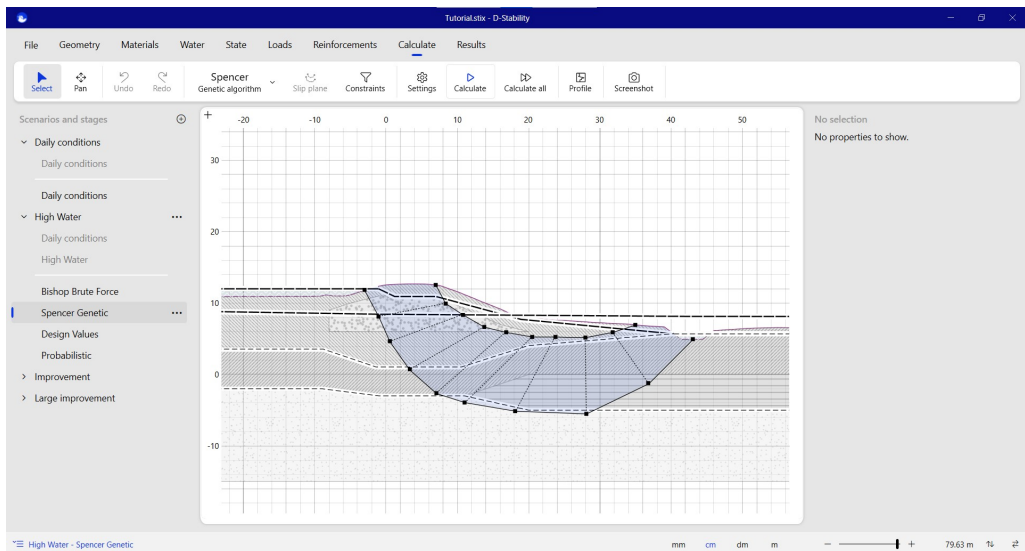


Figure 3.39 Define Spencer search area

Pressing the calculate button results in the following result. Note that the slip plane is constrained by the right side of the upper boundary.

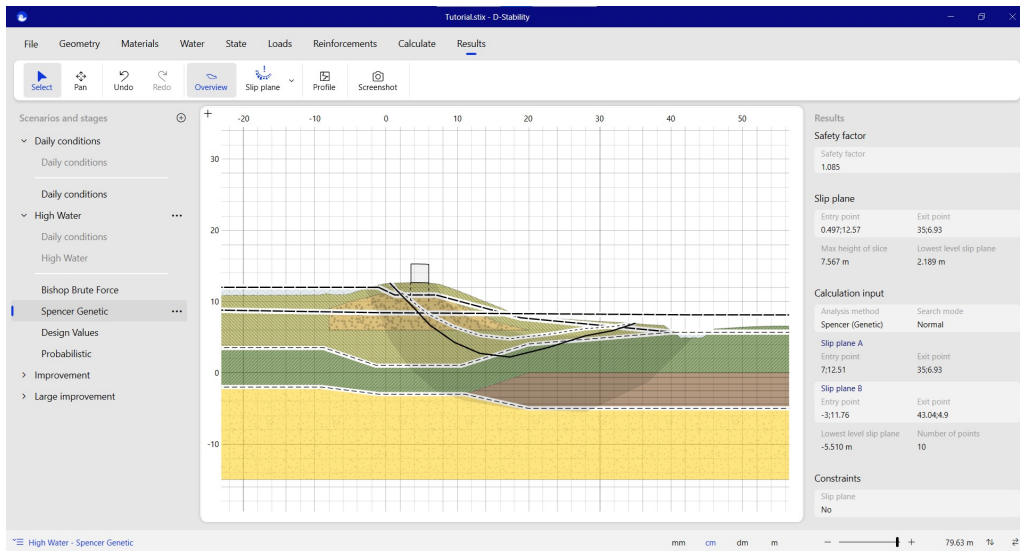


Figure 3.40 *Spencer result*

Pay attention to the dotted line in the Spencer slip plane. This is the thrust-line and one of the results of the calculation. An unrealistic slip plane causes an unrealistic thrust line and should therefore be discarded.

The yellow shading in the geometry represents the area in between the search boundaries. If the slip plane hits a boundary, it is advised to increase the search area. If the search area is too large, on the other hand, this can result in a lack of precision.

Inspecting the mobilized shear strength on the slip plane gives the following figure.

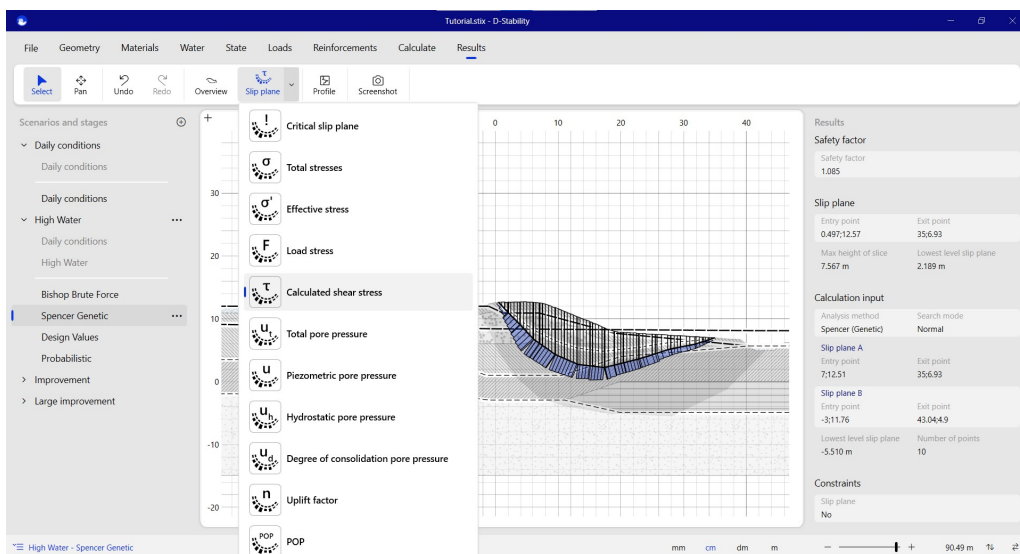


Figure 3.41 *Slip plane inspector*

3.16 Probabilistic analysis: design values

A new stage is added to make the analysis with design values.

The next step is to calculate the failure probability during the high water situation. A fully probabilistic calculation is too time-consuming to combine with an optimization method. First, a calculation with design values is made to find the representative slip plane. Then, the conditional failure probability of this slip plane is calculated.

A new stage is added to make the analysis with design values. After this a new stage is added for the probabilistic calculation as well. In the probabilistic stage, the representative slip plane from the design calculation is imported.

Note: D-Stability calculates the conditional failure probability, given an outside water level. To construct a fragility curve, one needs to repeat this process for several outside water levels. This fragility curve can be combined with the probability density function of the water distribution in order to calculate the failure probability of the cross section. This integration can, for example, be done with the probabilistic toolkit.

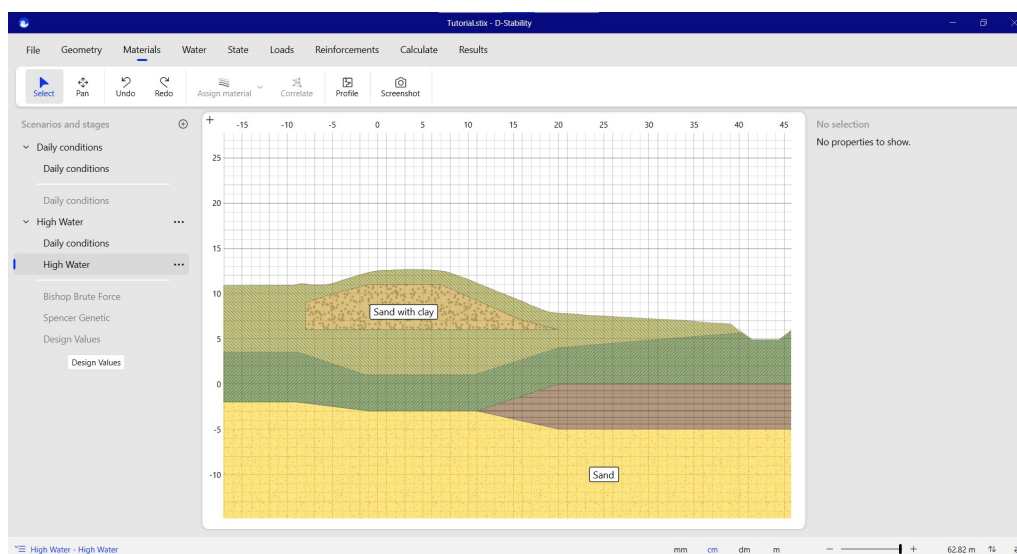


Figure 3.42 *Design values*

If the design values differ from the deterministic values, the optimization procedure needs to take place again as a different slip plane might be representative. In this tutorial, we will use the same values for the design calculation, therefore we can directly use the resulting circle from stage 2 (High water).

A single calculation for Bishop - Fixed point radius type is chosen as calculation method.

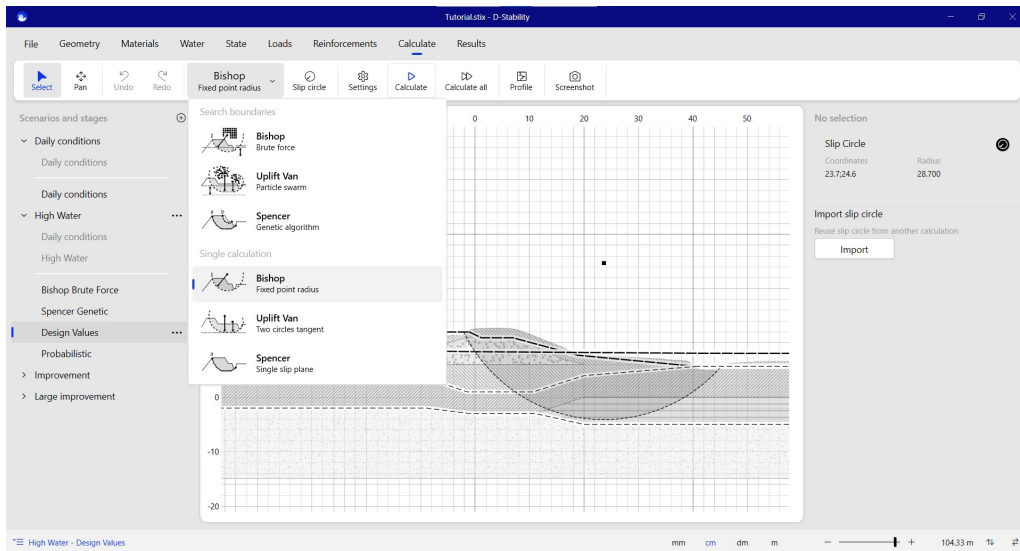


Figure 3.43 Making a single Bishop calculation

And the slip plane from stage 2, high water, is imported in the "Calculate" tab.

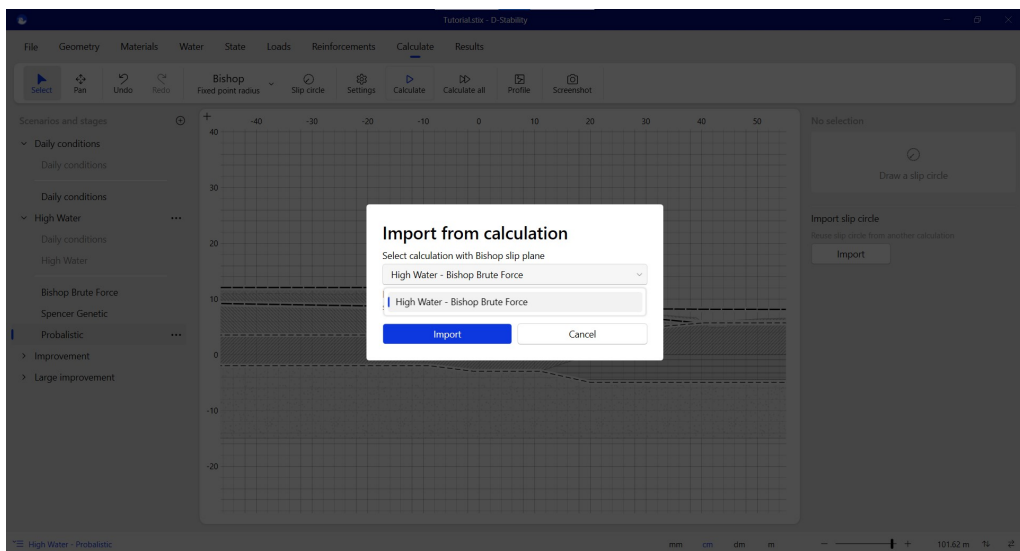


Figure 3.44 Import slip circle from another phase

All materials that are to be considered as stochastic, need to be marked as such and the mean and standard deviation need to be entered. This can be done in the "Materials" tab by selecting a layer and activating the "Probabilistic variables" of that layer. This needs to be done for all materials that are defined as stochastic.

Note: Note that only a log normal distribution can be used in D-Stability to define the distribution of the parameters. This is the most common type of distribution for geotechnical parameters. This is to prevent parameter values to become smaller than zero.



If the parameters within a material are correlated, the "r" to the right of the parameters connecting them can be selected. If it is blue, the correlation is active and the two

material properties will be fully correlated. If it is gray, the parameters are not correlated. More information about the correlation of parameters can be found in section 15.1.2.

Note: Only full correlation is possible. Partial or inverse correlation is not supported.



You can also correlate entire materials and state points. When selecting multiple materials or state points in the ribbon, one can press the "material correlation" or "state correlation" button to fully correlate the parameters. The user interface shows this correlation by drawing a line between the materials or state points.

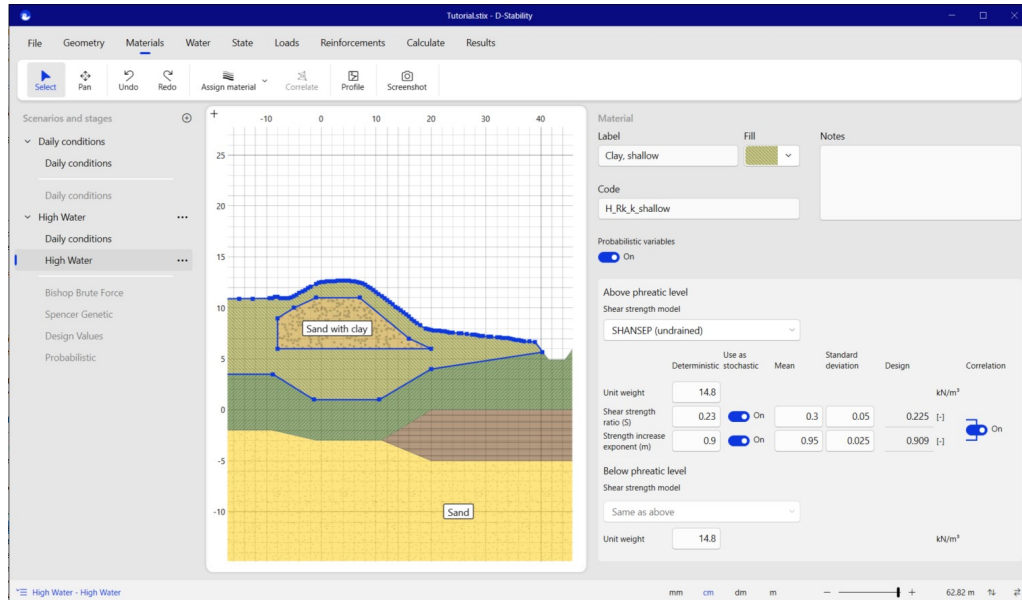


Figure 3.45 Defining probabilistic material properties and correlation

Note: More probabilistic parameters increases the calculation time.



In the calculation tab under settings, one can choose to calculate with the deterministic-, mean-, design- or probabilistic values. The latter can only be selected when using a single calculation method.

For this example, the design values are calculated to see if they give the same result as the deterministic values.

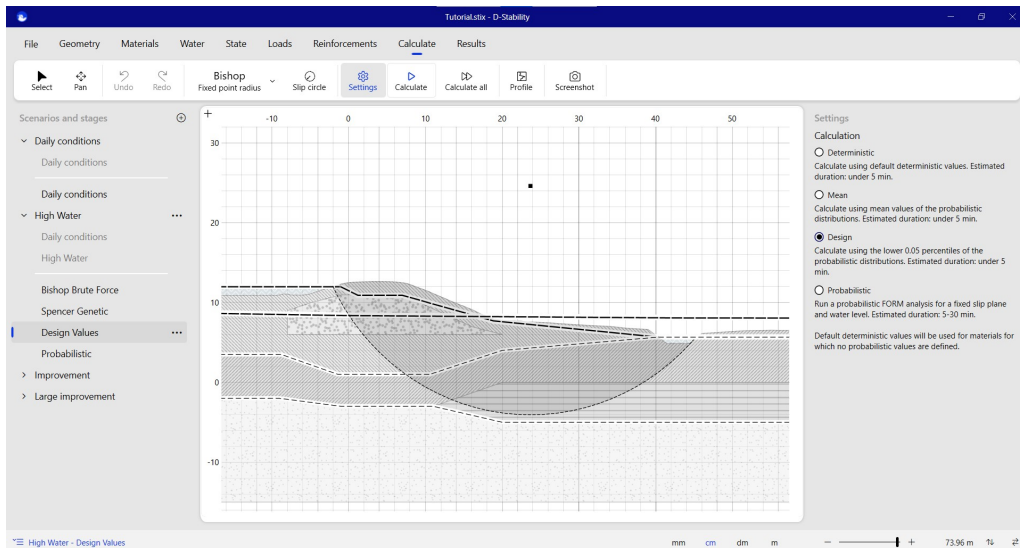


Figure 3.46 Choosing a design calculation

The slip circle can be inspected after a calculation with design values. This option will not be available after a probabilistic calculation. This option will be deactivated in all stages once a probabilistic calculation has been made. Rerunning the design value calculation enables the option again.

If you want to inspect the stresses after a probabilistic calculation, you need to do so in the corresponding previous deterministic stage.

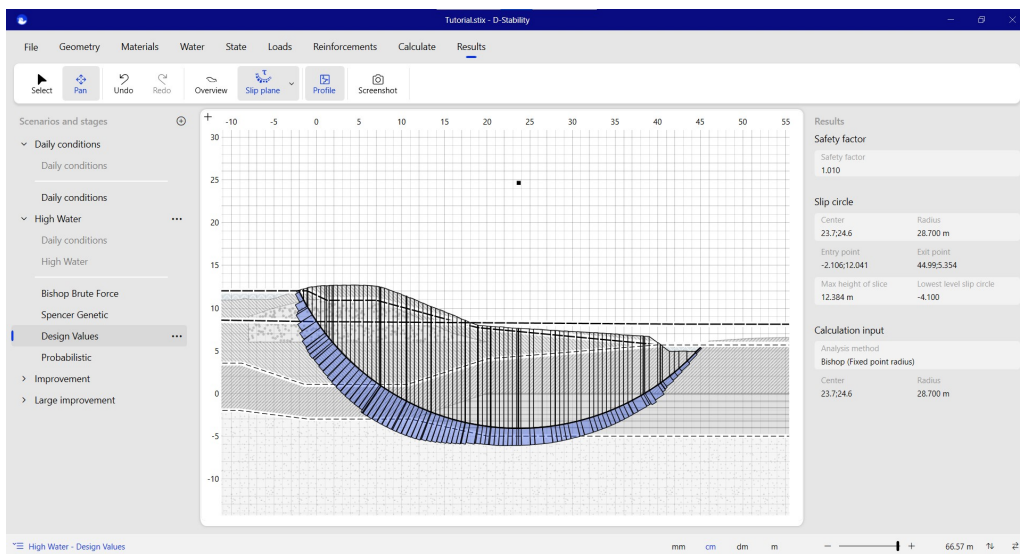


Figure 3.47 Results with design values

3.17 Correlation of state points

In the "State" tab, state points can be correlated, just like material properties. By selecting two state points, the "State correlation" button becomes active in the ribbon.

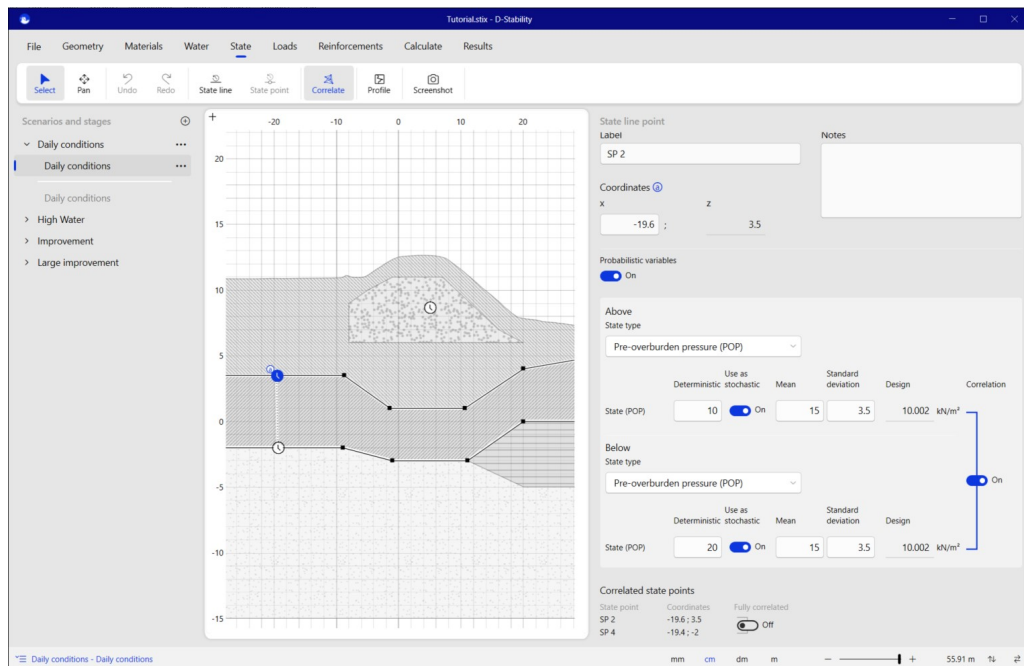


Figure 3.48 Correlation of state points

When correlating state points that lie on lines, like in the figure above, the bottom of one point is correlated to the top of the point below. If two points are correlated, this is indicated by a dotted line between the points just like with the material correlation.

If users correlate the upwards direction of a state point with the downwards one, this will be indicated with an "r" symbol connecting both parameters on the right hand side. In the example above, this would imply that the upwards direction of the point above is also fully correlated with the state point below.

If all state points are to be fully correlated (top and bottom) it is also possible to use the "fully correlated" switch at the bottom of the inspector area.

A point in a layer can also be correlated to state points on lines. In that case, there will always be full correlation as you cannot speak of "top" and "bottom" any more with a point inside a layer.

If the correlation is not possible, the gray "r" is dashed and clicking on it will not have any effect.

Note: Checking the influence factors (alpha) in the probabilistic results inspector on the right of the screen after the calculation is run is the best way to check whether the desired correlation has been used. Correlated parameters will give the same influence factors.



3.18 Probabilistic analysis: FORM analysis

The FORM analysis is performed next. In the "Calculate" tab, a probabilistic analysis can be chosen by selecting "Settings" in the ribbon. This option can only be activated once stochastic variables for (at least one) material(s) are defined. Note the extra parameter: the model factor. This factor takes the uncertainty of the model into account. If the model is exact, it can be taken account as a deterministic value of 1 with no standard deviation.

Note: More information about the FORM routine can be found in chapter 15, in the Reliability part of this manual.

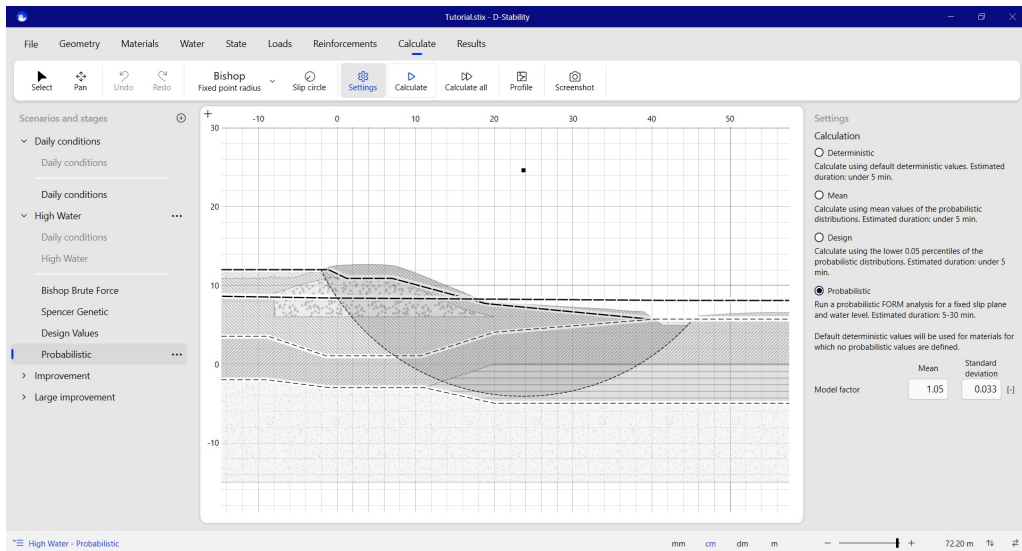


Figure 3.49 Fully probabilistic calculation

Running the probabilistic calculation gives the following result.

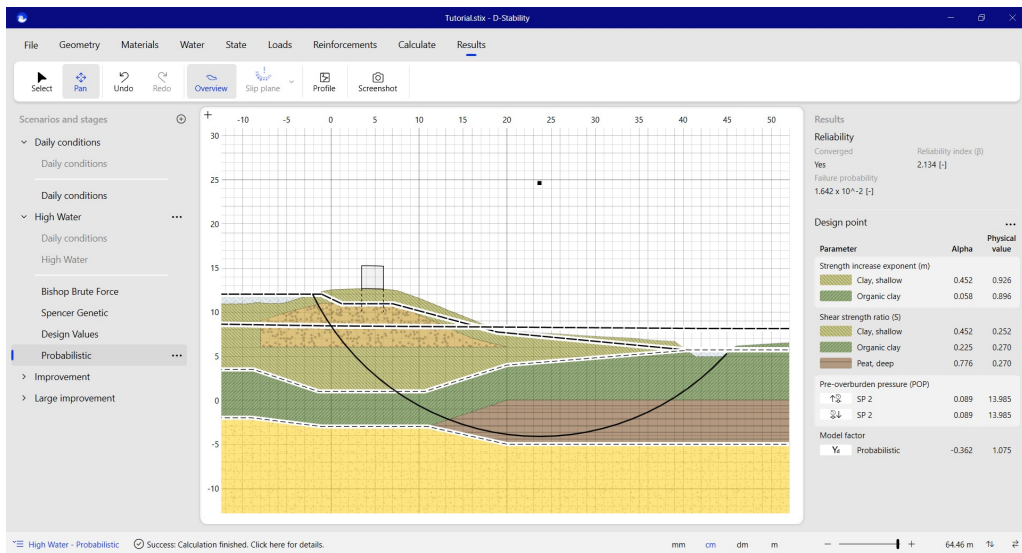


Figure 3.50 Result of a probabilistic calculation

In this case, the convergence has been achieved. This is not guaranteed. If the safety

factor is such that the Z function ($F_s - 1 = 0$) cannot be reached, the user will be informed that there is no convergence. This can be caused by a starting point too far from 1 or too little variance in the stochastic parameters.

Note: In the Z function mentioned above, the "1" is related to the model factor. The deviation on the model factor has direct influence on the Z function and thereby much influence.



At this time, one point on a fragility curve has been derived. This can be extended to a full fragility curve by repeating these steps for other outside water levels. For this tutorial, however, this embankment will be strengthened instead of further constructing the fragility curve.

The following parameters are used as steering criteria for the FORM analysis;

MaximumIterations	50
StepSize	0.01
RelaxationFactor	0.9
RelaxationLoops	3
EpsilonBeta	0.01

Using these parameters, one can reproduce the probability of failure with the Probabilistic Toolkit.

3.19 Probabilistic analysis: Monte Carlo Importance Sampling (MCIS) analysis

The MCIS analysis is performed if you combine a probabilistic analysis with a search algorithm. In the "Calculate" tab, a probabilistic analysis can be chosen by selecting "Settings" in the ribbon when an optimization analysis is selected. This option can only be activated once stochastic variables for (at least one) material(s) are defined. Note the extra parameter: the model factor. This factor takes the uncertainty of the model into account. If the model is exact, it can be taken account as a deterministic value of 1 with no standard deviation.

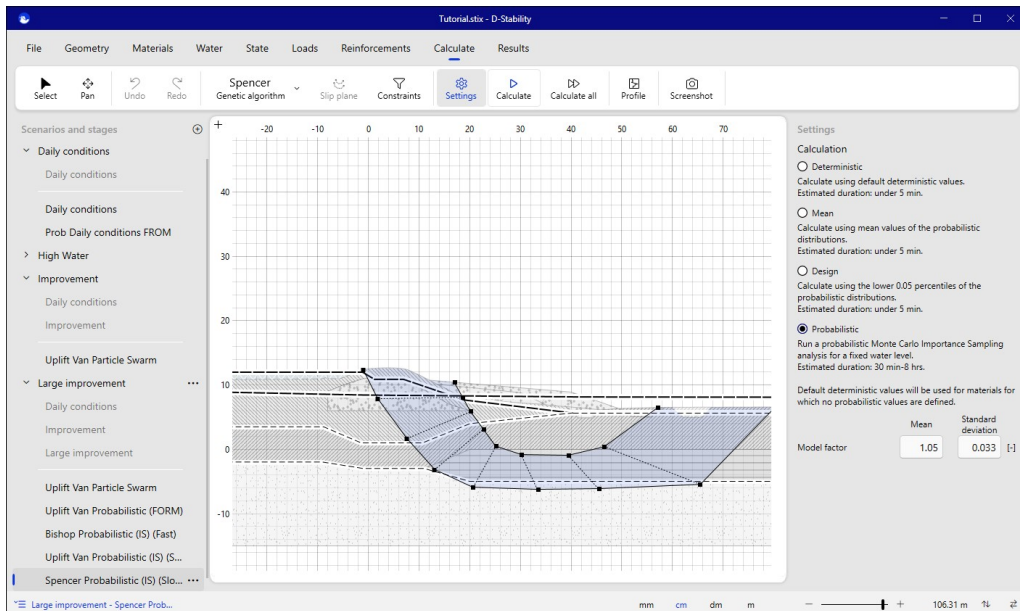


Figure 3.51 *The MCIS analysis*

Note: More information about the MCIS routine can be found in chapter 15, in the Reliability part of this manual.



MCIS is a relatively slow analysis. The calculation speed becomes longer in the case of:

- many parameters. Try to reduce the number of uncorrelated stochastic parameters below 10 or 15;
- a large β , especially with many variables as the starting point method becomes less predictive.

The following parameters are used as steering criteria for the MCIS analysis:

startpointmethod	sensitivity
maxbeta	8
VarianceFactor	1
MinVarianceLoops	1
MaxVarianceLoops	3
Var coeff failure	0.2
Min realizations	200
Max realizations	2000
Design point determination	Center of gravity
AutoMaximumSamplesNoResult	TRUE
EpsWeightSample	0.1

It is strongly advised to first carefully investigate the location of the slip plane. A good search space causes less noise in the search and therefore a more precise result.

It is also advised to use as stringent constraints as possible in a Spencer analysis. Only a few unrealistic Spencer slip plane results can greatly influence the MCIS result. If the expected result has 100% of the thrust line in the soil body, it is advised to set the constraint as such

The resulting slip plane of a MCIS analysis can be repeated with a FORM analysis to gain more trust in the result.

Both MCIS and FORM results can be used to construct a fragility curve.

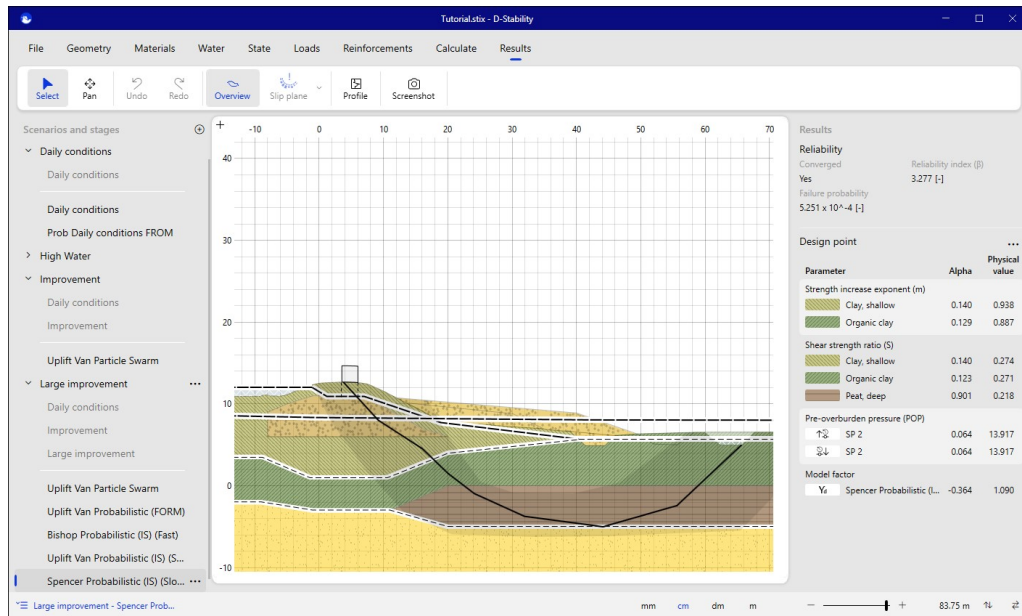


Figure 3.52 The result of an MCIS analysis

3.20 Berms and excavations

A new calculation stage is defined to design a berm. Water pressures are imported and the traffic load is defined. Next, the berm is drawn upon the geometry using the "draw berm" tool. A berm or an excavation must start and finish on the surface line.

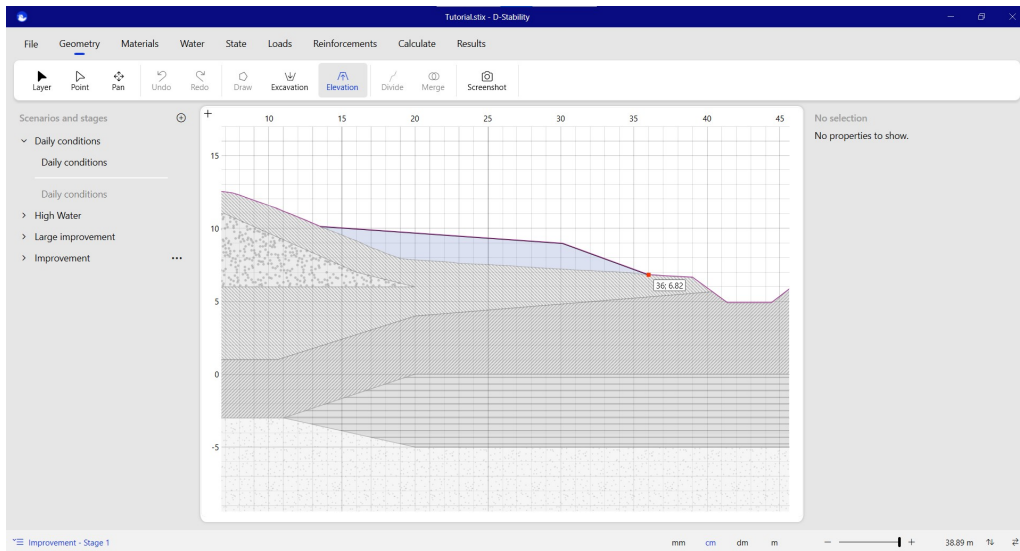


Figure 3.53 *Creating a berm*

Note: It is not possible to add any more shapes once that either an excavation or a berm has been added in a construction phase. The button for adding new shapes is disabled. Only more excavations or berms can be added.



In this tutorial, after drawing the berm, an excavation is drawn to represent a new ditch.

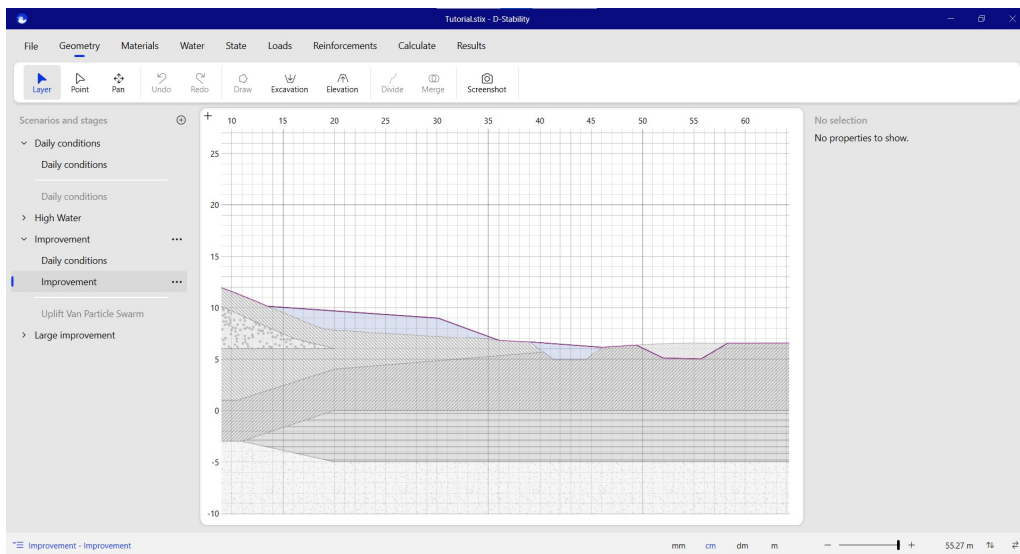


Figure 3.54 *Filling up the ditch and drawing a new excavation*

Materials are assigned to the newly drawn berms.

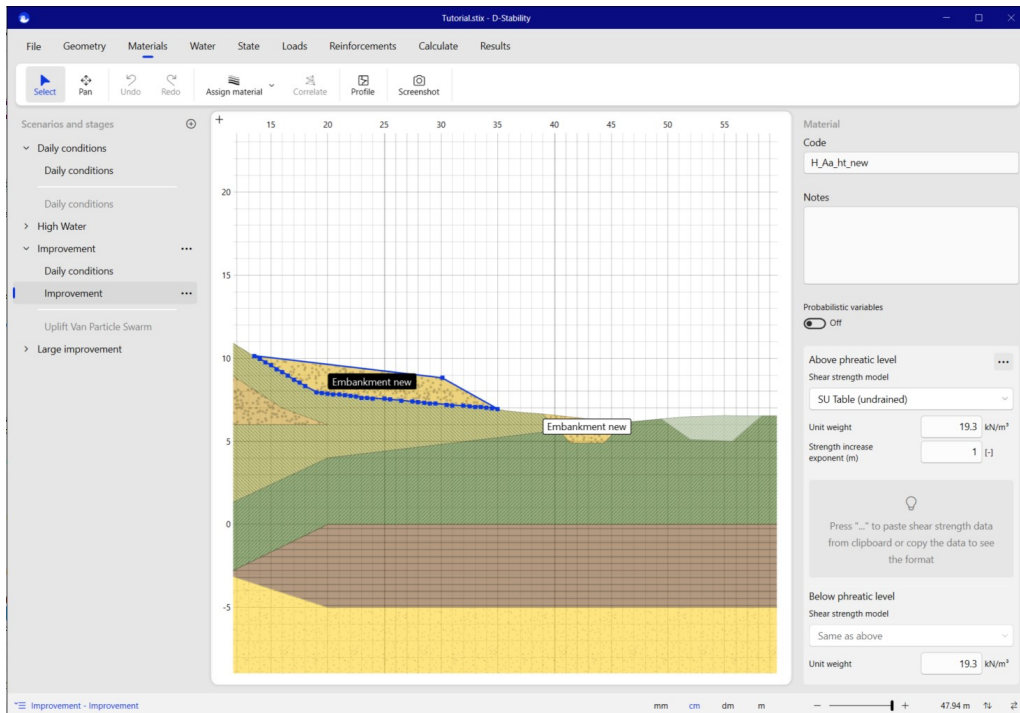


Figure 3.55 Assigning material to berm

Note that you cannot use the profile inspector until materials are assigned to the berm.

The inspector shows the initial state (POP) besides the berm. The next figures show that the yield stress remains virtually constant, but the POP disappears because the effective stress increases underneath the embankment.

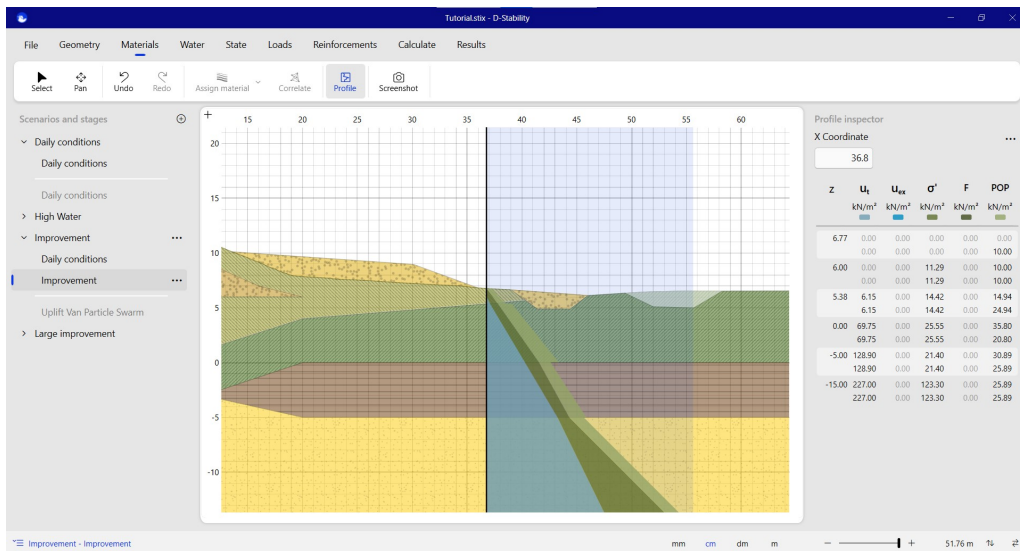


Figure 3.56 Inspecting POP besides the berm

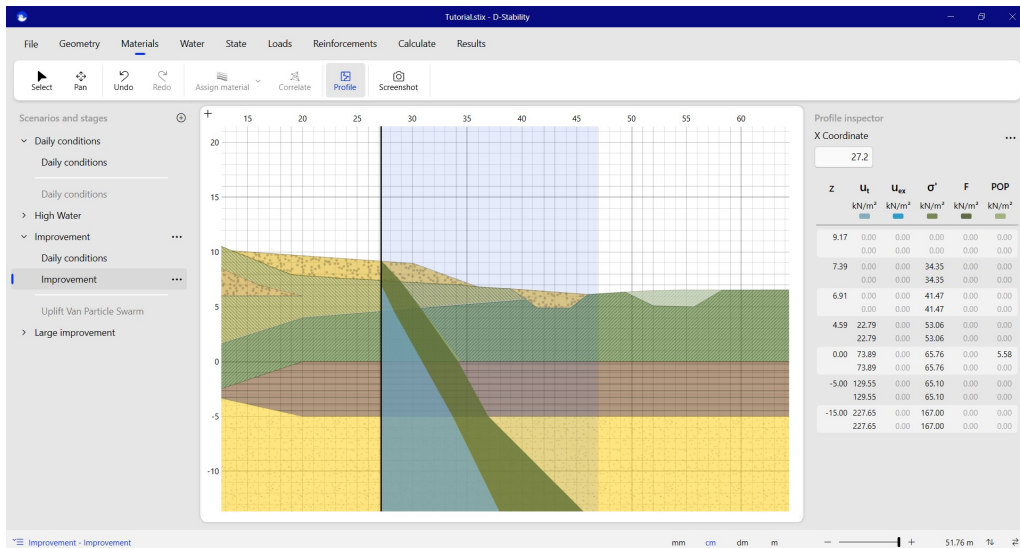


Figure 3.57 Inspecting POP underneath the berm

Below the ditch, the effective stress decreases and, therefore, the POP increases.

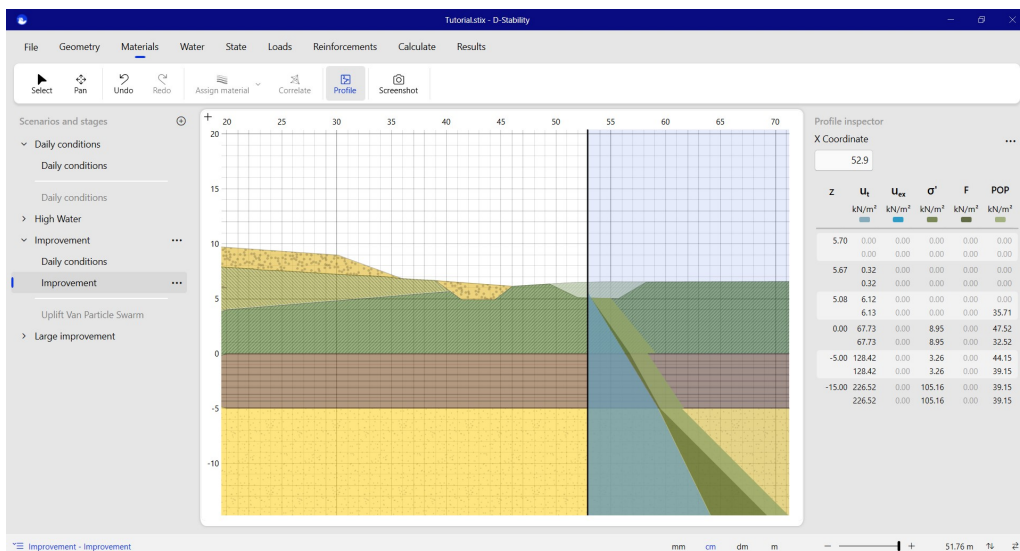


Figure 3.58 Inspecting the yield stress in the ditch

The safety factor of this new geometry is calculated using an Uplift-Van with Particle Swarm optimization in the "Calculate" tab. The active and passive search area need to be defined, just like the tangent scope.

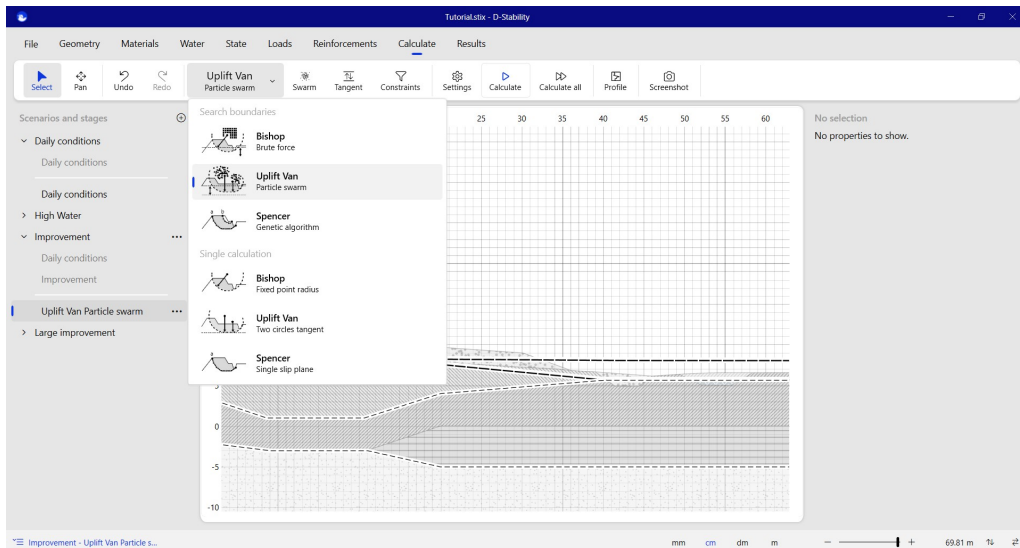


Figure 3.59 Making an Uplift-Van analysis

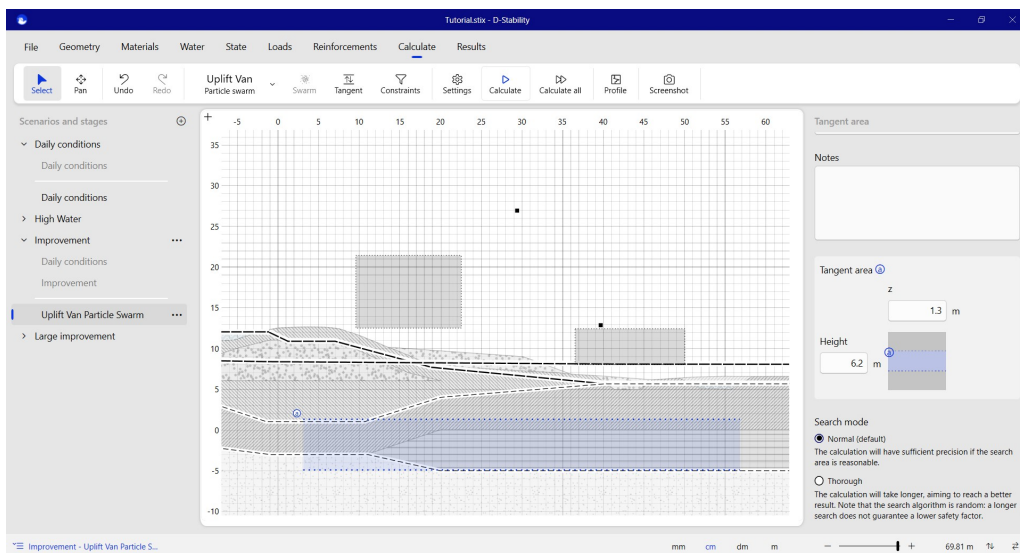



Figure 3.60 Defining the Uplift-Van search area

Note: This algorithm will seek outside the initial search area, but most precession is reached within the initial search scope. A large search area also means a decrease in precision. When in doubt, the user can choose for a "thorough" search and/or move the search area. 

The length of the berm is increased even further to increase the safety factor of the embankment. For this calumniation, a new state is created.

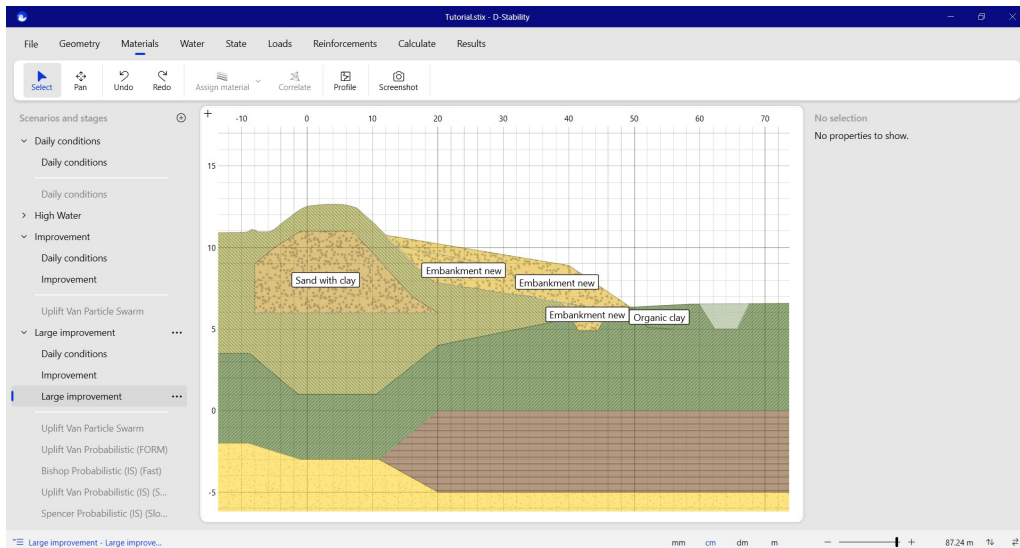


Figure 3.61 Increasing the berm length

After the particle swarm has found the optimal slip plane, this plane is imported to yet another stage such that a probabilistic calculation can be run. The run results in a lower failure probability.

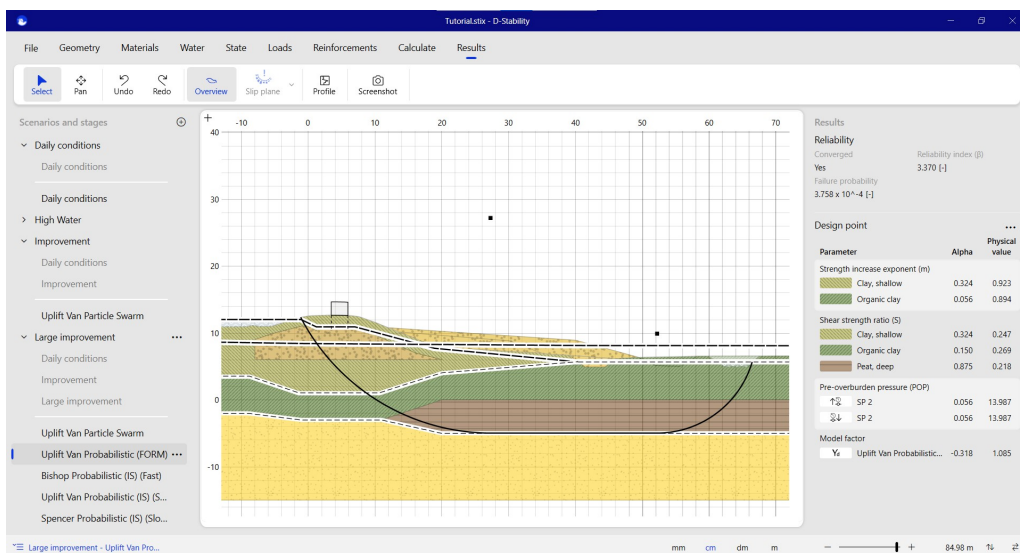


Figure 3.62 Determining the final conditional probability of failure

Note: A console is installed besides the D-Stability executable. This way, you can run D-Stability from the command line. This can be useful if you don't want to wait for the user interface to give results or if you are using external software to run D-Stability.



3.21 Exporting the fragility curve

D- Stability can help calculating conditional failure probabilities. The probabilities are conditional for an outside water level. The relationship between the outside water levels and the failure probabilities is called a fragility curve. To calculate the total failure probability of a flood protection embankment, the fragility curve needs to be multiplied

with the probability density function of the outside water levels. D-Stability has no knowledge of this distribution. This operation can be performed using external software, such as Excel, the Probabilistic Toolkit or with a Python script for HydraRing.

D-Stability offers the functionality to export the fragility curve, so it can be integrated wherever the user wants to. It is only possible to export a fragility curve after one or more probabilistic construction stages have been run. To do so, choose under "File", "Export", "Fragility Curve".

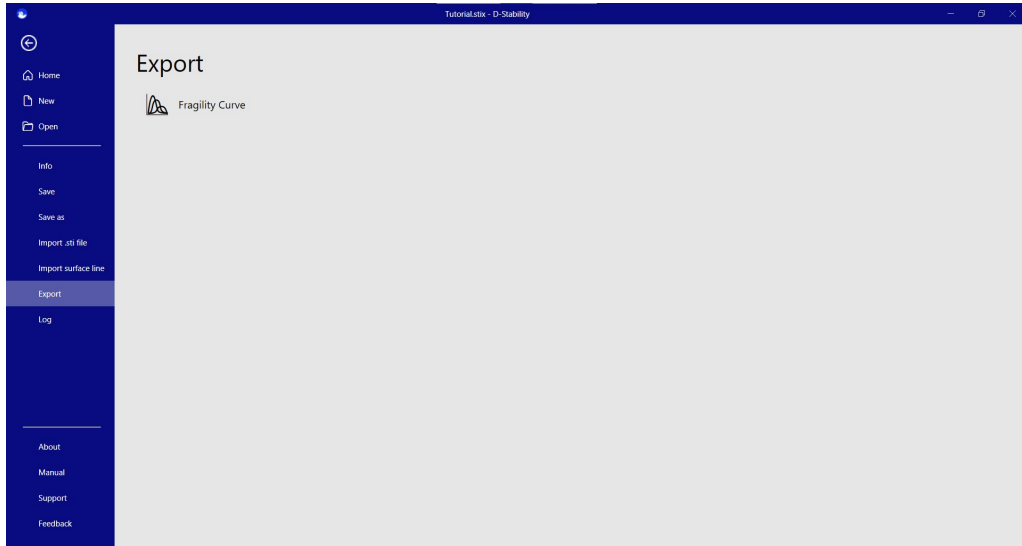


Figure 3.63 Export fragility curve screen

A preview is presented to inspect the shape of the curve. You can then select the stages to export.

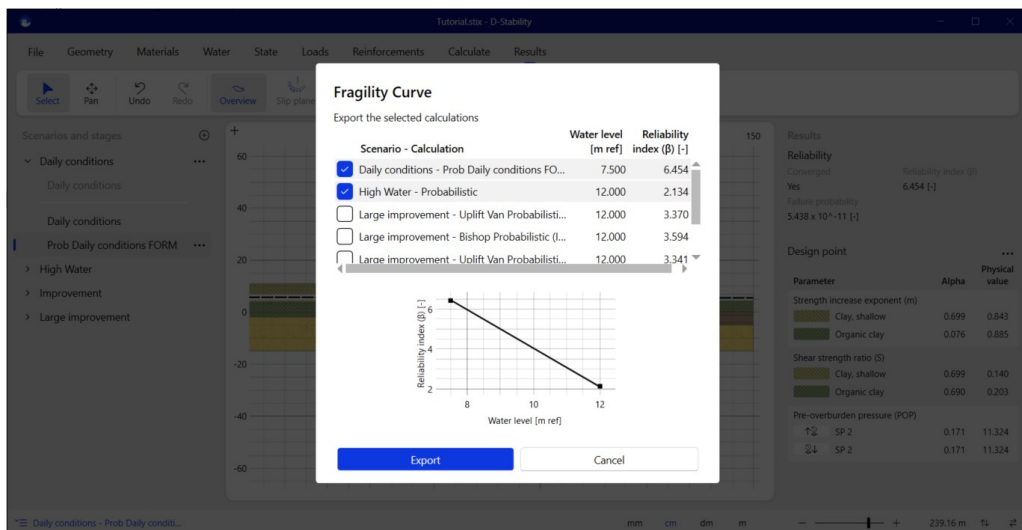


Figure 3.64 Exporting a fragility curve

When exporting the fragility curve, D-Stability writes a JSON file containing all information that external software could possibly needs to integrate the fragility curve over the distribution of the water load except, as indicated above, the probability

density function of the water level. Section 15.3 of the reference manual explains how to combine a fragility curve with a water load.

3.22 Parameter list in the application

The following parameters exist in the application.

subwindow	subsubwindow	variable	lower bound	upper bound	default
material	Mohr-Coulomb Advanced	Unit Weight	-infinite	infinite	0
		Cohesion	-infinite	infinite	0
		Frictional angle	-infinite	infinite	0
		Dilatancy angle	-infinite	infinite	0
	SHANSEP	Unit Weight	-infinite	infinite	0
		Sheer strenght ratio	-infinite	infinite	0
		Strenght increase exponent (m)	-infinite	infinite	1
	SU Table (undrained)	Unit Weight	-infinite	infinite	0
		Strenght increase exponent (m)	0	1	1
	Below phreatic level Mohr-Coulomb Advanced	Unit Weight	-infinite	infinite	0
		Unit Weight	-infinite	infinite	0
		Sheer strenght ratio	-infinite	infinite	0
	Below phreatic level SHANSEP	Strenght increase exponent (m)	-infinite	infinite	1
		Unit Weight	-infinite	infinite	0
Below phreatic level SU Teble (undrained)	Unit Weight	-infinite	infinite	0	
	Strenght increase exponent (m)	0	1	1	
Water		Unit weight of water	0	infinite	9.81
Waternet creator	Geometry	Embankment toe water side	-infinite	infinite	empty
		Embankment top water side	-infinite	infinite	empty
		Embankment Top land side	-infinite	infinite	empty
		Shoulder base land side	-infinite	infinite	empty
		Embankment toe land side	-infinite	infinite	empty
		Ditch embankment side	-infinite	infinite	empty

			Ditch bottom bankment side	em-	-infinite	infinite	empty	
			Ditch bottom side	land	-infinite	infinite	empty	
			Ditch land side		-infinite	infinite	empty	
Waternet creator	Water levels		Normative level		-infinite	infinite	empty	
			Mean level		-infinite	infinite	empty	
			Hinterland level		-infinite	infinite	empty	
		Water Phreatic offset	levels line	Embankment water side	top	-infinite	infinite	empty
	Embankment land side			top	-infinite	infinite	empty	
	Embankment water side			top	-infinite	infinite	empty	
		Water Drainage construction location	levels con-	Embankment land side	top	-infinite	infinite	empty
	Shoulder base side			land	-infinite	infinite	empty	
	Embankment land side			toe	-infinite	infinite	empty	
					-infinite	infinite	empty	
Waternet creator	Aquifer bottom aquifer layer		leakage length outwards	out-	-infinite	infinite	empty	
			leakage length inwards	in-	-infinite	infinite	empty	
	Aquifer inside aquitard		leakage length outwards	out-	-infinite	infinite	empty	
			leakage length inwards	in-	-infinite	infinite	empty	
Waternet creator	Aquitard layer		Head at land side		-infinite	infinite	empty	
			Head at water side		-infinite	infinite	empty	
			Intrusion length		-infinite	infinite	empty	
State line point	Above POP		State (POP)		-infinite	infinite	0	
			State (POP)		-infinite	infinite	0	
	Above OCR		State (OCR)		-infinite	infinite	1	
			State (OCR)		-infinite	infinite	1	
	Above stress	Yield		State (Yield stress)		-infinite	infinite	0
				State (Yield stress)		-infinite	infinite	0

State line point probabilistic	Above POP	State (POP)	-infinite	infinite	0	
		Mean	0.001	infinite	1	
		Standard deviation	0	infinite	0	
	Below POP	State (POP)	-infinite	infinite	0	
		Mean	0.001	infinite	1	
		Standard deviation	0	infinite	0	
	Above OCR	State (OCR)	-infinite	infinite	1	
		Mean	0.001	infinite	1	
		Standard deviation	0	infinite	0	
	Below OCR	State (OCR)	-infinite	infinite	1	
		Mean	0.001	infinite	1	
		Standard deviation	0	infinite	0	
	Above stress	Yield	State (Yield stress)	-infinite	infinite	0
			Mean	0.001	infinite	1
Standard deviation			0	infinite	0	
Below stress	Yield	State (Yield stress)	-infinite	infinite	0	
		Mean	0.001	infinite	1	
		Standard deviation	0	infinite	0	
Uniform load		Start	-1E9	endpoint	empty	
		End	startpoint	1,00E+09	empty	
		Magnitude	0	1,00E+27	10	
		Angle of distribution	0	89.999	0	
		Layer consolidation percentages	0	100	100	
Line load		X	-1E9	1,00E+09	empty	
		Z	-1E9	1,00E+09	empty	
		Angle	-360	360	0	
		Magnitude	0	Infinite	10	
		Angle of distribution	0	89	0	
Tree on slope		Wind Force	-infinite	infinite	10	
		Width of root zone	0	infinite	5	
		Angle of distribution	0	89,99	0	
Earthquake		Horizontal	-infinite	infinite	0	
		Vertical	-infinite	infinite	0	

		Free water factor	-infinite	infinite	0	
		Layer consolidation percentages	0	100	100	
Nail		X	-1E+9	1,00E+09	empty	
		Z	-1E+9	1,00E+09	empty	
		Direction	-infinite	infinite	0	
		Horizontal spacing	-infinite	infinite	0	
		Length	-infinite	infinite	3	
		Diameter nail	-infinite	infinite	0.1	
		Diameter grout	-infinite	infinite	0	
		Critical angle	-infinite	infinite	0	
		Maximum pull force	-infinite	infinite	0	
		Plastic moment	-infinite	infinite	0	
		Bending stiffness	-infinite	infinite	0	
		Lateral stress values	Distance	-infinite	infinite	0
			Sigma	-infinite	infinite	0
		Shear stress values	Distance	-infinite	infinite	0
		Sigma	-infinite	infinite	0	
Geotextile	Start coordinates	X	-1E+9	1,00E+09	empty	
		Z	-1E+9	1,00E+09	empty	
	End coordinates	X	-1E+9	1,00E+09	empty	
		Z	-1E+9	1,00E+09	empty	
		Effective Strenght	tens. 0	infinite	0	
		Reduction area	0	infinite	0	
Forbidden line	Start coordinates	X	-1E+9	1,00E+09	empty	
		Z	-1E+9	1,00E+09	empty	
	End coordinates	X	-1E+9	1,00E+09	empty	
		Z	-1E+9	1,00E+09	empty	
Bishop brute force	Search area	X	-1E+9	1,00E+09	empty	
		Z	-1E+9	1,00E+09	empty	
		Points vertical	1	100	empty	
		Points horizontal	1	100	empty	
		Resolution	0,01	100	1	
	Tangent area	Z	-1E+9	1,00E+09	empty	
		Lines	1	100	empty	
	Resolution	0,01	100	2		

Uplift van Particle swarm	Initial swarm area	X	-infinite	infinite	empty
		Z	-infinite	infinite	empty
		Height	0	infinite	empty
		Width	0	infinite	empty
	Tangent area	Z	-infinite	infinite	empty
		Height	0	infinite	empty
Spencer Genetic algorithm	Constraints	Minimum thrust line inside slices	0	100	0
		Minimum angle between slices	0	180	0
Bishop fixed point radius	Coordinates	X	-1E+9	1,00E+09	empty
		Z	-1E+9	1,00E+09	empty
		Radius	0	1,00E+09	empty
Uplift Van Two circles tangent	Coordinates	X a	Bound by geometry, not on border	Bound by geometry, not on border	empty
		Z a	-1E+9 depending on radius	1E+9 depending on radius	empty
		Radius a	almost 0, depending on distance between a and b	1,00E+09	
		X b	Bound by geometry, not on border		Point for defining radius of circle 'a'
		Z b	-1E+9 depending on radius	1E+9 depending on radius	Point for defining radius of circle 'a'
		Radius b			

Scientific Manual

4 Soil profile

4.1 Coordinate system

The horizontal axis is defined as the X-axis. The vertical axis is defined to be the Z-direction. Upwards is positive and downwards negative. Perpendicular to the cross section is the Y direction.

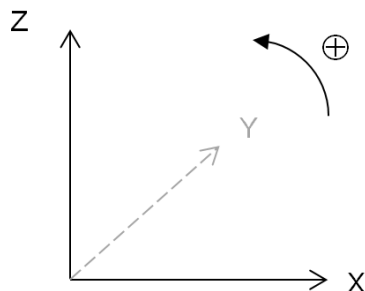


Figure 4.1 Coordinate system

4.2 Soil profile definition

A soil profile is a vertical cross section of the subsoil. The soil profile defines the soil properties in the subsoil at any location.

A soil profile is defined in two dimensions. It is assumed to continue infinitely in the direction perpendicular to the cross section.

The soil profile consists of

Points	The locations (x, z) , which are used in subsequent definitions;
Curves	Straight connections between two points;
Surface line	The line determining the surface level of the subsoil, consists of a sequence of points. The surface line is drawn purple as a guide. The surface line should progress always, so each point has an X-coordinate greater than or equal to its previous point;
Boundaries	The left and right side of the surface line (purple) for the edges of the possible analysis;
Phreatic line	Line from left to right boundary, which marks the border between dry and wet soil. Consists of a sequence of points. If no phreatic line is entered, then all soil is assumed to be dry;
Soil layers	Polygons defining a certain area in the soil profile. Polygons are defined by a closed set of curves, which are connected head by tail. Within a soil layer, the same soil or hydrological properties are valid. Exception: if the phreatic line intersects with the soil layer, the part above the phreatic line may have different properties than the part below the phreatic line;

The following restrictions apply to a soil profile

The following figure shows a soil profile. This soil profile has nine soil layers. Some layers have the same soil properties.

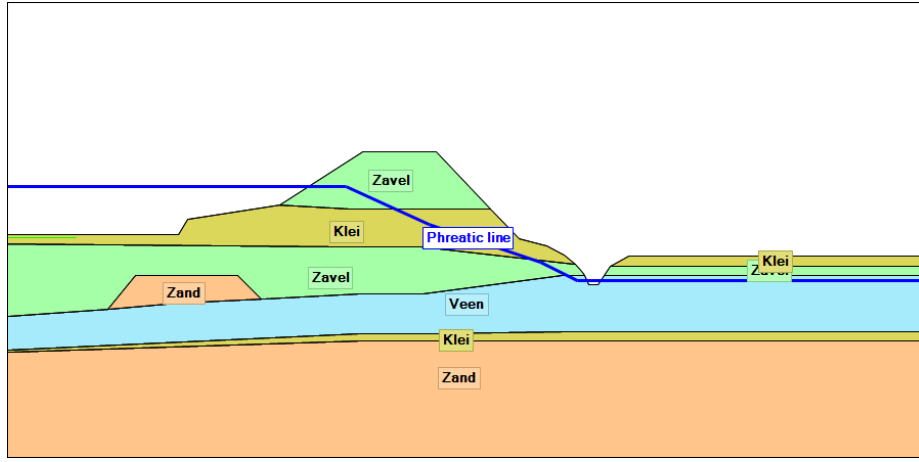


Figure 4.2 Soil profile

4.3 Vertices

A vertex is a point in the geometry that does not lie exactly in between two other points on a line. Such a vertex point causes changes in the data values in the profile that makes it impossible to linearly interpolate. All bending points in Figure 4.2 are vertex points.

The pre-processor of the kernel determines the stresses in the all vertex points before an optimization routine in order to speed up the optimization. This causes an individual calculation to last a little longer, but speeds up the optimization.

The stress inspector also uses the pre-processor to draw the stresses over depth. The inspector possibly does not draw a point correctly if there is a jump in stresses elsewhere then in a vertex point. The kernel itself will always determine these values correctly.

4.4 Soil and water pressure

Based on the soil profile, we can derive the following pressures due to the soil weight and phreatic line.

The soil weight at any given depth z is given by

$$\sigma_{\text{soil}}(x, z) = \sum_{\text{layers } i} (\gamma_{\text{dry}} \times h_{\text{dry}} + \gamma_{\text{wet}} \times h_{\text{wet}}) \quad (4.1)$$

The pressure due to the free water is given by

$$\sigma_{\text{water}}(x) = (z_{\text{phr}} - z_{\text{surf}}) \times \gamma_{\text{water}} \geq 0 \quad (4.2)$$

The hydrostatic pore pressure, which is the pressure due to water within the subsoil u_{hydro} is

$$u_{\text{hyd}}(x, z) = (z_{\text{phr in soil}} - z) \times \gamma_{\text{water}} \geq 0 \quad (4.3)$$

where

z_{phr}	is the level of the phreatic line at x ;
z_{surf}	is the level of the surface line at x ;
$z_{\text{phr in soil}}$	is the minimum of z_{phr} and z_{surf} at x ;
h_{dry}	is the thickness of layer i above z_{phr} and above z at x ;
h_{wet}	is the thickness of layer i below z_{phr} and above z at x ;
γ_{dry}	is the dry unit weight of layer i , in kN/m^3 ;
γ_{wet}	is the wet unit weight of layer i , in kN/m^3 ;
γ_{water}	is the water unit weight, in kN/m^3 (default 9.81 kN/m^3);

5 Pore pressure

Objective: To calculate pore pressures on any given location.

5.1 Hydraulic pore pressure

The hydraulic pore pressure u_{PL} is the pore pressure due to the presence of water in the subsoil. The hydraulic pore pressure depends on the position of the phreatic line and the hydraulic head at various locations.

D-Stability has two ways of defining the hydraulic head.

5.1.1 Hydraulic heads by lines

The head lines represent the piezometric level φ at the location of linked reference lines. A reference line is a geometrical line on which the defined piezometric level applies.

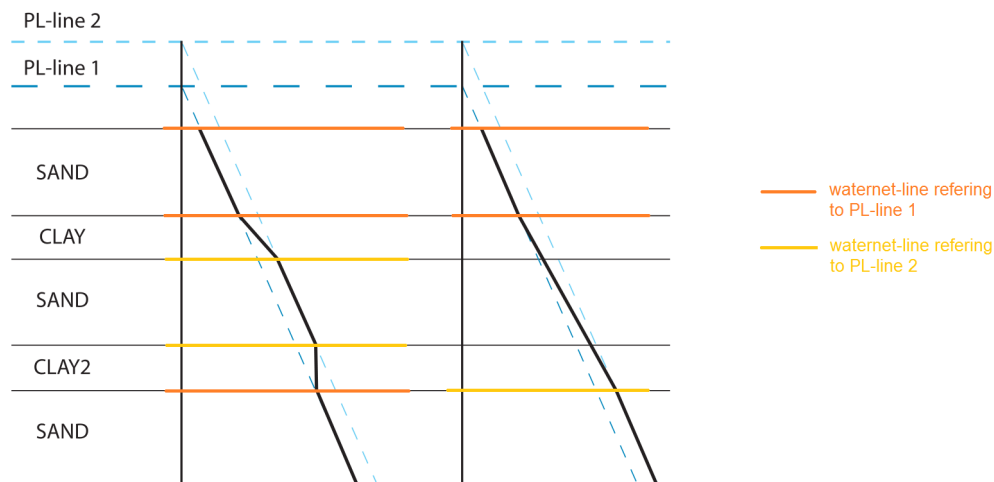


Figure 5.1 Calculation of the hydraulic pore pressures (from piezometric level lines)

Note: Contrary to what the above figure presumes, the reference line(s) do not have to (but may) follow the layer boundaries and to be horizontal. A reference line can be defined anywhere in the soil profile.



The following input is required:

Head line(s),	The X- and Z-coordinates of the points belonging to the head line(s) line must be defined. the first head line is phreatic, this can later be changed
Reference line(s)	The X- and Z-coordinates of the points belonging to the reference line(s) must be defined. The head line associated to each reference line needs also to be defined.

The unit weight water is by default set to 9.81 kN/m³.

By using several reference lines, the piezometric level can be defined at any location. Between reference lines, the piezometric level will be derived by linear interpolation. The piezometric level is derived as follows:

$$\varphi(x, z) = \frac{z - z_{\text{below}}}{z_{\text{above}} - z_{\text{below}}} \times \varphi_{\text{above}} + \frac{z_{\text{above}} - z}{z_{\text{above}} - z_{\text{below}}} \times \varphi_{\text{below}} \quad (5.1)$$

where

- z_{above} is the level of the nearest reference line at x above (x, z) ;
- z_{below} is the level of the nearest reference line at x below (x, z) ;

The following special reference lines are always applied

- The phreatic line is a reference line and head line in one;
- The surface line is a reference line and has the phreatic line as its head line. Therefore the head in the free water will always be the phreatic level. Any reference lines in the free water are ignored.

The pore water pressure in a point due to piezometric levels is:

$$u_{\text{PL}}(z) = \begin{cases} z < z_{\text{phreatic}} & (\varphi(z) - z) \times \gamma_{\text{water}} \geq 0 \\ z \geq z_{\text{phreatic}} & 0 \end{cases} \quad (5.2)$$

where

- z_{phreatic} is the level of the phreatic line in m;
- $\varphi(z)$ is the hydraulic head at depth z derived from the reference lines (see Equation (5.1)) in m;
- γ_{water} is the unit weight of water in kN/m^3 .

5.2 Pore pressure due to degree of consolidation

The effective weight σ'_{weight} of a layer i is equal to

$$\sigma'_{\text{weight}}(x, z) = \gamma_{\text{dry}} \times h_{\text{dry}} + (\gamma_{\text{wet}} - \gamma_{\text{water}}) \times h_{\text{wet}} \quad (5.3)$$

where

- h_{dry} is the thickness of layer i above z_{phreatic} and above z at x in m;
- h_{wet} is the thickness of layer i below z_{phreatic} and above z at x in m;
- γ_{dry} is the unsaturated (i.e. dry) unit weight of layer i , in kN/m^3 ;
- γ_{wet} is the saturated (i.e. wet) unit weight of layer i , in kN/m^3 ;
- γ_{water} is the volumetric weight of the water, in kN/m^3 .

The degree of consolidation determines which part of the overburden of an overlying soil layer is carried by effective stress, and which part by (excess) pore pressure. This degree ranges between 0% and 100%.

The pore pressure induced by the degree of consolidation $U_{i,z}$ in layer z by addition of layer i is:

$$u_{\text{DOC}}(x, z) = \begin{cases} z < z_{\text{phreatic}} & \sum_{\text{layers } i} \sigma'_{\text{weight}} \times \frac{100 - U_{i,z}}{100} \\ z \geq z_{\text{phreatic}} & 0 \end{cases} \quad (5.4)$$

where

- k is the number of layers;
- $\sigma'_{i,\text{weight}}$ is the effective weight of layer i at (x, z) , see Equation (5.3) (note that σ'_{weight} will be 0 for layers below the layer of (x, z))
- $U_{i,z}$ is the provided relative degree of consolidation in layer z (the layer in which (x, z) is located) due to layer i , in %.

Examples of excess pore pressures by soil self-weight

Table 5.2 shows an example of a three layered soil structure, where there are different degrees of consolidation.

Table 5.2 Different degrees of consolidation in different layers

Layer i (top to bot- tom)	Degree of consolidation in layer i by addition of layer j	Effective stress [%]	Pore pressures [%]
1	100	1	100	0
2	70	1	70	30
	100	2	100	0
3	60	1	60	40
	90	2	90	10
	100	3	100	0

The effective stress in a point in layer 3 is equal to 60% of the effective weight of layer 1, plus 90% of the effective weight of layer 2, plus 100% of the effective weight of the part of layer 3 above the point.

The excess pore pressure at the same spot is equal to $(100\% - 60\%) = 40\%$ of the effective weight of layer 1 plus $(100\% - 90\%) = 10\%$ of the effective weight of layer 2 plus $(100\% - 100\%) = 0\%$ of the effective weight of the part of layer 3 above the bottom of the slice. This example assumes that the phreatic line is located above layer 2.

By defining the degree of consolidation for the load of each layer above the actual layer, and for the weight of the actual layer itself, it is possible to simulate different stages of a construction process. If, for example, one extra layer is placed on the surface as a new load, the early stages of construction can be calculated by assigning a low degree of consolidation in underlying layers with low permeability due to the weight of the new layer.

For points above the phreatic line, it is possible to choose whether pore (excess/under) pressures are to be used to affect the effective stress.

5.3 Pore pressure from loads

The extra pore pressure due to loads is:

$$u_{\text{load}}(x, z) = \begin{cases} z < z_{\text{phreatic}} & \left(1 - \frac{U_{\text{load},z}}{100}\right) \times \sigma_{\text{load}} \\ z \geq z_{\text{phreatic}} & 0 \end{cases} \quad (5.5)$$

where:

- $U_{load,z}$ is the given degree of consolidation to the layer in which (x, z) is located due to the load (100 in case of permanent loads);
- σ_{load} is the increase of the total stress at location (x, z) due to the load, see Equation (9.6) and Equation (9.9)

5.4 Pore pressure due to earthquake

Earthquake forces will generate excess pore pressures in soil layers that do not reach fully drained. The excess pore pressures are determined by taking into account the degree of consolidation per layer. This degree of consolidation ensures that part of the vertical acceleration results in an increase in effective stress. The other part results in excess pore pressure. The earthquake pore pressure includes the change in hydrostatic pressure due to vertical quake component. The excess pore pressure u_{quake} generated by the earthquake is:

$$u_{quake}(x, z) = \begin{cases} z < z_{phreatic} & \sigma_{quake;water} + \sigma_{quake;soil} \times \left(1 - \frac{U_{quake,z}}{100}\right) \\ z \geq z_{phreatic} & 0 \end{cases} \quad (5.6)$$

where:

- $\sigma_{quake;water}$ is the earthquake water pressure (see Equation (9.11));
- $\sigma_{quake;soil}$ is the earthquake soil pressure (see Equation (9.10));
- $U_{quake,z}$ is the given degree of consolidation of the layer in which (x, z) is located ($0 \leq U_{quake,j} \leq 100\%$);

5.5 Total pore pressure and effective stress

The excess pore pressure u_{excess} is the pore pressure which exceeds the hydraulic pore pressure u_{PL} . The excess pore pressure is obtained by adding the following contributions:

$$u_{excess} = u_{DOC} + \sum_{loads} u_{load} + u_{quake} \quad (5.7)$$

The excess pore pressure due to the wind loading of trees is zero, because trees are supposed to be non temporary.

The total pore pressure u is the sum of the hydraulic pore pressure and the excess pore pressure

$$u = u_{PL} + u_{excess} \quad (5.8)$$

where

- u_{PL} is the pore pressure derived from the PL-lines, see Equation (5.2) ;
- u_{DOC} is the pore (excess/under) pressure derived from the degree of consolidation, see Equation (5.4);
- u_{load} is the extra pore pressure from temporary distributed loads, see Equation (5.5);
- u_{quake} is the extra pore pressure due to vertical quake, see Equation (5.6).

The pore pressure derived from the PL-lines represents (u_{PL}) the situation without any loads being applied, while the extra pore pressures due to the consolidation process (u_{DOC}) and temporary loads (u_{load}) are the result of the extra loading of soils with a low permeability.

The total stress $\sigma(x, z)$ is:

$$\sigma(x, z) = \sigma_{\text{soil}} + \sum_{\text{trees}} \sigma_{\text{tree}} + \sum_{\text{loads}} \sigma_{\text{load}} + \sigma_{\text{quake;soil}} + \sigma_{\text{water}} \geq 0 \quad (5.9)$$

where

σ_{soil}	is the stress due to soil weight (see Equation (4.1)) ;
σ_{tree}	is the stress due to a tree (see Equation (9.16));
σ_{water}	is the stress due free water above the soil surface (see Equation (4.2)) ;
σ_{load}	is the increase of the total stress at depth z due to a load, see Equation (9.6) for line loads and Equation (9.9) for uniform loads.
$\sigma_{\text{quake;soil}}$	is the increase of the total stress at depth z due to an earthquake, see Equation (9.10) .

D-Stability determines the vertical effective stress σ'_v at (x, z) , using:

$$\sigma'_v(x, z) = \sigma - u \geq 0 \quad (5.10)$$

where u is the total pore pressure (see [Equation \(5.8\)](#)) and σ is the total stress (see [Equation \(5.9\)](#)).

Since the effective stress is truncated at zero, the vanished stress is added to the calculation pore pressure u_{calc} as follows:

$$u_{\text{calc}} = \begin{cases} \sigma - u \geq 0 & u \\ \sigma - u < 0 & \sigma \end{cases} \quad (5.11)$$

6 Shear strength models

Objective: To calculate the shear strength τ at any given point in the soil profile and valid for a given angle of the slip plane.

Given:

- The shear strength model to be applied at the given point. Usually the shear strength model is defined per soil in the soil profile;
- The effective stress σ' at the given point.

6.1 MohrCoulomb model (drained): classic and advanced

When selecting the material model Mohr-Coulomb, D-Stability will determine the maximum available shear strength using the following equation (Davis, 1968):

$$\tau = c \times \frac{\cos \psi \times \cos \varphi}{1 - \sin \psi \times \sin \varphi} + \sigma'_n \times \frac{\cos \psi \times \sin \varphi}{1 - \sin \psi \times \sin \varphi} \quad (6.1)$$

where:

- c is the cohesion at the given location, in kN/m²;
- φ is the friction angle at the given location, in degree ;
- ψ is the dilatancy at the given location, in degree (default 0, $0 \leq \psi \leq 90$);
- σ'_n is the normal effective stress at the given location, in kN/m². The normal effective stress is determined within the limit equilibrium methods, see [chapter 7](#).

It should be noted that the definition of maximum available shear strength, equation (6.1) includes the dilatancy angle, which is different from the classical definition typically used in many handbooks on geotechnical engineering. When selecting $\psi = \varphi$, equation (6.1) transforms into the classical definition of the classic Mohr-Coulomb failure criterion:

This is the well-known Mohr-Coulomb definition of the failure line. By choosing Mohr-Coulomb classic, $\psi = \varphi$ is used which results in the classical Mohr-Coulomb behavior.

Assuming $\varphi \neq \psi$ gives so called non-associative behavior. When using $\psi = 0$, the shear strength becomes

$$\tau = c \times \cos \varphi + \sigma' \times \sin \varphi.$$

This way, plasticity can be taken into account when describing the strength. The following subsections provide more details on the background of equation (6.1) and selecting values for φ and ψ .

6.1.1 Introduction

D-Stability enables the use of different shear strength models to prescribe the maximum available shear strength along a potential sliding plane. One of these models is the Mohr-Coulomb (drained) model. Hereafter referred to as the MC-model. The D-Stability implementation of the MC-model requires the dilatancy angle, *varpsi*. The use of the dilatancy angle in the MC-model differs from the classical Mohr-Coulomb criterion as discussed in many textbooks, e.g. Verruijt (2012).

This text provides the theoretical background for including the dilatancy angle in the strength criterion. Next a comparison to constitutive models, as used in finite element analysis, is presented. Finally, some practical comments are presented in using the dilatancy angle in the strength criterion.

6.1.2 Theoretical background

Discussion on the soil strength that actually develops along a sliding plane has a long history. In that discussion Roscoe (1970) presents the results of 10 years of research at Cambridge University. The research comprehends the study on the stability of retaining walls and the mobilisation of the active and passive soil resistance. An important conclusion of the studies is that the rupture plane is not the plane along which the $(\tau/\sigma)_{max}$ is mobilised and the conventional Mohr – Coulomb failure criteria should be reconsidered. As stated by Roscoe (1970):

... Perhaps the most important fundamental error made in conventional methods of analysis, in which a shape is assumed for the rupture surface, is that the limiting maximum value of the stress ratio acts on that surface...

To follow the reasoning that lead to this conclusion, first the angle of principle stress, θ , the angle of principal strain increment, ξ and principal stress increment, χ are introduced, see the figure underneath. It should be noted that Roscoe (1970) uses the symbol ψ for the angle of principal stress, which conflicts with the use of ψ to represent the dilatancy angle as adopted in D-Stability.

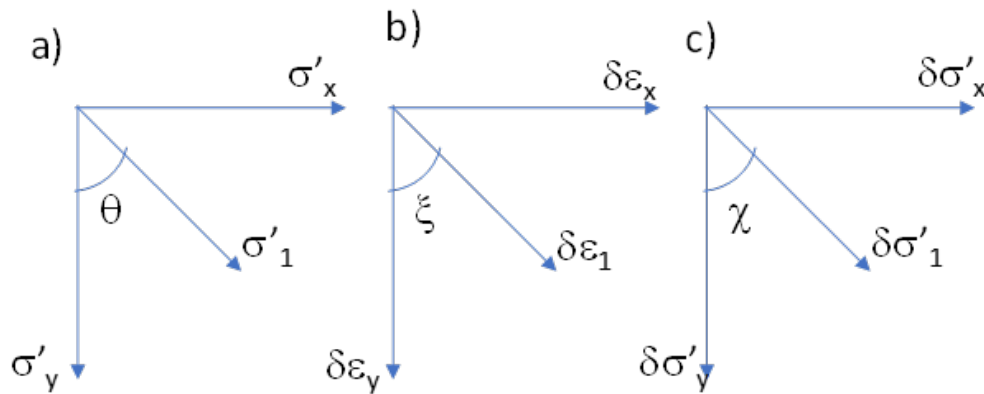


Figure 6.1 Definition of a-angle of principle stress, θ , b- the angle of principal strain increment, ξ and c-the angle of principal stress increment, χ

Figure 6.2 shows the results of two direct simple shear test results on Leighton Buzzard sand as presented by Roscoe (1970). The figure shows the development in the angles of principal effective stress θ , principal strain increment ξ and principal effective stress increment, χ . In which it should be noted that Roscoe (1970) uses the symbol φ for ψ .

Figure 6.2 shows that initially the angles of principal stress, θ , principal strain increment, ξ and principal stress increment, χ differ. After some deformation, when plasticity dominates soil behavior, the angle of principal strain increment, ξ aligns with the angle of principal effective stress, θ and not the angle of stress increment, χ .

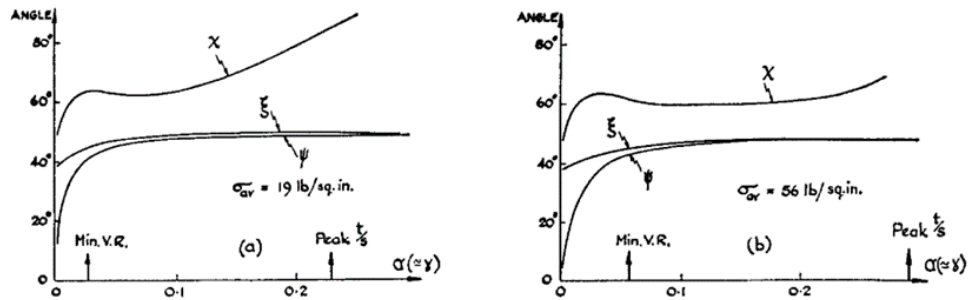


Fig. 9. Curves showing angles made with the vertical of directions, ψ of σ_1 , ξ of $\dot{\epsilon}_1$ and χ of $\dot{\sigma}_1$ (see Fig. 6(c)) during simple shear tests on medium dense ($e_0=0.64$) sand at $\sigma'_{av}=\text{constant}$: (a) 19 lb/sq. in., (b) 56 lb/sq. in.

Figure 6.2 Results of Direct Simple Shear tests on Leighton Buzzard sand, from Roscoe (1970). The symbol ψ in this figure stands for the angle of principal effective stress, θ 19 lb/sq in = 131 kPa and 56 lb/ sq in = 386 kPa

In the tests on the stability of retaining walls, the soil deformation and mobilised shear strength was studied by applying a rotation of the retaining wall while monitoring the response of the soil. The tests include the use of many lead balls that were placed in the soil surrounding the retaining wall. After a test was finished the exact position of the balls was determined using the Röntgen technique. From the observed displacements strain and strain increments were determined.

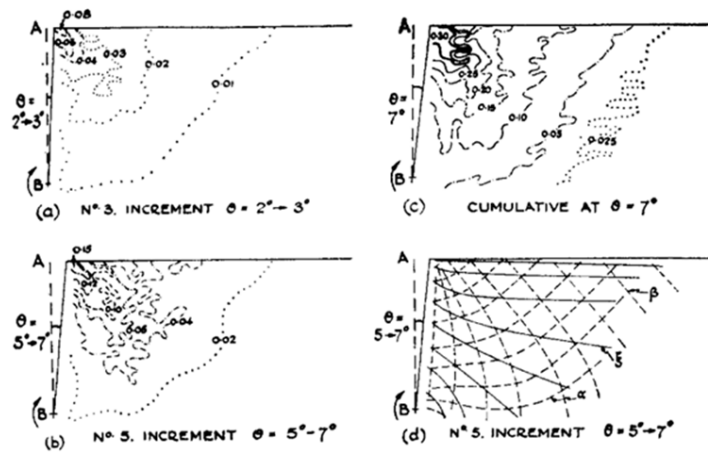


Fig. 24. Typical contours of incremental or cumulative shear strain and zero-extension line mesh at various stages of rotation of wall AB about its toe B into loose sand. Test PH ($e_0=0.77$). (a) and (b) Contours of maximum shear strain rate $\dot{\gamma}$, (c) contours of maximum shear strain γ , (d) α and β zero-extension lines and directions ξ of $\dot{\epsilon}_1$ during $\theta=5^\circ \rightarrow 7^\circ$

Figure 6.3 Typical test result from Roscoe (1970)

The test results reveal the location of zero extension lines, indicated by α and β in Figure 6.4. The rupture plane develops along one of the zero extension lines. The test results also reveal the position of lines with constant angle of principal strain increment, the ξ - lines. The zero extension lines, α and β cut the ξ -lines with angle of $[45 - (\psi/2)]$, with ψ representing the dilation angle.

Plastic behaviour of large soil volumes can be described using velocity characteristics and stress characteristics. The velocity characteristics coincide with the zero extension lines and are described by:

$$[h] \frac{dx}{dy} = \tan \left[\xi \pm \left(\frac{\pi}{4} - \frac{\psi}{2} \right) \right] \quad (6.2)$$

For a perfect plastic material, stress characteristics provide the lines along which the friction angle is mobilised, is the maximum τ/σ . The direction of the stress characteristics is given by:

$$[h] \frac{dx}{dy} = \tan \left[\theta \pm \left(\frac{\pi}{4} - \frac{\varphi'}{2} \right) \right] \quad (6.3)$$

Figure 6.2 illustrates that during plastic deformation the angle of principal strain increment, ξ , coincides with the angle of principal effective stress, θ ; $\xi = \theta$. The direction of the velocity characteristics, the zero extension lines which represent the rupture plane, equation (6.1) only corresponds to the direction of the stress characteristics, the plane along which friction angle is completely mobilised, equation (6.2), when $\varphi = \sigma'$. For φ is not equal to σ' the rupture plane will not follow the plane for which the friction angle is completely mobilised.

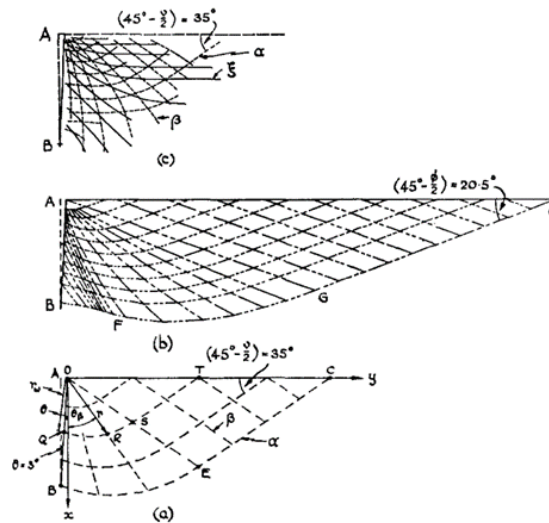


Fig. 30. Simultaneous field of characteristics for wall AB after rotating ($\theta=3^\circ$) about toe B into dense sand ($e_0=0.51$) during test PE: (a) simple assumed velocity characteristics for $\nu=20^\circ$, (b) Sokolovski (1965) stress field for $\varphi=49^\circ$ and δ' distribution given by S_1, S_3 in Fig. 20(a), (c) observed zero-extension line field (velocity characteristics)

Figure 6.4 Stress and strain increments observed after a rotation of a retaining wall, from Roscoe (1970), the symbol ν is used for angle of dilatancy which is represented by ψ in this text

It should be noted that constant volume deformation, undrained deformation, is found for $\varphi = \sigma'$ and the rupture plane does follow the zero-extension line. For drained behaviour, typically when φ is not equal to σ' the rupture plane will typically not follow the plane along which the friction angle is completely mobilised.

Figure 6.4 shows stress and strain increments near failure in one of the tests presented by Roscoe (1970). The figure clearly shows the difference between the stress characteristics, Figure 6.4b and the zero extension lines, Figure 6.4c.

The findings of Roscoe (1970) have consequences for slip plane analysis. In limit equilibrium methods a failure plane is assumed and equilibrium of forces or momentum for that failure plane is checked. When prescribing the maximum shear strength along that failure plane by the completely mobilised friction angle; $\varphi = \sigma' = (\varphi = \sigma')_{\max}$ it is implicitly assumed that $\varphi = \psi'$. As shown above, this is only correct for undrained, constant volume, conditions. It should be noted, that when applying the Mohr-Coulomb criteria in limit equilibrium methods, the maximum shear strength is described by $\varphi' = \sigma = (\varphi = \sigma')_{\max}$ and implicitly $\varphi = \psi'$ is assumed.

The shear strength mobilised along a zero-extension line, as depicted by Figure 4c, is given by Davis (1968):

$$\tau = c \times \frac{\cos \psi \times \cos \varphi}{1 - \sin \psi \times \sin \varphi} + \sigma'_n \times \frac{\cos \psi \times \sin \varphi}{1 - \sin \psi \times \sin \varphi} \quad (6.4)$$

When selecting $\varphi' = \psi$, equation (6.4) transforms into the classical definition of the Mohr-Coulomb failure criterion:

$$\tau = c + \sigma' \times \tan \varphi' \quad (6.5)$$

For $\psi = 0$ follows:

$$\tau = c \times \cos \varphi' + \sigma' \times \sin \varphi' \quad (6.6)$$

The angle between the slip plane and principal stress direction is found in Figure 6.4b and c, as the horizontal ground level behind the retaining wall is aligned with principal stress direction. For the Mohr-Coulomb criterion, $(\varphi = \sigma')$ max is assumed along the sliding plane and the sliding plane is assumed to coincide along the stress characteristics, show by Figure 6.4b. The angle between ground level and slip plane is for the MC criterion given by $(45 - \varphi'/2)$. For the Roscoe / Davis criterion the slip plane is found along the zero-extension line as given by Figure 6.4c and corresponding angle is $(45 - \psi/2)$.

Vardoulakis (1980) en Vermeer (1982) show by mathematical exercise that the angle between a slip plane and principal stress direction is bounded by $(45 - \varphi'/2)$ and $(45 - \psi/2)$. The Mohr -Coulomb and Davis criterion provide lower and upper boundary.

Several authors have published on the development and location of sliding planes in granular materials. Typically, these papers have strong fundamental approach and results are not easily translated to practical engineering.

Saada et al (1994) discusses test results that indicate the shear plane development in undrained tests on clay. As shown above the differences between the Mohr-Coulomb criterion and the Roscoe and Davis approach vanishes for undrained behaviour.

Kwak et al (2020) discuss the development of a rupture plane in a triaxial compression tests on clay. Using particle image velocimetry (PIV) analysis, the rupture plane is visualised in different stages of the test.

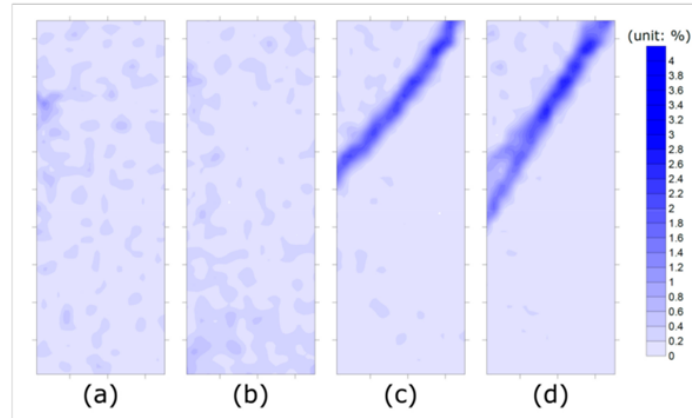


Figure 13. Increasing shear strain for OC1: (a) initial; (b) peak; (c) softening; and (d) steady state.

Table 3. Inclination angles for each stage with the internal friction and dilatation angle.

Description	Stage	ϕ'	ψ	$\theta_{Measured}$	θ_{MC}	θ_R	θ_A
NC1	Softening	37.1°	13.2°	52.1°	63.6°	51.6°	57.6°
	Steady state	36.7°	7.1°	59.2°	63.4°	48.6°	56.0°
NC2	Softening	36.9°	8.3°	49.6°	63.5°	49.2°	56.3°
	Steady state	36.1°	1.5°	56.1°	63.1°	45.8°	54.4°
OC1	Softening	39.0°	12.8°	51.7°	64.5°	51.4°	58.0°
	Steady state	37.9°	9.4°	56.3°	64.0°	49.7°	56.8°
OC2	Softening	38.7°	17.8°	52.3°	64.4°	53.9°	59.1°
	Steady state	38.1°	9.3°	55.2°	64.1°	49.7°	56.9°

Figure 6.5 Development of a failure plane in clay in a triaxial compression test, from: Kwak et al. (2020)

The failure plane development is subdivided in four stages, a) initial stage, b) peak, c) softening and d) steady state. The failure plane becomes only visible in the softening stage. During the softening stage, the failure plane develops and the inclination changes slightly. Kwak et al. (2020) compare the inclination of the sliding plane, $\sigma_{measured}$ with the predicted inclination by the Mohr Coulomb model, σ_{mc} , the Roscoe approach, σ_r and the solution presented by Arthur (1978), σ_A . The value for σ_A is given by $\sigma_A = 45 + (\psi + \phi')/4$.

For the steady state conditions $\sigma_{measured}$ was best reproduced by σ_A . While in the softening phase $\sigma_{measured}$ was best reproduced by σ_r . It should be noted that for the tests discussed in Roscoe (1970) the applied deformations were relatively small and steady state conditions along the sliding were probably not reached.

Teunissen (2016) links the theory described above to the practice of slip plane analysis. At failure, the maximum shear strength along a sliding plane should be described, using $\sin(\phi')$, which assumes $\psi = 0$. However, typically soil parameters are derived from axial symmetric testing conditions while calculations are conducted for plane strain conditions. The difference in shear strength mobilised in axial symmetric and plane strain conditions is discussed by, among others, Wroth (1984). Teunissen (2016) shows that the difference in shear strength due to the difference between the Mohr – Coulomb criterion and the Roscoe / Davis approach is largely counter balanced by the difference in shear strength for plane strain and axial symmetric conditions.

6.1.3 Numerical simulation

To test how the strength of soil predicted by the Mohr-Coulomb model in finite element analysis is influenced by the dilatancy angle, a series of direct simple shear test simulations has been made. The simulations are made using the PLAXIS soil test module, version 2019. The exact implementation of the MC-model in PLAXIS is presented in the PLAXIS manual.

For reasons of clarity the strength criterion by Davis (1968) is repeated:

$$\tau = c \times \frac{\cos \psi \times \cos \varphi}{1 - \sin \psi \times \sin \varphi} + \sigma'_n \times \frac{\cos \psi \times \sin \varphi}{1 - \sin \psi \times \sin \varphi} \quad (6.7)$$

for $\varphi' = \psi$ follows:

$$\tau = c + \sigma' \times \tan \varphi' \quad (6.8)$$

For $\psi = 0$ follows:

$$\tau = c \times \cos \varphi' + \sigma' \times \sin \varphi' \quad (6.9)$$

The applied soil properties are given in the table underneath. The initial vertical stress is $\sigma'_{yy} = 100 \text{ kN/m}^2$ in each simulation. In a direct simple shear test, the vertical stress acts perpendicular to the sliding and $\sigma_y = \sigma_n$. With $c' = 0$ the classical MC criterion provides $\tau = 100 \tan(30) = 57,7 \text{ kN/m}^2$, equation (6.8). The Roscoe / Davis approach, for $\psi = 0$, results in $\tau = 100 \sin(30) = 50 \text{ kN/m}^2$, equation (6.9).

simulation	1	2	3	4
γ , [kN/m ³]	0	0	0	0
c' [kN/m ²]	0	0	0	0
φ' [°]	30	30	30	30
ψ [°]	0	30	0	30
E [kN/m ²]	5000	5000	5000	5000
ν [-]	0,33	0,33	0,33	0,33
K_0^a	0,5	0,5	2	2

The K_0 -value refers to the initial stress conditions at the start of the shearing phase.

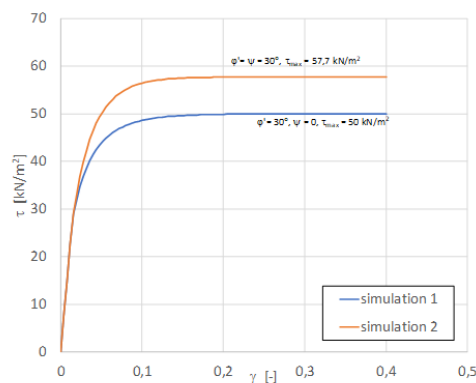


Figure 6, Stress – strain relation for simulations 1 and 2, $K_0 = 0.5$

Figure 6.6 Stress – strain relation for simulations 1 and 2, $K_0 = 0.5$

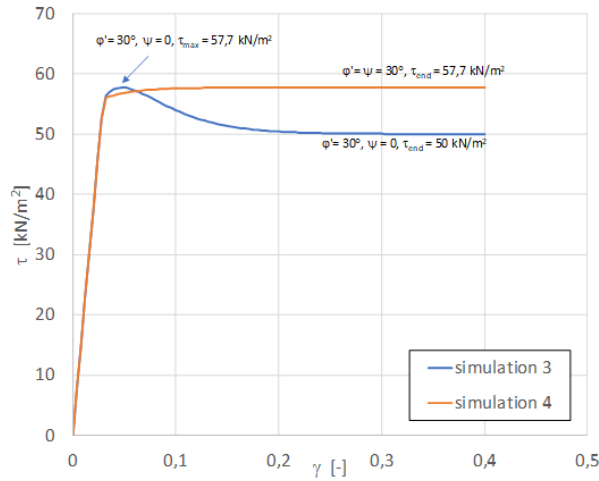


Figure 6.7 Stress – strain relationship for simulations 3 and 4, $K_0 = 2,0$

Figure 6.6 shows that for using $\psi = \varphi$, the shear strength on the sliding plane is determined by $\sigma' n \times \tan(\varphi')$ and the classical Mohr-Coulomb strength criterion is found. For $\psi = 0$ follows that the obtained strength is determined by $\sigma' n \times \sin(\varphi')$, conform the Roscoe / Davis approach.

The influence of the horizontal stress is remarkable, for $K_0 = 2$, as presented in Figure 7, follows, $\psi = 0$ a peak strength at $\sigma' n \times \tan(\varphi')$ and a final strength at $\sigma' n \times \sin(\varphi')$. It should be noted that the mathematical description of the Mohr-Coulomb model does not include softening. The observed softening is caused by the stress rotation caused by the applied shear deformation. For $\psi = \varphi'$, no peak is observed and mobilised shear strength follows from equation (6.1).

The simulations presented by Figure 6.6 and Figure 6.7 support the use of equation (6.3) in prescribing the maximum available shear strength along a sliding plane.

6.1.4 Advice on the use of the dilatancy angle ψ in D-Stability

As explained above Teunissen (2016) shows that in the daily practice of slope stability analysis two effects play a role that roughly undo each other:

- The classical MC-criterion is used on a prescribed failure plane and shear strength is determined by $\tan(\varphi')$, where $\sin(\varphi')$ should be more appropriate, see equation (3).
- Soil parameters are typically determined from axial symmetric laboratory tests and count for axial symmetric stress conditions, while these parameters are typically applied in plane strain calculations.

Wroth (1984) and others indicate that the difference in strength for axial symmetric and plane strain conditions is given by:

$$\phi'_{ps} \approx \frac{9}{8} \phi'_{tc} \quad (6.10)$$

In which ϕ'_{tc} represents the friction angle in triaxial compression and ϕ'_{ps} the friction angle in plane strain stress conditions.

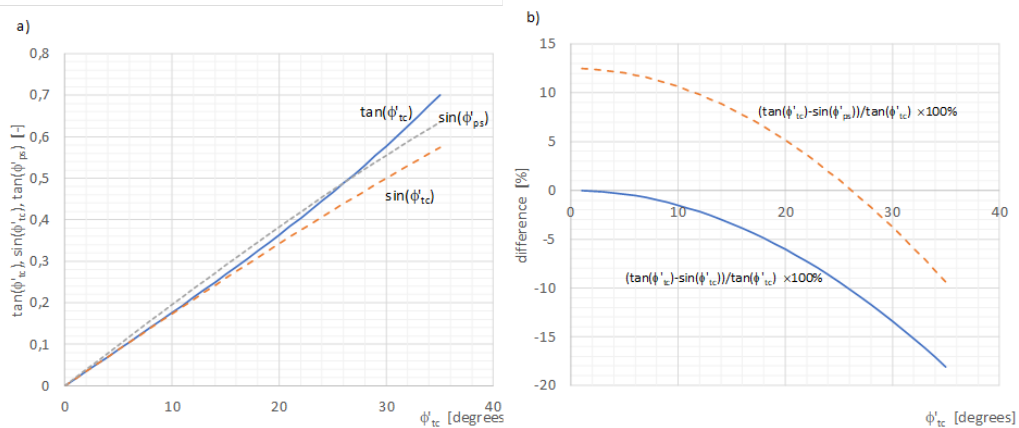


Figure 6.8 The difference in using triaxial compression and plain strain

Figure 6.8 shows that when using $\sin(\varphi'_{tc})$ instead of $\tan(\varphi'_{tc})$ the prescribed maximum shear strength for a certain stress will drop. However, when correcting for plane strain conditions and using $\sin(\varphi'_{ps})$, the difference with $\tan(\varphi'_{tc})$ reduces. For the range of typical values for φ'_{tc} for soils, $20 < \varphi'_{tc} < 35$ the difference in using $\sin(\varphi'_{ps})$ instead of $\tan(\varphi'_{tc})$ is in the order of ≈ 5 percent.

The conventional MC-criterion is found in D-Stability, when for the dilation angle the same value is selected as applied for the friction angle, $\psi = \varphi'$. It should be noted that the default value in D-Stability gives $\psi = 0$ and the conventional MC-criterion is not found by default.

Only in special cases $\psi \neq \varphi'$ should be selected. Examples of these special cases are for example:

- When the corresponding difference in axial symmetric plane strain stress conditions are accounted for or in some way acknowledged;
- When comparing the results produced by D-Stability to finite element calculation results that include the use of advanced material models;
- When assessing slope stability according to the Dutch regulations, MinlenM (2016) on water retaining structures (where the corresponding difference in axial symmetric plane strain; stress conditions and differences between compression and extension conditions and its uncertainties are accounted for in the model uncertainty factor).

In selecting the ψ -parameter to be used in D-stability, the following considerations play a role:

Classical MC-Criterion

- The classical MC-criterion is found for $\psi = \varphi'$. The Mohr-Coulomb classic model gives default $\psi = \varphi'$.

Roscoe – Davis approach

- The Roscoe / Davis approach is found for $\psi = \varphi'$;
- It can be used by selecting Mohr-Coulomb advanced in D-Stability;
- This approach should only be used when the difference between plane strain conditions, for which the calculations are conducted and the axial symmetric conditions for which the soil parameters typically are derived for, is acknowledged or accounted for;
- A typical value for clays is $\psi = 0$ degrees;

- When applying shear strength at large deformation, for example at critical state or residual strength, $\psi = 0$ is suggested for clays and sands.

6.1.5 References regarding Mohr Coulomb advanced model

- Davis E.H. (1968) Theories of plasticity and the failure of soil mass in: Soil Mechanics, selected topics (Lee editor), Butterworth, London
- Kwak T-Y., Park K-H., Kim J., Chung C-K., Baek S-H (2020) Shear band characterization of clayey soils with particle image velocimetry journal of applied sciences 10, 1139; doi:10.3390/app10031139
- Minlen M (2016) Schematiseringshandleiding Macrostabiteit binnenwaarts, Ministerie van Infrastructuur en Milieu
- Roscoe K.H. (1970) The influence of strains in soil mechanics (tenth Rankine lecture) Géotechnique 20 no 2 p 129 - 170
- Saada A.S., Bianchini G.F., Liang L. (1994) Cracks, bifurcation and shear bands propagation in saturated clays Géotechnique 44 no 1 p 35-64
- Teunissen J.A.M. (2016) Wrijving in sterkteberekeningen, Geotechniek, juli 2016, p 8-13
- Vardoulakis I., (1980) Shear band inclination and shear modulus of sand in biaxial tests Int. J. Numer. Anal. Methods Geomech. 4:103-119.
- Vermeer P.A. (1982) A simple shear band analysis using compliances in: IUTAM Conference on Deformation and Failure of Granular Materials, Delft
- Verruijt A. (2012) Soil Mechanics, Delft University of Technology free downloadable: <https://ocw.tudelft.nl/wp-content/uploads/SoilMechBook.pdf>
- Wroth C.P. (1984) The interpretation of in situ soil tests Géotechnique 34 no 4 p 449-489, DOI 10.1680/geot.1984.34.4.449

6.2 SHANSEP (undrained)

The Shansep formulation of undrained shear strength uses two material parameters (S and m) and one state parameter (σ'_y).

6.2.1 Yield stress

The effective vertical stress takes the history of the soil into account. We assume that the soil retains the maximum experienced effective stress (also called yield stress) σ'_y per location in the subsoil. The relation between the yield stress and the effective stress (see Equation (5.9)) is defined by the POP (the pre-overburden pressure) parameter:

$$\sigma'_y = \sigma'_v + \text{POP} \quad (6.11)$$

or by the OCR (over consolidation ratio) parameter:

$$\sigma'_y = \sigma'_v \times \text{OCR} \quad (6.12)$$

where

- σ'_y is the vertical yield stress in kN/m²;
- σ'_v is the vertical effective stress (see Equation (5.10)) in kN/m²

- POP is the provided pre-overburden pressure (this parameter is usually used to take into effect the effect of a preconsolidation in kN/m²;
- OCR is the provided over consolidation ratio (this parameter is usually used to take into account the effect of aging); [-]

It is indicated whether the POP or OCR is to be used.

6.2.2 Calculating the undrained shear stress

The kernel will calculate the shear stress along the slip plane from the ratio S between the undrained shear strength and the yield stress, according to the following equation:

$$\tau = s_u = \begin{cases} \sigma'_v > 0 & \sigma'_v \times S \times \left(\frac{\sigma'_y}{\sigma'_v}\right)^m \\ \sigma'_v = 0 & 0 \end{cases} \quad (6.13)$$

where

- S is the provided ratio between the undrained shear strength s_u and the yield stress [-];
- m is strength increase exponent [-];
- σ'_v is the effective stress [kN/m²] (see Equation (5.10));
- σ'_y is the maximum experienced vertical yield stress [kN/m²] (see Equation (6.11) or Equation (6.12));

6.2.3 Yield stress field

Yield stresses, nor POP or OCR values, are not given at each location in the soil profile, but in a limited set of points in layers or along reference lines. This section describes how the yield stresses from these set of points are used to calculate the yield stress at any given location (x , z).

In order to do so, a number of stress points are defined. In Figure 6.9, there is one layer with four stress points.

Each stress point contains a value p for either POP, OCR, σ'_y or s_u . All stress points (within a construction stage, see section 6.2.4) contain the same parameter type p . This value can be converted to the yield stress using Equation (6.11), Equation (6.12) or Equation (6.13).

The way yield stress values are interpolated between points is provided by yield stress lines, similar to reference lines and head lines (see section 5.1.1). Each yield stress line is contains a number of stress points, which define the value of a stress related parameter p .

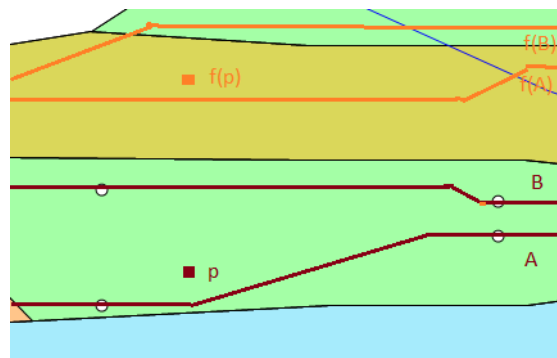


Figure 6.9 Yield stress points

Yield stress lines can be created along a reference line or around a layer. Values along a reference line can be different above then below. When a state point is placed inside a material, the inside values will be according to the entered yield value, the outside values will be zero.

Note: Combining state points in a layer and state lines in one building phase can be dangerous. The layer will have "zero" outside. Therefore, the state line will interpolate linear to this zero value. State points and state lines better not be used in the same building phase. Always check the results with the profile inspector.



When the value of a location between yield stress lines is requested, the value is interpolated. First an interpolation is performed in x -direction, then in z -direction. The interpolation is always linear, but the parameter which is regarded as linear is either σ'_y , POP, OCR or s_u . This linear parameter is provided. The yield stress or another value p at location (x, z) is interpolated as follows:

$$p_{\text{interpolated}} = \frac{z - z_A}{z_B - z_A} \times p(A) + \frac{z_B - z}{z_B - z_A} \times p(B) \quad (6.14)$$

where

- p is the provided linear parameter, one of POP, OCR, σ'_y or s_u ;
- A is the nearest yield stress reference line below p ;
- B is the nearest yield stress reference line above p ;
- $p(A)$ is the parameter value at the line A ;
- $p(B)$ is the parameter value at the line B ;

Using Equation (6.11), Equation (6.12) and Equation (6.13), the yield stress at any location and depending on the interpolation parameter p will be

$$\sigma'_y(x, z) = \begin{cases} \text{POP} & \sigma'_v + \text{POP}_{\text{interpolated}} \\ \text{OCR} & \sigma'_v \times \text{OCR}_{\text{interpolated}} \\ \sigma'_y & \sigma'_{y, \text{interpolated}} \\ s_u & \sigma'_v \times \left(\frac{s_{u, \text{interpolated}}}{\sigma'_v \times S} \right)^{\frac{1}{m}} \end{cases} \quad (6.15)$$

where

- $\text{POP}_{\text{interpolated}}$ is the interpolated POP value, using Equation (6.14) and $p = \text{POP}$;
- $\text{OCR}_{\text{interpolated}}$ is the interpolated OCR value, using Equation (6.14) and $p = \text{OCR}$;
- $\sigma'_{y, \text{interpolated}}$ is the interpolated OCR value, using Equation (6.14) and $p = \sigma'_y$;
- $s_{u, \text{interpolated}}$ is the interpolated OCR value, using Equation (6.14) and $p = s_u$;

6.2.4 Construction stages

Construction stages are primarily used to derive a proper yield stress field. Each previous state is taken into account when determining the current yield stress.

The development of yield is due to past fluctuations of effective stress can be described by building stages, where each stage has a soil profile, hydraulic circumstances, state and external loads. For example, there can be two stages, the first stage with daily circumstances

and the second with the high water situation. Another example is the simulation of a construction in several stages, where each stage represents a construction phase and has an additional soil layer in the soil profile.

Note: The previously known reference level defined the surface line without recent embankments or excavations. This reference level is replaced by two stages, which differ at the level of the reference line and is therefore no longer supported. This reference line will not be imported when importing an old .sti file.



Since we assume that the yield stress is retained during stages, but can be increased if a higher effective stress occurs in the current stage n , we can write

$$\sigma'_{y,\text{stage } n} = \max(\sigma'_{y,\text{stage } n-1}; \sigma'_y \geq \sigma'_v) \quad (6.16)$$

where

- $\sigma'_{y,\text{stage } n-1}$ is the yield stress of the previous stage using the same Equation (6.16) or 0, if no previous stage is available [kN/m²];
- σ'_y is the yield stress derived from the yield stress field (see Equation (6.15)) [kN/m²];
- σ'_v is the effective stress (see Equation (5.10)) [kN/m²];

Using Equation (6.13), the shear strength in the last construction stage becomes

$$\tau = s_u = \begin{cases} \sigma'_v > 0 & \sigma'_v \times S \times \left(\frac{\sigma'_{y,\text{last stage}}}{\sigma'_v}\right)^m \\ \sigma'_v = 0 & 0 \end{cases} \quad (6.17)$$

- $\sigma'_{y,\text{last stage}}$ is the yield stress of the last stage, see Equation (6.16) in [kN/m²];

6.3 Su table (undrained)

6.3.1 Introduction

Transitional soils (dilatant silty clays) or wet embankment material above the phreatic line do not always behave conform a SHANSEP material. In this case, it is possible to enter the relationship between the effective stress en the undrained shear strength directly through a *Su Table*.

When using the *Su Table* shear strength model, D-Stability will determine the shear strength at the bottom of a slice using the provided Su table.

The Su table represents an undrained material model. When this table is used with its default values (m=1), the strength of the material will not be effected by changing effective stresses in the current construction phase. If the strength is influenced by changing effective stresses, this can be realized with the parameter m, see section 6.3.3.

The SU table allows for a user defined relationship between the effective stress and the undrained shear strength within a material/layer. The undrained shear strength is based upon field- and/or lab tests and is turned into an average or design table through a statistical analysis. This average- or design value represents the undrained shear strength of the in-situ

situation of the soil. An example is given in the next figure. The bold line represents the average value, the bottom dashed line the design values given a log-normal distribution.

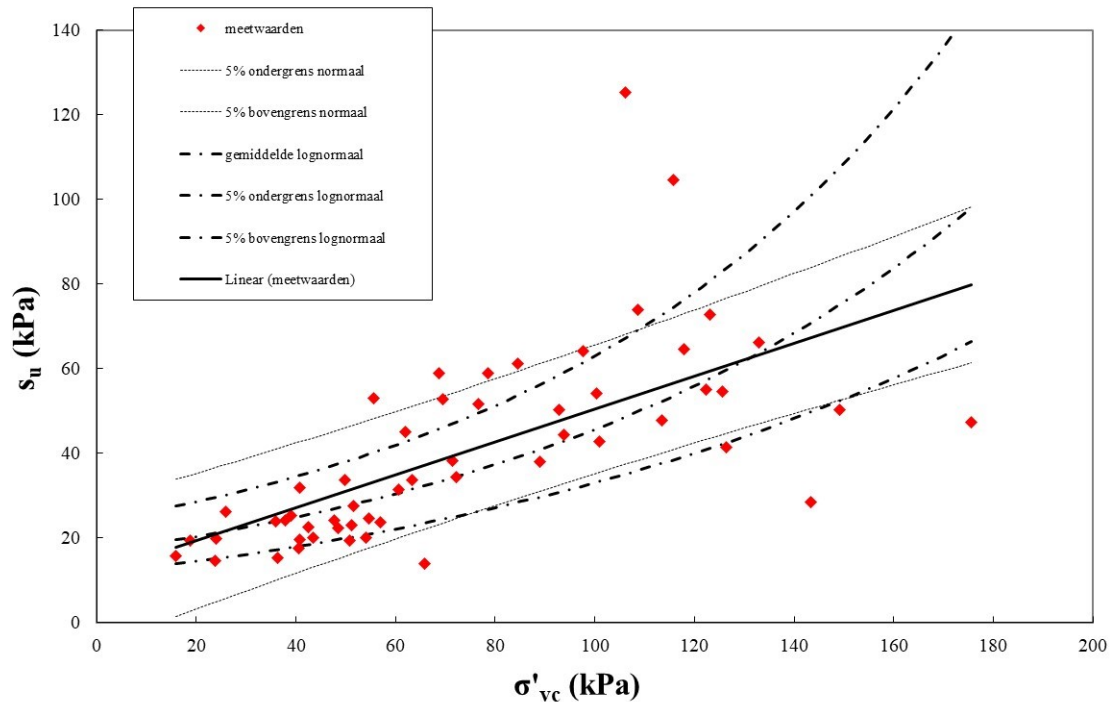


Figure 6.10 Average and design values of the undrained shear strength - effective stress relationship based upon statistical analysis of lab tests

Note: When effective stresses change in a construction phase, one cannot directly read the new S_u from the table. This table is valid at the bottom of the slices. Scaling of the strength due to changing effective stresses happens through the SHANSEP parameter 'm', see section 6.3.3



Each table is defined as a list of S_u -points where each point consists of an effective stress value combined with its belonging undrained shear strength (S_u) value. Linear interpolation takes place between the points.

Note that if the calculated effective stress for which the table is being interpolated exceeds the maximum effective stress in the table, the S_u value belonging to the last S_u -point is returned. If the first S_u point in the table has an effective stress > 0 , D-Stability interpolates from the first point to the origin.

6.3.2 Format of the table

The table can be pasted into D-Stability by clicking on the dots at the right above the selected S_u table (undrained) shear strength model.

The format of the table can be copied to the clipboard using the GUI of D-Stability. This empty table can be extended with the values the user has derived.

The S_u table is described as plane text in ASCII format and can be edited in, for example, Notepad. Copy/paste from Excel works in most cases, depending upon your regional settings.

The data must contain two columns. The first column contains the effective stress, the second column the undrained shear strength at that stress. The content must adhere to the following specifications:

- the decimal separator must be a "," (comma) or a "." (period);
- the list separator must be a ";" (semicolon), ":" (colon) or a "tab";
- all numbers must be positive;
- the numbers in the first column must be in ascending order.

If no strength is defined at zero effective stress, the point (0,0) is added to the table. The strength remains constant to the right of the last point in the table.

6.3.3 Scaling over 'm'

The stress-strength relationship of an undrained material can depend upon its history. The undrained shear strength under normal circumstances (initial stage) can be scaled to the shear strength during a high water situation (current stage). Scaling happens through the following formula:

$$S_{u_{current}} = S_{u_{table}} \times \left(\frac{\sigma'_{v;current}}{\sigma'_{v;max}} \right)^{1-m} \quad (6.18)$$

where:


$S_{u_{current}}$ is the undrained shear strength at the current stage (high water situation) in [kN/m²];

$S_{u_{table}}$ is the undrained shear strength under daily circumstances, as defined in the Su table in [kN/m²];

$\sigma'_{v;current}$ is the effective stress in the current stage [kN/m²];

$\sigma'_{v;max}$ is the highest effective stress in the previous construction stages kN/m²];

m is the strength increase exponent [-];

Note: if $m=1$, no scaling will take place and strength will remain as defined in the previous phase with the highest effective stresses. In that case, the undrained strength does not change as effective stresses change in current stage. 

Note: if $m=0$, the scaling will be linear with changing effective stresses. 

6.3.4 Graphical representation of the scaling over 'm'

This section walks through five construction stages to show how the undrained shear strength is scaled through the stages and changing effective stresses. The following stages are considered.

- 1 Stage 1: daily circumstances.
- 2 Stage 2: high water situation.
- 3 Stage 3: strengthening of the embankment.
- 4 Stage 4: no changes (consolidation period).
- 5 Stage 5: high water after strengthening.

The strength is determined at the bottom of one given slice from 'm' and the Su table as follows.

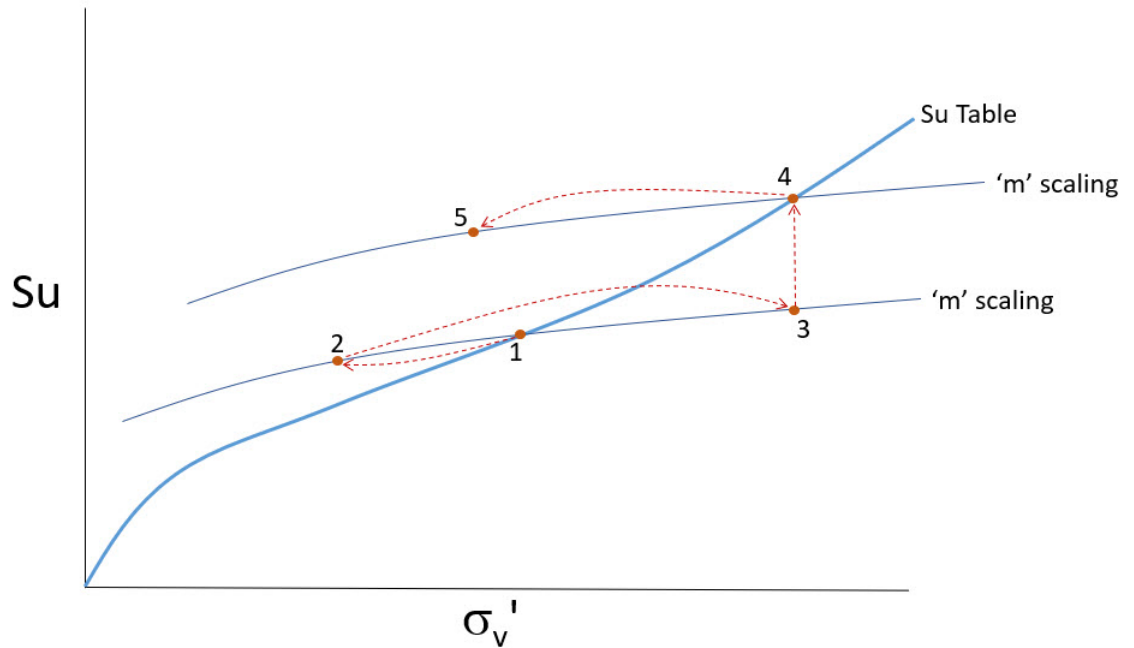


Figure 6.11 Scaling over m along the five construction stages

The effects on the S_u and thereby the safety factor are as follows.

- 1 Stage 1: Under the daily circumstances, all stress history effects are incorporated in the SU table and therefore the SU will be used "as is" in the Su Table. State points and state lines will be ignored if the Su Table material model is used.
- 2 Stage 2: Decreasing effective stresses - for example due to high water - cause scaling over 'm'. The safety factor decreases, but not as rapidly as the SU table itself.
- 3 Stage 3: The strengthening of the embankment increases the strength by scaling along the m line. The safety factor increases, but slower than the Su table itself would imply. This is due to the fact that this step implies an undrained loading step.
- 4 Stage 4: In this stage, a previous stage with higher effective stresses is available (stage 3). This stage is now the reference ($\sigma'_{v;max}$ from formula 6.9) in the SU table where stage 1 was the reference until now. The safety factor between stage 3 and stage 4 will increase. This is due to the fact that the model implies you return to the Su Table after consolidation.
- 5 Stage 5: Decreasing effective stresses cause scaling over 'm' again, but from a higher reference point. The safety factor decreases, but will remain higher as in stage 2 because the scaling is initiated from a higher point due to a higher $\sigma'_{v;max}$ in the past.

It is important to note that the safety factor increases between stages 3 and 4, even though no changes are made. This is due to a higher $\sigma'_{v;max}$ in stage 3 that become available in stage 4. The step from stage 3 to stage 5 can also be made directly, stage 4 is given in this example for illustration purposes.

6.3.5 SU tables in probabilistic analysis

Unlike all other parameters, a *Su Table* does not have a standard deviation but a variation coefficient.

Other parameters have a "deterministic" value, a "mean" value and a standard deviation to calculate the design value (5% lower bound). This way, the deterministic value is known along with the mean and the design value. In calculation settings, the user must choose in which mode the analysis is run.

As only one SU table is present with its variation coefficient, the D-Stability does not know whether this table is a design- or an average table. D-Stability uses the SU table as follows in the available calculation settings:

- Deterministic: the table is used "as is."
- Average: the table will be used "as is." It is assumed that the table contains average values.
- Design: the table is assumed to contain average values. Therefore, the table is scaled to the lower 5th percentile using a log normal distribution and the variation coefficient.
- Probabilistic: the table is assumed to contain average values. Realizations will be drawn using the available variation coefficient, assuming a log normal distribution around this average table.

Please note that the user can use a design table in deterministic mode, but when switching to another mode, this table must contain average values.

6.4 Calculation shear strength

The formulation of the shear strength in the previous paragraphs can be written as

$$\tau = c_{\text{calc}} + \sigma'_n \times \tan \varphi_{\text{calc}} \quad (6.19)$$

where

- τ is the shear strength;
- σ'_n is the normal effective stress, see Equation (5.10);
- c_{calc} is an adapted soil strength, in such a way that all previous shear strength models are true;
- φ_{calc} is an adapted friction angle strength, in such a way that all previous shear strength models are true;

Depending on the shear strength model, the calculation strength c_{calc} is

$$c_{\text{calc}} = \begin{cases} \text{C-Phi mode} & c \times \frac{\cos \psi \times \cos \varphi}{1 - \sin \psi \times \sin \varphi} \\ \text{Undrained shear strength} & s_{u, \text{max}}, \text{ see Equation (6.17)} \end{cases} \quad (6.20)$$

and the calculation friction angle φ_{calc} is

$$\varphi_{\text{calc}} = \begin{cases} \text{C-Phi mode} & \arctan \frac{\cos \psi \times \sin \varphi}{1 - \sin \psi \times \sin \varphi} \\ \text{Undrained shear strength} & 0 \end{cases} \quad (6.21)$$

7 Limit equilibrium methods

7.1 Safety factor

The equilibrium methods all consider a provided slip plane. A slip plane is a route through the soil profile, for which the safety factor will be calculated, which is the indication whether the slip plane is stable.

The safety factor F_s is the number through which the strength parameters of each soil layer must be divided such that the soil body is exactly in equilibrium. The equilibrium criteria depend on the limit equilibrium method used, i.e. Bishop, Uplift-Van or Spencer.

The safety factor is a real number greater than 0, without dimension.

If the slip plane is not valid (see [section 8.2](#)) or if the safety factor cannot be calculated (because, for example the maximum number of iterations during an iterative procedure is reached), then D-Stability will not return a safety factor.

7.2 Method of slices

Several methods exist to determine a safety factor of a soil body against macro stability. This kernel uses so called slices. Vertical lines divide the soil body into these slices (see [Figure 7.1](#)). For each slice, the different soil parameters, effective stresses and pore water pressures are calculated. These physical properties at the bottom of the slice are said to be representative for the slice. The slices are defined such that the properties of the slice do not change in horizontal direction. This holds true for all existing stresses and strength properties.

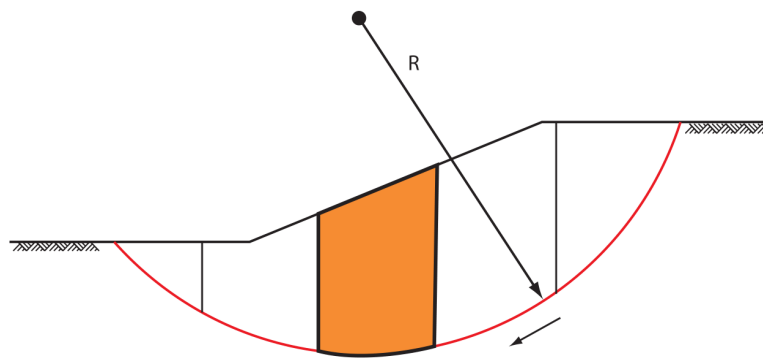


Figure 7.1 Slip plane including method of slices

7.2.1 Subdivision into slices

D-Stability automatically divides the slip plane into slices in accordance with the following criteria:

- Within one slice, the slice bottom does not intersect with layer boundaries and/or PL-lines;
- Within one slice, the slice bottom does not intersect with layer boundaries and the phreatic line, headlines, reference waternet lines, yield lines;
- Within one slice, the slice bottom does not intersect with load distribution lines;
- The entire base of any slice, which is part of the slip circle, is located totally within one soil layer and completely above or below the phreatic line.

In addition, D-Stability follows the following procedures in case a slide plane intersects the soil surface at more than two points. This is possible with a ditch as well as with a dike. In this case the largest area between two intersection points is taken to be the slide plane. If the plane cuts the surface of the geometry at only one point, the plane is rejected and is not processed any further. This latter case may occur when the geometry has not been defined wide enough so that slide planes reach the outer boundaries of the geometry, or when the slide planes just touches the surface at one point.

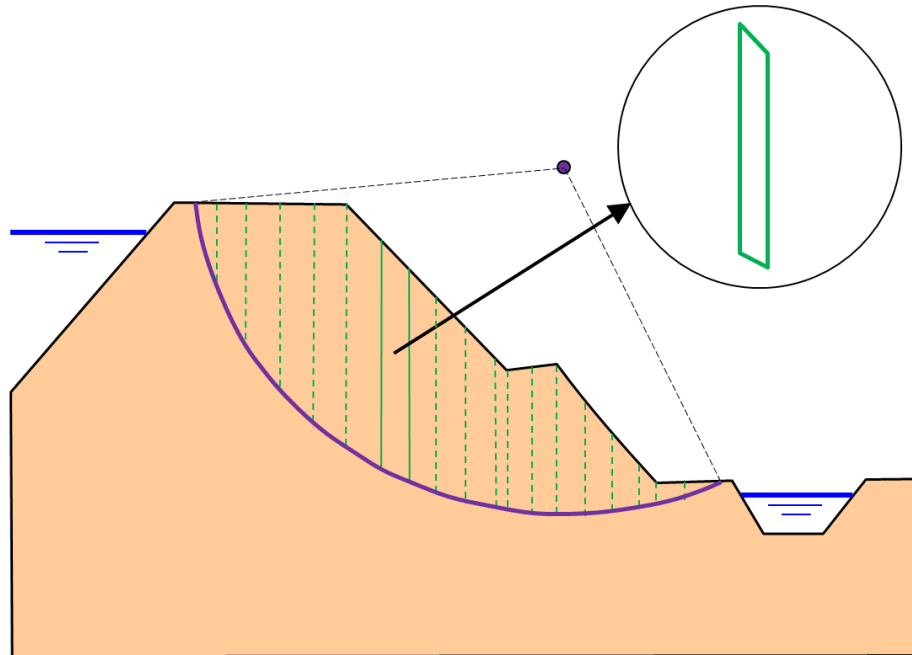


Figure 7.2 Global view of one slice

Slice boundaries are defined by

- all vertex points (see [section 4.3](#));
- intersection points of layers and the slip plane;
- nodes on non-circular slip planes;
- maximum provided slice width;
- load distribution lines;
- head lines;
- waternet reference lines.

The maximum width of a slice is provided. If the slice is wider, it will be divided into the lowest number of slices such that the maximum width is smaller than the maximum provided slice width.

7.2.2 Slice properties

The weight of the slice is given by

$$G = \sigma_{\text{soil}} \times b \quad (7.1)$$

where

G	is the weight of the slice [kN/m]
σ_{soil}	is the weight above the bottom of the slice
b	is the width of the slice [m]

The following properties are assigned to a slice (at the bottom of the slice)

- Geometrical properties (see section 7.2.2.1);
- Soil pressure σ_{soil} , (see Equation (4.1)) ;
- Weight of the slice (G , see Equation (7.1));
- Total pore pressure (u_{calc} , see Equation (5.11));
- Excess pore pressure (u_{excess} , see Equation (5.7));
- Effective stress σ'_v , see Equation (5.10));
- Yield stress (yield stress σ'_y , see Equation (6.11) and Equation (6.12));
- Calculation shear strength (c_{calc} , see Equation (6.20));
- Calculation friction angle (φ_{calc} , see Equation (6.21));
- Shear stress (τ , see Equation (6.19), value depends on the equilibrium method and is calculated during the equilibrium method);

If the bottom of the slice is very close to the boundary of a soil layer, the most unfavorable values will be used for c_{calc} and φ_{calc} . In fact, the shear strength τ (see Equation (6.19)) should have the least unfavorable value, but since the normal stress σ'_n is unknown yet, the effective stress σ'_v is used. This approximation is only carried out for slices with an almost horizontal bottom, because then we can assume that $\sigma'_n \approx \sigma'_v$. The approximated shear strength τ_{approx} is

$$\tau_{\text{approx}} = c_{\text{calc}} + \sigma'_v \times \tan \varphi_{\text{calc}} \quad (7.2)$$

The approximated shear strength τ_{approx} is calculated just above and below a soil boundary. From the side which gives the lowest result, the slice parameters c_{calc} and φ_{calc} are used.

7.2.2.1 Geometrical properties

The following geometrical properties are assigned to a slice

i	[-]	Number of the considered slice
n	[-]	Total number of slices in which the sliding part of the ground mass is divided. For Uplift-Van: $n = n_{\text{left}} + n_{\text{horiz}} + n_{\text{right}}$.
n_{left}	[-]	Number of slices in which the left sliding part of the ground mass is divided (Uplift Van)
n_{horiz}	[-]	Number of slices in which the horizontal sliding part of the ground mass is divided (Uplift Van)
n_{right}	[-]	Number of slices in which the right sliding part of the ground mass is divided (Uplift Van)
l_i	[m]	Length of arc at bottom of slice i : $l_i = b_i / \cos \alpha_i$
b_i	[m]	Width of slice i

h_i	[m]	Height of slice i
dx_i	[m]	Horizontal distance from the centre point of the circle to the centre of the upper boundary of slice i
dz_i	[m]	Vertical distance from the centre point of the circle to the centre of the upper boundary of slice i
x_i	[m]	Horizontal coordinate of the middle of slice i
$z_{i,top}$	[m NAP]	Vertical coordinate of the middle top of slice i
$z_{i,bottom}$	[m NAP]	Vertical coordinate of the middle bottom of slice i
α_i	[°]	Slide plane angle of slice i
β_i	[°]	Slope angle of slice i

7.3 Driving and resisting moments

The methods Fellenius, Bishop and Uplift-Van require moments to calculate the safety factor. These moments are described in this paragraph. The following symbols are used:

F_s	[-]	Safety factor
R	[m]	Radius of the slip circle (Bishop)
R_{left}	[m]	The radius of the left slip circle (Uplift Van)
R_{right}	[m]	The radius of the right slip circle (Uplift Van)
x_c	[m]	X co-ordinate of the center of the slip circle (Bishop)
$x_{c,left}$	[m]	The X-coordinate of the left slip circle (Uplift Van)
$x_{c,right}$	[m]	The X-coordinate of the right slip circle (Uplift Van)
z_c	[m NAP]	Z co-ordinate of the center of the slip circle (Bishop)
$z_{c,left}$	[m NAP]	The Z-coordinate of the left slip circle (Uplift Van)
$z_{c,right}$	[m NAP]	The Z-coordinate of the right slip circle (Uplift Van)

7.3.1 Driving moments

7.3.1.1 Driving soil moment

The driving soil moment $M_{D;soil}$ is the moment caused by the mass of the soil within the slip circle around its center:

$$M_{D;soil} = \sum_{\text{slices } i} G_i \times (x_c - x_i) \quad (7.3)$$

where

G_i is the weight of the soil in slice i (see [Equation \(7.1\)](#));

7.3.1.2 Driving water moment

The water moment is the contribution two water moments:

$$M_{D;water} = M_{Water;Top} + M_{Water;Side} \quad (7.4)$$

where:

$M_{Water;Top}$ is caused by the water forces (due to free water on surface) acting on the top of the slice, see [Equation \(7.5\)](#);

$M_{Water;Side}$ is caused by the water forces (due to free water on surface) acting on the side of the slice, see [Equation \(7.6\)](#) and [Equation \(7.7\)](#).

Water forces (due to free water on surface) acting on the top of the slice
 The water forces acting on and within the soil slice. When there is free water on the surface of the geometry and within the boundaries of the slip circle, it can have a positive or negative effect on the safety factor. The driving water moment M_{water} for a slice is calculated as follows:

$$M_{\text{Water;Top}} = \sum_{\text{slices } i} (x_i - x_c) \times W_{v;i} + (z_c - z_{\text{top};i}) \times W_{h;i} \quad (7.5)$$

where:

$W_{v;i}$ is the vertical component of the water force on top of slice i , in kN:

$$W_{v;i} = -\max[0; (z_{\text{phreatic}} - z_{\text{top};i})] \times \gamma_{\text{water}} \times b_i$$

$W_{h;i}$ is the horizontal component of the water force on top of slice i , in kN:

$$W_{h;i} = \max[0; (z_{\text{phreatic}} - z_{\text{top};i})] \times \gamma_{\text{water}} \times b_i \times \tan \beta_i$$

All other symbols are defined in section 7.2.2.1.

Water forces (due to free water on surface) acting on the side of the slice

Because of vertical layer boundaries, it is possible to have a surface with a vertical component. If this vertical component is part of the slip circle, D-Stability will place a slice to the left and right of this vertical. The moment caused by the free water on the top of both slices is calculated using the above formula (see Equation (7.5)). The force and moment of the free water against the vertical component of the surface (now also the side of a slice) is not taken into account by the above formula. Instead, D-Stability separately calculates the horizontal free water force and the moment caused by it.

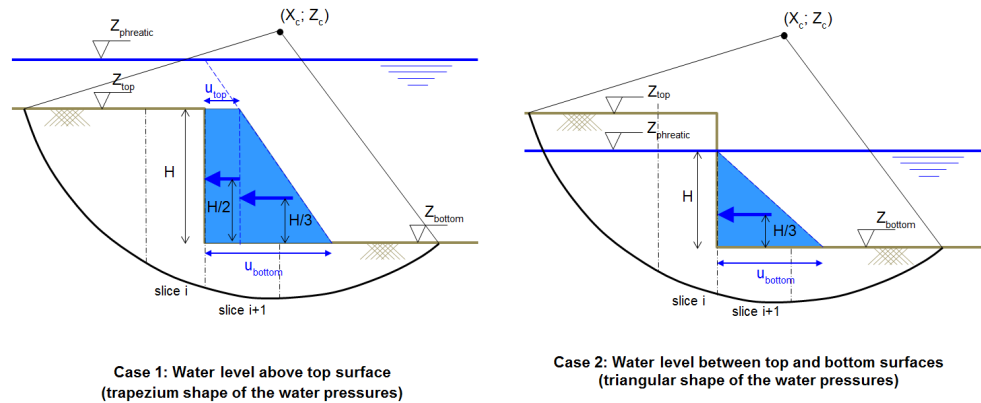


Figure 7.3 Horizontal water pressures (due to free water) acting on the side of a slice in case of vertical layer boundary

- If the phreatic line is above the top surface, the shape of the horizontal water pressures against the side of the slice is trapezium (case 1 in Figure 7.3):

$$M_{\text{Water;Side}} = u_{\text{top}} H \left(Z_c - \left(Z_{\text{bottom}} + \frac{H}{2} \right) \right) + \frac{H}{2} (u_{\text{bottom}} - u_{\text{top}}) \left(Z_c - \left(Z_{\text{bottom}} + \frac{H}{3} \right) \right) \quad (7.6)$$

- If the phreatic line is between the top and the bottom surfaces, the shape of the horizontal water pressures against the side of the slice is triangular (case 2 in Figure 7.3):

$$M_{\text{Water;Side}} = \frac{H}{2} u_{\text{bottom}} \left(Z_c - \left(Z_{\text{bot}} + \frac{H}{3} \right) \right) \quad (7.7)$$

where

H is the height of the saturated soil along the vertical layer boundary:

$$H = \min(Z_{\text{phreatic}}; Z_{\text{top}}) - \min(Z_{\text{phreatic}}; Z_{\text{bottom}})$$

If the soil within the slip plane height is dry, then $H = 0$.

u_{top} is the water pressure at the top of the saturated soil level:

$$u_{\text{top}} = (Z_{\text{phreatic}} - \min(Z_{\text{phreatic}}; Z_{\text{top}})) \times \gamma_w$$

u_{bottom} is the water pressure at level Z_{tangent} :

$$u_{\text{bottom}} = (Z_{\text{phreatic}} - Z_{\text{bottom}}) \times \gamma_w$$

Z_{top} is the top level of the vertical part;

Z_{bottom} is the bottom level of the vertical part.

Refer to [section 7.2.2.1](#) for the definitions of the other symbols.

7.3.1.3 Driving load moment

The (part of the) uniform loads ([section 9.2](#)) and the line loads ([section 9.1](#)) located within the confines of a slip circle creates a moment $M_{\text{D;load}}$ around the slip-circle center point. The uniform loads also refer to the uniform loads, which resemble a tree load (see [section 9.4](#)).

$$M_{\text{D;load}} = \sum_{j=1}^{n_{\text{loads}}} F_j \times \Delta w_j \times \Delta X_j + \sum_{l=1}^{n_{\text{lines}}} F_l \times \Delta X_l \quad (7.8)$$

with:

$$\Delta X_j = X_c - \frac{\max(X_{1;\text{left}}; X_{\text{begin};j}) + \min(X_{n;\text{right}}; X_{\text{end};j})}{2}$$

$$\Delta X_l = X_c - \frac{\max(X_{1;\text{left}}; X_l) + \min(X_{n;\text{right}}; X_l)}{2}$$

$$\Delta w_j = \min(X_{n;\text{right}}; X_{\text{end};j}) - \max(X_{1;\text{left}}; X_{\text{begin};j})$$

where:

F_j is the magnitude of uniform-load number j , in kN/m^2 ;

$X_{\text{begin};j}$ is the X coordinate of the starting point of load j ;

$X_{\text{end};j}$ is the X coordinate of the ending point of load j ;

$X_{1;\text{left}}$ is the X coordinate of the left side of slice 1 (i.e. entry point of the slip circle);

$X_{n;\text{right}}$ is the X coordinate of the right side of slice n (i.e. exit point of the slip circle);

Δw_j is the width of the part of the uniform-load j located within the confines of a slip circle;

ΔX_j is the X-coordinate at the middle of the part of the uniform-load j located within the confines of a slip circle;

ΔX_l is the X-coordinate of the line-load l located within the confines of a slip circle;

Refer to [section 7.2.2.1](#) for the definitions of the other symbols.

7.3.1.4 Driving earthquake moment

The driving moment of slip circles increases due to the earthquake coefficients. To simplify the calculation, it is assumed that the groundwater in the soil mass has the same extra acceleration as the soil in this mass. This extra moment $M_{D;\text{soil};\text{quake};\text{H}}$ called additional horizontal driving soil moment due to earthquake is

$$M_{D;\text{soil};\text{quake};\text{H}} = k \times \left| a_h \times \sum_{\text{slices } i} G_i \times (z_{\text{cg};i} - z_c) \right| \quad (7.9)$$

with $z_{\text{cg};i}$ as the center of gravity at the bottom of the slice (x, z) :

$$z_{\text{cg};i}(x, z) = \frac{\sum_{\text{layers } j} \bar{z}_j \times \sigma_j}{\sum_{\text{layers } j} \sigma_j} \quad (7.10)$$

$$k = \begin{cases} 1 & \text{if } M_D > 0 \\ -1 & \text{if } M_D < 0 \end{cases} \quad (7.11)$$

where

- \bar{z}_j is the mean vertical level of layer j along vertical x ;
- σ_j is the weight of soil layer j , see Equation (4.1) (a phreatic line divides a layer in two parts);
- a_h is the given horizontal earthquake factor (i.e. acceleration coefficient);
- G_i is the weight of the soil in slice i (see Equation (7.1)), in kN/m;
- $z_{\text{cg};i}$ is the vertical co-ordinate of the centre of gravity of slice i , in m;
- M_D is the total driving moment (given by Equation (7.15)) without the contribution of $M_{D;\text{soil};\text{quake};\text{H}}$;

Refer to section 7.2.2.1 for the definition of the other symbols.

The coefficient to increase the vertical gravitation has the following influence on soil stress, slice weight, driving moment and water pressure:

The additional driving soil moment due to vertical acceleration of the earthquake is as follows:

$$M_{D;\text{soil};\text{quake};\text{V}} = a_v \times \sum_{\text{slices } i} G_i \times (x_c - x_i) \quad (7.12)$$

where

- a_v is the vertical earthquake factor (i.e. acceleration coefficient);
- G_i is the weight of the soil in slice i (see Equation (7.1)), in kN/m;

Refer to section 7.2.2.1 for the definition of the other symbols.

The free water coefficient simulates the temporary draw down of the water. The free water moment is modified according to equation:

$$M_{D;\text{water};\text{quake}} = -M_{D;\text{water}} \times c_{fw} \quad (7.13)$$

where:

- $M_{D;\text{water}}$ is the driving water moment in kNm, see Equation (7.4);
- c_{fw} is the provided free water factor.

This results in the total driving earthquake moment

$$M_{D;\text{quake}} = M_{D;\text{soil};\text{quake};H} + M_{D;\text{soil};\text{quake};V} + M_{D;\text{water};\text{quake}} \quad (7.14)$$

where, H and V correspond to the horizontal and vertical components respectively.

7.3.1.5 Total driving moment

The total driving moment is given by

$$M_{\text{Driving}} = M_{D;\text{soil}} + M_{D;\text{water}} + \sum_{\text{loads}} M_{D;\text{load}} + M_{D;\text{quake}} \quad (7.15)$$

where

$M_{D;\text{soil}}$	is the driving soil moment (see Equation (7.3));
$M_{D;\text{water}}$	is the driving water moment (see Equation (7.4));
$M_{D;\text{load}}$	is the driving load moment (see Equation (7.8));
$M_{D;\text{quake}}$	is the driving quake moment (see Equation (7.14));

7.3.2 Resisting moments

7.3.2.1 Resisting moment from soil

Shear stresses and normal effective stresses act along the slip circle. The shear stresses prevent the soil mass from slipping. The resisting moment $M_{R;\text{soil}}$ is defined as the moment caused by the shear stresses along the slip plane.

$$M_{R;\text{soil}} = R \times \sum_{i=1}^n \tau_i \times l_i \quad (7.16)$$

where:

τ_i	is the shear stress along bottom of slice (see Equation (6.19)). Since τ_i depends on the equilibrium method, its value can be determined during the calculation of the safety factor;
----------	---

Refer to section 7.2.2.1 for the definitions of the other symbols.

7.3.2.1.1 Limited inclination of the slip plane

In the formula for the calculation of the shear stresses (τ), a problem arises for large negative values of the angle α . For these negative values, a large value for τ will be calculated, but this is unrealistic. To prevent this from happening, the value for α is therefore restricted to $\varphi/2 - 45^\circ$. This means that α never obtains a value less than $\varphi/2 - 45^\circ$. To illustrate this, see the following table where the τ and restricted τ' are given for various values of α and restricted α' .

In Figure 7.4, the value of the other parameters in the formula for τ is as follows:

$$\begin{aligned} c &= 0 \text{ kN/m}^2 \\ \varphi &= 20^\circ \\ \sigma'_v &= 10 \text{ kN/m}^2 \\ F_s &= 1 \end{aligned}$$

The minimum value for α becomes: $\varphi/2 - 45^\circ = -35^\circ$. The relation plus the assumption is displayed in Figure 7.4.

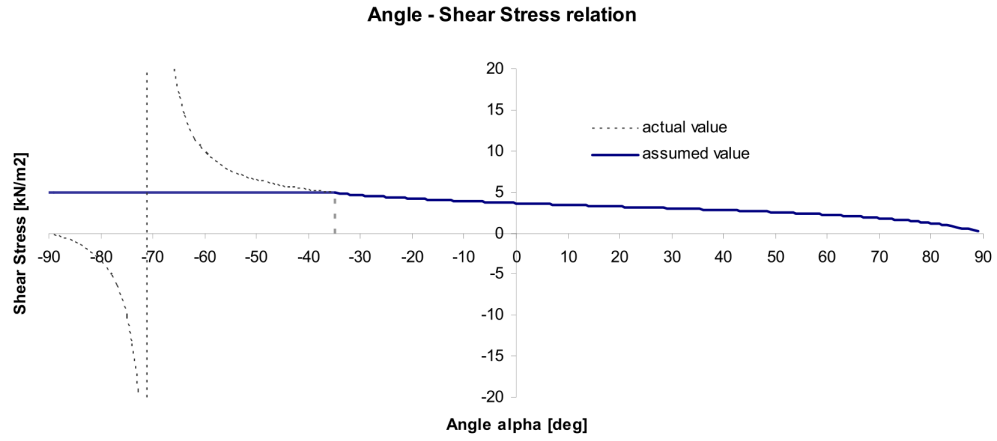


Figure 7.4 Relation angle α - Shear Stress for $\alpha_{\min} = 35^\circ$

If $F_s \neq 1$, the restricted angle α_{red} is:

$$\alpha_{\text{red}} = \max \left(\alpha; \frac{1}{2} \arctan \left(\frac{\tan \varphi}{F_s} \right) - \frac{\pi}{4} \right) \quad \text{with: } \alpha = \begin{cases} \alpha & \text{if } M_D \leq 0 \\ -\alpha & \text{if } M_D > 0 \end{cases}$$

7.3.2.2 Resisting moment from end section

The resisting moment is increased by $M_{R;\text{end section}}$, the resistance at the edges of a sliding section in the out-of-plane direction, due to the undrained shear strength:

$$M_{R;\text{end section}} = \frac{1}{F_s} \frac{1}{L/2} \sum_{i=1}^n \left(b_i \times \sum_{j=1}^{k_i} M_{j;su} \right) \quad (7.17)$$

with:

$$M_{j;su} = h_j s_{u;j;\min} (Z_c - Z_{j;\text{avg}}) + \frac{h_j}{2} |s_{u;j;\text{bot}} - s_{u;j;\text{top}}| (Z_c - Z_{j;\text{cg}})$$

$$s_{u;j;\min} = \min (s_{u;j;\text{bot}}; s_{u;j;\text{top}})$$

$$Z_{j;\text{avg}} = \frac{Z_{j;\text{bot}} + Z_{j;\text{top}}}{2}$$

$$Z_{j;\text{cg}} = Z_{j;\text{bot}} - \begin{cases} h_j/3 & \text{if } s_{u;j;\text{top}} < s_{u;j;\text{bot}} \\ 2h_j/3 & \text{if } s_{u;j;\text{top}} > s_{u;j;\text{bot}} \end{cases}$$

where:

- F_s is the safety factor of the equilibrium method;
- h_j is the thickness of layer j in slice i ;
- k_i is the number of layers along slice i ;
- L is the provided expected length of the sliding surface in the out-of-plane direction (i.e. cross section perpendicular to the cross section plane);
- n is the number of slices;
- $s_{u;j;\text{bot}}$ is the undrained shear strength at the bottom of layer j in slice i ;
- $s_{u;j;\text{top}}$ is the undrained shear strength at the top of layer j in slice i ;
- $Z_{j;\text{bot}}$ is the level at the bottom of layer j in slice i ;
- $Z_{j;\text{top}}$ is the level at the top of layer j in slice i .

Refer to [section 7.2.2.1](#) for the definition of the other symbols.

Note: This extra resisting moment is calculated only for the *Bishop* model in combination with



an undrained shear strength model.

7.3.2.3 Total resisting moment

The total driving moment is given by

$$M_{\text{Resisting}} = M_{\text{R;soil}} + M_{\text{R;geotextile}} + M_{\text{R;nail}} + |M_{\text{R;end section}}| \quad (7.18)$$

where

- $M_{\text{R;soil}}$ is the resisting soil moment (see Equation (7.16));
- $M_{\text{R;geotextile}}$ is the resisting geotextile moment (see Equation (10.1));
- $M_{\text{R;nail}}$ is the resisting nail moment (see Equation (10.5));
- $M_{\text{R;end section}}$ is the resisting end section moment (see Equation (7.17));

7.4 Bishop

7.4.1 Method according to A. W. Bishop

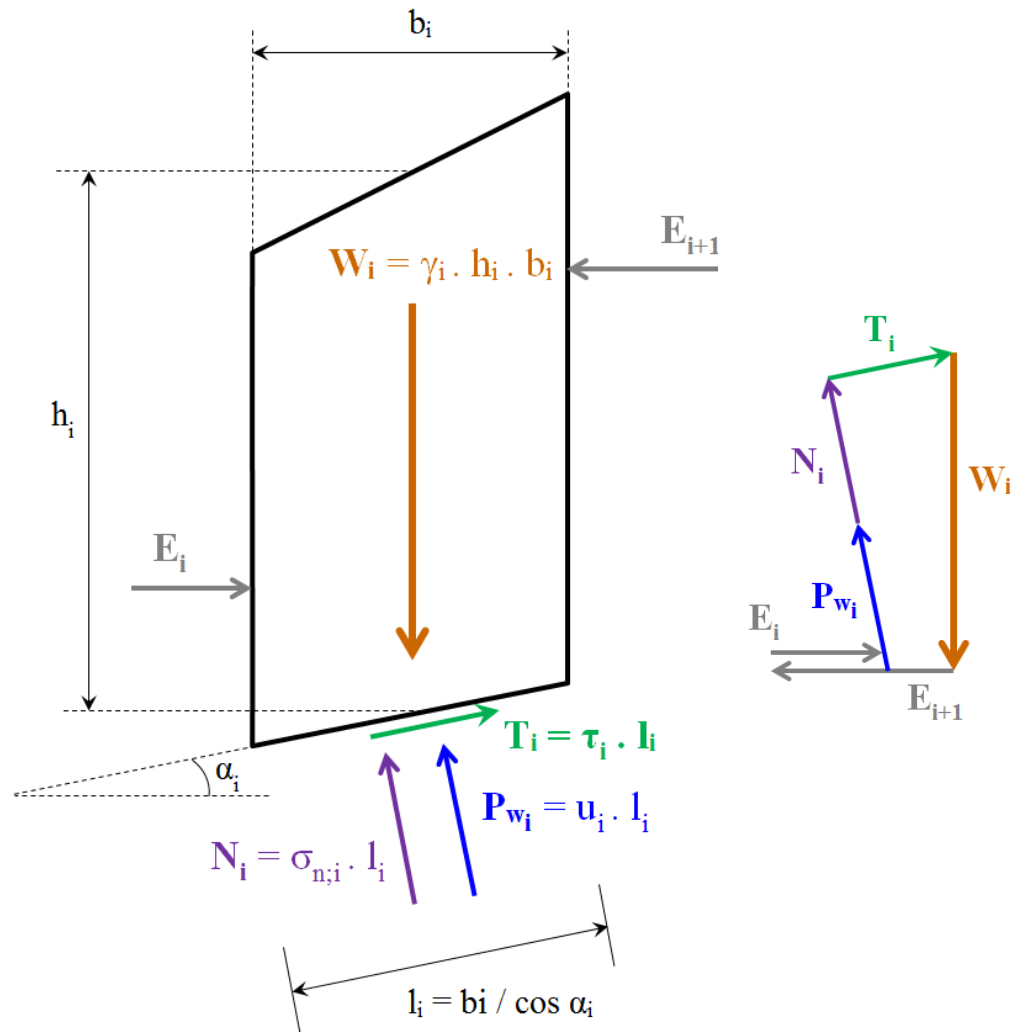
The Bishop method is applicable to a circular slip plane. By definition, the safety factor F_S is found when the slide plane is in limit state of equilibrium. The method (Bishop, 1955) is based on the assumption that the forces acting on both sides of any slice have zero resultant in the vertical direction. For each slice, a closed polygon of forces can be drawn. This implies force equilibrium in both horizontal and vertical directions per slice. The length of the horizontal line in the closed polygon of forces is a measure of the difference between the right and the left inter-slice forces.

The sum of all inter-slice forces is generally not zero, so that the horizontal balance of the total sliding mass is not satisfied. By reducing the soil parameters (the tangent of the friction angle and the cohesion) with the safety factor F_S , the moment equilibrium of the total sliding mass is satisfied.

Bishop defines the safety by the reduction factor that can be applied to cohesion and (the tangent of) the friction and dilatency. This means that only with Bishop's method the equilibrium of vertical forces is preserved. Therefore Bishop's method is preferred over Fellenius.

The equilibrium evaluation of a slice includes the forces and pressures in Figure 7.5.

Figure 7.5 Force equilibrium for one slice in the method of slices



The following table gives the definitions of the forces given in Figure 7.5:

- W_i is the weight of slice i , in kN/m;
 - T_i is the shear force along of slice i , in kN/m;
 - E_i is the interaction force of slice i with the slice at the left side, in kN/m;
 - E_{i+1} is the interaction force of slice i with the slice at the right side, in kN/m;
 - P_{w_i} is the water force acting on the base of slice i , in kN/m;
 - N_i is the (total) normal reaction of the soil acting on the base of slice i , in kN/m;
- Refer to [section 7.2.2.1](#) for the definition of the other symbols used in Figure 7.5.

The next sections describe how the different moments are calculated for a slice.

7.4.2 Equilibrium

The vertical equilibrium of the force acting on the slice writes:

$$\begin{aligned} \sum F_v = 0 &= -W_i + U_i \cdot \cos \alpha_i + N'_i \cdot \cos \alpha_i + T_i \cdot \sin \alpha_i \\ &= -\gamma_i \cdot h_i \cdot b + u_i \cdot l_i \cdot \cos \alpha_i + \sigma'_{n;i} \cdot l_i \cdot \cos \alpha_i + \frac{\tau_i}{F_s} \cdot l_i \cdot \sin \alpha_i \end{aligned}$$

which leads to:

$$\sigma'_{n;i} = \sigma'_{v;i} - \frac{\tau_i}{F_s} \cdot \tan \alpha_i \geq 0 \quad (7.19)$$

where

- $\sigma'_{v;i}$ is the effective stress at the base of slice i (see Equation (5.10))
- τ_i is the shear strength at the bottom of slice i (see Equation (6.19))

Repeating Equation (6.19), we know already that

$$\tau_{i,\text{calc}} = c_{i,\text{calc}} + \sigma'_{n;i} \times \tan \varphi_{i,\text{calc}} \quad (7.20)$$

Substitution of Equation (7.19) into Equation (7.20) leads to:

$$\tau_i = \frac{c_{i,\text{calc}} + \sigma'_{v;i} \times \tan \varphi_{i,\text{calc}}}{1 + \tan \alpha_i \times \frac{\tan \varphi_{i,\text{calc}}}{F_s}} \geq c_{i,\text{calc}} \quad (7.21)$$

where

- $\sigma'_{v;i}$ is the vertical effective stress at the bottom of slice i , in kN/m² (see Equation (5.10));
- $c_{i,\text{calc}}$ is the calculation strength at the bottom of slice i , in kN/m² (see Equation (6.20));
- $\varphi_{i,\text{calc}}$ is the calculation internal friction angle of the soil at the bottom of slice i , in degree (see Equation (6.21));
- α_i is the angle at bottom of slice, in degree;
- F_s is the safety factor (see Equation (7.22)).

7.4.3 Safety factor

The safety factor F_s for stability of slip circles is expressed by:

$$F_s = \frac{M_{\text{Resisting}}}{M_{\text{Driving}}} \quad (7.22)$$

where

- $M_{\text{Resisting}}$ is the resisting moment, see Equation (7.18);
- M_{Driving} is the driving moment, see Equation (7.15);

For Bishop, substitution of Equation (7.21) in the expression for the safety factor Equation (7.22) yields to Equation (7.23), an expression in which the safety factor occurs at both sides. D-Stability therefore determines the safety value for Bishop in iterative fashion, starting with a first estimate of the safety factor of 1.0. The result of the calculation (on the left) is used as a next estimate and this process continues until $|F_N - F_{N-1}| = 0.001$ or a maximum number of iterations has been made in which case no result is obtained.

$$F_s = \frac{R \sum_{i=1}^n \left(\frac{b_i}{\cos \alpha_i} \frac{c_i + \sigma'_{v;i} \tan \varphi_i}{1 + \tan \alpha_i \frac{\tan \varphi_i}{F_s}} \right) + M_{R;\text{geotextile}} + M_{R;\text{nail}} + |M_{R;\text{end section}}|}{M_{\text{Driving}}} \quad (7.23)$$

7.5 Uplift-Van

7.5.1 Method according to M. Van

The Uplift-Van method is applicable to a dual circular slip plane. The slip plane consists of an active circle, a passive circle and an horizontal bar between them.

High pore pressures at the horizontal interface of weak layers with an underlying permeable sand layer can cause reduction or even complete loss of shear resistance at this plane. This can yield an uplift failure mechanism, which is schematically drawn in Figure 7.6.

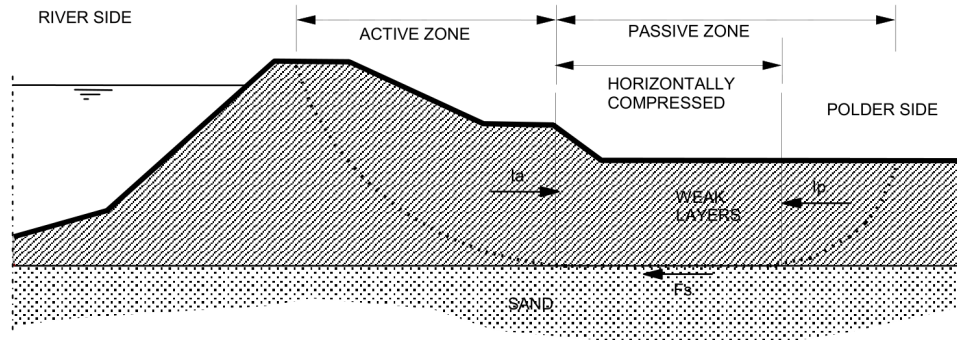


Figure 7.6 Uplift failure mechanism

The passive side of the slip plane is elongated in order to find equilibrium of horizontal forces. Van's method (Van, 2001) therefore assumes that the total slip plane is composed of a horizontal part bounded by two circular parts. The safety factor is determined using equilibrium of the horizontal forces acting on the compressed area between the active and passive slip circles.

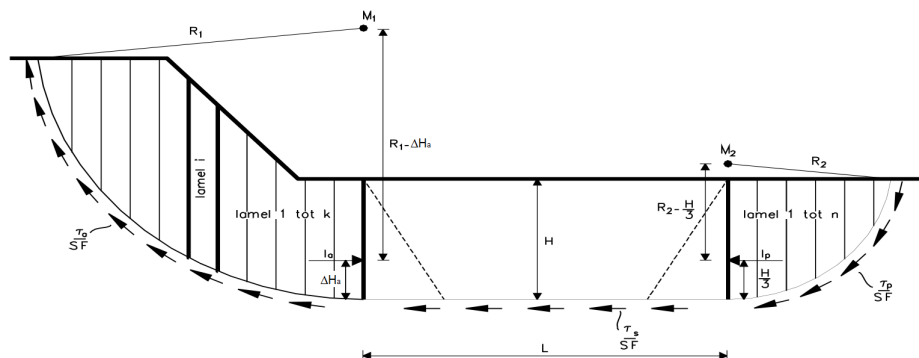


Figure 7.7 Van-Uplift Stability derivation

7.5.2 Driving moment of the circular parts

The total driving moment of the circular parts is the contribution of different components:

$$M_{D;\text{total};\text{left}} = M_{D;\text{soil};\text{left}} + M_{D;\text{water};\text{left}} + M_{D;\text{load};\text{left}} + M_{D;\text{quake};\text{left}} \quad (7.24)$$

$$M_{D;\text{total};\text{right}} = M_{D;\text{soil};\text{right}} + M_{D;\text{water};\text{right}} + M_{D;\text{load};\text{right}} + M_{D;\text{quake};\text{right}} \quad (7.25)$$

where:

$M_{D;\text{soil};\text{left}}$ is the driving soil moment at left side, in kNm/m, see Equation (7.3);

$M_{D;\text{soil};\text{right}}$ is the driving soil moment at right side, in kNm/m, see Equation (7.3);

$M_{D;water;left}$	is the driving water moment at left side, in kNm/m, see Equation (7.26);
$M_{D;water;right}$	is the driving water moment at right side, in kNm/m, see Equation (7.27);
$M_{D;load;left}$	is the driving external load moment at left side, in kNm/m, see Equation (7.8);
$M_{D;load;right}$	is the driving external load moment at right side, in kNm/m, see Equation (7.8);
$M_{D;quake;left}$	is the driving earthquake moment at left side, in kNm/m, see Equation (7.14);
$M_{D;quake;right}$	is the driving earthquake moment at right side, in kNm/m, see Equation (7.14);

The subscript *left*, is to say that the corresponding moment is calculated around the left circle, which is confined by the slices 1 to n_{left} . The subscript *right*, is to say that the corresponding moment is calculated around the right circle, which is confined by the slices $n - n_{right} + 1$ to n .

7.5.2.1 Driving water moments of the circular parts

The water moment is the contribution of three water moments:

$$M_{D;water;left} = M_{WaterTop;left} + M_{WaterSide;left} - M_{PoreBar;left} \quad (7.26)$$

$$M_{D;water;right} = M_{WaterTop;right} + M_{WaterSide;right} + M_{PoreBar;right} \quad (7.27)$$

where:

$M_{WaterTop;left}$	is caused by the water forces (due to free water on surface) acting on the top of the slice at left side, see Equation (7.28);
$M_{WaterTop;right}$	is caused by the water forces (due to free water on surface) acting on the top of the slice at right side, see Equation (7.29);
$M_{WaterSide;left}$	is caused by the water forces (due to free water on surface) acting on the side of the slice at left side, see Equation (7.30) and Equation (7.32);
$M_{WaterSide;right}$	is caused by the water forces (due to free water on surface) acting on the side of the slice at right side, see Equation (7.31) and Equation (7.33);
$M_{PoreBar;left}$	is caused by the pore pressures acting on the left bar, see Equation (7.34);
$M_{PoreBar;right}$	is caused by the pore pressures acting on the right bar, see Equation (7.35).

Water forces (due to free water forces on surface) acting on the top of the slice

The water moment is the moment caused by the water forces acting on and within the soil slice. When there is free water on the surface of the geometry and within the boundaries of the slip circle, it can have a positive or negative effect on the safety factor. The driving water moment due to free water forces acting on slices is calculated as follows:

$$M_{WaterTop;left} = \sum_{i=1}^{n_{left}} (X_i - X_{c;left}) \times W_{v;i} + (Z_{c;left} - Z_{i;top}) \times W_{h;i} \quad (7.28)$$

$$M_{WaterTop;right} = \sum_{i=n-n_{right}+1}^n (X_i - X_{c;right}) \times W_{v;i} + (Z_{c;right} - Z_{i;top}) \times W_{h;i} \quad (7.29)$$

where:

$W_{v;i}$	is the vertical component of the water force on top of slice i , in kN/m: $W_{v;i} = -\max[0; (Z_{phreatic} - Z_{top;i})] \times \gamma_w \times b_i$
$W_{h;i}$	is the horizontal component of the water force on top of slice i , in kN/m: $W_{h;i} = \max[0; (Z_{phreatic} - Z_{top;i})] \times \gamma_w \times b_i \times \tan \beta_i$

Refer to section 7.2.2.1 for the definitions of the other symbols.

Horizontal water forces (due to free water forces) acting on the side of the slice
 With the introduction of vertical layer boundaries, it became possible to have a surface with a vertical component. If this vertical component is part of the slip circle, D-Stability will place a slice to the left and right of this vertical. The force and moment of the free water against the vertical component of the surface (now also the side of a slice) must be taken into account (see Figure 7.3).

- If the phreatic line is above the top surface, the shape of the horizontal water pressures against the side of the slice is trapezium (case 1 in Figure 7.3):

$$M_{\text{WaterSide;left}} = u_{h;\text{top}} \times H \times \left(Z_{c;\text{left}} - \left(Z_{\text{bottom}} + \frac{H}{2} \right) \right) + \frac{H}{2} (u_{h;\text{bottom}} - u_{h;\text{top}}) \times \left(Z_{c;\text{left}} - \left(Z_{\text{bottom}} + \frac{H}{3} \right) \right) \quad (7.30)$$

$$M_{\text{WaterSide;right}} = u_{h;\text{top}} \times H \times \left(Z_{c;\text{right}} - \left(Z_{\text{bottom}} + \frac{H}{2} \right) \right) + \frac{H}{2} (u_{h;\text{bottom}} - u_{h;\text{top}}) \times \left(Z_{c;\text{right}} - \left(Z_{\text{bottom}} + \frac{H}{3} \right) \right) \quad (7.31)$$

- If the phreatic line is between the top and the bottom surfaces, the shape of the horizontal water pressures against the side of the slice is triangular (case 2 in Figure 7.3):

$$M_{\text{WaterSide;left}} = \frac{1}{2} H \times u_{h;\text{bottom}} \times \left(Z_{c;\text{left}} - \left(Z_{\text{bottom}} + \frac{H}{3} \right) \right) \quad (7.32)$$

$$M_{\text{WaterSide;right}} = \frac{1}{2} H \times u_{h;\text{bottom}} \times \left(Z_{c;\text{right}} - \left(Z_{\text{bottom}} + \frac{H}{3} \right) \right) \quad (7.33)$$

where:

- H is the height of the saturated soil along the vertical part:
 $H = \min(Z_{\text{water}}; Z_{\text{top}}) - \min(Z_{\text{water}}; Z_{\text{tangent}})$
 If the soil within the slip plane height is dry, then $H = 0$.
- $u_{h;\text{top}}$ is the hydrostatic pressure at level Z_{top} :
 $u_{h;\text{top}} = (Z_{\text{water}} - \min(Z_{\text{water}}; Z_{\text{top}})) \times \gamma_w$
- $u_{h;\text{bottom}}$ is the hydrostatic pressure at level Z_{bottom} :
 $u_{h;\text{bot}} = (Z_{\text{water}} - Z_{\text{bottom}}) \times \gamma_w$
- Z_{top} is the top level of the vertical part.
- Z_{bottom} is the bottom level of the vertical part.

Horizontal pore pressures acting on both bars of the horizontal part (i.e. circle's end)
 An Uplift-Van calculation consists of two circle parts and an horizontal part. Equilibrium for the circle parts must include pore pressure against such a part, as illustrated in Figure 7.8.

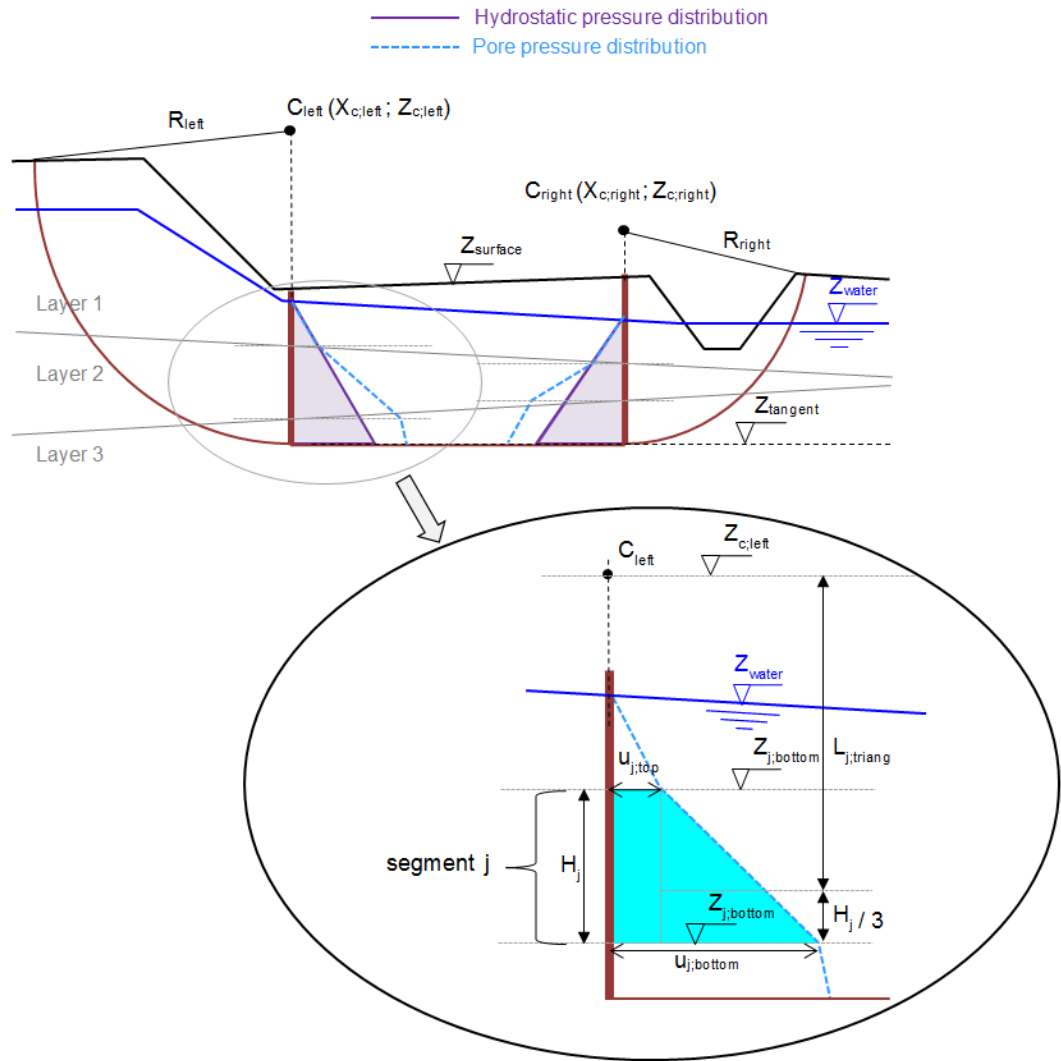


Figure 7.8 Schematization of the pore pressure distribution on bars

$$M_{\text{PoreBar:left}} = \sum_{j=1}^{n_{\text{segments:left}}} \min(u_{j;\text{top}}; u_{j;\text{bottom}}) \times H_j \times \left| Z_{c;\text{left}} - \left(Z_{j;\text{bottom}} + \frac{1}{2} H_j \right) \right| \quad (7.34)$$

$$+ |u_{j;\text{top}} - u_{j;\text{bottom}}| \times \frac{1}{2} H_j \times L_{j;\text{triang}}$$

$$M_{\text{PoreBar:right}} = \sum_{j=1}^{n_{\text{segments:right}}} \min(u_{j;\text{top}}; u_{j;\text{bottom}}) \times H_j \times \left| Z_{c;\text{right}} - \left(Z_{j;\text{bottom}} + \frac{1}{2} H_j \right) \right| \quad (7.35)$$

$$+ |u_{j;\text{top}} - u_{j;\text{bottom}}| \times \frac{1}{2} H_j \times L_{j;\text{triang}}$$

where:

$n_{\text{segments};\text{left}}$	is the number of segments having a linear pore pressure distribution along the left bar;
$n_{\text{segments};\text{right}}$	is the number of segments having a linear pore pressure distribution along the right bar;
H_j	is the height of segment j along the considered bar;
$u_{j;\text{top}}$	is the pore pressure at level $Z_{j;\text{top}}$;
$u_{j;\text{bottom}}$	is the pore pressure at level $Z_{j;\text{bottom}}$;
$Z_{j;\text{top}}$	is the top level of segment j along the considered bar;
$Z_{j;\text{bottom}}$	is the bottom level of segment j along the considered bar;
$L_{j;\text{triang}}$	is the arm of the resulting force of the triangular part of the pore pressure distribution for segment j along the considered bar:
	$L_{j;\text{triang}} = \begin{cases} Z_{c;\text{left}} - (Z_{j;\text{bottom}} + \frac{1}{3}H_j) & \text{if } u_{j;\text{top}} < u_{j;\text{bottom}} & \text{for left bar} \\ Z_{c;\text{left}} - (Z_{j;\text{top}} - \frac{1}{3}H_j) & \text{if } u_{j;\text{top}} \geq u_{j;\text{bottom}} & \text{for left bar} \\ Z_{c;\text{right}} - (Z_{j;\text{bottom}} + \frac{1}{3}H_j) & \text{if } u_{j;\text{top}} < u_{j;\text{bottom}} & \text{for right bar} \\ Z_{c;\text{right}} - (Z_{j;\text{top}} - \frac{1}{3}H_j) & \text{if } u_{j;\text{top}} \geq u_{j;\text{bottom}} & \text{for right bar} \end{cases}$

7.5.2.2 Determination of active and passive sides

The left side is considered as active if:

$$M_{D;\text{total};\text{left}} > M_{D;\text{total};\text{right}}$$

This leads therefore to:

$$M_{D;\text{total};\text{act}} = \max(M_{D;\text{total};\text{left}}; M_{D;\text{total};\text{right}}) \quad (7.36)$$

$$M_{D;\text{total};\text{pas}} = \min(M_{D;\text{total};\text{left}}; M_{D;\text{total};\text{right}}) \quad (7.37)$$

where:

$M_{D;\text{total};\text{left}}$ is the total driving moment at left side, see Equation (7.24);

$M_{D;\text{total};\text{right}}$ is the total driving moment at right side, see Equation (7.25).

7.5.3 Resisting moment of the circular parts

Shear stresses and normal effective stresses act along the slip circle. The shear stresses prevent the circular soil mass from slipping. The resisting moment is defined as the moment caused by the shear stresses along the circular arc around the center of the slip circle:

$$M_{R;\text{soil};\text{left}} = R_{\text{left}} \times \sum_{i=1}^{n_{\text{left}}} \tau_i \times l_i \quad (7.38)$$

$$M_{R;\text{soil};\text{right}} = R_{\text{right}} \times \sum_{i=n-n_{\text{right}}+1}^n \tau_i \times l_i \quad (7.39)$$

with:

$$\tau_i = \frac{c_i + \sigma'_{v;i} \times \tan \varphi_i}{1 + \tan \alpha_i \times \frac{\tan \varphi_i}{F_s}} \geq c_i \quad (7.40)$$

where

τ_i is the shear stress along bottom of slice i , in kN/m²;

$\sigma'_{v;i}$ is the vertical effective stress at the bottom of slice i , in kN/m², see Equation (5.10);

F_s is the safety factor, see Equation (7.57).

The derivation of Equation (7.40) is similar to the derivation of Equation (7.21).

7.5.4 Horizontal forces

7.5.4.1 Soil resistance force along horizontal part I_s

The horizontal resisting force acting along the horizontal part is:

$$I_s = \sum_{i=n_{\text{left}}+1}^{n_{\text{right}}-1} \frac{(c_i + \sigma'_{v;i} \times \tan \varphi_i) \times l_i}{F_s} \quad (7.41)$$

where:

j is the sign of the force;

$\sigma'_{v;i}$ is the vertical effective stress at the bottom of slice i , in kN/m^2 , see Equation (5.10);

Refer to section 7.2.2.1 for the definitions of the other symbols.

7.5.4.2 Earthquake force along horizontal part $F_{\text{quake;horiz}}$

The horizontal resisting force acting along the horizontal part is:

$$F_{\text{quake;horiz}} = \sum_{i=n_{\text{left}}+1}^{n_{\text{right}}-1} \sigma_{\text{h;quake};i} \times l_i \quad (7.42)$$

where:

$$\sigma_{\text{h;quake};i} = a_h \times \sigma_{\text{soil};i} \quad (7.43)$$

$\sigma_{\text{h;quake};i}$ is the stress caused by horizontal acceleration of an earthquake due to the soil weight at the bottom of slice i , in kN/m^2 ;

$\sigma_{\text{soil};i}$ is the weight above the bottom of slice i , in kN/m^2 (see Equation (4.1));

Refer to section 7.2.2.1 for the definitions of the other symbols.

7.5.4.3 Resulting water force along horizontal part $F_{\text{water;horiz}}$

The resulting water force along the horizontal part is the contribution of the water force due to (free) water on surface and of the pore pressures applying on the bars:

$$F_{\text{water;horiz}} = F_{\text{w;surf;left}} - F_{\text{w;surf;right}} + F_{\text{u;left}} - F_{\text{u;right}} \quad (7.44)$$

with:

$$F_{\text{w;surf;left}} = \frac{1}{2} [\max(Z_{\text{phreatic;left}}; Z_{\text{surf;left}}) - Z_{\text{surf;left}}]^2 \times \gamma_w \quad (7.45)$$

$$F_{\text{w;surf;right}} = \frac{1}{2} [\max(Z_{\text{phreatic;right}}; Z_{\text{surf;right}}) - Z_{\text{surf;right}}]^2 \times \gamma_w \quad (7.46)$$

$$F_{\text{u;left}} = \sum_{j=1}^{n_{\text{segments;left}}} \min(u_{j;\text{top}}; u_{j;\text{bottom}}) \times H_j + |u_{j;\text{top}} - u_{j;\text{bottom}}| \times \frac{1}{2} H_j \quad (7.47)$$

$$F_{\text{u;right}} = \sum_{j=1}^{n_{\text{segments;right}}} \min(u_{j;\text{top}}; u_{j;\text{bottom}}) \times H_j + |u_{j;\text{top}} - u_{j;\text{bottom}}| \times \frac{1}{2} H_j \quad (7.48)$$

where:

$Z_{\text{surf;left}}$ is the surface level at vertical $X = X_{\text{c;left}}$

$Z_{\text{surf;right}}$ is the surface level at vertical $X = X_{\text{c;right}}$

$Z_{\text{phreatic;left}}$ is the phreatic level at vertical $X = X_{\text{c;left}}$

$Z_{\text{phreatic;right}}$ is the phreatic level at vertical $X = X_{\text{c;right}}$

$n_{\text{segments;left}}$ is the number of segments having a linear pore pressure distribution along the left bar;

$n_{\text{segments;right}}$	is the number of segments having a linear pore pressure distribution along the right bar;
H_j	is the height of segment j along the considered bar;
$u_{j;\text{top}}$	is the pore pressure at level $Z_{j;\text{top}}$;
$u_{j;\text{bottom}}$	is the pore pressure at level $Z_{j;\text{bottom}}$;
$Z_{j;\text{top}}$	is the top level of segment j along the considered bar;
$Z_{j;\text{bottom}}$	is the bottom level of segment j along the considered bar.

See also [Figure 7.8](#) for the definition of the symbols.

7.5.4.4 Resulting horizontal force at active side I_a

Moment equilibrium around active circle center yields [Equation \(7.49\)](#) for the resulting force I_a at active side.

$$I_a = \frac{|M_{D;\text{act}}| - \frac{|M_{R;\text{soil;act}}|}{F_s}}{R_{\text{act}} - \Delta H_{\text{act}}} \quad (7.49)$$

with:

$$M_{R;\text{soil;act}} = \begin{cases} M_{R;\text{soil;left}} & \text{if the left side is active, see section 7.5.2.2} \\ M_{R;\text{soil;right}} & \text{if the right side is active, see section 7.5.2.2} \end{cases} \quad (7.50)$$

where:

$M_{D;\text{act}}$	is the total active driving moment, see Equation (7.36) ;
$M_{R;\text{soil;left}}$	is the soil resisting moment at left side, see Equation (7.38) ;
$M_{R;\text{soil;right}}$	is the soil resisting moment at right side, see Equation (7.39) ;
ΔH_{act}	is the arm of the active force I_a compare to the tangent level;
R_{act}	is the radius of the active circle;
F_s	is the safety factor that has to be determined, see Equation (7.57) .

7.5.4.5 Resulting horizontal force at passive side I_p

Moment equilibrium around passive circle center yields [Equation \(7.51\)](#) for the resulting force I_p at passive side.

$$I_p = \frac{|M_{D;\text{pas}}| - \frac{|M_{R;\text{soil;pas}}|}{F_s}}{R_{\text{pas}} - \Delta H_{\text{pas}}} \quad (7.51)$$

with:

$$M_{R;\text{soil;pas}} = \begin{cases} M_{R;\text{soil;left}} & \text{if the left side is passive, see section 7.5.2.2} \\ M_{R;\text{soil;right}} & \text{if the right side is passive, see section 7.5.2.2} \end{cases} \quad (7.52)$$

where:

$M_{D;\text{pas}}$	is the total passive driving moment, see Equation (7.37) ;
$M_{R;\text{soil;left}}$	is the soil resisting moment at left side, see Equation (7.38) ;
$M_{R;\text{soil;right}}$	is the soil resisting moment at right side, see Equation (7.39) ;
ΔH_{act}	is the arm of the active force I_a compare to the tangent level;
ΔH_{pas}	is the arm of the passive force I_p compare to the tangent level;
R_{pas}	is the radius of the passive circle;

R_{act} is the radius of the active circle;
 F_s is the safety factor that has to be determined;

7.5.5 Safety factor

7.5.5.1 Determination of the arm of the active force I_a

The resulting horizontal force at passive side of the compressed soil I_p is assumed to act above the tangent line, at 1/3 of the height of the bar. This assumption is relatively correct as no free water on surface is present at the polder side (i.e. $F_{w,surf;left} = 0$).

$$\Delta H_{pas} = \frac{1}{3} H_{pas} \quad (7.53)$$

where H_{pas} is the height of the bar at passive side.

The resulting horizontal force at active side of the compressed soil I_a is assumed to act above the interface with the sand, at a distance ΔH_{act} of the weak soil layers. To determine the arm ΔH_{act} of force I_a , the moments equilibrium around the bottom of the horizontal line (i.e. $Z_{tangent}$) is used:

$$\Delta H_{act} = \frac{\Delta H_{pas} \times I_p + M_{water;pas} - M_{water;act}}{I_a} \quad (7.54)$$

with:

$$M_{water;act} = \begin{cases} M_{water;left} & \text{if the active side is the left side} \\ M_{water;right} & \text{if the active side is the right side} \end{cases}$$

$$M_{water;pas} = \begin{cases} M_{water;left} & \text{if the passive side is the left side} \\ M_{water;right} & \text{if the passive side is the right side} \end{cases}$$

$$M_{water;left} = F_{w,surf;left} \times \Delta H_{w,surf;left} + M_{PoreBar;left} \Big|_{tangent}$$

$$M_{water;right} = F_{w,surf;right} \times \Delta H_{w,surf;right} + M_{PoreBar;right} \Big|_{tangent}$$

$$\Delta H_{w,surf;left} = Z_{surf;left} + \frac{1}{3} (Z_{phreatic;left} - Z_{surf;left}) - Z_{tangent}$$

$$\Delta H_{w,surf;right} = Z_{surf;right} + \frac{1}{3} (Z_{phreatic;right} - Z_{surf;right}) - Z_{tangent}$$


where:

$F_{w,surf;left}$ is the horizontal water force on left bar due to (free) water on surface, see Equation (7.45);
 $F_{w,surf;right}$ is the horizontal water force on left bar due to (free) water on surface, see Equation (7.46);
 $Z_{surf;left}$ is the surface level at vertical $X = X_{c;left}$;
 $Z_{surf;right}$ is the surface level at vertical $X = X_{c;right}$;
 $Z_{phreatic;left}$ is the phreatic level at vertical $X = X_{c;left}$;
 $Z_{phreatic;right}$ is the phreatic level at vertical $X = X_{c;right}$;
 $Z_{tangent}$ is the bottom level of the horizontal part;
 $M_{PoreBar;left} \Big|_{tangent}$ is the moment around the tangent line due to pore pressures along the left bar. It is similar to $M_{PoreBar;left}$ in Equation (7.34) except that the rotational point $Z_{c;left}$ is replaced with $Z_{tangent}$;
 $M_{PoreBar;right} \Big|_{tangent}$ is the moment around the tangent line due to pore pressures along the right bar. It is similar to $M_{PoreBar;right}$ in Equation (7.35) except that the rotational point $Z_{c;left}$ is replaced with $Z_{tangent}$.

The substitution of Equation (7.49) and Equation (7.53) in Equation (7.54) yields to Equation (7.55), an expression in which distance ΔH_{act} occurs at both sides. D-Stability

therefore determines this distance in iterative fashion, starting with a first estimate of the distance of $\Delta H_{act} = \frac{1}{3} H_{act}$. The result of the calculation (on the left) is used as a next estimate and this process continues until $|\Delta H_{act;N} - \Delta H_{act;N-1}| < 0.001$ or a maximum number of iterations has been made in which case no result is obtained.

$$\Delta H_{act} = \frac{\frac{1}{3} H_{pas} \times I_p + M_{water;pas} - M_{water;act}}{\frac{|M_{D;act}| - \frac{|M_{R;soil;act}|}{F_s}}{R_{act} - \Delta H_{act}}} \quad (7.55)$$

Note: If either I_a or I_p is negative, the iterative procedure describes above is not performed, and ΔH_{act} stays equal to its initial value $\frac{1}{3} H_{act}$. 

7.5.5.2 Equilibrium of horizontal forces

The equation for equilibrium of horizontal forces yields:

$$I_a + I_p + I_s + F_{water;horiz} + F_{quake;horiz} = 0 \quad (7.56)$$

Substitution of Equation (7.49) and Equation (7.51) into the equation for equilibrium of horizontal forces Equation (7.56) finally yields Equation (7.57) for the safety factor:

$$F_s = \frac{\frac{|M_{R;soil;pas}|}{R_{pas} - \Delta H_{pas}} + \frac{|M_{R;soil;act}|}{R_{act} - \Delta H_{act}} - I_s \times F_s}{\frac{|M_{D;pas}|}{R_{pas} - \Delta H_{pas}} + \frac{|M_{D;act}|}{R_{act} - \Delta H_{act}} + F_{water;horiz} + F_{quake;horiz}} \quad (7.57)$$

The substitution of Equation (7.41) (I_s), Equation (7.52) ($M_{R;soil;pas}$) and Equation (7.50) ($M_{R;soil;act}$) in Equation (7.57) yields to Equation (7.58), an expression in which F_s occurs at both sides. D-Stability therefore determines the safety factor in iterative fashion, starting with a first estimate of $F_0 = 1$. The result of the calculation (on the left) is used as a next estimate and this process continues until $|F_{s;N} - F_{s;N-1}| < 0.001$ or a maximum number of iterations has been made in which case no result is obtained.

$$F_s = \frac{\frac{\left| \sum_{i=n_{begin;pas}}^{n_{end;pas}} \frac{c_i + \sigma'_{v;i} \tan \varphi_i}{1 + \tan \alpha_i \frac{\tan \varphi_i}{F_s}} l_i \right|}{1 - \frac{\Delta H_{pas}}{R_{pas}}} + \frac{\left| \sum_{i=n_{begin;act}}^{n_{end;act}} \frac{c_i + \sigma'_{v;i} \tan \varphi_i}{1 + \tan \alpha_i \frac{\tan \varphi_i}{F_s}} l_i \right|}{1 - \frac{\Delta H_{act}}{R_{act}}}}{\frac{|M_{D;pas}|}{R_{pas} - \Delta H_{pas}} + \frac{|M_{D;act}|}{R_{act} - \Delta H_{act}} + F_{water;horiz} + F_{quake;horiz}} \times \sum_{i=n_{left}+1}^{n_{right}-1} (c_i + \sigma'_{v;i} \tan \varphi_i) l_i \quad (7.58)$$

with:

$$n_{begin;pas} = \begin{cases} 1 & \text{if the passive side is the left side} \\ n_{right-1} & \text{if the passive side is the right side} \end{cases}$$

$$n_{end;pas} = \begin{cases} n_{left} & \text{if the passive side is the left side} \\ n & \text{if the passive side is the right side} \end{cases}$$

$$n_{begin;act} = \begin{cases} 1 & \text{if the active side is the left side} \\ n_{right-1} & \text{if the active side is the right side} \end{cases}$$

$$n_{end;act} = \begin{cases} n_{left} & \text{if the active side is the left side} \\ n & \text{if the active side is the right side} \end{cases}$$

7.6 Spencer

7.6.1 Method according to E. Spencer

The Spencer method is applicable to a non constrained slip plane. This plane is defined by an entrance point, an exit point and a number of traversal points, between which there is a straight connection.

By definition, the safety factor F_s is found when the slide plane is in limit state of equilibrium. To fulfill this requirement, each slice must have equilibrium of moments, horizontal and vertical forces. The Spencer method (Spencer, 1967) satisfies those three conditions of equilibrium. The method itself is not constrained to any shape of slip plane and can therefore be used to freely search the slip plane with the least resistance.

7.6.2 Safety factor

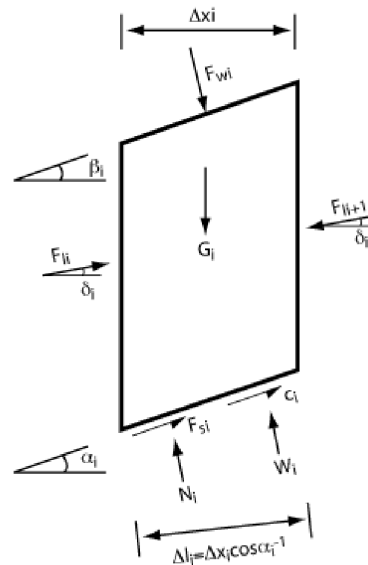


Figure 7.9 Interslice forces according to Spencer method

where:

α_i	Slide plane angle [°]
β_i	Slope angle [°]
δ_i	Interslice force angle [°]
φ_i	Internal friction angle along slip surface [°]
h_i	Slice height [m]
x_i	Slice width [m]
c_i	Cohesion along slip surface [kN/m ²]
F_s	Safety factor [-]
G_i	Weight [kN]
F_{li}	Interslice force [kN]
N_i	Effective normal force at bottom [kN]
F_{si}	Shear force along the bottom [kN]
F_{wi}	Water force on slope [kN]
L_i	Length of sliding plane [m]
W_i	Water pressure against bottom [kN]
x_i	Distance interslice force – sliding plane [m]

$$F_{wi} = \frac{\sigma_{\text{water}} \times b_i}{\cos \alpha_i} \quad (7.59)$$

$$G_i = \sigma \times b_i \quad (7.60)$$

$$W_i = u \times b_i \quad (7.61)$$

$$F_{\text{left};i} = F_{\text{right};i-1} \quad (7.62)$$

The difference in the top and bottom angle θ is

$$\theta_i = \alpha_i - \beta_i \quad (7.63)$$

The additional force F_{slice} on the slice is calculated as follows

$$F_{\text{slice}} = F_{w,i} \sin(\theta_i) - G_i \sin(\alpha_i) + \frac{c_i L_i}{F_s} + \frac{F_{w,i} \sin(\theta_i) + G_i \sin(\alpha_i) - W_i L_i}{F_s} \quad (7.64)$$

The fraction at the left and right side of the slice are defined as follows

$$f_{\text{left};i} = \cos(\alpha_{i-1} - \delta_i) + \frac{\tan \varphi_{i-1}}{F_s} \times \sin(\alpha_{i-1} - \delta_i) \quad (7.65)$$

and

$$f_{\text{right};i} = \cos(\alpha_i - \delta_i) + \frac{\tan \varphi_i}{F_s} \times \sin(\alpha_i - \delta_i) \quad (7.66)$$

Calculation of the interslice force F_{l_i} at intersection i :

$$F_{l,i+1} = \frac{f_{\text{right};i} \times F_{l,i} + F_{\text{slice}}}{f_{\text{left};i+1}} \quad (7.67)$$

The interslice force is considered as a resultant of three forces acting on a slice side:

- shear force along this side

- effective normal force
- water force

The angle of interslice forces of the first and last (fictitious) interslice force is set to zero implying horizontal forces. The angles of the other forces are set to δ . The fictitious interslice force acting on the first slice is zero. Now the (fictitious) force needed to ensure equilibrium at the end of the slide plane can be calculated.

The projected interslice forces in x and z direction are

$$F_{l,i,x} = F_{l,i} \cos \delta_i \quad (7.68)$$

and

$$F_{l,i,z} = F_{l,i} \sin \delta_i \quad (7.69)$$

$$f_{z,i} = x_{i-1} + \frac{1}{2} b_i \tan \alpha_i \quad (7.70)$$

By considering the equilibrium of moments round the center bottom point of the slice, the position of the resultant of interslice force is found in the following way

$$z_{l,i} = \frac{f_{z,i} F_{l,i-1,x} - \frac{1}{2} b_i F_{l,i-1,z}}{F_{l,i,x}} - \frac{\frac{1}{2} b_i F_{l,i,z} - \sin \beta_i F_{w,i}}{F_{l,i,x}} + \frac{1}{2} b_i \tan \alpha_i \quad (7.71)$$

The distance between the first fictitious interslice force and the sliding plane is zero. Now, calculating from the first to the last but one slice, the distance can be calculated between the last but one interslice force and the sliding plane. To keep the equilibrium of moments a fictitious rest moment (M_{rest}) is required for the last slice. M_{rest} can be calculated in the following way:

$$M_{rest} = x_{proj,n+1} F_{l,n,x} - \frac{1}{2} b_{n+1} F_{l,n,z} - F_{w,n+1} \alpha_{n+1} \sin \beta_{n+1} \quad (7.72)$$

For calculation of the rest moment, a working line for the rest force (F_{rest}) is defined by the horizontal line through point M. The solution procedure of the Spencer method consists of the search for F and δ in such a way that both $F_{rest} = 0$ and $M_{rest} = 0$. The search for the correct values for F and δ is carried out by means of an iterative model, using the following steps:

- Choose starting values for F and δ .
- Iterate formula 1 until $F_{rest} = 0$. F is adapted while δ is kept constant.
- Iterate formula 2 and 3 with the final values of the interslice forces from step 2 until $M_{rest} = 0$. F is kept constant while δ is adapted.
- With the values of F and δ that were gained by step 2 and 3, repeat the process from step 2 until $F_{rest} = 0$ and $M_{rest} = 0$.

Iteration of Equation (7.67) (step 2) is ended when the absolute value of rest force is less than ϵ . Iteration of Equation (7.71) and Equation (7.72) (step 3) is ended when the absolute value of the rest moment is less than ϵ . The complete iteration process is ended when the absolute values of both the rest force and the rest moment are less than 10° . As a starting value, a safety factor of 1.1 is assumed. The program calculates a starting value for δ in the following way:

$$\delta_{start} = \frac{\delta_{min} + \delta_{max}}{2} \quad (7.73)$$

In the calculation of the interslice forces from Equation (7.67), a division is made by factor:

$$\cos(\alpha_i - \delta_i) + \frac{\tan \varphi + \sin(\alpha_i - \delta_i)}{F_s} \quad (7.74)$$

At a certain combination of δ and F , this can lead to a division by zero. This critical combination can be found by:

$$\cos(\alpha_i - \delta_i) + \frac{\tan \varphi + \sin(\alpha_i - \delta_i)}{F_s} = 0 \quad (7.75)$$

This leads to:

$$\delta_{i,min} = \alpha_i - \left[\pi + \arctan \left(-\frac{F_s}{\tan \varphi} \right) \right] \quad (7.76)$$

or:

$$\delta_{i,max} = \alpha_i - \arctan \left(-\frac{F_s}{\tan \varphi} \right) \quad (7.77)$$

With this, the critical values of $\delta_{i,max}$ and $\delta_{i,min}$ can be calculated as a function of the starting value of F . The maximum of all $\delta_{i,max}$ is δ_{max} . The denominator of formula 2 includes $\cos(\delta_i)$. The denominator becomes zero when $\delta = -\frac{1}{2} \pi$ or $\delta = +\frac{1}{2} \pi$.

When δ_{min} is less than $-\frac{1}{2} \pi$, then $\delta_{min} = -\frac{1}{2} \pi$

When δ_{max} is larger than $+\frac{1}{2} \pi$, then $\delta_{max} = +\frac{1}{2} \pi$

8 Optimization procedures

The objective of the search algorithms is to find the slip plane with the minimum safety factor F_S (see [chapter 7](#)) given a limit equilibrium method.

In a geometry, an infinite number of slip planes can occur. Therefore, a search algorithm needs to find which slip plane is representative.

8.1 Search area

Each optimization procedure needs a search area. A search area defines the limits of the characteristics of the slip planes to be investigated. Each optimization procedure will generate slip planes within these limits and each of the slip plane with the lowest safety factor. depending on the limit equilibrium method, the search areas are defined in a different way.

8.1.1 Search area for Bishop

The search area for Bishop is defined by a rectangle and a tangent scope. By defining a square with centre points for slip circles and a number of tangent lines, all combinations of possible slip planes are investigated. The search area is three-dimensional as there are three parameters to be optimized (x , z and r).

8.1.2 Search area for Uplift-Van

The search area for Uplift-Van (see [section 7.5](#)) has two rectangular zones and an area for the horizontal tangent lines. The search is five-dimensional as there is another circle centre to be found.

8.1.3 Search area for Spencer

The Spencer calculation is based on an unconstrained plane with a number of bending points including the start and end point (see [section 7.6](#)).

Each slip plane point represents a dimension and therefore the items in a dimension represent the position of a bending point. For each dimension / bending point a minimum and maximum point has to be provided. Each dimension is fixed with a minimum value of 0 and a maximum value of 1.

In the optimization procedure, a bending point is determined between the minimum and maximum point, depending on the item value. For the first and last point, these point will be on the surface line and for all other points on a line between the minimum and maximum point of that bending point.

The search area is N-dimensional, with N the number of bending points.

A generated slip plane can be invalid if the slip plane does not progress in x direction. Such slip planes will be excluded.

8.2 Slip plane constraints

A slip plane may need to meet additional constraints. The constraints can be defined to prevent some slip planes from being calculated, because they are regarded as harmless or impossible.

8.2.1 General constraints on all slip planes

8.2.1.1 Minimal circle depth

The minimal slice depth of the highest slice in the slip plane is input.

8.2.1.2 Minimal circle length
The minimal slice length is input. Default, the value is set to 0 meter, which means that no check on the length will be performed. If the minimal slice length is > 0 m, then the check will be performed.

8.2.1.3 Entry and exit point constraints
The entry point of a slip plane may be restricted in the X-direction.

8.2.2 Constraints on Spencer slip planes

Some limitations apply to Spencer slip plane, in order to get the most realistic slip plane:

- The slip plane must progress, so the X-coordinate of a next point must be greater than the X-coordinate of a previous point
- The angle between the slices can be limited by a maximum value, with a default of 0°.
- The thrust line in the soil body: the percentage of horizontal force-points in slices must be more than a minimum value, with a default of 0%. This thrust line is drawn in the results after a Spencer calculation.

8.3 Single slip plane

This is in fact no optimization procedure, because it will process only one slip plane. It will be useful when the slip plane is already known or fixed, such as in a probabilistic analysis.

8.4 Grid search (Bishop)

The grid search is defined by a set of calculations that are all executed. The result with an optimum (minimum or maximum value) is said to be representative.

A grid search has a number of dimensions, called N. Each dimension contains a number of numeric items. All item combinations, also called points, are evaluated with a provided function. In essence, the grid search does no more than sequentially evaluating all these points and return the point with the optimum value.

Each dimension has a number of items which should be evaluated. The items can be defined as follows:

- a range with a minimum and maximum value and the number of steps into which the range should be subdivided
- an enumerated list of values

Possibly one item cannot be evaluated, because its input is regarded as invalid (see [section 8.2](#)). In that case, not any number should be returned by the function. It will never be regarded as the optimum.

8.4.1 Move grid if optimum is on edge

If, in any dimension, the optimum is on the edge of a dimension, the edge will be extended one step in the direction of the edge. This extension can happen in several dimensions at the same time.

Only dimensions with at least three items can be moved and the items should be defined as minimum/maximum/steps. Per dimension this feature is optional.

This process will be repeated until the optimum is not on the edge of the dimension area any more.

8.5 Genetic algorithm (Spencer)

The genetic algorithm is an optimization procedure used to find the representative slip plane within the search area. A genetic algorithm is particularly efficient in solving optimization problems that are not well suited for standard optimization algorithms, including problems in which the objective function is discontinuous, non-differentiable, stochastic, highly non-linear, or has a large number of variables. The genetic algorithm follows the procedure from Figure 8.1.

8.5.1 General genetic algorithm

In a genetic algorithm, a population of candidate solutions (individuals) to an optimization problem is evolved toward better solutions. Each candidate solution has a set of properties. In the case of this kernel, a set of properties that describe the slip plane. These properties evolve over a number of generations towards an optimal solution.

The evolution starts from a population of randomly (parabolic) generated individuals and is an iterative process, with the population in each iteration called a generation. In each generation, the safety factor (fitness) of every individual in the population is evaluated. This happens through a given limit equilibrium method (the fitness function). Slip planes with a low safety factor are considered to be more fit.

When evolving from one generation to the next, two individuals are combined (see section 8.5.1.1 and section 8.5.1.2) to make a new genome (individual). This genome is possibly modified (mutated, see section 8.5.1.3) to form a new child. Two children “fight” to decide which one will go to the next generation, see section 8.5.1.4. Elitism is introduced (section 8.5.1.4) to make sure the best solution thus far will not be lost. The algorithm terminates when a given number of generations have passed (section 8.5.1.6).

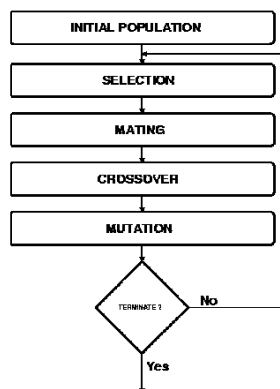


Figure 8.1 Procedure of the genetic algorithm

Default options are defined for a normal or thorough search. The options are defined in the following sections.

8.5.1.1 Initialization

Like in any other optimization method an initial guess of the final outcome is required. This guess concerns a choice of all individual genes in the population. In many problems the influence of the individual genes is fully independent. By implication, a random choice of the values of the genes between its appropriate limits is adequate.

In some problems a weak connection between the gene values is observed. An example is a free slip plane in slope analysis. Such a plane must be as flexible as possible in order to allow a wide variety of shapes. However, buckling planes will not survive as they have a surplus of resisting power. It is better to exclude these already at initialization.

From these perspectives, so far, two ways of initialization are defined:

- Uniform:

$$\frac{g_n - g_{min}}{g_{max} - g_{min}} = \eta_n \quad \text{with } 0 < \eta_n < 1 \quad (8.1)$$

- Parabolic:

$$\frac{g_n - g_{min}}{g_{max} - g_{min}} = \begin{cases} (\eta_A - \eta_B) \left(\frac{1}{\eta_C} \frac{n-1}{N-1} - 1 \right)^2 + \eta_B & \text{if } \frac{1}{2} < \eta_C < \infty \\ (\eta_A - \eta_B) \left(\frac{1}{1-\eta_C} \frac{N-n}{N-1} - 1 \right)^2 + \eta_B & \text{if } -\infty < \eta_C < \frac{1}{2} \end{cases} \quad (8.2)$$

with $0 < \eta_A < 1$ and $0 < \eta_B < 1$

In the uniform case every gene has its own random number. The corresponding value of the gene ranges between its minimum and maximum value. These bounds may even be different for every gene. The parabolic case is defined by three random numbers. They are chosen in such a way that the parabola for all genes ranges between 0 and 1.

Note that η_c is the relative position of the parabola's extreme. If this position is located outside the gene's position, the available space is not uniformly filled up, since the extreme enforces an extra offset. Therefore, it could be decided to fix the extreme always in the gene's range, $0 < \eta_c < 1$.

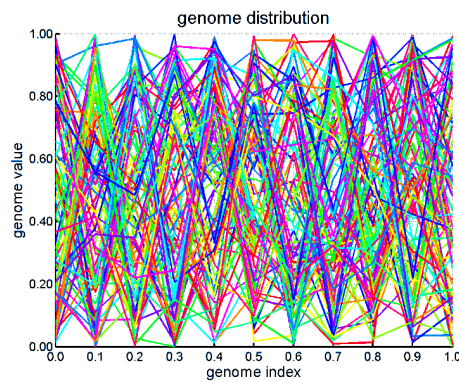


Figure 8.2 An entire population of uniformly defined individuals

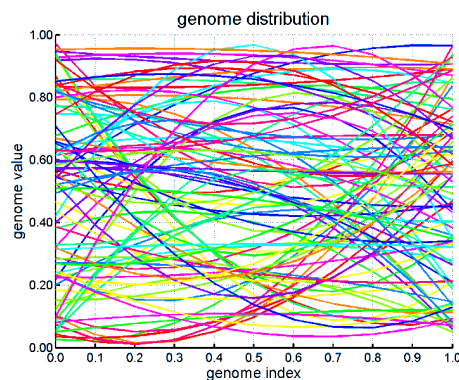


Figure 8.3 An entire population of quadratically defined individuals

8.5.1.2 Parental selection

Selection options specify how the genetic algorithm chooses parents for the next generation. The simplest selection method is a uniform random choice within the population. Parents are selected according to their index:

$$P[m] = G_m \quad m = \text{int}(\eta M) \quad (8.3)$$

This selection type is implemented in the kernel. More advanced options exist, based on the fitness scaling function or a remainder approach but are not (yet) implemented.

Crossover

The crossover rules realize the combination of two parents to form children for the next generation. Several types are in use, which meet certain specific demands in the problem at hand. Three of them are implemented in the kernel. The crossover mask is a vector of choices: “0” for the mother and “1” for the father.

Scattered

The father and mother are combined by having a completely random crossover mask. This works well for a small genome with independent genes, like for Bishop’s and Van’s method in slope stability. Mathematically, the crossover mask reads:

$$\chi = (0|1)_n \quad n = 1 \dots N \quad (8.4)$$

For every index a random choice between “0” and “1” is performed. The “0” selects the gene of the mother, the “1” the gene of the father. Visually, a scattered crossover looks as follows.

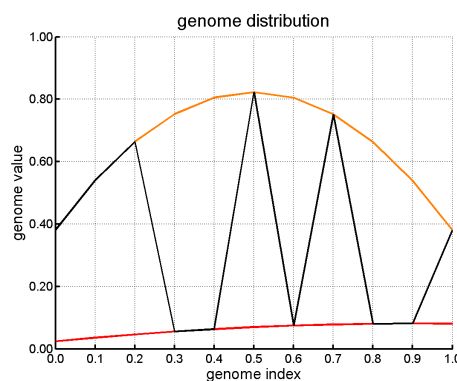


Figure 8.4 Scattered crossover between two parents

Index:	0	0.1	0.2	0.3	0.4	0.5	0.6	0.7	0.8	0.9	1
	1	1	1	0	0	1	0	1	0	0	1

A scattered genome initiation is ineffective for a genome with (weakly) connected genes, like a free slip surface in slope stability. Here, a random combination of well balanced parents will create chaotic children and therefore rarely better solutions. One of the other types is preferred, here.

Single Point

A single point crossover will combine the first part of one parent with the second part of the other parent. Mathematically, it is defined:

$$\chi = \{0 \dots 0, 1 \dots 1\} \quad (8.5)$$

For genome types which specify a coherent object, like a slip plane in slope stability, it will facilitate a more smooth convergence. In that case, the beginning of one plane will be

combined with the end of another plane. Such a plane will be more successful than a randomly shaped one.

paragraph*Double point

A double point crossover combines the middle of one slip plane with the edges of another. The definition is:

$$\chi = \{0\dots0, 1\dots1, 0\dots0\} \tag{8.6}$$

The figure below shows a double point crossover between two parents.

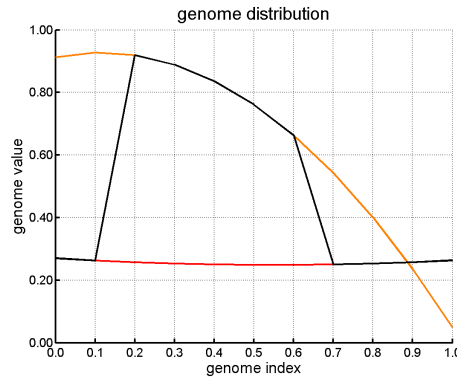


Figure 8.5 Double point crossover between two parents

Index:	0	0.1	0.2	0.3	0.4	0.5	0.6	0.7	0.8	0.9	1
	0	0	1	1	1	1	1	1	0	0	0

8.5.1.3 Mutation

Mutation options specify how the genetic algorithm makes small random changes in the individuals in the population to create mutation children. Mutation provides genetic diversity and enables the genetic algorithm to search a broader space. Three options are implemented in the kernel. The mutation mask is a vector of selected normalized gene values, similar to the initialization in (2) and (3). Three masks are defined, a jump, creep and an inversion.

Jump

Jump applies a completely random mutation mask

$$\mu = \eta_n \quad n = 1\dots N \tag{8.7}$$

A jump is suitable in slope stability when Bishop's or Van's method are applied. It helps finding the global minimum by jumping out of a local minimum. With Spencer's method, such a random change may paralyze the computation of the slip plane.

The jump method applies only for one point of the genome.

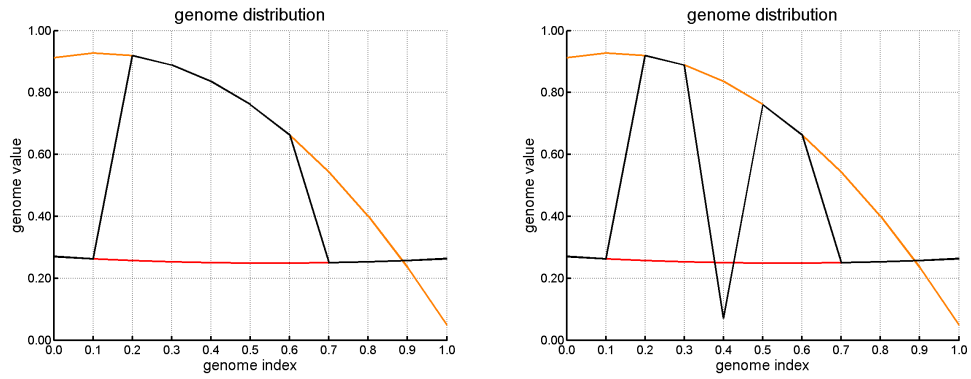


Figure 8.6 Left: initial genome; Right: genome after jump mutation

Creep

Instead of choosing a random mutation, one can choose to mutate with a small change. For example, one parameter can change 10% as a mutation.

The creep method applies only for one point of the genome. A Creep Reduction factor must be specified. This reduction factor is the maximum percentage a point can change. The mutation is random between zero and the maximum percentage.

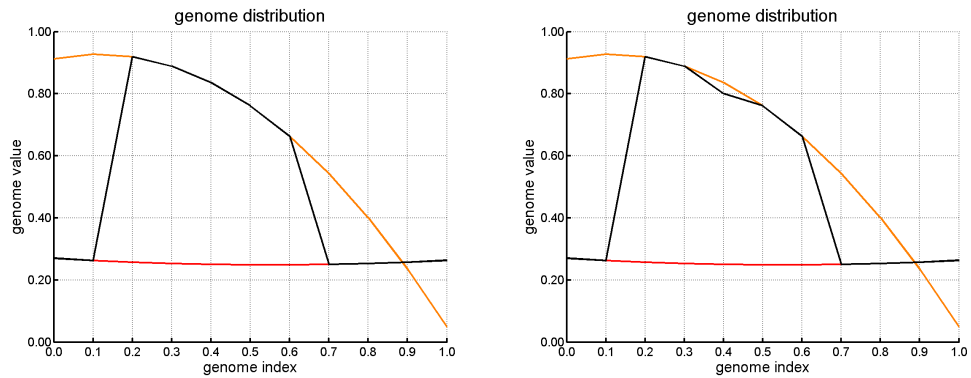


Figure 8.7 Left: initial genome; Right: genome after creep mutation

Inversion

An inversion is the inverse of the entire genome. It can be implemented in different ways. One can only invert in one direction, for example the height of the Spencer slices. For Bishop's method one can change the X and Y value of the genome, or mirror the X and mirror the Y relative to the boundary conditions. Not all inverses are possible. With Van's method it is useless to invert the two slip circles because their positions cannot be interchanges without violating the consistency rules of the program.

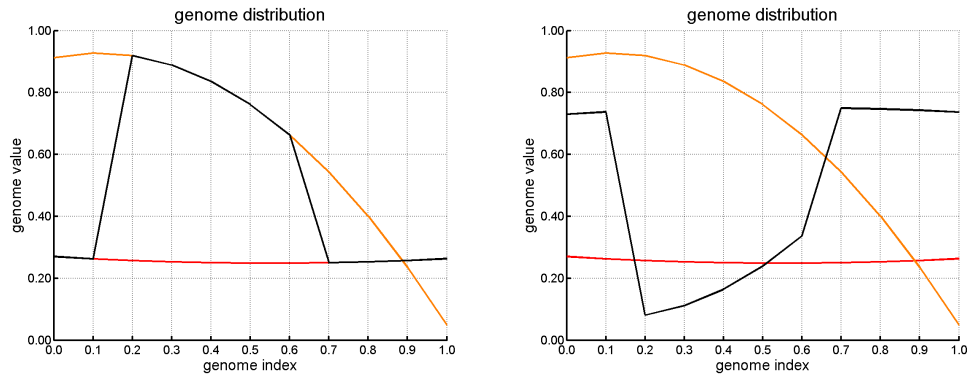


Figure 8.8 Left: initial genome; Right: genome after inversion

8.5.1.4 Child selection

The routine uses “tournament selection” to determine the strongest child. This means that the program chooses the individual with the highest fitness (i.e. lowest safety factor) to on to the next generation. This causes quick conversion to a minimum but little diversion

8.5.1.5 Elitism

The genetic algorithm uses elitism. The elite is passed directly through to the next generation. The size of the elite is variable.

8.5.1.6 Stop Criterion

The search terminates after a fixed number of generations. This number is variable.

8.5.1.7 Chaos in the algorithm

A genetic algorithm ought to be completely chaotic. The disadvantage of starting with a “random seed” is that every run will result in a slightly different answer. This makes it very difficult as a given problem does not result in a unique answer. The kernel does not use a “random seed” for drawing random numbers and will therefore always return exactly the same answer.

8.6 APSO algorithm (Uplift-Van)

The APSO (Adaptive Particle Swarm Optimization) algorithm is an algorithm that uses a population and performs a number of steps to improve a population. The algorithm uses particles. Each particle consists of a number of parameters, such as a coordinate in a sliding plane. The parameter values are normalized, so they all have a value between 0 and 1. Of each particle the model result is calculated.

The step from one population to the next is given by

$$X_{i,APSO}^{t+1} = \begin{cases} r_c < C & (1 - \beta) X_i^t + \beta B_i^t + \alpha r_a \\ r_c > C & X_i^t \end{cases} \quad (8.8)$$

with

$$\alpha = \delta^t \quad (8.9)$$

where

i	is the index number of the parameter in the particle;
X	represents the particle;
t	is the generation step in the iteration process;
B	is the best particle found so far;
C	is a given cross over fraction [0, 1];
β	is the parameter convergence factor [0, 1];
δ	is the parameter step size [0.1, 0.99];
r_c	is a random number, generated per parameter, particle and generation [0, 1];
r_a	is a random number, generated per parameter, particle and generation [-1, 1];

The algorithm keeps an elite, which consists of the best particles found so far. The elite has size K . To improve the population, the APSO algorithm is combined with a differential evolution algorithm, which is defined by

$$X_{DE,i}^{t+1} = \begin{cases} r_c < C & B_i^t + F \times (E_{r1,i}^t - E_{r2,i}^t + E_{r3,i}^t - E_{r4,i}^t) \\ r_c > C & X_i^t \end{cases} \quad (8.10)$$

where

F	is the given differential weight;
E	are particles in the elite;
$r1, r2, r3, r4$	are random index numbers in the elite;

Combining these algorithms, the next particle is defined as

$$X_i^{t+1} = \begin{cases} r_s < S & X_{APSO,i}^{t+1} \\ r_s > S & X_{DE,i}^{t+1} \end{cases} \quad (8.11)$$

where

S	is the APSO/DE separation factor, which linearly declines from 0.9 in the first generation to 0.1 in the last generation;
r_s	is a random number, generated per particle and generation [0, 1];

Using a random factor, in each iteration and per each particle it is decided whether the new particle comes from Equation (8.8) or from Equation (8.10). This is a random process which uses the APSO/DE separation factor S . Next there is another random process, which uses the cross over fraction C , which decides per parameter in the particle whether the value comes from Equation (8.8) or from Equation (8.10).

9 External loads

Objective

To calculate the stress σ_{load} due to external loads given a requested location (x, z) .

9.1 Line loads

A line load can be placed in or on the soil structure, and is assumed to continue infinitely in the direction perpendicular to the geometry plane. The angle of the load can be chosen freely, as long as there is a vertical downward component. The distribution angle determines the way the load spreads in the soil structure.

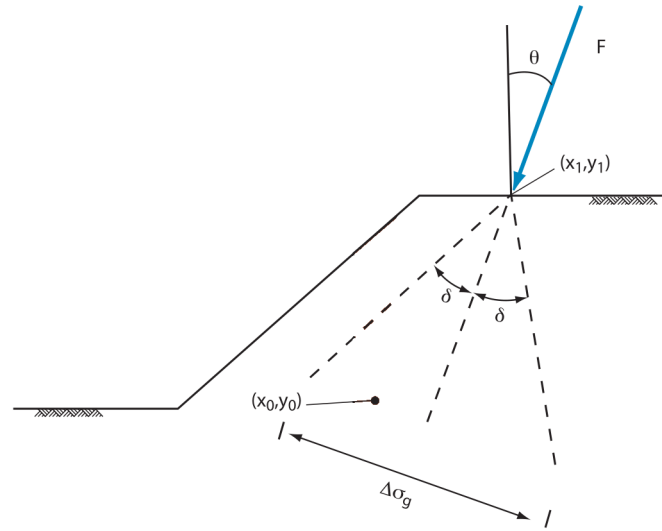


Figure 9.1 Line load

The width $\Delta\sigma_g$ over which the load is spread at a location (x, z) is found by rotating the system around the application point $(x_{\text{load}}, z_{\text{load}})$ of the load by the direction angle θ . The translated point becomes

$$x_{\text{rot}} = (x - x_{\text{load}}) \times \cos \theta - (z - z_{\text{load}}) \times \sin \theta + x_{\text{load}} \quad (9.1)$$

$$z_{\text{rot}} = (z - z_{\text{load}}) \times \cos \theta + (x - x_{\text{load}}) \times \sin \theta + z_{\text{load}} \quad (9.2)$$

where

- θ is the angle of load with the vertical axis, in radians;
- x is the X co-ordinate of the requested location, in m;
- z is the Z co-ordinate of the requested location, in m;
- x_{load} is the X co-ordinate of line load, in m;
- z_{load} is the Z co-ordinate of line load, in m;


The influence zone of the line is limited by a distribution angle. The influence limits $x_{\text{rot};\text{infl};\text{start}}$ and $x_{\text{rot};\text{infl};\text{end}}$ at a given z_{rot} are given by

$$x_{\text{rot;infl;start}} = x_{\text{load}} - (z_{\text{load}} - z_{\text{rot}}) \times \tan \delta \quad (9.3)$$

$$x_{\text{rot;infl;end}} = x_{\text{load}} + (z_{\text{load}} - z_{\text{rot}}) \times \tan \delta \quad (9.4)$$

where

δ is the load distribution angle, in radians.

Note: If the distribution zone of the line load intersects the surface line, the distribution zone is still limited by $x_{\text{rot;infl;start}}$ and $x_{\text{rot;infl;end}}$ and is not bounded by the soil width. 

In case the distribution angle δ is zero, the influence zone would become zero. This is not allowed, because the pressure would become infinite at an infinitely small influence zone. In that case the influence zone is set to a small value $\Delta\sigma_{\text{g;min}}$, default value 0.01 m. The influence zone $\Delta\sigma_{\text{g}}$ over which the load is spread, becomes

$$\Delta\sigma_{\text{g}} = \begin{cases} \theta > 0 & x_{\text{rot;infl;end}} - x_{\text{rot;infl;start}} \\ \theta = 0 & \Delta\sigma_{\text{g;min}} \end{cases} \quad (9.5)$$

The vertical pressure, which is the load divided by the width $\Delta\sigma_{\text{g}}$, is:


$$\sigma_{\text{load}} = \begin{cases} x_{\text{rot;infl;start}} \leq x_{\text{rot}} \leq x_{\text{rot;infl;end}} & \frac{F \times \cos \theta}{\Delta\sigma_{\text{g}}} \\ x_{\text{rot}} < x_{\text{rot;infl;start}} \vee x_{\text{rot}} > x_{\text{rot;infl;end}} & 0 \end{cases} \quad (9.6)$$

where

σ_{load} is the stress due to the line load at the requested location, in kN/m²;

F is the magnitude of the line load, in kN;

θ is the angle of load with the vertical axis, in radians;

Note: The line load can be situated in or on the soil structure. 

Besides an increase of the total stress, line loads located in the confines of the slip circle also contributes to the driving moment of the slip circle. This moment is added to the driving load moment. See [section 7.3.1.3](#).

9.2 Uniform loads

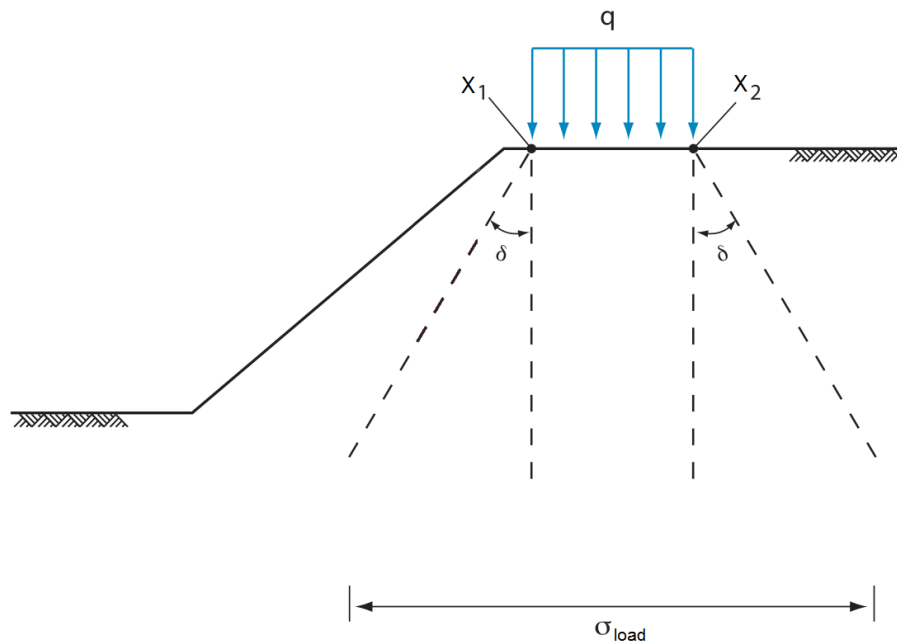


Figure 9.2 Uniform Load


The influence zone of a uniform load is limited by a distribution angle. The influence limits $x_{\text{infl};\text{start}}$ and $x_{\text{infl};\text{end}}$ at a given z are given by

$$x_{\text{infl};\text{start}} = x_{\text{start}} - (z_{\text{start}} - z) \times \tan \delta \quad (9.7)$$

$$x_{\text{infl};\text{end}} = x_{\text{end}} + (z_{\text{end}} - z) \times \tan \delta \quad (9.8)$$

where

x_{start}	is the horizontal co-ordinate where load starts, in m;
z_{start}	is the vertical co-ordinate where load starts, in m NAP;
x_{end}	is the horizontal co-ordinate where load ends, in m;
z_{end}	is the vertical co-ordinate where load ends, in m;
δ	is the distribution angle of the load, in degree;

Note: If the distribution zone of the uniform load intersects the surface line, the distribution zone is still limited by $x_{\text{rot};\text{infl};\text{start}}$ and $x_{\text{rot};\text{infl};\text{end}}$ and is not bounded by the soil width. 

The uniform load(s) will increase the total stress. This increase at a given location (x, z) is calculated using the following formula:

$$\sigma_{\text{load}} = \begin{cases} x_{\text{infl};\text{start}} \leq x \leq x_{\text{infl};\text{end}} & \frac{x_{\text{end}} - x_{\text{start}}}{x_{\text{infl};\text{end}} - x_{\text{infl};\text{start}}} \times q \\ x < x_{\text{infl};\text{start}} \vee x > x_{\text{infl};\text{end}} & 0 \end{cases} \quad (9.9)$$

where

σ_{load}	is the increase of the total stress, in kN/m ² ;
q	is the magnitude of the distributed load, in kN/m ² ;
x_{start}	is the horizontal co-ordinate where load starts, in m;
x_{end}	is the horizontal co-ordinate where load ends, in m;
$x_{\text{infl;start}}$	is the horizontal co-ordinate where load has influence at z , see Equation (9.7) ;
$x_{\text{infl;end}}$	is the horizontal co-ordinate where load has influence at z , see Equation (9.7) ;
δ	is the distribution angle of the load, in degree;

Besides an increase of the total stress, the load also contributes to the driving moment of the slip plane. The part of the load located within the confines of a slip circle creates a moment around the slip-circle center point (See [section 7.3.1.3](#)). This moment is added to the total driving moment.

9.3 Earthquake

In D-Stability it is possible to simulate the influences of earthquake forces. The earthquake forces induce several forces, stresses and moments. The influences of these earthquake forces are incorporated in D-Stability by so-called earthquake coefficients. These coefficients give the mass (of soil and water) an additional horizontal and vertical acceleration. Earthquake is taken into account in [section 5.4](#) and [section 7.3.1.4](#).

Earthquake forces will generate excess pore pressures in layers that are not fully drained. The pressure $\sigma_{\text{quake;soil}}$ generated by the earthquake is

$$\sigma_{\text{quake;soil}}(x, z) = a_v \times \sigma_{\text{soil}} \quad (9.10)$$

where

a_v	is the given vertical acceleration coefficient;
σ_{soil}	is the soil weight at (x, z) , see Equation (4.1) ;

The earthquake pressure includes the change in hydrostatic pressure due to vertical quake component, which is:

$$\sigma_{\text{quake;water}}(x, z) = a_v \times u_{\text{hydro}} \quad (9.11)$$

where

a_v	is the vertical acceleration coefficient;
u_{hydro}	is the hydrostatic pore pressure (see Equation (4.3)) ;

9.4 Tree on slope

The effect of the wind in the trees is equivalent to the effect of two uniform loads at both sides of the application point, one positive, the other one negative (Figure 9.3).

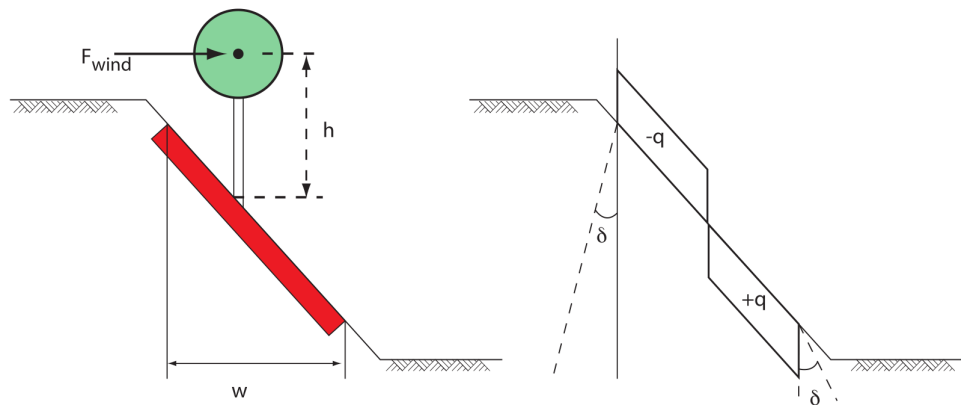


Figure 9.3 Representation of the effect of wind on trees

The uniform loads are generated in such a way that they reflect the moment, caused by the wind on the tree, around the root of the tree. Note that negative loads are not drawn in the profile inspector, so the effect can only be seen on one side of the tree.

This moment is

$$M_{\text{tree}} = -F_{\text{wind}} \times h \quad (9.12)$$

where

- F_{wind} is the magnitude of the wind, in kN/m;
- h is the height of the tree (the application point of the wind), in m;

The uniform loads will have a magnitude, in such a way that they would lead to the same moment. The magnitude of the equivalent uniform load q is:

$$q = \frac{M_{\text{tree}}}{(w/2)^2} \quad (9.13)$$

where

- w is the horizontal width of the root zone, in m.

Using Equation (9.9), the increase of stress at location (x, z) at the left and at the right side within the influence zone are:

$$\sigma_{\text{tree;left}} = \frac{-q \times w}{w + 2 \times (z_{\text{surface}} - z) \times \tan \delta} \quad (9.14)$$

$$\sigma_{\text{tree;right}} = \frac{q \times w}{w + 2 \times (z_{\text{surface}} - z) \times \tan \delta} \quad (9.15)$$

where

z_{surface} is the z -coordinate at the surface line at x ;

and leads to the total stress of the tree σ_{tree}

$$\sigma_{\text{tree}} = \sigma_{\text{tree;left}} + \sigma_{\text{tree;right}} \quad (9.16)$$

10 Reinforcements

Objective: To calculate the resisting moment due to reinforcements

10.1 Resisting moment from geotextiles

Geotextiles can be used to reinforce and improve the stability of slopes. The geotextile introduces a force that can act at the boundary of a slip circle (see Figure 10.1).

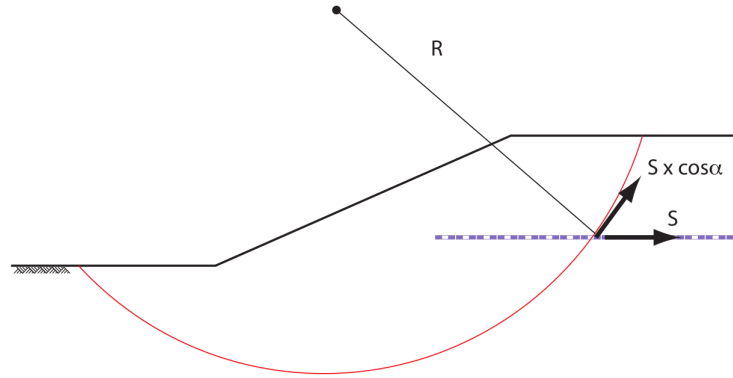


Figure 10.1 Resisting contribution by geotextiles

When calculating the safety factor, an extra resisting moment due to the geotextile $M_{R;geotextile}$ is introduced:

$$M_{R;geotextile} = R \times S \times \cos \alpha \quad (10.1)$$

with:

$$S = \frac{L_{min}}{L_{red}} \times T_f \leq T_f$$

$$L_{min} = \min \left(\sqrt{(X_{start} - X_{inter})^2 + (Y_{start} - Y_{inter})^2}; \sqrt{(X_{end} - X_{inter})^2 + (Y_{end} - Y_{inter})^2} \right)$$

where:

L_{min}	is the minimum embedding length, in m;
L_{red}	is the defined reduction area in m;
R	is the radius of the slip circle;
S	is the mobilized tensile strength in kN;
T_f	is the defined tensile strength in kN/m;
$(X_{inter}; Y_{inter})$	is the intersection point between the slip circle and the geotextile;
$(X_{start}; Y_{start})$	is the defined start point of the geotextile;
$(X_{end}; Y_{end})$	is the defined end point of the geotextile;
α	is the angle between the geotextile and the tangent line along the circle where the geotextile intersects the slip circle, in degrees.

Note: If the minimum embedding length L_{min} is larger than the reduction area L_{red} , then



100% of the strength is mobilized (i.e. $S = T_f$).

The contribution of the geotextile depends on the vertical distance between the slip circle center and the geotextile. Therefore, for acquiring a larger safety factor, it is required that this distance is relatively large. Only geotextiles that intersect a slip circle contribute to the resisting moment.

10.2 Resisting moment from nails

Soil nailing is a technique to reinforce and strengthen the existing ground by installing closely spaced steel bars, called nails. The bars are usually installed into a pre-drilled hole and then grouted into place or drilled and grouted simultaneously. They are usually installed at a slight downward inclination. A rigid or flexible facing (often pneumatically applied concrete otherwise known as shotcrete) or isolated soil nail heads may be used at the surface.

Nails are taken into account in the calculation by considering the forces generated at the intersection with the slip circle (Figure 10.2):

- the lateral force F_N , parallel to the nail;
- the shear force F_D , perpendicular to the nail.

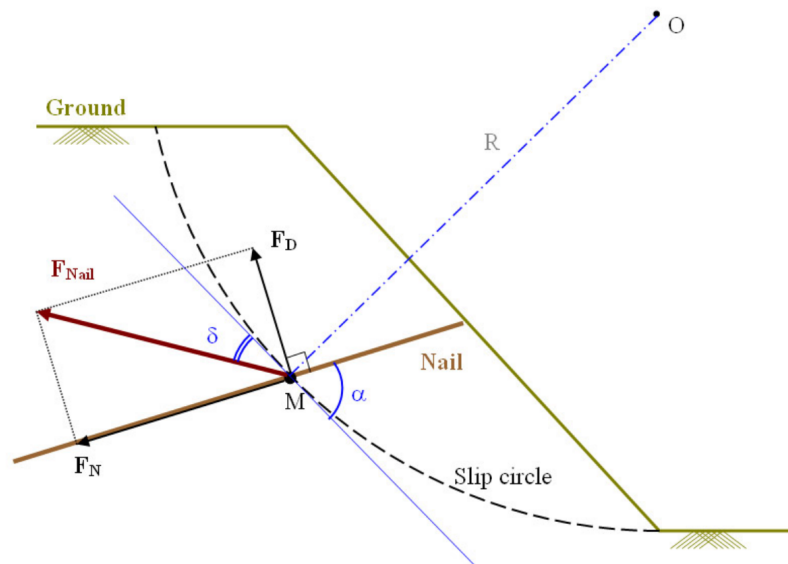


Figure 10.2 Resisting contribution by nails

The design method used for the calculation of both forces F_N and F_D is based on the Clouterre recommendations (Clo, July 1993) considering four failure criteria:

- section 10.2.1 the tensile resistance at the soil-nail interface is reached;
- section 10.2.2 the soil fails in bearing below the nail;
- section 10.2.3 the tensile and shear resistance of the nail is reached;
- section 10.2.4 the (stiff) nail breaks in bending.

The vector F_{nail} (F_N , F_D) must be located within the stability domain satisfying the four criteria mentioned above. The program determines the vector giving the maximum F_N and the minimum F_D . This is illustrated in Figure 10.3 where criteria 1 and 3 are relevant.

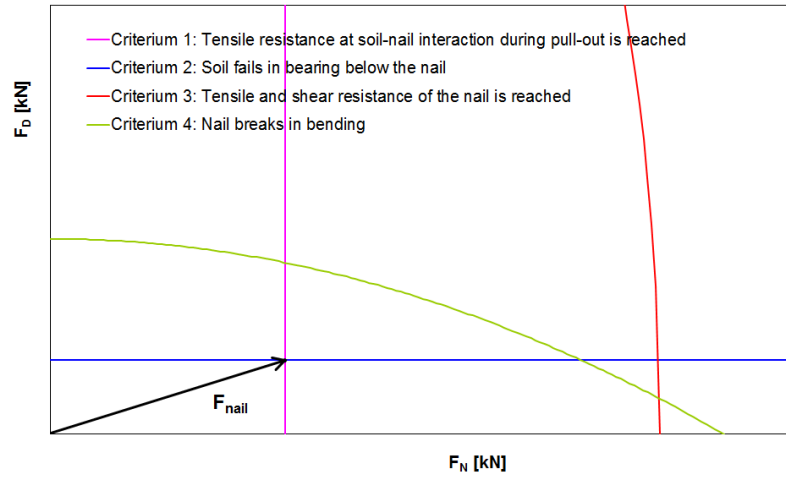


Figure 10.3 Representation of the four criteria in the $F_N - F_D$ diagram to determine F_{nail}

Influence of the critical angle

Depending on the value of α (angle between the nail and the tangent line along the circle where the nail intersects the slip circle) compared to the value of the critical angle α_{critical} , F_N or F_D can be neglected:

- If $\alpha < \alpha_{\text{critical}}$, the shear force is neglected:

$$\begin{aligned} F_N &= \min(F_{N;1}; F_y) \\ F_D &= 0 \end{aligned} \quad (10.2)$$

- If $\alpha \geq 90^\circ - \alpha_{\text{critical}}$, the lateral force is neglected:

$$\begin{aligned} F_N &= 0 \\ F_D &= \min\left(F_{D;2}; \frac{F_y}{2}; F_{D;4}\right) \end{aligned} \quad (10.3)$$

where:

$F_{N;1}$ is the limit resistance to pull-out between ground and bond, given by Equation (10.6);

$F_{D;2}$ is the limit shear force when soil fails in bearing below the nail, given by Equation (10.9);

$F_{D;4}$ is the limit shear force when nail breaks in bending, given by Equation (10.14);

F_y is the yield force in tension, as input value;

The total force in the nail is:

$$F_{\text{nail}} = \sqrt{F_D^2 + F_N^2} \quad (10.4)$$

The extra resisting moment $M_{R;\text{nail}}$ due to the nail is:

$$M_{R;\text{nail}} = M_D + M_N \quad (10.5)$$

with:

$$M_D = F_{\text{nail}} \times \cos \delta \times R$$

$$M_N = F_{\text{nail}} \times \sin \delta \times \tan \varphi_{\text{calc}} \times R$$

where:

- M_D is the moment due to the projection of F_{nail} on the tangent line along the circle, in kNm;
- M_N is the moment due to soil friction, in kNm;
- r is the radius of the slip circle, in m;
- δ is the angle between the nail force F_{nail} and the tangent line along the circle where the nail intersects the slip circle:
- $$\delta = \alpha - \arctan\left(\frac{F_D}{F_N}\right)$$
- α is the angle between the nail and the tangent line along the circle where the nail intersects the slip circle
- φ_{calc} is the effective friction angle of the soil at the intersection point, see Equation (6.21).

10.2.1 Tensile resistance at soil-nail interaction during pull-out

Reaching the pull-out capacity of soil nails can be assessed by the following criteria:

$$F_N \leq F_{N;1} = \tau_{\text{max}} \times \pi \times D \times L_a \quad (10.6)$$

where:

- τ_{max} is the ultimate frictional resistance to pull-out between ground and bonded length, in kN/m². If *Input of ultimate shear stress along nail* is selected, then τ_{max} is determined using a stress table using distance L_{shear} . If *Input of bond stress diagram (sigma, tau)* is selected, then τ_{max} is determined using the bond stress table.
- D is the borehole diameter, in m;
- L_a is the adherence length beyond the failure surface, in m.
- L_{shear} is the distance from nail head used in the shear stress curve ($L - \tau_{\text{max}}$ curve), in m:
- $$L_{\text{shear}} = \begin{cases} L_2 + 0.5 L_1 & \text{if facing or bearing plate is used} \\ L_2 + 0.5 L_1 & \text{if no facing or bearing plate is used and if } L_1 < L_2 \\ 0.5 L_2 & \text{if no facing or bearing plate is used and if } L_1 \geq L_2 \end{cases}$$
- L_1 is the length from failure surface to end nail, in m;
- L_2 is the length from failure surface to head nail, in m: $L_2 = L - L_1$.

10.2.2 Soil/nail normal reaction: soil fails in bearing below the nail

The nail is consider as a beam on elastic supports (i.e. soil):

$$EI \frac{d^4 y}{dz^4} + E_s \times y = 0 \quad (10.7)$$

where

- EI is the stiffness of the nail, in kNm²;
- E_s is the Young's modulus of the soil determined from the following empirical formula, in kN/m²:
- $$E_s = \frac{\alpha \times \sigma'_v}{CR \times \left[\left(\frac{2}{9}\right) 2.65^\alpha + \frac{1}{6} \alpha \right]}$$
- α is the rheological coefficient of the soil, in m;
- CR is the compression ratio of the soil:
- $$CR = \frac{C_c}{1 + e_0}$$
- σ'_v is the effective stress at the intersection point between the nail and the slip circle (see Equation (5.10)).

The soil plastification occurs at:

$$y = \frac{p_u \times D}{E_s} \quad (10.8)$$

The limit shear force is therefore:

$$F_{D;2} = \frac{1}{2} \times p_u \times D \times L_0 \quad (10.9)$$

where

p_u is the ultimate lateral stress. In D-Stability, it can either be:
 – user-defined if *Input of ultimate lateral stress along nail* is selected. In this case, p_u is determined using the lateral stress table using distance L_2 .
 – automatically calculated by the program if *Use soil parameters c, phi / su* is selected. In this case, the program uses the following empirical formulas, depending on the shear strength model, in kN/m²:

$$p_u = \begin{cases} 3 \sigma'_v \times K_p & \text{with } K_p = \frac{1 + \sin \varphi_{\text{calc}}}{1 - \sin \varphi_{\text{calc}}} & \text{for } c, \varphi \text{ models} \\ 9 s_u & & \text{for } s_u \text{ models} \end{cases}$$

D is the borehole diameter, in m;

L_0 is the reference length, in m, defined as:

$$L_0 = \left(\frac{4EI}{E_s} \right)^{\frac{1}{4}}$$

L_2 is the length from failure surface to head nail, in m.

σ'_v is the effective stress at the intersection point (see Equation (5.10)).

φ_{calc} is the effective friction angle of the soil at the intersection point (see Equation (6.21)).

10.2.3 Tensile and shear resistance of the nail

The maximum shear stress criterion, also known as Tresca's criterion, predicts that failure of a ductile material (e.g. nail in this case) occurs when the maximum shear stress (τ_{max}) at a given point in the nail reaches the yield shear stress (τ_y) obtained from a uni-axial tensile test:

$$\tau_{\text{max}} = \tau_y \quad (10.10)$$

With respect to 2D stress, the maximum shear stress (τ_{max}) is related to the difference in the two principal stresses σ_1 and σ_3 by the following equation:

$$\tau_{\text{max}} = \frac{1}{2} (\sigma_1 - \sigma_3) \quad (10.11)$$

For a tensile test, $\sigma_1 = \sigma$ and $\sigma_3 = 0$, so that:

$$\tau_{\text{max}} = \frac{1}{2} \sigma \quad (10.12)$$

Similarly, the yield strength in shear (τ_y) is related to the yield strength in tension (σ_y) by:

$$\tau_y = \frac{1}{2} \sigma_y \quad (10.13)$$

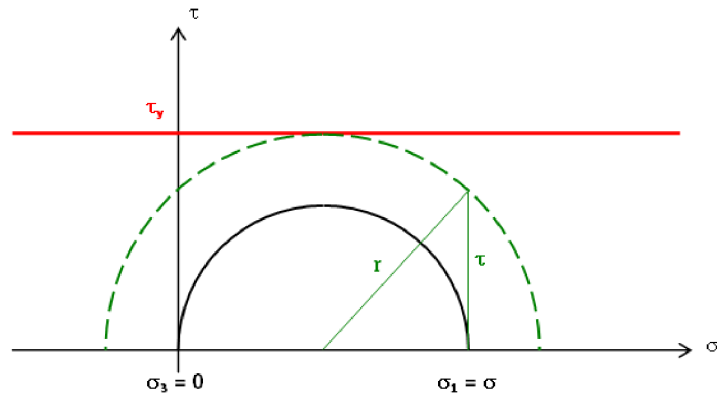


Figure 10.4 Representation of the Tresca's criterion by Mohr's circle

To represent this yield criterion graphically, Mohr's circles are used (Figure 10.4). It indicates that the yielding occurs if the radius of the Mohr's circle reaches τ_y , which writes:

$$r^2 = \tau^2 + \left(\frac{1}{2}\sigma\right)^2 \leq \tau_y^2 = \left(\frac{1}{2}\sigma_y\right)^2 \quad (10.14)$$

After integration of this equation over the cross-section S of the nail, the maximum shear stress criterion finally becomes:

$$4F_D^2 + F_N^2 \leq F_y^2 \quad (10.15)$$

where $F_y = S \times \sigma_y$ is the yield force in tension.

10.2.4 Soil/nail normal reaction: nail breaks in bending

The plastification of the nail occurs for a limit shear force of:

$$F_{D;4} = 1.62 \frac{M_{\max}}{L_0} \left(1 - \left[\frac{F_N}{F_y}\right]^2\right) + 0.24 \times p_u \times D \times L_0 \quad (10.16)$$

where:

- D is the borehole diameter, in m;
- F_y is the provided yield force in tension;
- p_u is the ultimate lateral stress, see Equation (10.9);
- L_0 is the reference length, in m, defined as:

$$L_0 = \left(\frac{4EI}{E_s}\right)^{1/4}$$

11 Waternet Creator

The waternet creator creates water pressures in the geometry based on parameters and boundary conditions. It is one of several ways to determine the water pressures in the cross section.

11.1 Waternet lines

The waternet creator generates waternet lines for both inwards and outwards calculations.

The waternet creator goes through a number of steps to generate pore pressures:

- 1 Validation of soil profile (section 11.1.1);
- 2 Validation of the hydraulic conditions (section 11.1.2);
- 3 Schematisation of phreatic plane (section 11.1.3);
- 4 Schematisation of the waternet-lines and their associated piezometric heads (section 11.1.4);
- 5 Calculation of pore pressures by means of waternet-lines (section 11.1.5).

Note: When using the automatic procedure, the unit weight of water γ_w is set equal to 9.81 kN/m³.



11.1.1 Conditions under which the automatic generation works

Under certain circumstances, the kernel must be able to produce the water pressures in the geometry. If the following circumstances are met, the water pressures will be schematized following the guidelines [Technisch Rapport Waterspanningen bij dijken (2004)] during a high water tide.

The requirements to automatically produce water pressures are as follows:

- Minimum of one and maximum of two aquifers;
- The aquifers reach from one boundary to the other (CNS 8);
- The generator only works if the high water table is on the left side.

11.1.2 Required input

For the schematisation of the phreatic lane and the piezometric heads, a distinction is made between four geo-hydrological scenario's:

- Case 1A : Clay dike on underground with clay and peat layers (see Figure 11.1);
- Case 1B : Clay dike on underground with sand layers (see Figure 11.1);
- Case 2A : Sand dike on underground with clay and peat layers (see Figure 11.2);
- Case 2B : Sand dike on underground with sand layers (see Figure 11.4).

The parameters listed in Table 11.1 are required to generate the water pressures.

Table 11.1 Parameters for generating water pressures in geometry, inner stability

Symbol	Unit	Description
Dike/bottom material		Choice between four geo-hydrological scenario's: 1A, 1B, 2A and 2B, see above for more information.
Z_{polder}	m NAP	The water level in the ditches in the polder.
MHW	m NAP	Outside high water level.
GHW	m NAP	Mean high water level.
$\varphi_{\text{PL2};\text{in}}$	m NAP	The hydraulic head of PL2 inwards at the top of the penetration zone of the deep compressible layers. When there are no specific measurements available, then the mean high water level (GHW) is the recommended input.
$\varphi_{\text{PL2};\text{out}}$	m NAP	The hydraulic head of PL2 outwards at the top of the penetration zone of the deep compressible layers. When there are no specific measurements available, then the mean high water level (GHW) is the recommended input.
$L_{\text{intrusion}}$	m	The intrusion length is the height of the penetration zone of the water pressures into an aquitard. This is the zone at the bottom of the deep compressible layers, where the piezometric head is affected by fluctuations in the first aquifer below. This is an input value. In practice, the intrusion length is set to 3.0 m for tidal areas, and to 1.0 m for the other areas.
$\lambda_{\text{PL3};\text{in}}$	m	The inward leakage length in the aquifer related to PL3.
$\lambda_{\text{PL3};\text{out}}$	m	The outward leakage length in the aquifer related to PL3.
$\lambda_{\text{PL4};\text{in}}$	m	The inward leakage length in the aquifer related to PL4.
$\lambda_{\text{PL4};\text{out}}$	m	The outward leakage length in the aquifer related to PL4.
Use default offsets	bool	If true, the default offsets will be used. If false, the user-defined values ($A_{\text{offset};\text{user}}$, $B_{\text{offset};\text{user}}$, $C_{\text{offset};\text{user}}$ and $D_{\text{offset};\text{user}}$) will be used.
Adjust PL3 and PL4 for uplift	bool	If true and if uplift indeed occurs, PL3 and PL4 will be lowered to a value in which uplift just no longer occurs. Refer to section 11.1.4.3 for more details. If false, PL3 and PL4 will not be adjusted.
$A_{\text{offset};\text{user}}$	m	The user-defined offset for the creation of PL1 (phreatic lane) under outer crest line.
$B_{\text{offset};\text{user}}$	m	The user-defined offset for the creation of PL1 (phreatic lane) under inner crest line.
$C_{\text{offset};\text{user}}$	m	The user-defined offset for the creation of PL1 (phreatic lane) under inner shoulder.
$D_{\text{offset};\text{user}}$	m	The user-defined offset for the creation of PL1 (phreatic lane) under inside toe.
$Z_{\text{B};\text{initial}}$	m NAP	The initial height of PL1 (phreatic lane) under outer crest line.
$Z_{\text{C};\text{initial}}$	m NAP	The initial height of PL1 (phreatic lane) under inner crest line.
Drain pipe	bool	The availability of a drain pipe. If true, the coordinates of the middle of the drain pipe (X_{drain} and Z_{drain}) must be given.
X_{drain}	m	(Only relevant if a drain pipe is present) The horizontal X-coordinate of the drain pipe, if present.
Z_{drain}	m NAP	(Only relevant if a drain pipe is present) The vertical Z-coordinate of the drain pipe, if present.

The outward calculations, the level of the phreatic plane at river side is GLW instead of GHW.

11.1.3 Schematisation of phreatic plane

In D-Stability the phreatic plane is referred to as “Phreatic Line”.

The procedure sets out the location of the phreatic line at a maximum of 6 points: A to F, see figures below. The level of the phreatic line is defined by entering a number of vertical offsets relative to the outer water level or the ground level. The location of the phreatic line between the points is determined on the basis of linear interpolation.

Lower levels relative to the reference point/plane are stated as positive values. When schematizing a rise in the phreatic plane under the crest, the offset should be stated as a negative value.

Table 11.2 lists the created points of the phreatic plane for all the scenario's.

Table 11.2 Schematisation of the phreatic plane for the different scenario's

P	Cases 1A and 1B Clay dikes (see Figure 11.1)	Case 2A Sand dike on clay (see Figure 11.2)	Case 2B Sand dike on sand (see Figure 11.4)
A	Intersection of the river water level with the outer slope (determined automatically).	Intersection of the river level with the outer slope (determined automatically).	Intersection of the river water level with the outer slope (determined automatically).
B	River water level minus offset, with default offset 1 m, limited by minimum value $Z_{B;initial}$, see section 11.1.3.2.	River water level minus offset, with default offset $0.5 \times (Z_A - Z_E)$, limited by minimum value $Z_{B;initial}$, see section 11.1.3.2.	Linear interpolation between point A and point E, limited by minimum value $Z_{B;initial}$, see section 11.1.3.2.
C	River water level minus offset, with default offset 1.5 m, limited by minimum value $Z_{C;initial}$, see section 11.1.3.2.	Linear interpolation between point B and point E, limited by minimum value $Z_{C;initial}$, see section 11.1.3.2.	Linear interpolation between point A and point E, limited by minimum value $Z_{C;initial}$, see section 11.1.3.2.
D	Linear interpolation between point C and point E, unless the user defines an offset $D_{offset;user}$ with respect to the surface level.	Linear interpolation between point B and point E, unless the user defines an offset $D_{offset;user}$ with respect to the surface level.	Linear interpolation between point A and point E, unless the user defines an offset $D_{offset;user}$ with respect to the surface level.
E	Surface level at dike toe minus offset, with default offset 0 m.	Surface level at dike toe minus offset, with default offset $-0.25 \times (Z_A - Z_E)$.	Surface level at dike toe minus offset, with default offset $-0.25 \times (Z_A - Z_E)$.
F	Intersection point polder level with ditch (is determined automatically).	Intersection point polder level with ditch (is determined automatically).	Intersection point polder level with ditch (is determined automatically).

Note: : For sand dike (i.e. case 2A and 2B), if a drainage construction is present in the dike (see Figure 11.3 and Figure 11.5), the phreatic plane goes directly to the middle of the



drainage construction (after point A) and does not pass along the inner slope (i.e. segment before point E in Figure 11.2). The phreatic line, as result of the drainage, can not be situated below the water polder level.

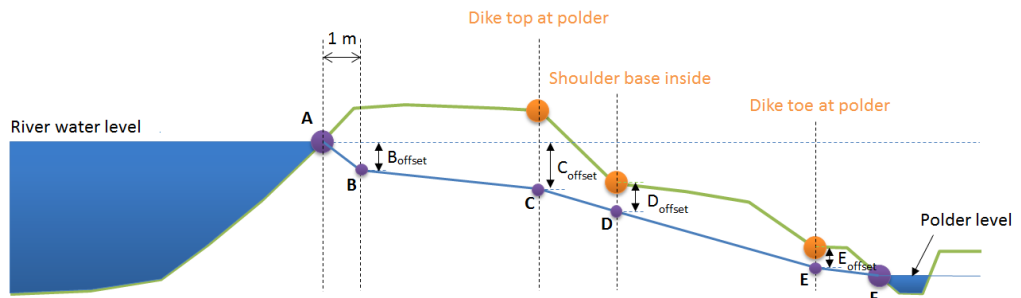


Figure 11.1 Schematisation of the phreatic plane for clay dikes (scenario's 1A and 1B)

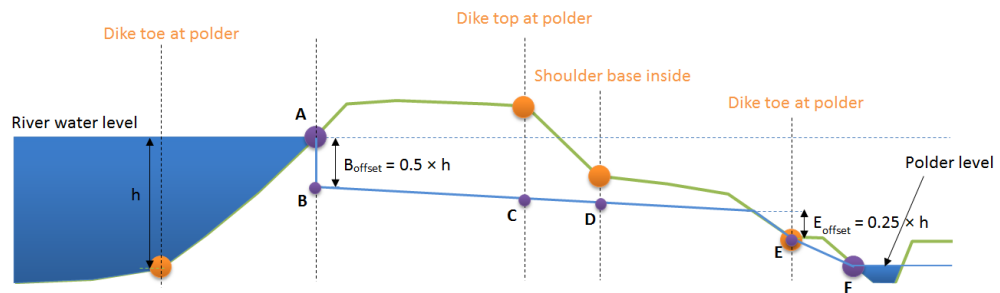


Figure 11.2 Schematisation of the phreatic plane for sand dike on clay/peat underground (scenario 2A), without drainage construction

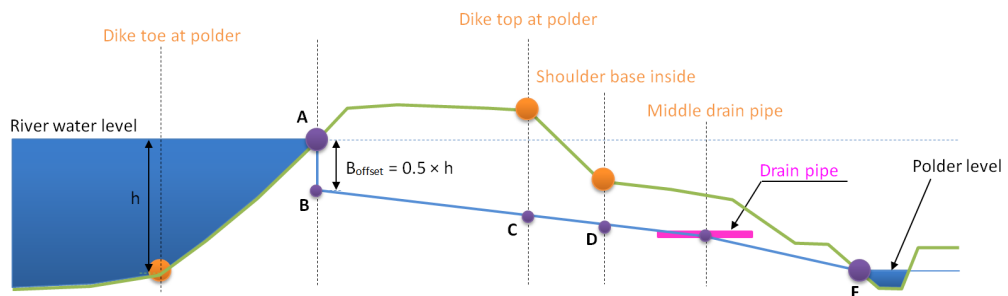


Figure 11.3 Schematisation of the phreatic plane for sand dike on clay/peat underground (scenario 2A), with drainage construction

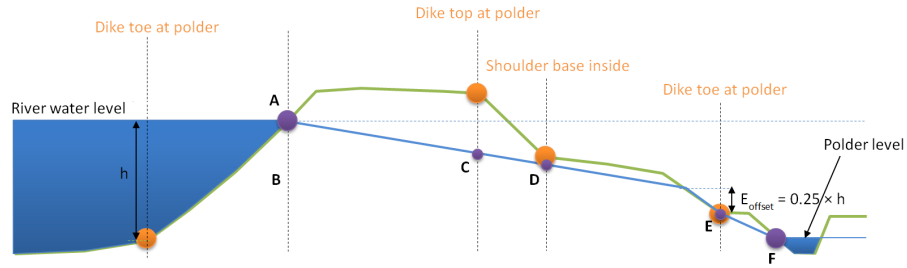


Figure 11.4 Schematisation of the phreatic plane for sand dike on sand underground (scenario 2B), without drainage construction

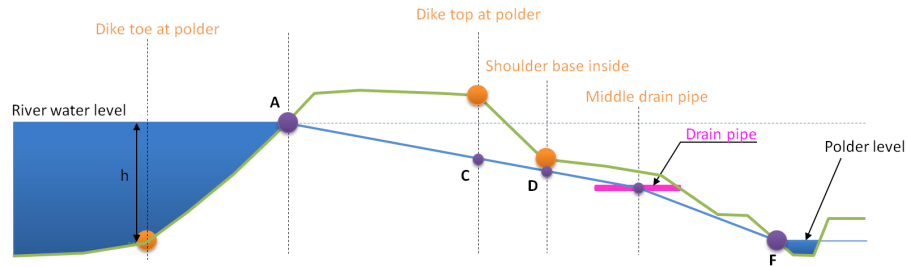


Figure 11.5 Schematisation of the phreatic plane for sand dike on sand underground (scenario 2B), with drainage construction

11.1.3.1 Particular cases

The checks below apply to the four scenario's.

Free water

The procedure must check that the phreatic plane along the dike does not extend beyond the slope. If this is the case, the location is automatically adapted to follow the surface level one centimeter lower.

Free water in the polder side is allowed. However the polder water level is limited by the surface level outside (right geometry boundary).

No ditch, no shoulder

If there is no shoulder, point D will be omitted. If there is no ditch, the offset at point E will be continued with a limit of 1 cm below the surface line.

Phreatic line goes up

The procedure must ensure that the location of the phreatic plane is not below the stated polder level at points D and E as a result of the stated offsets. If this is the case, the location of the phreatic plane will automatically be matched to the polder level. In addition, the procedure must ensure that the phreatic plane at points D and E is not higher than at the preceding points (see Figure 4.4). Point C may be higher than point B.

11.1.3.2 Minimum values below dike crest

The phreatic levels at points B and C is limited by user-defined minimal values:

- $Z_{\min;\text{crest river}}$, the minimum value below the dike top at river;
- $Z_{\min;\text{crest polder}}$, the minimum value below the dike top at polder.

The minimum value below point B when point B does not correspond to the dike top at river must be deduced by interpolation or extrapolation between points $(X_{\text{crest river}}; Z_{\min;\text{crest river}})$ and $(X_{\text{crest polder}}; Z_{\min;\text{crest polder}})$.

11.1.4 Schematisation of the piezometric heads

Table 11.3 gives an overview of the various piezometric lines and associated schematisation.

Table 11.3 Overview and description of piezometric lines

Piezometric line	Description
Phreatic line	For stability calculations with a stationary phreatic plane. The schematisation for PL1 is described in section 11.1.3 .
PL2	The pore pressure at the top of the penetration layer. The PL2 is not affected by the piezometric head in the underlying aquifer and it is constant (in other words, there is no damping) over the entire width of the cross-section. The user enters the value for PL2, as well as the thickness of the penetration layer. PL2 will be created only if the thickness of the penetration layer > 0 m.
PL3	Pore pressure in the bottom aquifer. The form of PL3 is given in Table 11.5 . The value for PL3 at the inner toe depends on the stated leakages lengths $\lambda_{\text{PL3};\text{in}}$ and $\lambda_{\text{PL3};\text{out}}$. These leakage lengths express the degree to which PL3 is damped to PL2. A high value means no damping (PL3 is constant). And a low value suggests full damping to PL2. If no value has been entered for PL2, the polder water level will be used.
PL4	Pore pressure in an intermediate aquifer (if present). The schematisation for PL4 is similar to that described for PL3. However, PL3 should be read as PL4. Note: Both PL3 and PL4 use different leakage lengths.

11.1.4.1 Schematisation of piezometric head PL2

For the schematisation of PL2, a linear interpolation is used between the hydraulic head of PL2 inwards $\varphi_{\text{PL2};\text{out}}$ at left geometry boundary and the hydraulic head of PL2 outwards $\varphi_{\text{PL2};\text{in}}$ at right geometry boundary.


$$\varphi_2(X) = \frac{\varphi_{2;\text{in}} - \varphi_{2;\text{out}}}{X_{\text{right}} - X_{\text{left}}} \times (X - X_{\text{left}}) + \varphi_{2;\text{out}} \quad (11.1)$$

Table 11.4 Points of PL2

Point	X-coordinate [m]	Z-coordinate [m NAP]
Left	X_{left} is the left geometry boundary	$Z_{\text{left}} = \varphi_{\text{PL2};\text{out}}$ with $\varphi_{\text{PL2};\text{out}} < \text{GHW}$
Right	X_{right} is the right geometry boundary	$Z_{\text{right}} = \varphi_{\text{PL2};\text{in}}$ with $\varphi_{\text{PL2};\text{in}} < \text{GHW}$

11.1.4.2 Schematisation of piezometric heads PL3 and PL4

Table 11.5 lists the created points of PL3 and PL4.

Note: For scenario “Sand dike on sand” (2B), only PL1 (Phreatic line) is created (not PL2, PL3 and PL4) even if one or more aquifers are present and the pore pressures are hydrostatic (i.e. with respect to the phreatic line). 


Note: For scenario “Clay dike on sand” (1B), PL4 will not be created even if an in-between aquifer is present. 

Table 11.5 Points of head lines PL3 and PL4

Point	Scenario's 1A and 2A Dike on clay (see Figure 11.6)	Scenario 1B Clay dike on sand (see Figure 11.7)
Left geometry boundary	$\varphi_3 = \varphi_4 = \text{MHW}$	
Outer dike teen	$\varphi_3 = \varphi_4 = \text{MHW}$	
Outer dike top	$\varphi_3 = \varphi_{3;\text{crest out}}$ (see Equation (11.2)) $\varphi_4 = \varphi_{4;\text{crest out}}$ (see Equation (11.3))	Linear interpolation
Inner dike teen	φ_3 calculated with Equation (11.4) φ_4 calculated with Equation (11.5) or linearly interpolated in cases where uplift occurs in a uplift zone of 20 m (for shorter zone where uplift occurs, it is not linearly interpolated).	$\varphi_3 = \varphi_4 = \text{surface level}$
First uplift location	φ_3 calculated with Equation (11.4) and maximum the uplift potential. φ_4 calculated with Equation (11.5) and maximum the uplift potential.	not applicable
First uplift location + 20 m	φ_3 calculated with Equation (11.4) and maximum the uplift potential. φ_4 calculated with Equation (11.5) and maximum the uplift potential.	not applicable
Right geometry boundary	φ_3 calculated with Equation (11.4) and for situations where uplift occurs PL3 goes down with a slope 1:100 with respect to the uplift potential in the uplift zone. φ_4 calculated with Equation (11.5) and for situations where uplift occurs PL4 goes down with a slope 1:100 with respect to the uplift potential in the uplift zone.	$\varphi_3 = \varphi_4 = \text{surface level}$

where:

$\lambda_{PL3;in}$	is the user-defined inward leakage length, see Table 11.1;
$\lambda_{PL3;out}$	is the user-defined outward leakage length, see Table 11.1;
$\lambda_{PL4;in}$	is the user-defined inward leakage length, see Table 11.1;
$\lambda_{PL4;out}$	is the user-defined outward leakage length, see Table 11.1;
GHW	is the user-defined mean high water level, see Table 11.1;
$\varphi_2(X)$	is head 2 at location X , calculated on basis of the gradient of PL2 between the user-defined values $\varphi_{2;out}$ and $\varphi_{2;in}$, see Equation (11.1);
ΔX	is the distance between point X , an arbitrary punt lying on the polder side of the dike, and de outer crest of the dike.

If this is no PL2, the polder level is used in Equation (11.2) until Equation (11.5).

11.1.4.3 Checking for uplift

If the input property “Adjust PL3/PL4 for uplift” (see Table 11.1) is enabled, the waternet creator will determine whether there is any uplift from the inner toe to the inside geometry limit. The formula from the VTV (2006) is used for this purpose, together with the initial schematisation for the piezometric heads :

$$F_{\text{uplift}} = \frac{\sigma_g}{\sigma_w} \quad (11.6)$$

If uplift is calculated within the uplift zone, PL3 and/or PL4 are lowered to a value in which uplift just no longer occurs, in other words to the point at which there is an unstable equilibrium (see Figure 11.8).

First uplift location

The check of uplift takes place for each geometry point, starting from the inner toe of the dike, and also every 50 cm, so that for a descending surface level from dike toe until inside geometry limit without in-between points the first uplift point can be determined anyway.

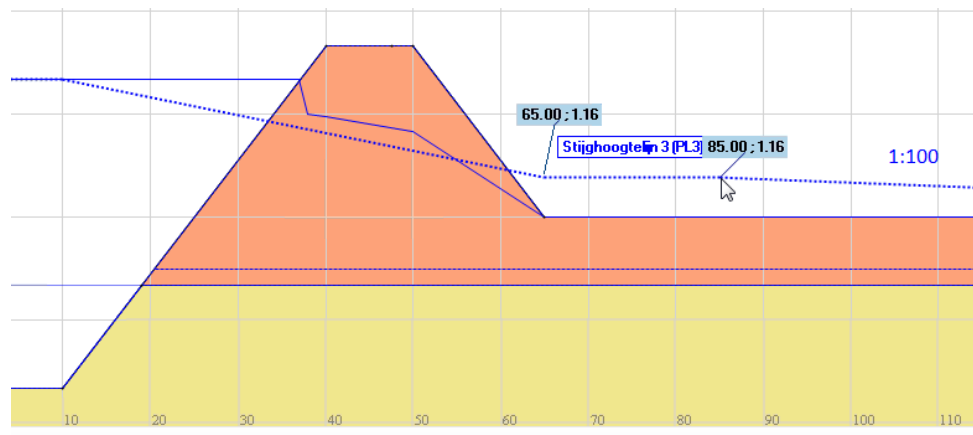


Figure 11.8 Lowering of piezometric head in the presence of uplift. D-Stability checks for uplift starting at the inner toe and extending to the edge of the profile and adapts the piezometric head accordingly until an unstable equilibrium is attained.

Uplift length

A fixed uplift zone length of 20 meters is assumed. After the uplift zone length of 20 m, PL3 and PL4 go to PL2 with a slope of 1:100.

When there is a ditch present and the first uplift location is situated between innertoe and the ditch, the uplift zone does not end at 20 meters after the first uplift location, but ends at 20 meters after the ditch dike side. So the uplift zone can be longer than 20 meters.

11.1.5 Schematisation of the pore pressures by means of waternet-lines

The aquifers must be defined from bottom to top (in the direction of the surface). A piezometric line (PL3) is assigned to the deep aquifer (see Figure 11.9). The pore pressures in the penetration layer are schematised using PL2. PL4 will be allocated to any additional aquifer (see Figure 11.10).

If several aquifers are stacked in succession one above the other, the same PL must be allocated to all of them, assuming a hydrostatic range for the pore pressures. The separation between the aquifer and cohesive layer is then determined by the top of the highest aquifer in the stack.

For the purposes of the stability calculations, the piezometric heads are schematised in the vertical direction using linear interpolation in the soft layers. A hydrostatic range is assumed in the soil layers where the phreatic plane is located and the aquifers.

If two in-between aquifers or more are defined, only the highest in between aquifer is relevant.

If the interpolation mode hydrostatic is given for a layer in the *.soil file, the kernel uses this interpolation mode instead of the above (automatic). This user-defined interpolation method must reach from one boundary to the other.

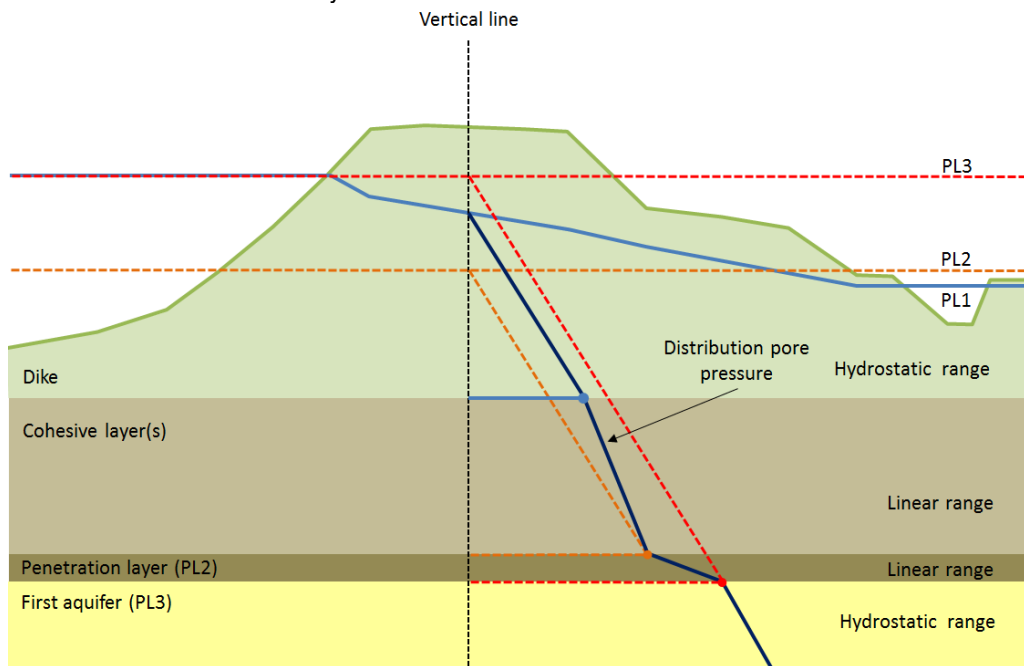


Figure 11.9 Schematisation of pore pressures when there is a single aquifer

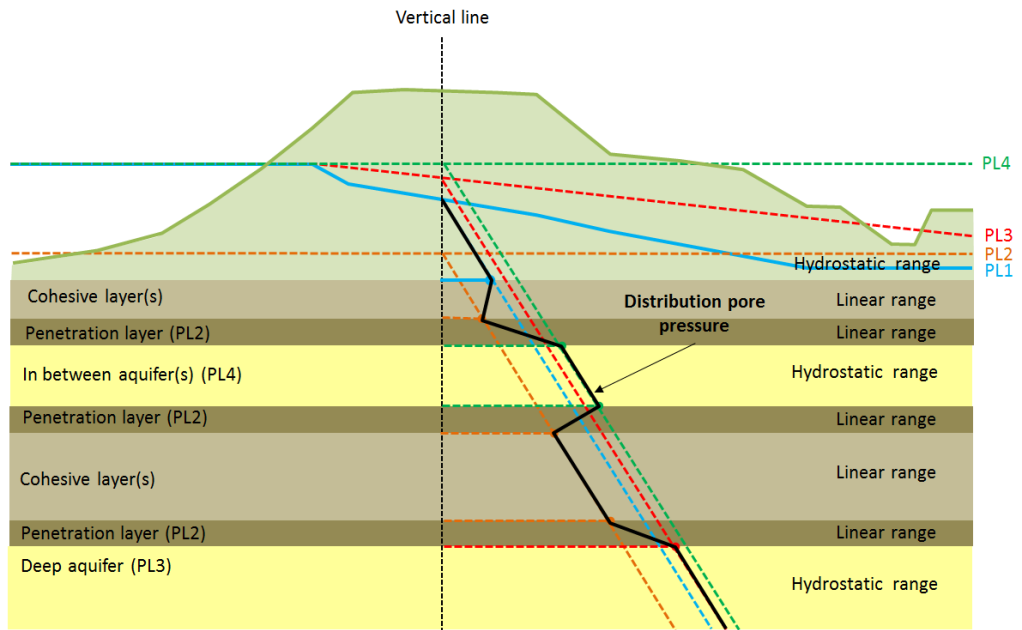


Figure 11.10 Schematisation of pore pressures when there is an in-between aquifer

Reliability analysis

12 Introduction

Reliability approaches are commonly allowed to be used in standards like the Eurocode and the Dutch WBI, for both structural and geotechnical design. Taking this into account, the D-Stability software supports the following reliability approaches:

- Semi-probabilistic analysis - [chapter 14](#),
- Full-probabilistic analysis with First Order Reliability Method (FORM) - [chapter 15](#),

All approaches require the definition of the stochastic variables (i.e. distribution type and corresponding parameters) of the load and strength variables - see [chapter 13](#).

The type of analysis can be chosen under Calculation - Settings. Here one can choose a calculation with deterministic values, mean values, characteristic values or a fully probabilistic analysis (with a fixed slip circle and a fixed water level).

13 Stochastic distributions

In order to support both the semi- and the full- probabilistic analyses, D-Stability always applies a log-normal probability distribution for all stochastic variables. The distribution is characterized by a mean μ and a standard deviation σ or a variation coefficient V .

13.1 Distribution properties

13.1.1 Mean

To calculate the mean value of parameter x , one can straightforwardly evaluate the following equation:

$$\mu(x) = \frac{1}{n} \sum_{i=1}^n x_i \quad (13.1)$$

where n is the number of samples.

13.1.2 Standard deviation

The standard deviation quantifies the uncertainty in a parameter:

$$\sigma(x) = \sqrt{\frac{1}{n-1} \sum_{i=1}^n (x_i - \mu)^2} \quad (13.2)$$

This uncertainty can also be defined with the variation coefficient V .

$$V = \frac{\sigma}{\mu} \quad (13.3)$$

where σ is the standard deviation and μ is the mean.

13.1.2.1 Determining standard deviation

In practice the following guidelines are used to determine a value for the standard deviation (σ_{total}) when processing soil test results. The input value of the standard deviation is composed of a statistical contribution of several factors:

- inherent soil variability
- systematic uncertainty contribution by soil testing
- the transformation from measurements to parameters

The D-Stability calculation assumes a homogeneous soil distribution. For a complete description of the uncertainty in the soil the effect of spatial fluctuations in the standard deviation must also be included. A suitable expression for the standard deviation can be derived, by applying Vanmarcke's random field theory (Vanmarcke, 1983). Combination of this expression with a systematic contribution yields:

$$\sigma_{\text{total}} = \sqrt{(\mu \cdot V_{\text{sys}})^2 + \left(\frac{1}{n} + \Gamma^2 + \gamma_v \cdot (1 - \Gamma^2)\right) \left(\frac{t}{u} \cdot \sigma_{\text{stat}}\right)^2} \quad (13.4)$$

with:

$$\Gamma^2 = 1 - \frac{1}{n_{\text{verticals}}} \cdot \sum_{i=1}^{n_{\text{verticals}}} \sigma_{\text{stat},i}^2 \quad (13.5)$$

$$\gamma_v = \max\left(\pi \cdot \frac{D_v}{d_{\text{layer}}}; 1\right) \quad (13.6)$$

where

- μ is the mean value of the variable under study, x , as shown in Equation (13.1);
- σ_{stat} is the statistical standard deviation value of the variable under study, x , as shown in Equation (13.2);
- n is the number of samples available for the variable under study, x ;
- V_{sys} is the variation coefficient V that quantifies the systematic uncertainty by soil testing and by the transformation from measurements to parameters. A usual value is 0.1 for cohesion, and 0.04 for the friction angle
- Γ defines the ratio between the average standard deviation along separate verticals and the global standard deviation. Γ assumes the value 0 if the standard deviation expresses the uncertainty in horizontal direction on the mean value. Γ assumes the value 1 if the standard deviation expresses the uncertainty in horizontal direction on a local value. A value of 0.5 is often applicable ($\Gamma^2 = 0.25$), assuming regular dimensions for (a) the width of the shearing volume, (b) the horizontal correlation length and (c) the regions of test sampling;
- u is the parameter from a normal distribution Φ_N , which corresponds to the following $P(x < \text{value}) = \Phi_N(u)$;
- t is the parameter from a t-student distribution, which depends on the number of samples n . The parameter becomes equal to u for large values of n ;
- γ_v defines the ratio between the vertical scale of fluctuation (correlation length) D_v and the thickness of the layer d_{layer} that is intersected by the slip plane. A usual value for D_v is 0.25 m.

13.1.3 Density functions

The Probability Density Function (PDF) $f(x)$: This is a function which indicates the likelihood of occurrence of a random chosen value x , relative to other values;

The Cumulative Density Function (CDF) $F(x)$: This is a function which indicates the probability that a random chosen value y is less or equal than x . It is related to $f(x)$ as

$$F(x) = P(y < x) = \int_{-\infty}^x f(y) dy \quad (13.7)$$

13.2 Distribution types

13.2.1 Standard normal distribution

The standard normal distribution is a normal distribution with mean $\mu = 0$ and deviation $\sigma = 1$. The standard normal distribution is unlikely to occur in the real world, but is used internally in probabilistic calculations.

The probability density function is

$$\varphi(u) = \frac{1}{\sqrt{2\pi}} e^{-u^2/2} \quad (13.8)$$

and the cumulative density function, or in other words the non exceeding probability, is

$$\Phi(u) = \int_{-\infty}^u \varphi(v) dv \quad (13.9)$$

Since there is no closed form to express Φ , it is approximated by approximation formula 26.2.17 for Normal Probability Function, Handbook of Mathematical Functions, Abramowitz & Stegun.

Other distribution types are converted to the standard normal distribution. The physical value in another distribution type, called x , is converted to a value u in the standard normal distribution, in such a way that the non exceeding probability of x is equal to the exceeding probability of u . With Φ the cumulative density function of the standard normal distribution, the converted value u is

$$u(x) = \Phi^{-1}(F(x)) \quad (13.10)$$

13.2.2 Normal distribution

The cumulative density function is

$$F_{\text{normal}}(x) = \Phi(u) \quad (13.11)$$

with the conversion function to the standard normal distribution

$$u(x) = \frac{x - \mu}{\sigma} \quad (13.12)$$

or inversely

$$x(u) = \mu + \sigma \cdot u \quad (13.13)$$

where

μ is the mean value, see [Equation \(13.1\)](#);
 σ is the standard deviation, see [Equation \(13.2\)](#);

13.2.3 Log-normal distribution

If parameter $y = \ln(x)$ has a normal distribution, then parameter x has a log-normal distribution. A log-normal distribution always yields values higher than a given shift (usually 0, denoted by c). The normal and log-normal distributions are similar for small ratios between the standard deviation and the mean.

The cumulative density function is

$$F_{\text{lognormal}}(x) = \Phi(u) \quad (13.14)$$

with the conversion function to the standard normal distribution

$$u(x) = \frac{\ln(x - c) - \mu}{\sigma} \quad (13.15)$$

or inversely

$$x(u) = c + e^{\mu + \sigma \cdot u} \quad (13.16)$$

When the mean m (see [Equation \(13.1\)](#)) and variance v (see [Equation \(13.2\)](#)) are given, the location μ and scale σ are calculated as follows

$$\sigma^2 = \ln \left(1 + \left(\frac{v}{m - c} \right)^2 \right) \quad (13.17)$$

and

$$\mu = \ln(m - c) - \frac{\sigma^2}{2} \quad (13.18)$$

14 Semi probabilistic analysis

In this approach, also called design value approach, calculations are made with combinations of unfavourable values of input parameters for resistance and loads. The unfavourable values are called design values.

They are determined by applying a partial factor on the unfavourable characteristic value, commonly defined by a confidence limit of 95%. The characteristic value of parameter follows from a stochastic distribution, usually defined by mean and standard deviation, where the standard deviation quantifies the uncertainty.

In D-Stability calculations the calculated safety factor must be larger than the required value:

$$F_s > F_{\text{required}}$$

14.1 Design value

A design value x_{design} of a soil strength variable x is determined by using the following equation:

$$x_{\text{design}} = \frac{x_{\text{charac}}}{f_{\text{partial}}} \quad (14.1)$$

where f_{partial} is the partial factor, used by D-Stability to reduce the characteristic strength to lower values. Usually $f_{\text{partial}} \geq 1.0$. The D-Stability software supplies defaults for the value of f_{partial} that are based on the Dutch NEN standards.

14.2 Characteristic value

Per parameter type, a specific confidence level p_{conf} is used, which is a probability. Usually, the confidence limit is 0.05 for strength parameters (parameters which increase the safety factor (see section 7.1) when the parameter value is increased) and 0.95 for load parameters (parameters which decrease the safety factor when the parameter value is increased)

The corresponding value in the standard normal space is calculated as follows

$$u_{\text{charac}} = \Phi^{-1}(p_{\text{conf}}) \quad (14.2)$$

where Φ is the cumulative density function of the standard normal distribution (see Equation (13.9));

Using the stochastic variable definition of a parameter, the corresponding x_{charac} can be derived.

14.2.1 Characteristic value (normal)

A characteristic value of a normally distributed soil variable x is determined from the following equations:

$$x_{\text{charac}} = \mu + u_{\text{charac}} \times \sigma \quad (14.3)$$

which is Equation (13.13) applied to u_{charac} .

14.2.2 Characteristic value (lognormal)

A characteristic value of a log-normal distributed variable x is determined by using the following equation:

$$x_{\text{charac}} = c + e^{\mu + u_{\text{charac}} \cdot \sigma} \quad (14.4)$$

which is Equation (13.16) applied to u_{charac} .

14.3 Stress tables

D-Stability determines a standard deviation of the soil strength variable, from stress tables, by application of the following procedure:

- first, it calculates per layer the average normal stress along the slip plane $\sigma_{\text{normal.ref}}$;
- then, it determines the value of the standard deviation at this reference normal stress from the characteristic and mean value of the shear strength:

$$\sigma[\tau] = \frac{\tau_{\text{ref.characteristic}} - \mu[\tau_{\text{ref}}]}{u_{\text{charac}}} \quad (14.5)$$

During probabilistic analysis, the D-Stability software will use the shear strength at the reference normal stress τ_{ref} as the random stochastic parameter per layer, and scale the shear strength values at other normal stress levels:

$$\tau = \frac{\sigma_{\text{normal}}}{\sigma_{\text{normal.ref}}} \times \tau_{\text{ref}} \quad (14.6)$$

Note: Stress tables are characterized by this one stochastic parameter, whereas the c-phi model is characterized by two: "cohesion" and "friction angle".



15 Full probabilistic analysis

Following the recommendation of the "Handreiking faalkansanalyse macrostabiliteit" document (Schweckendiek *et al.*, 2017), one must keep in mind the following steps when performing a full-probabilistic analysis of macrostability:

- i via a sensitivity analysis define the difference between the safety factor achieved with:
 - mean and design values,
 - low and high water levels,
 - etc.
- ii based on this sensitivity analysis and resulting slip planes, choose the water levels necessary to build a fragility curve,
- iii per water level (and corresponding schematisation of the pore water pressures), choose the relevant slip plane(s) and perform a FORM analysis (per slip plane),
- iv These individual analysis are a fragility point. Per water level, the lowest achieved reliability index (highest probability of failure) is used to define the fragility curve,
- v finally, the fragility curve is combined with the distribution of the water level and one failure probability is achieved for macrostability.

The explanations and equations shown in the precious chapters apply for step i, no further explanation is needed.

In step ii, the used is responsible of choosing the correct (value and amount) of water levels, so that a good fragility curve is achieved - more details in Schweckendiek *et al.* (2017).

15.1 FORM analysis

Step iii: the First order reliability method (FORM) is an approximation method, which is nowadays broadly used, accepted and validated in reliability analysis. In this method, approximations to the shape of the failure surface are made.

A FORM analysis cannot be used under all circumstances. In general, the precision of the FORM result decreases with a large number of stochastic parameters. In literature, it is often advised not to use a FORM analysis with more than 10 stochastic parameters. D-Stability usually converges with even 20 or more stochastic parameters, but the advice is to only define stochastic values for the parameters that influence the safety factor significantly.

The FORM analysis will only converge if the Z function can be reached within reasonable limits of the stochastic parameters. The solution space must be rather smooth.

The FORM analysis searches for the design point: The design point is, in standard normal space, the point in the parameter space with the highest probability density which leads to failure. In standard normal space this point corresponds with the point closest to the origin (point with all 0 coordinates). When the design point is found, the reliability index β can be evaluated as the distance between the origin and the design point (see Figure 15.1). The corresponding probability of failure is

$$p_{\text{failure}} = 1 - \Phi(\beta) \quad (15.1)$$

where Φ is the cumulative density function in the standard normal space (see Equation (13.9)).

The probability of failure found in this way is regarded to be a good approximation of the "real" probability of failure.

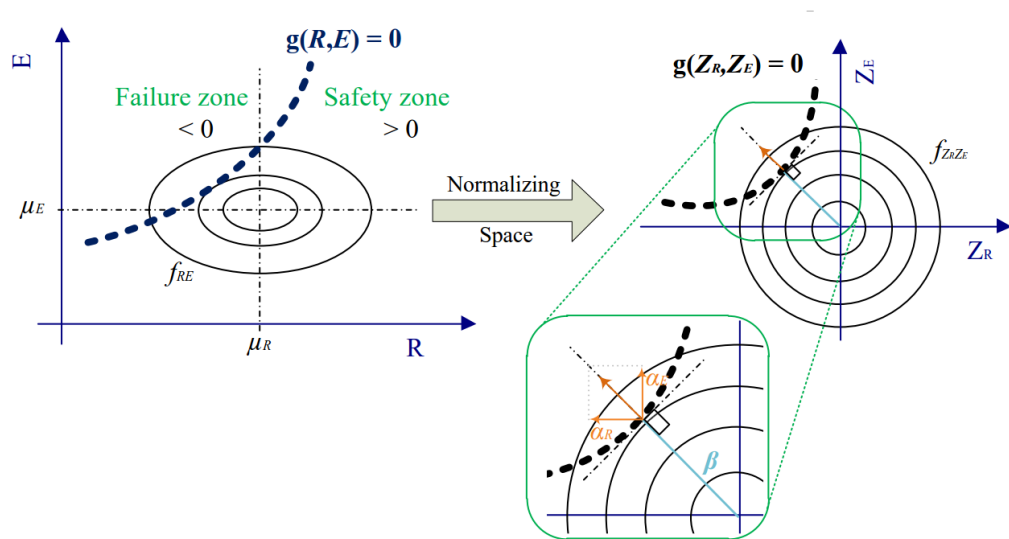


Figure 15.1 Schematic representation of FORM

To find the design point, the FORM analysis starts at the origin in the standard normal space and iterates to the design point. The FORM analysis uses a limit state function Z , which returns a negative value when failure occurs and a positive value when no failure occurs. D-Stability uses the following Z -function:

$$Z(u) = \frac{F_s(x(u))}{\gamma} - 1 \quad (15.2)$$

where

- u are the coordinates of the point in the standard normal space;
- x are the coordinates of the point in the "real" space. Conversion from u to x takes place using using the inverse of Equation (13.13) for normal distributions and Equation (13.16) for log-normal distributions;
- F_s is the safety factor found by section 7.1;
- γ is a model factor. The model factor is also defined as a stochastic variable and therefore has a corresponding coordinate in u ;

In each iteration step, the current point is moved closer to the design point. In the first iteration step, the current point is equal to the origin. Using a steepest descent, the next point is found, until a convergence criterion is fulfilled. The step move from the current point to the next point is calculated by

$$u_{j,i+1} = -\alpha_{j,i} \cdot |u_i| \cdot f_{relax} + u_{j,i} \cdot (1 - f_{relax}) \quad (15.3)$$

with the α value per coordinate

$$\alpha_j = \frac{\frac{\partial z_j}{\partial u_i}}{\left| \frac{\partial z}{\partial u} \right|} \quad (15.4)$$

where

j	is the index of a coordinate;
i	is the iteration index number;
$ u $	is the vector length of the current point;
f_{relax}	is the given relaxation factor. The relaxation factor prevents the algorithm from taking too big steps, which may cause divergence. Additionally, the FORM analysis reduces the relaxation factor a number of times by a factor 0.5 when no convergence is reached;
$\frac{\partial z_j}{\partial u_i}$	is the derivative in z to u_j ;
$\left \frac{\partial z}{\partial u} \right $	is the vector length of the derivative to all coordinates;

The α -values are sensitivity factors. These sensitivity factors allow us to assess the influence of each stochastic variable's uncertainty. This information can help choosing the necessary number of stochastic variables of a problem, i.e. the number of stochastic variables can be reduced, without compromising the accuracy of the reliability calculation.

A D-Stability FORM analysis is carried out with a fixed slip plane. Though in principle the analysis can be carried out with a search algorithm in each evaluation of Z , this is too time consuming. More information in [Schweckendiek et al. \(2017\)](#). The fixed slip plane is found with a semi probabilistic analysis.

15.1.1 Convergence

Convergence is reached when the following two criteria are met:

The Z -value must be close enough to zero. Suppose Z is linear with U close to the design point, we can write

$$\frac{|\Delta Z|}{|\Delta U|} = \left| \frac{\partial z}{\partial u} \right| \quad (15.5)$$

Since $\Delta Z = Z$ (because we take the difference with $Z = 0$) and we define the maximum allowed difference of u as ε_z , the convergence is calculated as

$$\frac{|Z|}{\left| \frac{\partial z}{\partial u} \right|} = \Delta U < \varepsilon_z \quad (15.6)$$

and

The beta value should not vary too much from step to step. This is defined as follows (with $\beta_{\text{estimated}}$ the predicted value of beta given at the previous step):

$$|\beta - \beta_{\text{estimated}}| < \varepsilon_\beta \quad (15.7)$$

The values ε_z and ε_β can be given by the user as diff failure and diff reliability.

Note: Start with few stochastic parameters to make sure the analysis converges easily. Build a more complex analysis from there by adding more stochastic parameters.



15.1.2 Correlations

Correlations define the dependency between stochastic variables. When two parameters are positively correlated, a higher encountered value in the first parameter leads to probably a higher value encountered in the second parameter. The correlation factor ρ_{pq} between two variables p and q is the Pearson correlation coefficient, which is:

$$\rho_{p,q} = \frac{\sum_i u_{p,i} u_{q,i}}{\sum_i u_{p,i} \sum_i u_{q,i}} \quad (15.8)$$

where

i is the index number of the observed value;
 p, q indicate variables;
 $u_{p,i}$ is the u-value corresponding with observed value x_i (see Equation (13.10), note that the distribution of variable p is derived already);

The FORM analysis is based on independent, in other words uncorrelated, parameters. Therefore each point u in the iteration process (see Equation (15.3)) is first converted to its correlated counterpart, before the safety factor is calculated.

Therefore, Equation (15.2) is replaced by the following calculation

$$Z(u) = \frac{F_s(x(u_{\text{correlated}}(u_{\text{uncorrelated}})))}{\gamma} - 1 \quad (15.9)$$

To get $u_{\text{correlated}}$, the following calculation is carried out:

$$u_{\text{correlated}} = L(u_{\text{uncorrelated}}) \quad (15.10)$$

where L denotes the lower triangle matrix originating in the Cholesky decomposition of the correlation matrix $[\rho] = LL^T$.

Note: The correlation matrix must be positive definite. If this is not the case, impossible correlations can be ignored by the reliability kernel. Parameters that are meant to be correlated might not be because of this reason. Always check your output!



The following parameters are used as steering criteria for the FORM analysis in D-Stability;

MaximumIterations	50
StepSize	0.01
RelaxationFactor	0.9
RelaxationLoops	3
EpsilonBeta	0.01

15.2 Monte Carlo and Monte Carlo Importance Sampling analysis

15.2.1 Crude Monte Carlo (MC)

Crude Monte Carlo sampling refers to the repeated sampling of the variables from the multivariate probability distribution function $f_X(x)$ (or, if the variables are mutually independent, sampling from the respective distribution functions $f_{X_1}(x_1), \dots, f_{X_n}(x_n)$). A single sample x_i refers to a vector of length n , where n is the number of random variables. For each sample x_i , the resulting value of limit state function $Z(x_i)$ is computed. The probability of failure is estimated as the ratio of samples for which $Z(x_i) < 0$, N_f , to the total number of samples, N :

$$\hat{P}_f = \frac{N_f}{N} = \frac{\sum_{i=1}^N I(Z(x_i))}{N} \quad (15.11)$$

where I is the indicator function, which is equal to unity when $Z < 0$, equal to zero when $Z \geq 0$. the figure shows a schematic view of the procedure for an example with two random variables X_1 and X_2 . Each dot represents a sampled pair (x_1, x_2) . Red grid points indicate failure ($Z < 0$), green grid point indicate no failure ($Z \geq 0$). The estimated probability of failure is equal to the number of the red dots divided by the total number of dots.

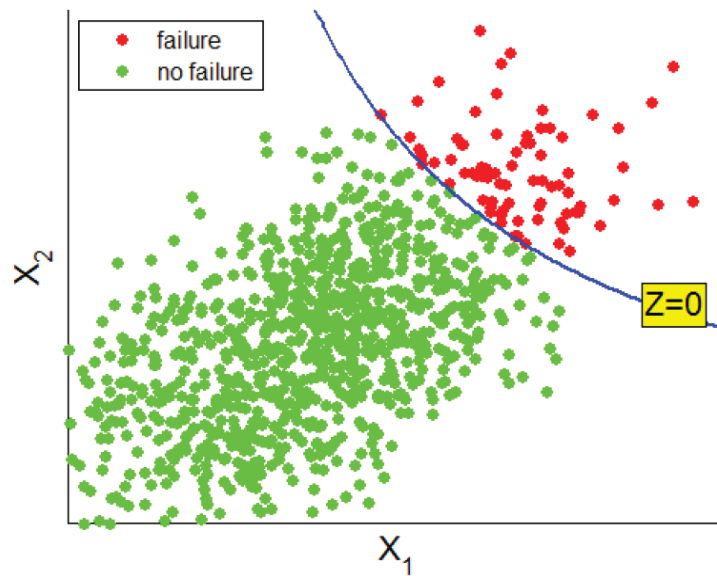


Figure 15.2 Schematic view of Monte Carlo sampling for an example with two random variables. Each dot represents a sampled pair (x_1, x_2) . Red dots indicate failure ($Z < 0$), green dots indicate no failure ($Z \geq 0$).

The required number of samples, N , to provide a reliable estimate of the probability of failure depends on the actual failure probability P_f and on the acceptable error in the estimate of P_f . Additionally, it depends on the acceptable probability that the real error is within the accepted range. This is because even though taking a large number of samples will most likely result in small errors (law of large numbers), it can never be fully guaranteed due to the random character of the Monte Carlo sampling. However, it is possible to take N large enough to guarantee with for example 95% or 99% certainty that the error in the estimate is within the acceptable range. This probability, P_k , can be expressed as:

$$P_k = \Phi(k) - \Phi(-k) \quad ; k > 0. \quad (15.12)$$

where Φ represents the standard normal distribution function, and k represents a sort of reliability index that the error is within the accepted range. The relation between k and P_k is schematically depicted in the figure below.

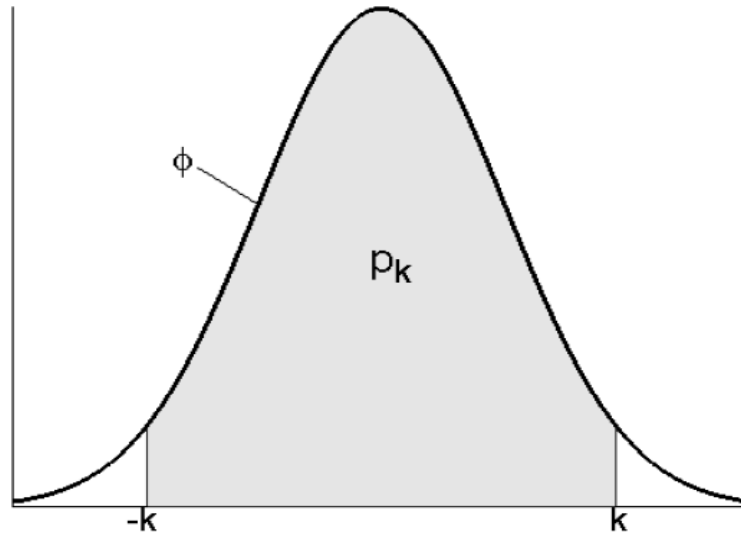


Figure 15.3 Relation between k and P_k according to equation (15.13). Function ϕ is the standard normal density function

For example, a probability of 95% corresponds with a k -value of 1.96, because 95% of samples from a standard normal distribution function have a value between -1.96 and 1.96 . In formula, k is defined as:

$$k = \Phi^{-1} \left(\frac{1 + P_k}{2} \right) \quad (15.13)$$

where P_k is the desired probability that the actual error is within the defined acceptable range. The required number of samples N can be estimated with the following formula (Melchers, 2002):

$$N = \frac{k^2}{\varepsilon^2} \left(\frac{1 - P_f}{P_f} \right) \quad (15.14)$$

where ε is the acceptable relative error in the estimate of P_f :

$$\varepsilon = \left(\frac{|\hat{P}_f - P_f|}{P_f} \right) \quad (15.15)$$

where \hat{P}_f is the Monte Carlo estimator of failure probability P_f .

Note that the required number of samples depends on the failure probability, which is not known in advance. Therefore, an estimate of the order of magnitude of the failure probability must be assumed, which can subsequently be revised during the Monte Carlo sampling procedure.

The table below shows the required number of samples for combinations of ε and P_f . The value of k in this example is taken equal to 1.96. The numbers from this table show that, taking into account that each sample involves an evaluation of the Z -function, crude Monte Carlo is a rather inefficient method (i.e. a large number of Z -function evaluations is required) especially for estimating small failure probabilities.

Table 15.3 Required number of samples with crude Monte Carlo for combinations of the acceptable relative error ε and actual probability of failure P_f . The value of k in equation (15.13) is taken equal to 1.96.

	ε		
P_f	0.10	0.05	0.01
10^{-2}	$4 \cdot 10^4$	$2 \cdot 10^5$	$2 \cdot 10^7$
10^{-3}	$4 \cdot 10^5$	$2 \cdot 10^6$	$2 \cdot 10^8$
10^{-4}	$4 \cdot 10^6$	$2 \cdot 10^7$	$2 \cdot 10^9$
10^{-5}	$4 \cdot 10^7$	$2 \cdot 10^8$	$2 \cdot 10^{10}$

15.2.2 Adaptive Importance Sampling (MCIS)

Adaptive Importance Sampling (MCIS) is an improvement of the Importance Sampling method. In general, Importance Sampling is sensitive to the user given start point. If not chosen well, the method might not give satisfactory results. In Adaptive Importance Sampling loops are used to improve the start point.

The algorithm of the Adaptive Importance Sampling is presented in the figure below.

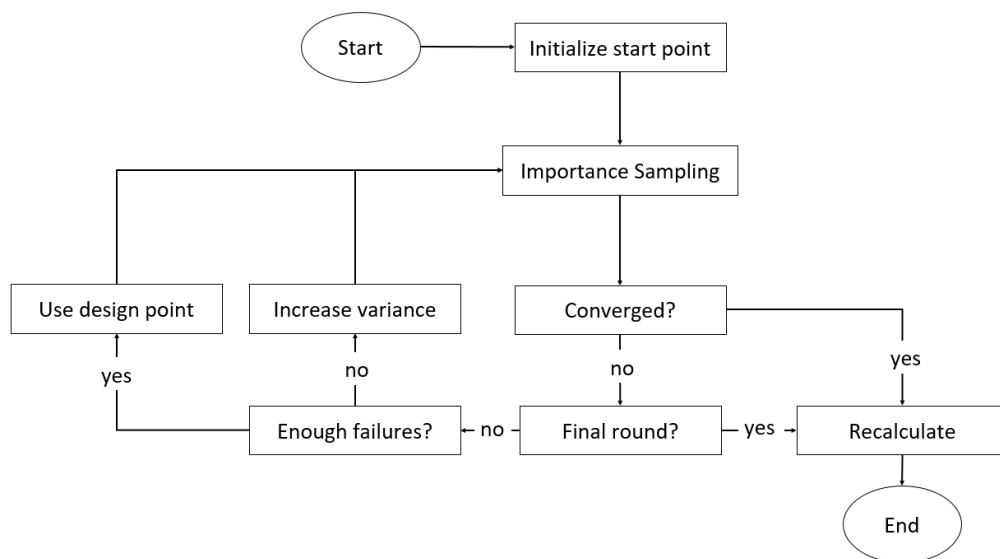


Figure 15.4 The algorithm of Adaptive Importance Sampling.

The individual steps are:

- **Initialize start point:** here one of the FORM start methods is used, the method can be selected by the user.
- **Importance Sampling:** in this step the Importance Sampling method is applied.
- **Converged?:** the convergence is reached when $\min\{N_{failed}/N, 1 - N_{failed}/N\} > \epsilon_{failed}$ where N_{failed} is the number of failed realizations and N is the total number of realizations. The value of ϵ_{failed} is specified by the user.
- **Final round?:** this step checks whether the last allowed round is reached, this is done to prevent endless loops. The maximal number of loops is specified by the user. Usually 5 rounds are enough.
- **Recalculate:** in this step the Importance Sampling is applied with a larger number of realizations. Here the last design point is used as the start point.

- **Enough failures?:** this step checks whether enough failures are found, this is the case when $N_{failed} > N_{enough}$. The value of N_{enough} is specified by the user.
- **Increase variance:** when there are not enough failures (hence $N_{failed} \leq N_{enough}$), then the variance coefficient is increased with a certain value. The value is specified by the user. With this value, the Importance Sampling calculation is repeated.
- **Use design point:** when there are enough failures (hence $N_{failed} > N_{enough}$), then the calculated design point is used as input for the next Importance Sampling calculation.

The following parameters are used as steering criteria for the MCIS analysis in D-Stability:

Startpointmethod	sensitivity
Maxbeta	8
VarianceFactor	1
MinVarianceLoops	1
MaxVarianceLoops	3
Var coeff failure	0.2
Min realizations	200
Max realizations	2000
Design point determination	Center of gravity
AutoMaximumSamplesNoResult	TRUE
EpsWeightSample	0.1

15.3 Fragility curve

Step iv: assuming that the user has found, per water level, the minimum reliability index (FORM analysis), the fragility curve is built and linear interpolation is considered between the existent, calculated fragility points (water levels).

Section 3.18 of the tutorial in this document explains how to export such a fragility curve using D-Stability.

It is important that enough points exist in the fragility curve, so that it correctly translates the failure behaviour, e.g. in case of uplift and/or over topping - more in [Schweckendiek et al. \(2017\)](#).

15.4 Combining Fragility Curve and water level

Step v: The combination of the fragility curve with the stochastic water level, is done via numerical integration over all water levels.

$$p_{\text{combined}} = \int_{u=-\infty}^{\infty} p_h(h(u)) \cdot \varphi(u) \partial u \quad (15.16)$$

where

- $h(u)$ is the water level corresponding to u , defined by a Gumbel distribution;
- p_h is the interpolated probability of failure between the fragility points of the fragility curve at a certain water level h ;
- $\varphi(u)$ gives the probability density corresponding to u , see [Equation \(13.8\)](#);

The integral is approximated by a summation from $u = -8$ to 8 , with step size 0.001 . The probability density is calculated by $\Phi(u + du) - \Phi(u)$.

The reliability, or β in the design point, is calculated as follows:

$$\beta = \Phi^{-1}(p_{\text{combined}}) \quad (15.17)$$

where Φ is the cumulative density function in the standard normal space (see Equation (13.9))

The design point, which is the combination of parameters with the highest probability density in the u -space, is found during the summation process. This value is the closest one to the origin, since we use only standard normal variables. The distance to the origin r is defined as

$$r = \sqrt{\varphi^{-1}(p_h)^2 + u^2} \quad (15.18)$$

The α_h value for the water level is calculated with the u -value in the design point:

$$\alpha_h = -\frac{u_{\text{design}}}{\beta} \quad (15.19)$$

The other alpha values, which correspond to soil and pore pressure parameters in the stability calculation, are interpolated values in the design point. They are normalized as follows:

$$\alpha_{\text{stab, normalized}} = \text{sign}(\alpha_{\text{stab}}) \cdot \sqrt{\alpha_{\text{stab}}^2 \cdot (1 - \alpha_h^2)} \quad (15.20)$$

where α_{stab} is the interpolated α -value in the fragility curve.

References

16 References

- July 1993. *Soil Nailing Recommendations-1991 for Designing, Calculating, Constructing and Inspecting Earth Support Systems Using Soil Nailing (English Translation)*. Tech. rep., Recommendations CLOUTERRE 1991.
- Bishop, A., 1955. "The Use of the Slip Circle in the Stability Analysis of Earth Slopes." *Geotechnique* 5: 7-17.
- Schweckendiek, T., M. van der Krogt, B. Rijnveld and A. M. Teixeira, 2017. *Handreiking Faalkansanalyse Macrostablieit*. Tech. Rep. 11200575-016-GEO-0005, Deltares.
- Spencer, E., 1967. "A method of analysis of the stability of embankments assuming parallel interslice forces." *Geotechnique* 17 (1): 11-26.
- Van, M., 2001. "New approach for uplift induced slope failure." In *XVth International Conference on Soil Mechanics and Geotechnical Engineering, Istanbul*, pages 2285-2288.
- Vanmarcke, M., 1983. *Random Fields, Analysis and Synthesis*. ISBN 0-262-22026-1. MIT Press.



BOI



Rijkswaterstaat
*Ministry of Infrastructure
and Water Management*

Deltares

Deltares

Deltares is an independent institute for applied research in the field of water and subsurface. Throughout the world, we work on smart solutions for people, environment and society.

Deltares

www.deltares.nl